

**School of Civil Engineering and the Environment**  
**University of Southampton**  
**United Kingdom**



**Development of granules-based technology for partial  
nitrification**

Thesis submitted for the degree of Doctor of Philosophy

Candidate: **Simone Cinquepalmi (26649306)**

Supervisor: **Dr. Yongqiang Liu**

Co-supervisor: **Prof. Sonia Heaven**

May 2020





# UNIVERSITY OF SOUTHAMPTON

## ABSTRACT

### FACULTY OF ENGINEERING AND THE ENVIRONMENT

Water and Environmental Engineering

Thesis for the degree of Doctor of Philosophy

## DEVELOPMENT OF GRANULES-BASED TECHNOLOGY FOR PARTIAL NITRIFICATION

Simone Cinquepalmi

Side-stream treatment is much more efficient and effective than returning the side stream to the main stream. Currently, partial nitrification followed by either denitrification or ANAMMOX process are being investigated intensively for nitrogen removal from the side stream to replace conventional nitrification-denitrification due to reduced energy and carbon inputs as well as less sludge production. As a precedent step, partial nitrification plays a critical role for the whole nitrogen removal process. Although there are a lot of research to investigate partial nitrification to improve its performance and stability, most of them focus on suspended sludge. Granular sludge as a kind of self-immobilized biofilm with compact structure and large size has distinct advantages such as high biomass retention, high capability to withstand the unfavourable environmental conditions (e.g. pH, toxic compounds and temperature) and loading shock compared with suspended sludge. Therefore, this study mainly focuses on the development of granule sludge based partial nitrification technology for side stream treatment.

In the first part of this study, the rapid granulation and the performance by granular sludge for partial nitrification were evaluated in four 3-L sequencing batch reactors. A rapid granulation strategy by forming heterotrophic granules first followed by converting heterotrophic granules to partial nitrifying granules was proposed and validated to shorten the reactor start-up time. With this newly proposed strategy for rapid partial nitrifying granulation, effects of ambient temperature and temperature at 30-33 °C (the temperature of side stream from anaerobic digestion tank), and COD/N ratio (5 and 20) on heterotrophic granulation were investigated. Heterotrophic granules were formed within 9 days at 18-23 °C and 11 days at 30-33 °C, respectively, which is faster than most reported granulation periods i.e. 2-4 weeks. By quickly decreasing COD/N ratio, nitrifying bacteria were enriched in the formed heterotrophic granules within 30 days to treat 100 mg N L<sup>-1</sup> influent nitrogen, due to the excellent retention of granular sludge in the reactors. On days 37 and 47, it can be claimed that heterotrophic granules have been fully converted into partial nitrifying granules in four reactors, which is around 35-50 days faster than the formation of nitrifying granules directly with suspended sludge by enriching nitrifying bacteria first. In addition, it was found that at lower temperature and COD/N, granules formed a bit more quickly. This part confirmed that the newly proposed strategy for the formation of partial nitrifying granules is very effective, which could be applied in the real situation to start up new reactors or quickly restart the crashed reactors.

After the formation of partial nitrifying granules, 4 reactors were operated to evaluate their long-term nitrogen removal performance. The reactor operated at 18-23 °C and 30-33 °C achieved specific ammonium oxidation rates of 0.598 and 0.346 mg N mg VSS d<sup>-1</sup>, respectively, with nitrogen loading rates of 1.7 and 2.4 g N L<sup>-1</sup> d<sup>-1</sup>, respectively, suggesting higher specific ammonium oxidation of nitrifying granules at ambient temperature than 30-33 °C. At both temperatures, ammonium removal efficiency is higher than 98% and nitrite accumulation efficiency is higher than 97%, indicating that temperature is not critical factor for granules to achieve partial nitrification. Although reactor performance was good, it was found that minerals were accumulated in granules gradually, resulting in mineral content as high as 80% after 70-day reactor operation. XRD analysis showed that Ca-phosphate in the form of hydroxyapatite (HAP) is the main inorganic compound in granules in accompany with small amount of CaCO<sub>3</sub> in the form of calcite. The second part of this work thus examined this mineral accumulation in partial nitrifying granules in details. Partial nitrifying granules from reactors were sorted into groups with different granule sizes. For the smallest group with granule size from 150 to 250 μm, two distinct colour granules, i.e. brown and yellow, were observed. For larger group with granule size above 710 μm, only brown granules were observed. For all brown granules with different size ranges, ash content of granules was higher than 70%. Both HAP and calcite were found in brown granules with different sizes, with the former preferentially accumulated in the larger granules. The Ca/P ratio in granules is at around 2, which is close to theoretical molar ratio of Ca/P in HAP. Cycle analysis showed that 15 mg L<sup>-1</sup> phosphate in the synthetic wastewater was removed by 60% in both particles range <600 μm and >2800 μm, which is mainly due to the reaction of phosphate with high calcium concentration in water, i.e. 100 mg/L Ca in this case (typical calcium concentration in tap water in Southampton) at alkaline conditions such as >8. Compact granule structure results in

high mass transfer resistance, which might further create a more alkaline environment in granules due to pH gradient to facilitate the precipitation of CaP. For yellow granules with size ranging from 150 to 250  $\mu\text{m}$ , ash content only was 3% and specific ammonia removal rate was  $35 \text{ mg N g}^{-1} \text{ h}^{-1}$ , indicating that yellow granules are newly formed fresh granules which play a major role for nitrogen removal in the reactors. Although the structure of partial nitrifying granules was very stable during 150 days operation, the gradual accumulation of minerals in granules actually led to the reduced microbial activity. Therefore, further investigation is needed to control the mineral accumulation and ash content increase.

Extracellular polymeric substances (EPS) were reported much higher in granular sludge than in suspended sludge because of the strong hydraulic selection pressure used to form granules, which can stimulate more EPS production to adhere cells to form compact aggregates. Furthermore, the interaction between EPS and metal ions, and the binding of metal ions with EPS provided localized high metal ion concentration, leading to a saturated local environment for inorganic precipitation, which were also widely reported especially in geography studies. The third part of this study thus intended to explore how mineral precipitates affect EPS analysis and the relationship between mineral precipitates and EPS in sludge and how to produce a reliable and accurate analysis of EPS with high mineral precipitates. It was found that high mineral precipitate in sludge mainly interfere protein analysis with the Lowry method. It was found that the highly bound Ca within EPS instead of free calcium ions in the solutions of extracted EPS, from partial nitrifying granules, reacted with Lowry reagents to form precipitates to interfere the optical density readings of spectrophotometer. How bound Ca with EPS can form inorganic precipitates with Lowry reagents was out of the study scope although it is very interesting with regard to the mechanism of the precipitate accumulation in partial nitrifying granules with high EPS content and high influent water hardness levels (in this case, high Ca ion concentration). But an improved protein analysis was found in this research work by simply prolonging the incubation time from 1 hr to 3 hr to allow newly formed precipitates to settle down to the bottom of cuvette to minimize the interference of suspended particles on optical density readings. After 3 hr incubation, the difference of optical readings with/without Calcium dropped from 38.6% to less than 0.1%, suggesting the effectiveness of this incubation prolongation for protein analysis with Lowry method.

Although partial nitrifying granules are more resistant to unfavourable conditions compared with suspended sludge, it is still unavoidable in some circumstances that nitrifying bacteria are inhibited such as at high salinity levels or high toxic compound levels. The fourth part of the study examined the reactivation of inhibited nitrifying granules as well as suspended nitrifying sludge by exerting a weak electric field (EF). The experiment studied the inhibition of partial nitrifying sludge with 2-4% salinity and 50-100 mg phenol  $\text{L}^{-1}$ , respectively. It was found that the application of  $2 \text{ V cm}^{-1}$  electric field for 90 minutes could increase the activity of nitrifying granules (that were not inhibited) by 30% compared to the control. Suspended sludge showed 164% and 169% more activity than control after EF treatment while intact granules showed 43% and 18% more activity compared with the control, at 2% and 4% salinity, respectively. However, different results were obtained for phenol inhibition tests. After phenol shock, all sludges were not able to recover their activity completely. The EF treated intact granules showed a recovery of 55% and 45%, after shock at 50 and 100 mg phenol  $\text{L}^{-1}$ , respectively. The suspended sludge showed only negligible recovery after phenol inhibition, indicating granules are more resistant to toxic compounds than suspended sludge. In addition, it is suggested that EF treatment is effective to reactivate nitrifying activity after unfavourable condition shock.

Overall, this study has demonstrated the rapid formation of partial nitrifying granules, which is promising for industrial application to shorten the reactor start-up period. The rapidly formed partial nitrifying granules also can maintain long-term stable operation, indicating its prospect to replace conventional partial nitrification by suspended sludge for side stream treatment. The mineral accumulation in partial nitrifying granules due to high water hardness level, however, needs further investigation to minimize its negative effects on the microbial activity although precipitation of CaP is favourable for phosphorus removal from side stream by partial nitrifying granules.

## LIST OF CONTENTS

ABSTRACT .....	iii
LIST OF CONTENTS .....	v
LIST OF TABLES .....	vii
LIST OF FIGURES .....	ix
ABBREVIATIONS .....	xiii
DECLARATION OF AUTHORSHIP .....	xvii
ACKNOWLEDGEMENTS .....	xviii
Chapter 1 .....	1
LITERATURE REVIEW AND RESEARCH OBJECTIVES .....	1
1.1. Literature review .....	3
1.2. Research objectives .....	26
Chapter 2 .....	29
FAST START-UP OF PARTIAL NITRIFYING GRANULES REACTOR AND ITS LONG-TERM STABLE OPERATION AT HIGH CALCIUM CONCENTRATION .....	29
2.1. Introduction .....	31
2.2. Materials and methods .....	33
2.3. Results .....	37
2.4. Discussion .....	49
2.5. Conclusions .....	54
2.6. Experimental weaknesses .....	54
Chapter 3 .....	57
PHYSICAL, CHEMICAL AND BIOLOGICAL CHARACTERISTICS OF PARTIAL NITRIFYING GRANULES TREATING MIDDLE STRENGTH AMMONIUM WASTEWATER WITH HIGH WATER HARDNESS LEVEL .....	57
3.1. Introduction .....	59
3.2. Materials and methods .....	61
3.3. Results .....	66

3.4. Discussion.....	86
3.5. Conclusions.....	89
3.6. Experimental weaknesses .....	90
3.7. Appendix.....	91
Chapter 4 .....	99
STUDY ON EPS EXTRACTION FROM SLUDGE WITH HIGH MINERAL CONTENT AND RELEVANT ACTORS FOR RELIABLE PROTEIN MEASUREMENTS.....	99
4.1. Introduction.....	101
4.2. Materials and methods .....	102
4.3. Results.....	105
4.4. Discussion.....	112
4.5. Conclusions.....	114
4.6. Experimental weaknesses .....	114
Chapter 5 .....	115
REACTIVATING AMMONIUM REMOVAL ACTIVITY OF NITRIFYING BIOMASS AFTER INHIBITION USING EXTERNAL ELECTROSTATIC FIELD .....	115
5.1. Introduction.....	117
5.2. Materials and methods .....	119
5.3. Results.....	122
5.4. Discussion.....	127
5.5. Conclusions.....	130
5.6. Experimental weaknesses .....	130
Chapter 6 .....	131
OVERALL DISCUSSION, CONCLUSIONS AND RECOMMENDATIONS FOR FUTURE WORK.....	131
6.1. Overall discussion .....	133
6.2. Overall conclusions .....	137
6.3. Recommendations for future work .....	138
List of references .....	141

## LIST OF TABLES

Table 1.1 - Costs of N removing or recovering by some of the mentioned technologies and comparison with the main biological nitrogen removal processes (Philips et al. 2011. IWA/WEF Nutrient Removal and Recovery, Miami). .....	5
Table 1.2 - Process requirements for some of the main biological technologies used in WWTPs (Ahn, 2006, Van Hulle et al., 2010, Mulder, 2003, Lackner et al., 2014) .....	24
Table 1.3 - Estimation of running energy demand for digester supernatant treatment, N content in the supernatant assumed to be 2.3 g NH <sub>4</sub> -N L <sup>-1</sup> ; source:(Magrí et al., 2013). .....	25
Table 2.1 – Operational conditions of experiment. ....	34
Table 2.2 - Ammonia removal performances and nitrite accumulation before and after biomass instability during phase 3 and after stable conditions were achieved during phase 4. ....	43
Table 2.3 - ICP-MS analysis. Preliminary results on the concentration of main elements within R3 and R4 granules ash on day 107, at the end of phase 3. ....	43
Table 2.4 – Saturation index results .....	44
Table 3.1 – Saturation index calculation parameters .....	63
Table 3.2 - Excitation and emission ranges detected with EEM for EPS analysis (Chen et al., 2003b, Wang and Zhang, 2010, Wang et al., 2014a). ....	65
Table 3.3 – Density, ash content and ICP-MS results of main elements concentrations within different size granules .....	69
Table 4.1 –EPS extraction sample with different dilutions and relative PN amount measured by Lowry’s method. ....	105
Table 4.2 – Proteins calibration curves with and without calcium addition. ....	109
Table 4.3 – Comparison between calibration curves after different incubation times. ....	110





## LIST OF FIGURES

Figure 1.1 - Oxygen and COD requirements for traditional nitrification/denitrification. ....	23
Figure 1.2 – a) Oxygen and COD requirements for PN/ANAMMOX and b) comparison of sludge production between traditional nitrification/denitrification and PN/ANAMMOX (Fux et al., 2002).....	24
Figure 2.1– SBR configuration of reactors used in the experiment. ....	33
Figure 2.2 - a) profiles of SVI <sub>5</sub> , b) MLVSS, c) sludge volume percentages with size smaller than 200 µm and d) sludge mean size over time during phase 1 in R3 (18-23 °C) and R4 (30-33 °C) with 200 mg NH <sub>4</sub> <sup>+</sup> -N L <sup>-1</sup> of influent N and COD/N of 5. ....	37
Figure 2.3 - a) profiles of SVI <sub>5</sub> , b) MLVSS, c) sludge volume percentages with size smaller than 200 µm and d) sludge mean size over time during phase 1 in R2 (COD/N at 20 and 50 mg NH <sub>4</sub> <sup>+</sup> -N L <sup>-1</sup> ) and R4 (COD/N at 5 and 200 mg NH <sub>4</sub> <sup>+</sup> -N L <sup>-1</sup> ) at operational temperature of 30-33 °C.....	38
Figure 2.4 - Profiles of nitrogen species and COD over the time during phase 2 in a) R1 and R2 and b) R3 and R4.....	39
Figure 2.5 - Profiles of nitrogen species over the time during phases 2-4 with COD reduced quickly to 0 and NH <sub>4</sub> <sup>+</sup> -N increased to certain values in a) R1 and R2 and b) R3 and R4.....	41
Figure 2.6 – Concentrations of a) free ammonia (FA) and b) free nitrous acid (FNA) over the operation time with the increased influent NH <sub>4</sub> <sup>+</sup> -N concentration. ....	41
Figure 2.7 – a) ash content, b) SVI <sub>5</sub> and c) MLSS-MLVSS along the whole experiment in the four reactors; in the first plot the three distinct stages, from left to right, of ash generation are shown (slight, high and negligible ash increase rate, respectively).....	42
Figure 2.8 – EDX analysis; preliminary elemental composition of the a) external and b) internal surfaces of R3 granules and c) external and d) internal surfaces of R4 granule during phase 4 (day 126). ....	45
Figure 2.9 - XRD analysis; the inorganic solid phases present within granules ash from R3 and R4 (day 121). ....	46
Figure 2.10 - SEM microscopy of R4 granules on day 113. a) External and b) internal surface of half cut granule, c) detail of a spherical structure on the granule external surface, c.1) crystal agglomeration on top of spherical structure, d) detail of external surface around the spherical structure on granule, e) details of bacillus and coccoid bacteria surrounded by an unknown clear material (arrow) and f) other bacteria embedded in EPS (white arrows). ....	47
Figure 2.11 - Stereomicroscopy images; granular biomass from a) R1, b) R2, c) R3 and d) R4, during stable operation on day 142. Black and white arrows represent a granule fragment and a normal entire granule, respectively. Bar = 1000 µm. ....	48
Figure 3.1 – Specific oxygen utilization rate (SOUR) of granules with different size ranges (y: yellow, b: brown). ....	66
Figure 3.2 – a) sAOR, PO <sub>4</sub> <sup>3-</sup> and Ca <sup>2+</sup> removal and Na <sup>+</sup> production in different sizes granules during batch tests; b)c) examples of batch test results from <600 µm.....	67
Figure 3.3 - Stereomicroscopy images of different sizes granules. a)b) 150-250(y) µm, c)d) 150-250(b) µm, e)f) 600-710 µm, g)h) 1400-2000 µm and i)j) >2800 µm granules. Blue, white, red, grey, green, orange and yellow	

arrows are flocs, mature granules, cauliflower-like particle, young granules, crystals, buds and cracks respectively. Bar = 1000 $\mu\text{m}$ . .....	71
Figure 3.4 - XRD results of different sizes granules; a) 150-250(y) $\mu\text{m}$ , b) 150-250(b) $\mu\text{m}$ , c) 300-425 $\mu\text{m}$ and d) 500-600 $\mu\text{m}$ . .....	72
Figure 3.5 – XRD results of different sizes granules; a) 710-1180 $\mu\text{m}$ , b) 1400-2000 $\mu\text{m}$ and c) >2800 $\mu\text{m}$ . .....	73
Figure 3.6 – Hypothetical description of granule’s surface (left) and internal layers (right) from SEM and SEM-EDX results; the different structures found within samples are illustrated just for convenience and to make the following pictures clearer. ....	74
Figure 3.7 – SEM morphology of 150-250(y) $\mu\text{m}$ granules; a) crystal-like particle overview and b) its surface, c) granule fragment overview and d) its surface. ....	75
Figure 3.8 – SEM morphology of 150-250(b) $\mu\text{m}$ granules; a) granule overview, a.1) granule with stereomicroscopy for comparison, b) crystal structure, c) plate-like spherical aggregate and d) crystal bar. ....	75
Figure 3.9 – SEM morphology of 300-425 $\mu\text{m}$ granules; a) granule overview, b) bud overview, c) left and d) right portion of the bud. ....	76
Figure 3.10 – SEM morphology of 500-600 $\mu\text{m}$ granules; a) group of granules, b) mature granule overview and c) crystal structure on its surface, d) young granule overview and e)f) its right portion and g) left portion. White and black arrows indicate the inorganic layer and clumps, respectively, formed on top of bacteria cells. ....	77
Figure 3.11 – SEM morphology of 710-1180 $\mu\text{m}$ granules; a) granule overview, b)c) bacteria and globular structures in a crack, d) bud and e) its surface, f) crystal structure at the bud base covered with EPS. ....	78
Figure 3.12 – SEM morphology of 1400-2000 $\mu\text{m}$ granules; a) entire granule overview, b) halved granule overview, c) external layer of the granule half, d) middle layer of the granule half and e)f) core of the granule half. f.1) shows a zoomed in of the inorganic crystal bar present in the granule half core. ....	79
Figure 3.13 – SEM morphology of >2800 $\mu\text{m}$ granules; a) granule overview, b) a white globule and c) bacilli on the granule surface, d) halved granule overview and e) crystal bars in its core.....	80
Figure 3.14 – EPS content from different sizes granules of a) proteins and b) polysaccharides. Extraction with formaldehyde/NaOH method; Lowry’s and Dubois’s procedures used for PNs and PSs determination, respectively. LB=loosely bound-EPS, TB=tightly bound-EPS. ....	81
Figure 3.15 – EEM results from a) LB-EPS and b) TB-EPS in <600 $\mu\text{m}$ , c) LB-EPS and d) TB-EPS in 710-1180 $\mu\text{m}$ , e) LB-EPS and f) TB-EPS in 1400-2000 $\mu\text{m}$ , g) LB-EPS and h) TB-EPS in > 2800 $\mu\text{m}$ . Except for TB in <600 $\mu\text{m}$ , which was diluted 16 times before analysis, all TB samples were diluted 64 times. The different regions encountered are described in Table 3.2. ....	83
Figure 3.16 – SEM-EDX spectroscopy results of the elements weight percentage of external and internal granule surface in a) 150-250(y) $\mu\text{m}$ , b) 150-250(b) $\mu\text{m}$ , c) 300-425 $\mu\text{m}$ ; d) 500-600 $\mu\text{m}$ , e) 710-1180 $\mu\text{m}$ , f) 1400-2000 $\mu\text{m}$ and g/h) >2800 $\mu\text{m}$ granules. For reference of the analysed granule portions see Figure 3.6. ....	85
Figure 3.17 – Ammonium, nitrite and nitrate concentrations along with pH during batch test of a) <600 $\mu\text{m}$ , b) 710-1180 $\mu\text{m}$ , c) 2000-2400 $\mu\text{m}$ and d) >2800 $\mu\text{m}$ granules.....	3.92
Figure 3.18 – $\text{Ca}^{2+}$ and $\text{PO}_4^{3-}$ concentrations during batch test of a) <600 $\mu\text{m}$ , b) 710-1180 $\mu\text{m}$ , c) 2000-2400 $\mu\text{m}$ and d) >2800 $\mu\text{m}$ granules. ....	3.93
Figure 3.19 – Mixture of different sizes granules before characterisation study. The arrow indicates a bud. ....	94

Figure 3.20 - Mixture of different sizes granules before characterisation study. The arrow indicates a bud. ....	95
Figure 3.21 - Mixture of different sizes granules before characterisation study. The arrow indicates a bud. ....	96
Figure 3.22 - Mixture of different sizes granules before characterisation study. The arrow indicates a bud. ....	97
Figure 3.23 – Mixture of different sizes granules before characterisation study. ....	98
Figure 4.1 – Extended calibration curve for proteins detection by Lowry’s method. ....	105
Figure 4.2 – Profile of EPS extracted with heat procedure; proteins and polysaccharides amount with and without dialysis in a) LB and b) TB-EPS of granules. EEM spectra from granules in c) LB and d) TB-EPS. Proteins and polysaccharides amount with and without dialysis in e) LB and f) TB-EPS of sludge. EEM spectra from sludge in g) LB and h) TB-EPS. ....	107
Figure 4.3 - Precipitates cloud observed during Lowry method incubation of a) blank (without and with $\text{Ca}^{2+}$ ) and b) last point (without and with $\text{Ca}^{2+}$ ) of BSA calibration curve. ....	108
Figure 4.4 – Proteins calibration curves done a) without and b) with $120 \text{ mg Ca}^{2+} \text{ L}^{-1}$ addition, c) correlation between added $\text{Ca}^{2+}$ concentration and absorbance after 1 h incubation. ....	109
Figure 4.5 – Spectrophotometric results of calibration curve a) without $\text{Ca}^{2+}$ addition (1 hour incubation) and b) with addition of $\text{Ca}^{2+}$ (3 hours incubation). ....	110
Figure 4.6 – Profile of EPS extracted with formaldehyde/NaOH procedure; proteins and polysaccharides amount with and without dialysis in a) LB and b) TB-EPS of granules. EEM spectra from granules in c) LB and d) TB-EPS. Proteins and polysaccharides amount with and without dialysis in e) LB and f) TB-EPS of sludge. EEM spectra from sludge in g) LB and h) TB-EPS. ....	111
Figure 5.1 – Electric field setup showing power supplier and the samples containing beaker. ....	120
Figure 5.2 – Sludge morphology and granulation process showed by stereomicroscopy; bar = $1000 \mu\text{m}$ . ....	122
Figure 5.3 – Pre-trials to measure the most suitable duration and intensity for the electric field treatment. a) sAOR after different treatment durations (at $2 \text{ Vcm}^{-1}$ ), b) the percentage increase/decrease of activity at the investigated duration compared to control, c) sAOR at different electric field intensities and durations and d) the percentage increase/decrease of activity at the investigated intensities and durations compared to control. ....	123
Figure 5.4 – Ammonium, nitrite and nitrate concentrations change during salinity batch test of a) the control, b) G4% after inhibition and c) G4% after electric field treatment. ....	124
Figure 5.5 – Activity test after salt inhibition and electric field treatment. a) sAOR and b) the percentage of activity increase/decrease compared to control after salt inhibition. c) sAOR and d) the percentage of activity enhancement compared to control after electric field treatment. ....	125
Figure 5.6 - Activity test after phenol inhibition and electric field treatment; a) sAOR and b) the percentage of activity decrease compared to control after phenol inhibition. c) sAOR and d) the percentage of activity enhancement compared to control after electric field treatment. ....	126



## ABBREVIATIONS

AC	Activated carbon particles
ALE	Alginate-like exopolysaccharides
AMO	Ammonia monooxygenase
ANAMMOX	Anaerobic ammonia oxidation
AOB	Ammonium oxidising bacteria
AOR	Ammonia oxidising rate
ARP	Ammonia recovery process
AS	Activated sludge
ATP	Adenosine tri-phosphate
C	Carbon
CaCO <sub>3</sub>	Calcium carbonate
CAL	Calcite
CANON	Completely autotrophic nitrogen removal over nitrite
CaPO <sub>3</sub>	Calcium phosphate
CO <sub>3</sub> <sup>2-</sup>	Carbonate
COD	Chemical oxygen demand
CO <sub>2</sub>	Carbon dioxide
CaP	Calcium phosphate
DEAMOX	Denitrifying ammonium oxidation
DO	Dissolved oxygen
DNA	Deoxyribonucleic acid
EBPR	Enhanced biological phosphorous removal
EDX	Energy dispersive X-ray spectroscopy
EDTA	Ethylenediaminetetraacetic acid
EEM	Excitation and emission matrix
EF	Electric field
EPS	Extracellular polymeric substance
ER	Exchange ratio
F/NaOH	Formaldehyde/Sodium hydroxide extraction
FA	Free ammonia (NH <sub>3</sub> )

FNA	Free nitrous acid (HNO <sub>2</sub> )
GAO	Glycogen accumulating organisms
GHG	Greenhouse gas
HA	Humic acid
HAO	Hydroxylamine oxidoreductase
HAP	Hydroxyapatite
HRT	Hydraulic retention time
HSP	Heat shock proteins
ICP-MS	Inductively coupled plasma emission spectrometer with mass spectroscopy
LB	Loosely bound EPS
MIP	Microorganisms-induced precipitation
MLSS	Mixed liquor suspended solids
MLVSS	Mixed liquor volatile suspended solids
N	Nitrogen
N/DN	Traditional nitrification/denitrification
N <sub>2</sub>	Di-nitrogen gas
N <sub>2</sub> O	Nitrous oxide
NADH	Nicotinamide adenine dinucleotide
NaHCO <sub>3</sub>	Sodium bicarbonate
NaOH	Sodium hydroxide
NAR	Nitrite accumulation rate
NH <sub>3</sub>	Ammonia or free ammonia
NH <sub>4</sub> <sup>+</sup>	Ammonium
NLR	Nitrogen loading rate
NO	Nitric oxide
NOB	Nitrite oxidising bacteria
NOR	nitrite oxidoreductase
NO <sub>2</sub> <sup>-</sup>	Nitrite
NO <sub>3</sub> <sup>-</sup>	Nitrate
NPR	Nitrite production rate
OLAND	Oxygen-limited autotrophic nitrification denitrification
OLR	Organic loading rate

PAO	Phosphate accumulating organisms
PBS	Phosphate buffer saline solution
pCO <sub>2</sub>	Carbon dioxide pressure
PIPES	piperazine-N,N' -bis(2-ethanesulfonic acid)
PN	Partial nitrification
PNs	Proteins
PN/A	Partial nitrification/ANAMMOX (two stages)
PS	Polysaccharides
PSA	Particle size analyser
PSB or PSF	Phosphate-solubilizing bacteria or fungi
rRNA	Ribosomal ribonucleic acid
sAOR	Specific ammonia oxidising rate
SBR	Sequencing batch reactor
SEM	Scanning electron microscopy
SI	Saturation index
SNA	Simultaneous partial nitrification/ANAMMOX (one stage)
sNOR	Specific nitrite oxidation rate
SRT	Sludge retention time
SVI <sub>5</sub> or SVI <sub>30</sub>	Sludge volume index after 5 or 30 minutes settling
TB	Tightly bound EPS
VFA	volatile fatty acids
WWTW	Wastewater treatment works (or Wastewater treatment plant, WWTP)
XRD	X-ray diffraction





## DECLARATION OF AUTHORSHIP

I, Simone Cinquepalmi

declare that this thesis and the work presented in it are my own and has been generated by me as the result of my own original research.

Development of granules-based technology for partial nitrification .....

I confirm that:

This work was done wholly or mainly while in candidature for a research degree at this University;

Where any part of this thesis has previously been submitted for a degree or any other qualification at this University or any other institution, this has been clearly stated;

Where I have consulted the published work of others, this is always clearly attributed;

Where I have quoted from the work of others, the source is always given. With the exception of such quotations, this thesis is entirely my own work;

I have acknowledged all main sources of help;

Where the thesis is based on work done by myself jointly with others, I have made clear exactly what was done by others and what I have contributed myself;

None of this work has been published before;

Signed: .....

Date: 2020 May 13<sup>th</sup>

## ACKNOWLEDGEMENTS

I would like to express my special appreciation and thanks to the supervisor Dr. Yongqiang Liu, the co-supervisor Prof. Sonia Heaven and the internal examiner Prof. Charles Banks for serving as my committee members even at hardship.

Thanks to Pilar and Dominic, with their precious help and their endless knowledge in the laboratory.

Grazie alla mia famiglia, alla quale questa tesi dedico, che anche se lontana, é stata sempre tanto vicina, per lungo tempo.

Un gracias a mi amigo, Santi, sin ti nunca esa tesis se habría acabado. Thanks to all class 2013-2017 friends from the lab, I will always remember you as very smart and wise, but also very open minded and cool people.

Un pensiero a te, Zio.

Un abrazo, Abuelo.

E, dulcis in fundo, un grazie infinito a Te, essenziale, instancabile compagna di vita (con e senza Ignazio).

**LITERATURE REVIEW AND RESEARCH OBJECTIVES**



## **1.1. Literature review**

### **1.1.1. Nitrogen and the environment**

#### ***1.1.1.1. N-producing human activities***

In the last century, the nitrogen (N) input in the environment has been disturbed by human activities; among them can be mentioned the Haber-Bosch process (synthetic fertilizers production), fossil fuels combustion, petroleum refining, ceramics and cement works, mining, textile and food processing (Cowling et al., 2001, EPA, 2003). The consequent use of water during these activities (e.g. for cleaning the machineries or for the gaseous waste streams scrubbing) has produced a great amount of high N-concentrated wastewaters. In addition, N from landfills leachates created by the urban activity in discharging municipal solid waste, the further increase of nitrogen-fixing legumes plantations and the application of soil N-fertilisers have all generated an expanded volume of N-rich wastewaters. Most of these waste streams arrive to the wastewater treatment works (WWTW), where together to the streams coming from residences (domestic/municipal) and institutions are treated before being released again in the environment (e.g. rivers, sea, lakes).

#### ***1.1.1.2. Environment and health***

The main problems caused by uncontrolled nitrogen release in the ecosystem are to be related to the forms  $\text{NH}_4^+$  (ammonium),  $\text{NO}_2^-$  (nitrite) and  $\text{NO}_3^-$  (nitrate), which represent a fundamental source of nutrients for both plants and algae; the presence of high concentrations of these nutrients in water bodies produces overgrowth of photosynthetic organisms, an example of which are the so called algal blooms (WHO, 2000). After a life cycle, death of both plants and algae generates the fast growth of bacteria; they remove the organic matter by depleting dissolved oxygen present in the aquatic environment, generating obvious harsh conditions for aerobic living beings. The high amount of dead plants also shields the sun light from deeper layers and generates unpleasant odours and colours within the water; an increase of acidity after the production of toxic sulphide ( $\text{H}_2\text{S}$ ) can also be a consequence of this dramatic situation. The whole process is generally called eutrophication and it has been recognized as a pollution problem in European, North American and Asian lakes and reservoirs since the mid-20<sup>th</sup> century (Rodhe, 1969). Normally, it affects water bodies characterised by a low turnover (coastal areas, lagoons, lakes, etc.) and, although sometimes it happens naturally, it mostly takes place because the ecosystem is not able to assimilate or recycle the great amount of nitrogen released by the human activities (EPA, 2003).

Uncontrolled nitrate and nitrite release also threatens human health, the two nitrogen species may cause the development of methemoglobinemia (infantile cyanosis) and carcinogenesis;  $\text{NO}_3^-$  is reduced to  $\text{NO}_2^-$  in the digestive system and once it gets in contact with the haemoglobin present in the blood, it interferes with the oxygen mechanism of transport. Sometimes the affected children are also described as blue babies, due to the suffocation accompanied by the change of skin colour to blue (Comly, 1945, Metcalf and Eddy, 2003). Studies reported cases of methemoglobinemia when values of nitrate in water were higher than  $10 \text{ mg L}^{-1}$ ; for this reason, the standard values of nitrates in drinking water should not exceed this concentration (EPA, 2003). Several investigations also reported cases of gastric cancer diagnosed in patients that have ingested high amounts of nitrates. They would be reduced to nitrites and react with amines and amides in the stomach, forming nitrosamines and nitrosamides; then, they would finally reach the colon and contribute to the induction of colon tumours (Lijinsky, 1977).

Nitrous oxide ( $\text{N}_2\text{O}$ ) is generally produced during fuel combustion and specific biological processes for ammonia removal from wastewater (Kampschreur et al., 2009); it is considered a very dangerous greenhouse gas (GHG)

and it has a global warming effect 350 times that of CO<sub>2</sub> (Van Hulle et al., 2010). Moreover, when N<sub>2</sub>O reacts with oxygen in the atmosphere, it gives rise to nitric oxide (NO), another notorious GHG.

Even if ammonium (NH<sub>4</sub><sup>+</sup>) is normally considered an important nutrient for life, it can eventually become toxic to fish; when pH rises above 8-9, most of it will be present in the un-ionised form (NH<sub>3</sub>), which may be lethal for fish at concentrations within the range 0.1-10 mg L<sup>-1</sup> (EPA, 2003). Moreover, as active chemical species, its uncontrolled release in the environment is considered a serious problem because it is oxidized by oxygen to different nitrogen forms, finally producing nitric acid, which generates soil acidification during precipitations.

### 1.1.2. Physicochemical N-removal processes

Therefore, even though nitrogen compounds are necessary nutrients for life, when the normal equilibrium of the different species is destabilised the results are severe issues for the surrounding environment. The current European legislation provides the discharging requirements of total N in urban wastewater treatment plants as low as 15 mg L<sup>-1</sup> and 10 mg L<sup>-1</sup> for person equivalent of 10000-100000 and higher than 100000, respectively (*Directive 91/271/EEC*). N can be removed from wastewaters by a variety of physicochemical and biological processes. For a specific application the available alternatives will be evaluated on cost aspects, chemical and energy requirements, operational experience and process reliability. The technology chosen to treat a specific wastewater stream depends on factors such as nitrogen and carbon concentrations, cost-effectiveness of the process, effluent requirements, stream temperature and pH level, presence of toxins or biological metabolism inhibiting compounds. However in practice the selection of either a biological or a physicochemical process is determined based on the N concentration of the wastewater and on the treatment cost-effectiveness (Mulder, 2003). When either N concentration is too low or higher than 5 g N L<sup>-1</sup> or C/N ratio is not favourable or the temperature is too low, or biological inhibitors or toxins reach too high concentrations, the physical-chemical methods are technically and economically more feasible (Metcalf and Eddy, 2003). Among them the main processes actually applied in WWTW are:

- *Ion-exchange*, NH<sub>4</sub><sup>+</sup> contained in the wastewater is adsorbed on a zeolite structure, basically replacing the positive ions (e.g. Na<sup>+</sup>, K<sup>+</sup>, Ca<sup>2+</sup>, Mg<sup>2+</sup>). Widely employed adsorbents, or exchangers, are clinoptilolite, analcime or chabazite (Hedström, 2001) and also the Ammonia Recovery Process (ARP) by chemisorption and vacuum can be mentioned (Fassbender, 2001).
- *Air stripping*, the wastewater is percolated from the top of a column reactor packed with inert material, an upward air-flow is pumped from the bottom and goes through the bed stripping the volatile NH<sub>3</sub> (Laureni et al., 2013).
- *Concentration by membrane filtration*, based on size exclusion (ultrafiltration and nanofiltration), or on a diffusive mechanism in which pressure is applied and water is forced to flow through a semi-permeable membrane in the opposite direction of the natural osmotic flow (reverse osmosis) (Masse et al., 2007).
- *Concentration by vacuum evaporation*, the wastewater is simply concentrated by water evaporation under vacuum condition.

- *Breakpoint chlorination*,  $\text{NH}_3$  in wastewater goes through a complete oxidation to gaseous N by reacting with chlorine ( $\text{Cl}_2$ ) (Pressley et al., 1972).
- *Struvite precipitation*, addition of  $\text{Mg}^{2+}$  and  $\text{PO}_4^{3-}$  that react with  $\text{NH}_4^+$  ion and produce struvite precipitates (Shin and Lee, 1998).

The listed technologies are effective in nitrogen removal and all of them, except for breakpoint chlorination, can recover nitrogen as a fertiliser or other valuable industrial by-products. Nevertheless, all these processes also share a common great amount of used chemicals and high costs of maintenance (Table 1.1); moreover, most of the concentrations of nitrogen in wastewaters treated in WWTWs are normally lower than  $2 \text{ g N L}^{-1}$  (EPA, 1993, Mulder, 2003). Therefore, recovery of nitrogen by chemical or physical technologies, at this moment, does not appear economically feasible; on the other hand, the biological processes still look like the most cost-effective and environmental friendly technology for wastewater treatment.

Table 1.1 - Costs of N removing or recovering by some of the mentioned technologies and comparison with the main biological nitrogen removal processes (Philips et al. 2011. IWA/WEF Nutrient Removal and Recovery, Miami).

Process	Cost (US\$ Kg $\text{N}^{-1}$ removed or recover)	Ammonia recovery
Air Stripping	2.40	Yes
Ion exchange (Clinoliptolite)	2.80	Yes
ARP: chemisorption + vacuum	6.72	Yes
Nitrification/Denitrification	1.80	No
Nitritation/Denitritation	0.90	No
Partial Nitrification/ANAMMOX	0.15	No

### 1.1.3. Biological N-removal processes

Traditionally, the process used for many years in WWTWs, and yet the preferred one for municipal streams, has been coupling the nitrification and the denitrification pathways to obtain an effluent within the limits of legislation; in this process the  $\text{NH}_4^+$  is oxidised to  $\text{NO}_3^-$  and then reduced to  $\text{N}_2$ . Recently, after more stringent limitations, the treatment plants started changing this trend to a more cost-effective process that aims to produce only  $\text{NO}_2^-$  (partial nitrification or nitritation), ceasing the reaction that otherwise would proceed to nitrate formation; nitrite would still be reduced to  $\text{N}_2$  gas by the following denitrification (denitritation). The resulting process is described as nitrification/denitrification over nitrite or partial nitrification/denitritation or nitritation/denitritation. Further reduction of operational costs can be obtained by the application of *ANAerobic*

*AMMonium OXidation* (ANAMMOX) after nitrification. The partial nitrification-ANAMMOX system, compared to the conventional nitrification-denitrification over nitrate, actually saves up to 63% of the costs of aeration and up to 100% of the costs for external carbon addition. Moreover, in the innovative system the carbon dioxide (CO<sub>2</sub>) and the sludge production are greatly minimised (Volcke et al., 2010, Agrawal et al., 2018). The partial nitrification-ANAMMOX can be either obtained in two different reactors (two-stage configuration) or in one single reactor (one-stage configuration) also called in some studies CANON or OLAND or DEAMOX.

Important biological-based technologies for nitrogen removal worth mentioning are also the phototrophic systems and the microbial electrochemical cell. The phototrophic systems take advantage of the energy from sunlight to remove COD and N from wastewater; two organisms are at the moment considered for streams treatment applications, the phototrophic purple bacteria (Hülsemann et al., 2014, Hülsemann, 2014, Hülsemann, 2016) and the microalgae (single-celled algae and cyanobacteria) (Gonçalves, 2017). In the electrochemical cells the oxidation and reduction reactions are separated by a membrane; the pH on the cathode side increases, generating the deprotonation of the ammonium to ammonia, which can easily be separated (Kuntke, 2018). Although there are some examples of application at full scale, both technologies are at the moment unable to achieve the discharge limits; this also explains why they are mainly used for tertiary treatment, otherwise an additional treatment step would be needed (Winkler, 2019).

Now, before the systems just cited are described with more details, comparing advantages and disadvantages for each of them, an introductory paragraph about activated and granular sludge application in wastewater treatment and importance of extracellular polymeric substance (EPS) will be described.

#### **1.1.4. Granular sludge technology**

##### ***1.1.4.1. Activated VS granular sludge***

Activated sludge is a very well-known and largely used process for wastewater treatment; so far, this technology has been used for more than a century and the principle behind it is basically the degradation of biodegradable organics by a wide range of different and specialised microorganisms that float suspended in the waste stream. This simple and effective technology, anyhow, has few drawbacks that can be listed as: (a) large space needed for separation of biomass from treated water; (b) high sensitivity of microbial community to high organic loads or toxic chemicals; and, even if lower than chemical and physical processes, (c) high costs of operation.

About twenty years ago, a new technology able to overcome those drawbacks was described for the first time, the granular sludge (Morgenroth et al., 1997, Dangcong, 1999, Tay et al., 2001a, Beun et al., 2002). Granules are compact, quasi-rounded aggregates of biomass and are considered a special case of biofilm growth, since they are not using any external carrier (e.g. in moving bed biofilm systems and fluidized bed or airlift reactors); they form by a fascinating, as well as not fully understood, self-immobilization process. Within the granular sludge several microbial communities create a strong interaction between each other, exchanging information and bio-products, all embedded in a sticky matrix of extracellular polymeric substance (EPS). Laboratory results have indicated several advantages of aerobic granular sludge over the counterpart aerobic suspended sludge, and they can be listed as follows:

- a) Good settling properties, shown by lower SVI<sub>30</sub> (<50 mL g<sup>-1</sup>) than conventional activated sludge (80 and 120 mL g<sup>-1</sup>). The particles settle 10 times faster (Xiao et al., 2008, Ni et al., 2009) and show settling velocity that can reach 50-90 m h<sup>-1</sup> (Gonzalez-Gil and Holliger, 2014), depending on the size and density. This means that treatment and clarification can be done in the same reactor, avoiding further



space and costs of operation for a large secondary clarifier tank to hold the wastewater to separate the suspended sludge.

- b) High biomass retention, which improves the volumetric conversion capacity and the possibility to treat waste streams at a relatively larger loading rate (Maszenan et al., 2011). This is also beneficial to cultivate slow growing bacteria, i.e. nitrifying and ANAMMOX bacteria (Gonzalez-Gil and Holliger, 2014), which reduces sludge bulking (Moy et al., 2002). Compared to flocculent sludge, granules can accommodate five times more biomass concentration (De Kreuk et al., 2005), which consequently allows the treatment works to use less land than conventional sludge based plants.
- c) Contains different environments, where both aerobic and anaerobic zones can be distinguished due to the oxygen and nutrients gradients along the radial direction (Liu et al., 2010a, Winkler et al., 2013b); this allows different biological processes to be simultaneously performed, i.e. nitrifying and denitrifying bacteria, phosphate accumulating organisms (PAO) and glycogen accumulating organisms (GAO), (Beun et al., 1999, De Kreuk et al., 2005, Qin and Liu, 2006) or partial nitrification and ANAMMOX (Vlaeminck et al., 2008, Shi et al., 2010). At the same time, costs of operation are reduced also because a higher surface area per volume of biomass can be achieved and there are no reactor configuration or support morphology constrains compared to conventional biofilm technology (de Kreuk and van Loosdrecht, 2004).
- d) High tolerance to shock loading or toxins and biological inhibiting chemicals, due to the increased mass transfer towards the internal layers and the high biomass concentration (Beun et al., 2000, Liu and Tay, 2004).

The application of granular sludge technology avoids using multiple tanks and recirculation piping and pumps, hence reducing the footprint and the operational costs of the wastewater treatment. This reduces the land needed compared to the aerobic sludge based plant by 75% and the energy consumption by 30%. This is also possible due to the high costs of sludge dewatering and transportation steps that would be drastically reduced with granules. Compared to activated sludge based processes, the operation costs for using aerobic granules could be reduced by 25% (Sarma and Tay, 2018a, Franca et al., 2018).

#### ***1.1.4.2. Granulation and factors influencing the process***

The importance of this technology is well described by the previous paragraph; in addition, further knowledge about long-term stability and internal biological interactions of granular sludge justify the need of a better understanding of the mechanism behind the particles formation and structural stability. The formation of aerobic granules is a gradual process in which the suspended activated sludge turns into granular sludge due to environmental stress conditions (Liu and Tay, 2002). Because a common rule to describe the exact moment in which the granule forms is hard to find in literature, three main rules are considered in this thesis to define when granular sludge is established: (a) values of  $SVI_5$  and  $SVI_{30}$  lower than  $80 \text{ mL g}^{-1}$  and  $<10\%$  difference between them; (b) 50% or more of biomass within the reactor represented by particle size greater than  $200 \mu\text{m}$ , since flocs size ranges normally between  $50$  and  $300 \mu\text{m}$ ; (c) well defined and clear particles outline, visible by microscope or naked eye (Dangcong et al., 1999, de Kreuk et al., 2007a, Liu and Tay, 2007, Liu et al., 2010b).

From the first time aerobic granular sludge was described, most research on the development of aerobic granular sludge or aerobic granulation process has been conducted using sequencing batch reactors (SBR) (Strous et al., 1998, Dapena-Mora et al., 2004, Liu and Tay, 2004, Rusalleda et al., 2008, López et al., 2008, Gao et al.,

2011a). The system works in cycles that can be 3 to 6 hours long; each cycle is defined by four phases: waste stream filling, reaction (aeration/stirring), settling time and discharging. Since most of the studies about aerobic granules have used the SBR system, it can be affirmed that this kind of configuration represents an important factor for aerobic granulation. Among the operational factors considered to influence granulation process, settling time, hydraulic retention time (HRT), hydraulic stress, loading rate, periodic starvation time and height to diameter (H/D) ratio are the most important.

The settling time acts as a hydraulic selection pressure on the sludge unable to settle lower than the discharging point, while the best settling particles will be retained in the reactor and begin the granulation process. Short settling times (i.e. 5 minutes) could generate large well settling aerobic granules in a SBR system, whereas a mixture of suspended biomass and not well settling granules were obtained when settling times longer than 15 minutes were used (Qin et al., 2004a, Qin et al., 2004b). The long settling time allowed not well settling flocculent sludge to be retained in the reactor; it has been reported that flocs show a higher bacteria activity compared to granular sludge due to higher mass transfer limitation for nutrients and oxygen in the latter (Li and Liu, 2005, Liu et al., 2005b). For this reason, the forming granules could be outcompeted by the flocs and granulation could fail. In addition, it was also described that short settling times could select cells with a higher surface hydrophobicity that enhanced the EPS content in the sludge (Gao et al., 2011b), hence, increasing the possibilities for cell-to-cell contact and formation of granules.

A factor influencing granules development is represented by the exchange ratio (ER); it is described as the liquid volume discharged at the end of the cycle over the total reactor working volume. There is some evidence that at higher ER a good granulation performance could be achieved; different ER have been tested and a high fraction of the biomass represented by granules could be obtained only if the ER was higher than 50-60%. For values lower than 40% a mixture of suspended sludge and granules could be observed.

The air bubbles up-flow during reaction (aeration) step creates hydrodynamic shear stress, creating an homogenous circular flow and localized vortex along the reactor height; thus a circular hydraulic attrition is constantly applied on the bacterial aggregates (Liu et al., 2005a). This attrition is a main force to shape the granules to a minimum surface free energy (Liu and Tay, 2002) and the height to diameter (H/D) ratio of the SBR column is an important parameter to control it. Different studies have reported the correlation of this parameter with the structure and the stability of the aerobic granules; higher shear force induced the formation of more compact, rounder, denser and smaller particles (Tay et al., 2004, Gao et al., 2011b), as well as more production of EPS (Ohashi and Harada, 1994). This will allow more contact among the cells and a stronger and more stable granules structure could be obtained (Liu et al., 2004b). It has been reported that the optimum air up-flow superficial velocity to produce aerobic granules should be  $>2.0 \text{ cm s}^{-1}$ . A velocity  $<1.2 \text{ cm s}^{-1}$  could indeed only lead to a flocculent biomass and between  $1.4\text{-}2.0 \text{ cm s}^{-1}$  unstable granules were achieved (Beun et al., 1999).

The HRT of the reactor is closely related to the cycle time in an SBR system. Very short HRT in SBR systems has reported biomass wash-out, since not enough time was allowed for the microorganisms to grow and reach a minimum aggregation to remain within the reactor. On the other hand, too long HRT has led to biomass hydrolysis, thus resulting in interfering with biological aggregation (Chen et al., 2003a, Pan et al., 2004). A nitrifying SBR operated at 24 h cycle time showed no granulation, but if reduced to 3 h the complete biomass wash-out was observed. On the other hand, at cycle times of 6 and 12 h nitrifying granules were obtained (Tay et al., 2002).

The reaction phase is divided in degradation (feast), where the substrate is reduced to a minimum, and starvation (famine), when substrate is no longer available. It is thought that bacteria subject to a feast/famine regime become more hydrophobic and increase the cell-to-cell contacts (Bossier and Verstraete, 1996, Liu et al., 2004b). Long starvation times have reported to increase the EPS production in the sludge, suggesting that EPS could be used by bacteria to counteract the environmental stress (Tay et al., 2001b, Chen and Strevett, 2003). On one hand, short starvation time could reduce granulation time, but too short periods were unfavourable for long-term stability (Liu and Tay, 2008, Wang, 2005). Extended starvation time instead showed longer granulation time, but also more granules integrity and smaller sizes (Gao et al., 2011b). However, aerobic granulation could not develop in a SBR with a periodic feast-famine regime present if other parameters were not properly controlled (Qin et al., 2004b, Qin et al., 2004a).

Several studies stated that aerobic granules could be obtained at different loading rates for both heterotrophic (Moy et al., 2002, Liu et al., 2003) and nitrifying (Yang et al., 2004a, Qin et al., 2004c, Tsuneda et al., 2003) granules. They showed that the effects of substrate loading rate on the granulation process were irrelevant; on the other hand, the physical characteristics of the aerobic granules strongly depended on it. For instance, the mean size of aerobic granules increased from ~2 to 4.2 mm when the organic loading rate (OLR) changed from 6 to 9 Kg COD m<sup>-3</sup> d<sup>-1</sup> (Moy et al., 2002). Except for a physical strength decrease at increasing OLRs and biological kinetics changes in aerobic granules, there were no significant differences in density, specific gravity, and sludge volume index (SVI) between granules developed at different loading rates, for what concerns dry biomass (Liu et al., 2003).

#### ***1.1.4.3. Minerals precipitation within granular sludge***

Granular sludge has recently attracted much interest due to the reported precipitation of minerals in different biological systems; for instance, calcium phosphate (CaPO<sub>4</sub>) minerals were observed in enhanced biological phosphorus removal (EBPR) (Mañas, 2011, Mañas et al., 2012b), in one-step partial nitrification/ANAMMOX (Gonzalez-Martinez et al., 2017, Johansson et al., 2017) and pure ANAMMOX (Lin et al., 2013a). Calcium carbonate (CaCO<sub>3</sub>) precipitation was instead reported in aerobic granular sludge processes (Ren et al., 2008, Liu et al., 2016a) and a mixture of both minerals was described in anaerobic granules treating black water (Cunha et al., 2018a).

Literature on the bulk precipitation of inorganic minerals in wastewater treatment processes has been extensive; it is common understanding that the main factors promoting bulk precipitation are pH, ions concentration (e.g. Ca<sup>2+</sup>, PO<sub>4</sub><sup>3-</sup>, CO<sub>3</sub><sup>2-</sup>, etc.), temperature and the presence of nucleation sites (Hammes and Verstraete, 2002, Dupraz et al., 2009, Mañas, 2011, Peng et al., 2018). On the other hand, it is only speculated that precipitation induced by bacteria within granular sludge is caused by: (a) the bacteria activity, (b) the micro-environments created within the granule due to mass transfer resistance and (c) the extracellular polymeric substance (EPS) composition (discussed in details later).

The uncontrolled production of inorganic precipitation can represent a disadvantage for the treatment works, since it can generate scaling issues by covering surfaces of heat exchangers, boilers, pipes and reactors (Rathinam et al., 2018). In addition, decreased biological activity of the aerobic granules (Ren et al., 2008, Liu et al., 2016a) and increased energy costs for mixing due to solidification in the reactors bottom (Van Langerak et al., 1998). Nevertheless, the increased amount of minerals within granular sludge was also reported to improve the bacteria aggregation and the granule structure stability and settling rate (Jiang et al., 2003, Lin et al., 2013a). Importantly, the removal of phosphorus (P) from wastewater within granular sludge has lately attracted the interests of the

scientific community; this is also explained by the fact that the recovery in the solid form of a valuable product (i.e. struvite and hydroxyapatite) without chemical or pH adjustment would be advantageous (Desmidt et al., 2015, Nancharaiyah et al., 2016, Peng et al., 2018, Sarma and Tay, 2018b).

Phosphorus (P) is an important nutrient for life but also an eutrophication agent if released in the environment. It is a necessary element for human activities (e.g. agriculture, food industry, household applications, etc.) (Desmidt et al., 2015) and it is mostly extracted from the phosphate rock deposits of  $P_2O_5$  (Vaccari and Strigul, 2011). Unfortunately, it is a not-renewable source and with population increase and the endless rising application of fertilisers, the depletion of the element has become an urgent problem that needs to be addressed. This is why P removal and recovery from wastewaters within granules that could be easily harvested and separated from the rest of reactor seems an appealing opportunity. The production of hydroxyapatite (HAP) by aerobic granules has convenient advantages over the struvite precipitation by crystalliser, since the mineral can be achieved without any pH adjustment, due to the gradients within the particles, or need of chemicals addition (e.g.  $MgCl_2$ , lime, etc.) or  $CO_2$  degassing, with a subsequent reduction of the WWTW costs.

There is an industrial market (e.g. implants filling and coating, synthetic bones, corrosion resistant materials, drug delivery, etc.) in which calcium phosphate could be used as a substitute of phosphate rock and been processed using the existing infrastructures (Tervahauta et al., 2014, Peng et al., 2018). Furthermore, HAP has been suggested as a *slow releasing fertiliser* for direct application to land (Singh and Agrawal, 2008). Although it is considered a slightly soluble compound in soil, there are different strategies to overcome this inconvenient; for instance, it could be applied in acidic soils (Qiu et al., 2015), it could be pre-treated with a slightly acid solution, or even applied together with phosphate-solubilizing bacteria or fungi (De-Bashan and Bashan, 2004). However, at the moment there are still environmental risks for the direct application to soil of inorganic granules produced from wastewater treatment; this is due to presence of not inactivated pathogens, heavy metals and not biodegradable organics contained in wastewater (Havukainen et al., 2016). Good results were obtained by Tervahauta et al. (2014) where HAP was produced by an anaerobic digestion system treating vacuum collected black water, which showed very low heavy metal concentrations; anyhow, more studies would still be needed in the future before the harvested biomass could follow the discharge directive limits and be directly used as a fertiliser in agriculture.

#### ***1.1.4.4. Extracellular polymeric substance (EPS)***

The biomass employed in wastewater treatment works is never present as a single cellular unit in the bulk solution but is constantly shown as aggregates, either flocculent or biofilm sludge, including granules. To keep the cells together is the extracellular polymeric substance (EPS), secreted by the bacteria under specific environment conditions (Sheng et al., 2010). Although the role played by EPS is not yet thoroughly understood, it is thought that it could help the adhesion to surfaces, increase the biofilm structure stability, provide cell-to-cell contact to favourite transport of information and it could represent some sort of protective barrier against environmental stresses (Wingender et al., 1999, Laspidou and Rittmann, 2002). This would also explain its importance for the granulation process, as explained in the previous paragraphs. Generally, a greater content of EPS was described in biofilm than in suspended sludge and it is mainly composed by polysaccharides, proteins, humic-like molecules, lipids and nucleic acids (Tay et al., 2001c, Adav and Lee, 2008). However, proteins (PNs) and polysaccharides (PS) are often the most present components and for this reason they are also the most analysed.

The PN/PS ratio has been described as an important parameter to describe the biofilm structure stability; there are studies reporting that a higher PNs concentration would justify a more stable aggregate structure (Adav and Lee,

2008, Zhu et al., 2013, Zhang et al., 2007), also showing association between increased PN's content during granulation and reduction when the particles disintegrated. On the contrary, other research states that PS instead would be more involved in the structure stability than PN's (Tay et al., 2001c); this was justified by the increased polysaccharides content under high hydrodynamic shear stress. In addition, reduced structure stability was linked to the increased PN/PS ratio in a study where concentration of PS present in the granule core was used by bacteria as carbon source when nutrients were insufficient (Sadri Moghaddam and Alavi Moghaddam, 2015); this could indeed explain a reduced granule structure stability due to the creation of internal empty spaces. Other studies in which nutrients mass transfer limitation generated a reduction of PS were also reported, specifically in an aerobic granular system showing excessive inorganic precipitation (Liu et al., 2015b) and in lithified layers of nature marine stromatolites (Kawaguchi and Decho, 2002). In these studies, the high amount of inorganic matter could increase the mass transfer limitation within the biofilm, causing the starving bacteria to utilise the PS as carbon source for growth. However, there is great confusion at the moment about EPS composition and roles on granular sludge, which is probably due to the not-fully standardised procedures to both extract EPS and to analyse its components. In addition, this is worsened by the interference between chemicals used for extraction and determination protocols and the extracted EPS components (Comte et al., 2006, D'Abzac et al., 2010).

EPS matrix has showed to be able to bind cations such as  $\text{Ca}^{2+}$ ,  $\text{Mg}^{2+}$ ,  $\text{Fe}^{2+}$ ,  $\text{Fe}^{3+}$  and  $\text{K}^{+}$ , as a not-specific process driven by the different elements concentration between the biomass and the bulk solution. This was suggested by the presence of alginate-like esopolysaccharides (ALE) molecules with their negative charges (i.e. carboxyl groups). The  $\text{Ca}^{2+}$  binding to the ALE chains was demonstrated among the most stable reaction compared to the other cations, as also explained by the formation of ALE-Ca-ALE bridges (Yu et al., 2001, Dupraz et al., 2009). These crosslinks can make the EPS structure more stable as described in some research (Wang et al., 2007b, Ren et al., 2008). However, in case of excessive accumulation of the metal, it also showed to induce precipitation of calcium carbonate and calcium phosphate crystals in an anaerobic granular system (Cunha et al., 2018a), which was justified by the action of EPS molecules in lowering the energy needed for crystals nucleation (Dupraz et al., 2009). The binding of ALE to other cations was also reported, for instance phosphorus was accumulating in granular sludge as K-struvite mainly because of the adsorption of ammonium to  $\text{K}^{+}$  present in EPS ALE (Lin et al., 2012). In a granular EBPR for P removal,  $\text{K}^{+}$ ,  $\text{Mg}^{2+}$  and  $\text{Ca}^{2+}$  were found in EPS as 44.7%, 27.7% and 28% of their total granule content (Wang et al., 2014b); it was described that the movement of these cations from the bacteria to the bulk solution was interfered with their accumulation in EPS. Also P was found to bind EPS and it was hypothesised this could take place through the changed conformation of the ALE-Ca-ALE bridges; an increase of cations amount, the absence of bulk chelating agents (e.g. VFAs as acetate) and an increased pH were described as the right conditions for the bridge to create enough space to allocate a molecule of  $\text{PO}_4^{3-}$  (Lin et al., 2013b, Sarma and Tay, 2018b). In aerobic granules for simultaneous nitrification/denitrification a concentration as high as 17.6% of total removed P was found in EPS (Huang et al., 2015) and its adsorption was also reported by its presence on the surface of dead cells in another study (Longnecker et al., 2010).

The extracellular polymeric substance has been extracted in several ways in literature; the used methods are generally classified in physical and chemical procedures. In the former category, centrifugation is often used as control and represents probably the mildest protocol. The speed normally used should be higher than 10000g, whereas when a speed lower than 5000g is used, it is likely just a matter of separating the solids from the extracted supernatant (Adav and Lee, 2008, Villain et al., 2010). Other extraction methods are heating (Wingender et al., 1999), cation exchange resin (Xie et al., 2012) and ultrasonication (Ramesh et al., 2006). The chemical methods are represented by addition of strong bases, surfactant, fixative, chelating agents; specifically, formaldehyde is paired with NaOH (Liu and Fang, 2002), formamide is used with NaOH (Adav and Lee, 2008), but also Ethylenediaminetetraacetic acid (EDTA) (Comte et al., 2006), ethanol (Adav and Lee, 2008) and

glutaraldehyde (Comte et al., 2006) were used alone. The cation exchange resin and the EDTA would act to remove the cations that would normally accumulate in EPS and weaken the structure stability; this would also be the case when raising the pH to >12 using bases, which would deprotonate and detach the cations. A mass of negative charges that repulse each other is formed and causes the EPS structure to crumble. The fixatives such as formaldehyde and formamide are employed to avoid lysis of the cells during the harsh procedures of extraction. They generally bind to amino, hydroxyl, carbonyl and sulfhydryl groups of proteins and nucleic acids of the cell membrane, therefore preventing the cells to lyse. Among these extraction procedures, the formaldehyde plus NaOH was often described with the highest extraction yield, without contaminating the solution with material from lysed cells (Comte et al., 2006, D'Abzac et al., 2010, Keithley and Kirisits, 2018). However, more recent research has reported that the combination of physical and chemical procedures would be more efficient than each alone (Adav and Lee, 2008, Zhang et al., 2012); for instance, sonication used before the formaldehyde plus NaOH incubation could improve the extraction yield, which was also due to the different sludge structure to extract the EPS from (suspended flocs or granules).

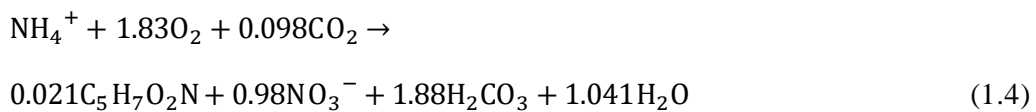
Among the analytical procedures for the PS determination in wastewater, are the colorimetric, gravimetric, enzymatic, titrating and chromatographic protocols. Among them, the most widely used methods due to their simplicity are the colorimetric phenol-sulfuric acid (Dubois et al., 1956) and anthrone method (Gaudy, 1962). On the other hand, the analytical procedures for PNs analyses are the colorimetric methods of modified Lowry, Bradford (Bradford, 1976) and bicinchoninic (BCA) (Smith et al., 1985), and the more complicated and expensive resonance light-scattering, proteomics, ion-exchange chromatography and excitation-emission matrix spectroscopy. However, the modified Lowry method (Frølund et al., 1995, Lowry et al., 1951) remains the most preferred due to the accurate results and the little interference by many compounds contained in wastewater (Lucarini and Kilikian, 1999); in addition, the modified version of this procedure also allows the simultaneous measurement of humic acid. However, it has been reported in literature that this method could produce poor reliability or strangely fluctuating values when analysing wastewater containing cations. Specifically, concentrations of 0.5 and 0.9 mmol L<sup>-1</sup> of Ca<sup>2+</sup> and Mg<sup>2+</sup>, respectively, showed unreproducible results (Xie and Burnell, 1994) or even a negative amounts of PN (Westgate and Park, 2010). This could be justified by the alkaline reagents contained in Lowry method, i.e. 5.7 g L<sup>-1</sup> of NaOH and 28.6 g L<sup>-1</sup> of Na<sub>2</sub>CO<sub>3</sub>, with a final pH>12. Indeed, the cations at such pH would react with carbonate and precipitate. Shen et al. (2013) demonstrated that technologies like dialysis and cation exchange resin could remove over 90% of both Ca<sup>2+</sup> and Mg<sup>2+</sup> (3 mmol L<sup>-1</sup>), therefore eliminating the Lowry method interference. The dialysis would act as a physical selective membrane that would discharge molecules/atoms in the sample that are larger than the 3.5 kDa pores size. On the other hand, the negative charges on the resin would chemically bind the positively charged cations, without reacting with the rest of sample. As described above, the EPS composition is able to bind to different cations in the bulk solution and produce the precipitation of inorganic minerals within the biofilm. It could be speculated that during the EPS extraction a portion of cations bound to such mixture of organic and inorganic matter could be found in the final extracted solution. However, the interaction of this kind of cations with the EPS extraction procedures and the Lowry method PN determination is not clear yet and further investigation would be needed.

## **1.1.5. Traditional nitrification-denitrification**

### ***1.1.5.1. Nitritation and nitrataion***

Nitrification is a process based on two different reactions, nitritation and nitrataion, with hydroxylamine as an intermediate. It is carried out by two chemolithoautotrophic bacteria that use NH<sub>4</sub><sup>+</sup> or NO<sub>2</sub><sup>-</sup> as energy to

synthesise biomass, CO<sub>2</sub> as the carbon source and O<sub>2</sub> as electron acceptor (Metcalf and Eddy, 2003). Commonly the most recognized genus of bacteria that carry out the ammonia oxidation belongs to the  $\beta$ -*Proteobacteria* subdivision; among all of them the *Nitrosomonas* is normally described, however, also *Nitrosococcus*, *Nitrospira*, *Nitrosovibrio* and *Nitrosolobus* can be included in this group. Since they oxidise NH<sub>4</sub><sup>+</sup> to NO<sub>2</sub><sup>-</sup> in aerobic environments they are also called aerobic ammonia oxidising bacteria (AerAOB or simply AOB). In the second reaction, in which the NO<sub>2</sub><sup>-</sup> is oxidised to NO<sub>3</sub><sup>-</sup>, the main responsible is generally from the *Nitrobacter* genus, even though several other genera such as *Nitrospira*, *Nitrospina*, *Nitrococcus*, and *Nitrocystis* are known to be involved (Teske et al., 1994, Rittmann and McCarty, 2001, Ahn, 2006). The members of this group are also called as nitrite oxidising bacteria (NOB). The Equations 1.1, 1.2, 1.3 and 1.4 show, respectively, the reaction of nitrification, nitratation, the overall reaction of nitrification and the overall nitrification reaction considering biomass production, respectively:



NH<sub>4</sub><sup>+</sup> is first oxidised to hydroxylamine (NH<sub>2</sub>OH) (not shown) by the membrane bound ammonia mono-oxygenase (AMO) and the hydroxylamine oxidoreductase (HAO) in AOBs. Then, the membrane-bound nitrite oxidoreductase (NOR) contained in NOBs will oxidise NO<sub>2</sub><sup>-</sup> to NO<sub>3</sub><sup>-</sup> (Sinha and Annachatre, 2007). During nitrification, for each g of NH<sub>4</sub><sup>+</sup>-N nitrified, 4.25 g of oxygen are used, 0.16 g of new nitrifying cells are produced and 7.07 g of alkalinity as CaCO<sub>3</sub> are destroyed. Therefore, nitrification is an acidifying process that needs alkalinity control; for each mole of NH<sub>4</sub><sup>+</sup> oxidised to NO<sub>3</sub><sup>-</sup>, two moles of HCO<sub>3</sub><sup>-</sup> need to be added to the medium (Bernat et al., 2012). It has been well described that the real substrates for AOB and NOB are the non-protonated species ammonia (NH<sub>3</sub> or free ammonia FA) and nitrous acid (HNO<sub>2</sub> or free nitrous acid FNA), respectively (Anthonisen et al., 1976). AOB and NOB are considered obligatory aerobic bacteria, even though it has been found that the former can oxidise ammonia also in anoxic environments.

#### 1.1.5.1.1. Nitrifying bacteria slow growth rate and system start-up

The chemolithotropic metabolism justifies the fact that nitrifying bacteria are quite slow growing microorganisms. For instance, the specific growth rates of AOB and NOB are 1 and 0.5 d<sup>-1</sup>, respectively, at 35 °C (Khin and Annachatre, 2004). A consequence of this is the long time needed for starting-up nitrifying processes, since it takes long time for the bacteria to reach a sufficient concentration in the system due to bacteria wash-out (Tay et al., 2002); however, this could even be longer if nitrifying granules were to be cultivated. In addition, to explain the slow growth rate is also the high degree of inhibition to a long list of chemicals; even ammonium and

nitrite in the protonated forms ( $\text{NH}_3$  and  $\text{HNO}_2$ ) showed to reduce both AOB and NOB activity (Anthonisen et al., 1976). Other reported inhibiting chemicals were phenol (Gao et al., 2017), heavy metals (Hu et al., 2003), antibiotics (Katsou et al., 2016), but also environment conditions like temperature and salinity (Gonzalez-Silva et al., 2016). Therefore, to insure the efficiency of nitrifying full-scale processes could sometime become challenging (Agrawal et al., 2018). Nitrifying granules processes are a fairly new technology but they play a fundamental role in the nitrogen removal from wastewater treatment (Sarma and Tay, 2018a); indeed, they represent an important defence for the autotrophic bacteria, due to the stronger and resistant structure that, differently from activated sludge, could reduce the extent of inhibition. In addition, the special biofilm structure would increase the retention time of the slow growing bacteria, avoiding wash-out from the system and shortening the start-up times. However, the risk of temporary change in waste stream quality, the increase of toxins content or a technical problem could still cause the nitrifying system failure. For instance, a case was described where the sudden reduction of oxygen in a simultaneous partial nitrifying/ANAMMOX reactor could generate system failure; stable conditions of the process could only be recovered after a month (Joss et al., 2011). This kind of situations would mean for the treatment works the need of purchasing new biomass, with consequent increase of the operational costs.

To improve the start-up of nitrifying activated and granular sludge systems, different studies have been reported in literature and, among others, worth of mention are: (a) selection of inoculum from specific wastewater treatment processes (e.g. anoxic/oxic tank, denitrifying tank, etc.) (Tsuneda et al., 2003, Shi et al., 2009, Shi et al., 2010); (b) operating systems choice (e.g. SBR, air-lift, etc.) (Song et al., 2013); (c) addition of activated carbon (AC) particles (Bartoli et al., 2010) or (d) ground anaerobic granules to enhance granulation (Tokutomi, 2004); (e) heterotrophic granules used as inoculum to improve biomass retention (Wan et al., 2013); (f) addition of metals and (g) application of magnetic field (Wang et al., 2012). Among these, it is believed that for reducing time of nitrifying granules systems start-up, the manipulation of the reactor operation would involve lower costs and would be preferred over those strategies needing accessory approaches such as AC dosage or magnetic field application.

The time needed for cultivation of nitrifying granules was reported initially as 300 days in an up-flow fluidised bed reactor (Tsuneda et al., 2003) and 120 days in an SBR (Shi et al., 2009, Shi et al., 2010). Shorter times were then achieved by using an SBR inoculated with activated sludge and fed with both COD and high ammonium concentration; nitrifying activity was detected after 80 days and partial nitrifying granules were obtained in 146 days (Wei et al., 2014). Partial nitrifying suspended biomass and partial nitrifying granules in a sequencing batch air-lift reactor were observed after 60 and 83 days, respectively (Song et al., 2013). Inoculating nitrifying sludge to a sequencing batch airlift reactor achieved partial nitrification and granules in 70 days (Kim and Seo, 2006). Nitrifying granules production was described in around 55 days in an SBR system (Chen et al., 2015); the inoculum used in the study was a suspended nitrifying biomass, produced in a previous experiment and stored for at least 2 months at  $4^\circ\text{C}$ . After reviving the microorganisms, the concentration of  $\text{NH}_4^+$  was rapidly increased from 200 till  $1000 \text{ mg N L}^{-1}$  in 55 days and kept constant until the end of operation. In the study, stepwise NLR increase (from 0.4 to  $2 \text{ g L}^{-1} \text{ d}^{-1}$ ) and short settling time (from 10 to 7 min) were the main change parameters to achieve a quick granulation of nitrifying biomass. FA inhibition of granulation at such NLR was previously described (Yang et al., 2004b, Wang et al., 2007a), but in this study it was avoided since  $\text{NH}_4^+$  concentration in the effluent was always close to zero after one single cycle. Moreover, the fast granulation was also possible due to the stepwise shortening of settling time from 10 to 7 minutes. However, Chen et al. (2015) used already nitrifying activated sludge as inoculum, which would explain the quick nitrifying granulation. On the other hand, the amount of the autotrophic bacteria in conventional activated sludge from sewage works would be much lower and the accumulation in the system could take quite long time. Thus, good biomass retention should be provided



to minimize the risk of biomass washout and to ensure a stable treatment; strategies to achieve biomass retention were reported as attachment to the surface of a carrier (De Prá et al., 2012) and entrapment in gel beads (Furukawa et al., 2009, Qiao et al., 2010). The inoculation of heterotrophic granules was described to enhance the nitrifying bacteria accumulation (Wang et al., 2016); however, fresh heterotrophic granules were used in that study but in practice their cultivation can take time and much longer would be needed if AOB selection over the NOB (partial nitrification, explained later) is required. As described before, the adjustment of reactor operation parameters (e.g. settling time, H/D ratio, HRT, shear stress, etc.) can improve the formation of granular sludge. It was described that by applying high OLR and short settling times, stable heterotrophic granules could be produced in one week, but the particles could be observed in the system already after 24 h (Liu and Tay, 2015). Therefore, if these two parameters were used to form heterotrophic granules and they were enriched by AOBs, the total start-up period for the formation of partial nitrifying granules could be reduced. Anyway, heterotrophic granulation failure was described in literature by using too short settling time or HRT (Qin et al., 2004b, Qin et al., 2004a, Tay et al., 2002) and at so strong selection pressure it is possible that slow growing bacteria would be easily washed out of the reactors. Hence, optimisation of operational strategies would be needed to quickly enrich the nitrifying bacteria without losing heterotrophic granules structure stability and, at the same time, to produce stable nitrifying granules.

#### *1.1.5.1.2. Nitrifying bacteria activity enhancement*

In the last decade, research on novel technologies that could improve biomass activity and growth rate in parallel to the reduction of inhibitory effects was reported. The application of electromagnetic field and ultrasound technology on biological processes for wastewater treatment has showed interesting results, reporting a variety of effects such as improved removal of pollutants, changes in cell membrane permeability, increased biomass growth rate and other promising effects. Although the factors behind the effectiveness of these technologies are still not well understood and under investigation, it could be speculated that it could be the cellular response to a stressful condition, as it could be considered the irradiation with ultrasound or electromagnetic waves. This could also be justified by the increase of 16S rRNA gene copies (Yin et al., 2016) or the activation of heat shock proteins (HSP) cascade reaction. A brief introductory description of these technologies is provided in the following paragraphs.

**MAGNETIC FIELD** - A magnetic field is generated by either solely a permanent magnet or an electromagnet in which movement of electric currents is provided; the latter can be made by using a power supplier connected to a quite long coiled wire, which should be applied around the biomass that needs treatment. The intensity of magnetic field used in wastewater treatment ranges between a couple of mT to hundreds. Different examples of applications were reported in literature. For instance, iron accumulation within nitrifying granules and the stimulation of EPS production was generated; granulation time in this system treating high N-strength synthetic wastewater was reduced from 41 to 25 days by applying a static magnetic field of 48 mT (Wang et al., 2012). In another study, ANAMMOX cultures inoculated in a lab-scale reactor showed that time for cultivation could be reduced by 25% and the  $\text{NH}_4^+$  removal activity increased by 30% compared to the untreated control by using a magnetic field with intensity of 60 mT (Liu et al., 2008). The AOB *Nitrosomonas europaea* growth rate was shown to be increased after static magnetic field at 17 mT was used; a range between 30 and 50 mT was described as improving the  $\text{NH}_4^+$  oxidation rate in a sequencing batch reactor by 77% (Filipič et al., 2015). Promising results were also reported on aerobic granules where the application of both permanent magnets with non-uniform magnetic field and an electromagnet with 3-5 mT uniform magnetic field could improve the COD and  $\text{NH}_4^+$  removal by 45-54% and 30-50%, respectively; in addition, EPS production at the low magnetic field intensities was increased of 77% compared to the untreated control (Liu et al., 2016b).

**ULTRASOUND** - The ultrasound technology was used in wastewater treatment for many applications that go from improvement of anaerobic biodegradability of sludge to enzyme increased activity, enhanced nutrients removal and more (Zhang and Jin, 2015). The sound waves (acoustic energy) are generated at frequencies higher than 20 kHz by ultrasound generators. Different examples of the beneficial effects of ultrasound were reported. The increased specific oxygen uptake was observed in activated sludge irradiated with ultrasound at 28kHz frequency and a power input of 50 W L<sup>-1</sup>; this was described to be generated by the higher activity of the enzyme protease and the increased amount of adenosine triphosphate which play important roles in bacteria activity (Zeng et al., 2006). In addition, the treatment effects were closely dependent on duration, showing negative effects after a too long irradiation. Low-intensity ultrasounds in conjunction with EDTA were showed to allow quicker recovery of ANAMMOX bacteria after inhibition by heavy metal Cu(II). An interesting effect was the increased heme c content, which was reported to increase the bacteria activity and growth rate (Zhang et al., 2015). The sound waves could produce a loosening of EPS and the granular sludge settling skills were improved. Another application of ultrasound technology was described as the inhibition of NOB activity in a partial nitrifying sequencing batch reactor treating a synthetic urine wastewater; ultrasounds with energy density of 0.09 kJ/mg VSS could generate enhancement of AOB activity up to a certain limit, after which the activity decreased. On the other hand, NOBs in the nitrifying activated sludge investigated were continuously inhibited and their amount reduced under the ultrasound effects (Zheng et al., 2015).

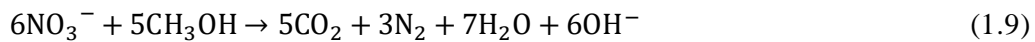
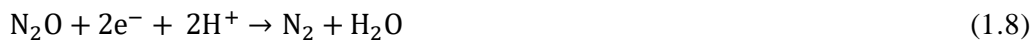
**ELECTRIC FIELD** - An electric field (EF) can be generated by providing a potential difference ( $\Delta\phi$ ) between two electrodes (or plates) placed at a certain known distance (d) by using a common power supplier. The intensity of the uniform EF generated is intended as  $E: \Delta\phi/d$ . This technology has been known for long time in the bio-medical filed (Thrivikraman et al., 2018), but recent studies for its application in biological wastewater treatment showed promising results. As for the other two technologies, improvement of bacteria activity and increased growth rate were reported. For instance, the enhancement of nitrogen removal of 25.6% after treatment with 2 V cm<sup>-1</sup> for 20 minutes was described in ANAMMOX biomass. The continuous application showed instead negative effects on the bacteria activity, but once the treatment was removed, complete recovery of the autotrophs was described (Qiao et al., 2013). In a similar way, at a specific voltage an enhanced organic carbon removal was observed in aerobic sludge (Alshawabkeh et al., 2004); on the contrary, a treatment longer than 24 h could generate biomass inhibition. The EF positive effects could be linked to the permeabilisation of the cellular membrane as also described in Chen et al. (2006a), where pores were observed on the bacteria surface. It could be speculated that this could facilitate the transportation of nutrients into the cells, therefore improving the bacteria activity. On the other hand, it was also reported that a too high intensity or long duration of treatment could generate a bactericide effect, by producing an irreversible membrane permeabilisation (Wang et al., 2018). It is therefore important to choose carefully these two parameters, to avoid either negligible or sterilising effects. The importance of EF effects on bacteria activity could be shown by the change of concentration of energetic molecules like adenosine triphosphate (Liu et al., 2015a, Ailijiang et al., 2016) or nicotinamide adenine dinucleotide (NAD/NADH) (She et al., 2006) in the biological system. The ammonia monooxygenase (AMO), hydroxylamine oxidoreductase (HAO) and nitrite oxidoreductase (NOR) are all enzymes important for nitrification reaction. The electric field was reported to increase activity of all of them with a consequently increased bacteria N removal activity and growth rate (Ge et al., 2015).

Compared to EF, the magnetic field and ultrasound technologies show some drawbacks, mainly represented by complicated theory behind the process and the need of expensive equipment (e.g. magnetic field detector, ultrasound generator, etc.). As explained before, to generate an electric field, relatively cost-effective equipment is needed. In addition, its promising effects have been well known for a long time, especially in bio-medical research (Thrivikraman et al., 2018), making of this technology an interesting candidate for varied applications in

wastewater treatment. However, most of the research in literature was done to establish that biomass removal activity and growth rate could be enhanced; on the other hand, to the best of our knowledge, studies on EF application on the recovery of lost activity due to bacteria inhibition (e.g. toxic chemicals) are still missing. In addition, submerging the electrodes in the same solution where biomass is present represents almost the only type of setup used at the moment. It has been reported that the viability of bacteria could be affected by their contact to the electrodes (Jackman et al., 1999) or by the possibility that toxic oxygen radicals could be generated (She et al., 2006). Also, choosing the material to use is of concern since dissolution of the electrode or production of by-products could reduce the positive EF effects on biomass. Therefore, it is thought that an external application of the electrodes as plates to the outside wall of a reactor could be advantageous and more beneficial for the system.

### ***1.1.5.2. Denitrification***

The denitrification process is carried out by various heterotrophic microorganisms, especially under oxygen-reduced or anoxic conditions, which oxidise  $\text{NO}_2^-$  to  $\text{N}_2$  by four steps (Equations 1.5 to 1.9). Bacteria with this metabolism are often found as Gram-negative  $\alpha$  and  $\beta$ -*Proteobacteria*, some examples are *Pseudomonas*, *Alcaligenes*, *Paracoccus* and *Thiobacillus*, whereas *Bacillus* can be found from the Gram-positive group and some halophilic Archaea such as *Halobacterium* (Balows et al., 1992). They use inorganic N as electron acceptor instead of  $\text{O}_2$  and organic matter as energy and carbon source, represented by methanol in the equation (Metcalf and Eddy, 2003).



According to the Equations, for each g of  $\text{NO}_3^-$ -N reduced 3.57 g of alkalinity (as  $\text{CaCO}_3$ ) are produced. The denitrifying bacteria first oxidise  $\text{NO}_3^-$  to  $\text{NO}_2^-$ , then to nitric oxide (NO) and to nitrous oxide ( $\text{N}_2\text{O}$ ), before it is released in the atmosphere as  $\text{N}_2$  (Wang and Ivanov, 2010). Several carbon sources have been used for denitrification in WWTW, such as methanol, acetate, ethanol, lactate and glucose (Akunna et al., 1993); since it is inexpensive, methanol is today the most widespread organic carbon source used for denitrification process (Rittmann and McCarty, 2001). The alkalinity concentration increases after the production of hydroxide and the carbonic acid concentration in the medium is reduced; so the tendency of denitrification is to partially reverse the

effects of nitrification and raise the pH of the biological reaction. For waters low in alkalinity, the recovery of alkalinity through denitrification can be a significant benefit. Denitrifying bacteria are facultative aerobes, in presence of both oxygen and nitrates they can choose the former as electron acceptor because the energy generated per unit weight of organic matter metabolized is higher. Therefore, it is essential to keep an anoxic environment so that the reduction of nitrates can occur; no conversion was observed at an oxygen concentration above  $0.2 \text{ mg L}^{-1}$  (Skerman and Mac Rae, 1957).

The traditional nitrification-denitrification process carried out in most of the WWTWs ensures high potential removal efficiency, high process stability and reliability, and relatively easy process control (Metcalf and Eddy, 2003). On the other hand, it requires large footprints and high operational costs (great amount of oxygen for nitrification and organic source for denitrification). Because the organic carbon present in some wastewaters with high N concentrations (e. g. landfill leachate, reject water) is quite limited, the complete removal of nitrogen by the traditional technology is not cost-effective (van Dongen et al., 2001); indeed, the requirement of added electron donors, such as methanol, makes the full-scale denitrification process quite expensive (Khin and Annachhatre, 2004). Generally, the traditional nitrification-denitrification is used for treating wastewaters with relatively low nitrogen concentrations like the domestic streams, however, high cost we still incurred for this technology (Van Hulle et al., 2010). Therefore, in modern installations the complete nitrification of  $\text{NH}_4^+$  to  $\text{NO}_3^-$  started to be substituted by nitrification to nitrite (or partial nitrification) followed by denitrification, which reduces oxygen, organic carbon and overall energy. In addition, further reduction of costs could be achieved by the complete substitution of denitrification with the *ANAerobic AMMonium OXidation* (ANAMMOX) process, following the partial nitrification tank, as explained in details later.

#### **1.1.6. Partial nitrification and long-term stability**

The partial nitrification reaction is the result of NOB activity inhibition, with  $\text{NO}_2^-$  accumulation in the effluent and no or little concentration of  $\text{NO}_3^-$  present; the oxidation of ammonium to nitrite in dedicated reactors can be achieved by means of different strategies: (a) moderately high temperatures; (b) combination of high pH and concentrations of  $\text{NH}_3$  and/or  $\text{HNO}_2$ ; (c) addition of inhibitors; (d) short SRT and HRT adjustment; (e) low concentration of DO; and (f) intermittent aeration.

##### ***1.1.6.1. High temperature***

The maximum specific growth rate of NOB at the temperature of  $35 \text{ }^\circ\text{C}$  is approximately only half of the one for the AOB ( $0.5$  and  $1 \text{ d}^{-1}$ , respectively) (Khin and Annachhatre, 2004). From experiments with pure cultures of AOB and NOB, an optimal temperature of  $35 \text{ }^\circ\text{C}$  for aerobic ammonium oxidizers and  $38 \text{ }^\circ\text{C}$  for nitrite oxidizers were observed (Grunditz and Dalhammar, 2001); the values of activation energy for the two groups of bacteria are within the range  $72\text{--}60 \text{ kJ mol}^{-1}$  and  $43$  to  $47 \text{ kJ mol}^{-1}$ , respectively (determined in studies between  $7$  and  $30 \text{ }^\circ\text{C}$ ) (Van Hulle et al., 2010). Therefore, at temperatures above  $25 \text{ }^\circ\text{C}$  a higher increase of the specific growth rate of AOB than that of NOB will occur (Hellings et al., 1998, van Dongen et al., 2001) and the former can effectively outcompete the latter (Brouwer et al., 1996).

An example of process using a relatively high temperature is the SHARON (*Single reactor system for High Activity ammonia Removal Over Nitrite*) system, described the first time by a research group from Delft University of Technology, The Netherlands (Hellings et al., 1998). In practice, the system is a chemostat operated at a temperature of  $35 \text{ }^\circ\text{C}$ , without biomass retention, in which sludge and hydraulic retention times are equal and lower than 1.5 days. In addition to high temperature, NOB wash-out was also possible because of the short retention time selected. Although this mechanism of NOB activity inhibition seems very practical, high

temperatures are not generally available, especially for sewage treatment operations because of the high costs of energy (Lackner et al., 2014).

#### **1.1.6.2. FA, FNA and pH**

The real substrates for AOB and NOB are  $\text{NH}_3$  and  $\text{HNO}_2$ , respectively (Anthonisen et al., 1976). At  $\text{pH} < 6.5$  the  $\text{NH}_3$  concentration becomes too low for sufficient growth of the AOB and vice-versa  $\text{HNO}_2$  is not sufficient for NOB growth at pH slightly alkaline; the reason is due to the pH-dependent equilibrium between the concentrations of  $\text{NH}_3/\text{NH}_4^+$  and  $\text{HNO}_2/\text{NO}_2^-$ . In addition, both AOB and NOB are inhibited by both FA and FNA; the former seemed to be affected at values between 8 and 120  $\text{mg L}^{-1}$  of FA, whereas the more sensitive NOB could be inhibited in a range between 0.08 and 0.82  $\text{mg L}^{-1}$ . On the other hand, FNA inhibition occurred at concentrations of 0.2-2.8  $\text{mg L}^{-1}$  for AOB and 0.06-0.83  $\text{mg L}^{-1}$  for NOB. Therefore, appropriate suppression of the NOB activity can be achieved by simply maintaining alkaline pH in presence of  $\text{NH}_3$ . In addition, NOB are particularly susceptible to a changing pH, whereas AOB seem more robust to this kind of environmental stresses (Abeling and Seyfried, 1992).

Several studies have applied high N concentrated wastewaters (e.g. reject water) or a step wise increase of NLR to inhibit NOB activity, with both suspended (Yang et al., 2010, Jin et al., 2013, Xing et al., 2013) and biofilm or granular sludge (Jin et al., 2008, Okabe et al., 2011, Zhang et al., 2011, Daalkhajjav and Nemati, 2013, Guillen et al., 2015) in continuous systems; good results were also described with SBR granular systems (Kim and Seo, 2006, Song et al., 2013, Wei et al., 2014). However, such strategy would not be suitable for stable nitrification in a system treating main-stream wastewater; the concentration of  $\text{NH}_4^+$  is, indeed, much lower than the concentrations described in those studies and FA would not be enough to inhibit NOB activity. Moreover, the long-term application of high concentrations of  $\text{NH}_3$  has often reported failure of nitrite accumulation, with an increase of  $\text{NO}_3^-$  in effluent due to an acclimation of NOB biomass (Turk and Mavinic, 1989, Peng and Zhu, 2006).

#### **1.1.6.3. Dissolved oxygen**

The oxygen half saturation constant ( $K_0$ ) of nitrification and nitratation kinetics varies in the range of 0.25-0.5  $\text{mg O}_2 \text{ L}^{-1}$  and 0.34-2.5  $\text{mg O}_2 \text{ L}^{-1}$ , respectively (Barnes and Bliss, 1983, Hanaki et al., 1990, Rittmann and McCarty, 2001, Bernat et al., 2012); this means that the AOB are able to use more efficiently the electron acceptor than the microorganisms of the second step of nitrification, thus growing faster than NOB. The normal dissolved oxygen (DO) concentration necessary for nitrification is 2-4  $\text{mg L}^{-1}$  and if it drops to concentrations lower than 2  $\text{mg L}^{-1}$  nitrification rate will be greatly decreased. At levels of DO in the reactor within the range 0.5 - 1.0  $\text{mg L}^{-1}$ , the growth rate of AOB is 2.6 times faster than that of NOB (Park and Noguera, 2004).

Low DO as strategy to enhance nitrification was used by both continuous and sequencing batch systems; the difference in DO values between those studies was mainly due to the type of biomass used, flocculent or biofilm/granular. Indeed, lower DO concentrations than 2  $\text{mg L}^{-1}$  were described in flocculent systems of both batch systems (López-Palau et al., 2011, Pan et al., 2014) and continuous ones (Ma et al., 2009, Yang et al., 2010, Jin et al., 2013, Chai et al., 2015); on the other hand, higher DO concentrations than 5  $\text{mg L}^{-1}$  were described for systems using biofilm in SBR (Shi et al., 2009, Vázquez-Padín et al., 2010, López-Palau et al., 2011, Song et al., 2013). Higher DO is generally expected in biofilm systems due to a gradient of oxygen along the thickness of particle (in case of granular biomass) (Liu et al., 2010a, Winkler et al., 2013b). Interestingly, among the continuous systems using biofilm described in literature, only a few were using high DO concentrations (Wan et al., 2013, Wan et al., 2014), whereas most of them used DO lower than 1.4  $\text{mg L}^{-1}$  (De Clippeleir et al., 2011,

Okabe et al., 2011, Zhang et al., 2011, De Clippeleir et al., 2013, Guillen et al., 2015). This is explained by the fact that the final effluent was characterised by an ammonium/nitrite ratio of around 1, good for a following ANAMMOX reaction; indeed, the low DO inside the biofilm may produce a partial inhibition also of AOB, producing a not complete  $\text{NH}_4^+$  oxidation.

A disadvantage of using low  $\text{O}_2$  is the production of a very important greenhouse gas (GHG), nitrous oxide ( $\text{N}_2\text{O}$ ). It is still debated what factors could generate this (GHG), but it is speculated that the presence of high  $\text{NO}_2^-$  in parallel to  $\text{NH}_4^+$ , the low content of organic carbon (low COD/N ratio) and limiting  $\text{O}_2$  concentrations, could induce AOBs to oxidise  $\text{NH}_4^+$  by  $\text{NO}_2^-$  as electron acceptor instead of  $\text{O}_2$ . This process is generally called *nitrifier denitrification* (Colliver and Stephenson, 2000, Desloover et al., 2011) and causes the  $\text{N}_2\text{O}$  release.

#### **1.1.6.4. Intermittent aeration**

In this strategy, the oxygen absence induces different metabolisms to compete for the same substrate. For instance, in case COD was provided, denitrification would take place by heterotrophic bacteria during the anoxic period, which would remove available  $\text{NO}_2^-$ ; when aeration was to start again,  $\text{NO}_2^-$  would no more be available for NOB metabolism, which would then be unable to reproduce and grow (Lemaire et al., 2008). In addition, after the anoxic period, the activity recovery of NOB has shown a delay of around 1.5 - 12 h (this time being function of the length of the anoxic stress) (Kornaros et al., 2010, Bournazou et al., 2013). The decay rate of AOB, on the other hand, resulted lower than that of NOB when exposed to anoxic conditions (Salem et al., 2006). Therefore, the intermittent aeration could create stimulation of AOB and at the same time inhibition of NOB activities.

Another important role played by intermittent aeration is the oxygen concentration within biofilm structures (e.g. granules) at beginning and end of aeration time. At beginning of aeration oxygen will not reach the internal layers of biofilm due to high activity of aerobic biomass (de Kreuk et al., 2007a, de Kreuk et al., 2007b, Yilmaz et al., 2008), but after the complete oxidation of COD and nitrification of  $\text{NH}_4^+$ ,  $\text{O}_2$  will fully penetrate the biofilm (Meyer et al., 2005); therefore, the  $\text{O}_2$  will possibly stop denitrification and stimulate  $\text{NO}_2^-$  oxidation. In literature,  $\text{O}_2$  penetration within the biofilm could be avoided by not reducing completely the  $\text{NH}_4^+$  content in wastewater; different studies, indeed, confirmed that ammonium residual in the effluent could be considered essential for NOB out-selection (Isanta et al., 2012, De Clippeleir et al., 2013, Regmi et al., 2014). To avoid NOB activity, then, the aeration could be preventively stopped before the substrate  $\text{NH}_4^+$  is completely removed; several investigations reported good and stable nitrification by real time control on the aeration time in sequencing batch systems, both for suspended (Fux et al., 2006, Lemaire et al., 2008, Li et al., 2011) and biofilm (Lochmatter and Holliger, 2014) systems. The aeration is generally stopped after a specific parameter set-point is detected by the sensor, e.g. ammonia valley by the pH probe or ammonia breakpoint on the signal generated by the DO probe (Peng and Zhu, 2006).

Intermittent aeration as strategy to avoid oxidation of  $\text{NO}_2^-$  to  $\text{NO}_3^-$  has been used widely for treatment of high N-strength wastewater, with SBR system with both suspended (Fux et al., 2006, Lemaire et al., 2008, Li et al., 2011, Pan et al., 2014) and granular (Li et al., 2013) biomass. For continuous systems, instead, studies applying intermittent aeration to granular systems are still missing; on the other hand, research using suspended sludge to treat domestic wastewater at 25 °C (Regmi et al., 2014) and a special biofilm system for reject water treatment (Yang et al., 2015) were reported. As for the strategy of using low  $\text{O}_2$  concentrations to induce partial nitrification, also with intermittent aeration the production of  $\text{N}_2\text{O}$  could be an issue.

### 1.1.6.5. HRT and bacteria growth rate

The hydraulic retention time (HRT) can be another parameter that controls  $\text{NO}_2^-$  shunt in the reactor; when a short hydraulic retention time is applied, nitrite oxidizing bacteria are likely washed out (Hellings et al., 1998). This selection depends on different minimum required sludge ages by the different microorganisms, indeed the maximum specific growth rate of NOB is half of the AOBs at temperature of 35 °C (Khin and Annachhatre, 2004). When substrate or DO is low, the specific growth rate of NOB ( $\mu_{\text{NOB}}$ ) becomes lower than the minimum rate needed by the biomass to reproduce within the reactor and not being washed-out:

$$\frac{1}{\text{SRT}} + \beta_{\text{NOB}} > \mu_{\text{NOB}} \quad (1.10)$$

$$\frac{1}{\text{SRT}_{\text{min}}} \approx \mu_{\text{NOB}} - \beta_{\text{NOB}} \quad (1.11)$$

In the Equations 1.10 and 1.11, SRT is the solids retention time of the system,  $\beta_{\text{NOB}}$  the NOB decay rate. To wash out NOB microorganisms, the  $\mu_{\text{NOB}}$  has to be lower than the sum of the inverse of  $\text{SRT}_{\text{min}}$  and biomass decay. On the other hand, the  $\text{SRT}_{\text{min}}$  is the minimum solids retention time that allows good biomass retention within a system (Metcalf and Eddy, 2003). Therefore, to select AOB retention over the NOB, the proper SRT should be designed.

Several studies have been described to use very different HRTs, but it seems that for SBR reactors, generally, the shortest value achieved could be 6 h with granular sludge (Kim and Seo, 2006, Vázquez-Padín et al., 2010, Lochmatter et al., 2014). On the other hand, continuous systems achieved HRTs as short as 1-2 h by using reactors with different kinds of biofilm (e.g. RBC, bio-fringes, carriers and sponges) (Chuang et al., 2007, De Clippeleir et al., 2011, Okabe et al., 2011, De Clippeleir et al., 2013, Daalkhajav and Nemati, 2013, Guillen et al., 2015). A continuous granular reactor was run at 5.4 h and no other systems with a shorter hydraulic retention time have been described (Jin et al., 2008). The HRT represents, therefore, a very critical parameter for stable nitrification, shorter retention times could increase AOB wash out, but too high HRTs could produce an increase of NOB activity and destabilisation of the process.

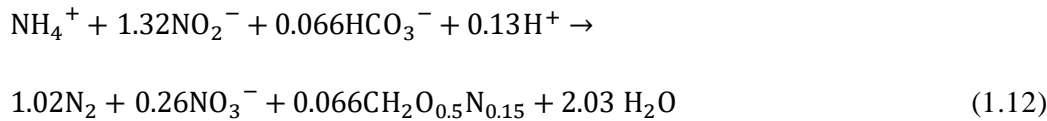
### 1.1.6.6. Inhibitors

The inhibition of NOB by hydroxylamine has been described (Hao and Chen, 1994, van der Star et al., 2008, Xu et al., 2012); these microorganisms have exhibited acute and irreversible toxicity towards the intermediate of nitrification and this may also cause  $\text{NO}_2^-$  build-up in a nitrifying system (Yang and Alleman, 1992). Another inhibitor described in literature was chlorate ( $\text{KClO}_3$ ), which selectively inhibited NOB but not AOB. Partial nitrification was achieved only by addition of chlorate in a granular reactor, no DO or temperature control were used (Xu et al., 2011). Formic, acetic, propionic and n-butyric acid were also found to have a certain inhibition on  $\text{NO}_2^-$  oxidation, whereas no obvious effects were observed for ammonium oxidation (Van Hulle et al., 2010).

### 1.1.7. ANAMMOX

The ANAMMOX pathway is carried out by a group of chemolithoautotrophic bacteria of the order *Planctomycete*. These microorganisms oxidise  $\text{NH}_4^+$  in absence of  $\text{O}_2$  using  $\text{NO}_2^-$  as the electron acceptor to

obtain N<sub>2</sub>; CO<sub>2</sub> is used as sole carbon source and reduced by the same NO<sub>2</sub><sup>-</sup> to produce biomass (Van de Graaf et al., 1996). The reaction carried out by ANAMMOX has been hypothesised as follows (Strous et al., 1999):



For each mole of NH<sub>4</sub><sup>+</sup> consumed 1.32 moles of NO<sub>2</sub><sup>-</sup> are reduced, 1.02 moles of N<sub>2</sub> gas and 0.26 moles of nitrate are produced. Two compounds are believed to be formed as intermediates, hydroxylamine (NH<sub>2</sub>OH) and hydrazine (N<sub>2</sub>H<sub>4</sub>) (not shown in Equation).

ANAMMOX shows a great potential since the total nitrogen removal rates achieved could be described as high as 26 g N L<sup>-1</sup> d<sup>-1</sup> by Tsushima et al. (2007) and 45 g N L<sup>-1</sup> d<sup>-1</sup> by Tang et al. (2010). However, to obtain an efficient treatment, a proper ammonium/nitrite ratio (1:1.32) should be provided to the system; therefore, ANAMMOX alone is generally not advisable in WWTW.

The ANAMMOX pathway shows very interesting and promising features for wastewater treatment and they can be listed as follows: (a) high nitrogen removal ability; (b) no requirement for external organic carbon source; (c) low production of excess sludge; (d) smaller reactor footprint (up to 50% less); (e) reduction of energy demand and power consumption up to 60-90% (comparison with traditional nitrification-denitrification); (f) reduction of greenhouse gas emissions (up to 90%), consumption of HCO<sub>3</sub><sup>-</sup> instead of CO<sub>2</sub> production (as in traditional denitrification). Therefore, this technology could be probably recognised one of the greatest breakthroughs of the present century in treatment of waste streams (Lackner et al., 2014, Agrawal et al., 2018).

### 1.1.8. Partial nitrification and ANAMMOX

Two configurations were described for the partial nitrification-ANAMMOX process: two-stage (PN/A), in which the two reactions take place in two separated reactors; one-stage or simultaneous nitritation and ANAMMOX (SNA), in which AOB and ANAMMOX bacteria are present in different layers of the same biofilm system. Most of the full-scale systems (88%) at the moment are represented by one-stage configuration and they are mainly located in Europe; however, there is currently a strong interest in side-stream treatment implementation in North America and China. The PN/A and SNA are mainly applied to side-stream wastewater treatment at the moment, where temperature and concentration of NH<sub>4</sub><sup>+</sup> are high enough; only few studies have reported the application of this technology to main-stream treatment with low temperature (10-17 °C) and/or low NH<sub>4</sub><sup>+</sup> (<100 mg N L<sup>-1</sup>) (Vázquez-Padín, 2009, De Clippeleir et al., 2011, Winkler et al., 2012b, Chang et al., 2013, Daverey et al., 2013, De Clippeleir et al., 2013, Hu et al., 2013, Wett et al., 2013). The main problems to face when applying this process to those conditions are: (a) very low growth rate of biomass due to the stringent temperatures of operation; (b) biomass wash-out due to low net biomass production at such low nitrogen concentration and high flow; (c) higher activity of NOB compared to AOB at low temperatures; and (d) high N<sub>2</sub>O emissions when two-stage configuration is applied (Morales et al., 2015, Schaubroeck et al., 2015).

The preference of one-stage configuration for full-scale processes is justified by: (a) high volumetric nitrogen removal rate (Van Hulle et al., 2010) and (b) significantly reduced investment costs due to the smaller footprint, lower energy for aeration and operation and lower consumption of alkalinity (Magrí et al., 2013); (c) reduced



inhibition of ANAMMOX by nitrite since its accumulation is avoided; (e) lower  $N_2O$  emissions than two-stage configuration, 0.4-1.3% compared to 2.3-6.6% of the nitrogen load (Kampschreur et al., 2008, Kampschreur et al., 2009, Joss et al., 2009, Desloover et al., 2011).

Although the two stage-configuration may seem less favourite from an economic point of view, it still shows some practical advantages for which further investigations are considered necessary; for instance it is important to mention the possibility of: (a) individual optimization of both reactions and process flexibility to a wider range of conditions (Wyffels et al., 2004, Veys et al., 2010); (b) no competition between ANAMMOX and denitrifiers for  $NO_2^-$ ; (c) absence of organic carbon,  $O_2$  and toxic compounds that could inhibit ANAMMOX (Jaroszynski and Oleszkiewicz, 2011). In addition, for high loaded waste streams the relatively high investment costs for a separated PN/A process would be compensated by possibility to retrofit previous tanks, by the lower operational costs and efficient nitrogen removal performance (Hao et al., 2001, Nielsen et al., 2005). Moreover, at the moment the main bottleneck of the ANAMMOX based processes application to the main-stream of WWTPs seems to be the proliferation of NOB which contribute to an excessive presence of  $NO_3^-$  in the effluent (De Clippeleir et al., 2013, Wett et al., 2013). Perhaps, the use of a two-stage reactor configuration could allow using a more efficient operational strategy to avoid the  $NO_2^-$  oxidizing bacteria development without affecting the ANAMMOX bacteria.

### 1.1.9. Energy requirements for wastewater nitrogen removal

For a specific application the available alternatives for nitrogen elimination need to be evaluated on a multitude of cost aspects, chemical and energy requirements, operational experience, process reliability and environmental impact. However, the selection of the best alternative is generally based on cost-effectiveness. For traditional nitrification-denitrification (N/DN) approximately 4.57 kg  $O_2$  and ~3.5 kg COD (methanol) are needed per kg of  $NH_4-N$  converted; when PN process is used, instead, it will result in 25% savings in electricity for oxygen pumping (3.43 kg  $O_2$   $kg^{-1}$   $NH_4-N$ ) and 40% savings in costs for COD addition (~2.1 kg COD  $kg^{-1}$   $NH_4-N$ ) (Figure 1.1). With PN/A and SNA, further costs for electricity for  $O_2$  pumping will be cut, no longer organic carbon will be necessary and sludge production will also be reduced (Figure 1.2b and c) (Ahn, 2006, Magrí et al., 2013, Lackner et al., 2014). Nitrate produced by the ANAMMOX bacteria in both PN/A and SNA would require a little amount of organic carbon to be reduced to  $N_2$  gas; however, most real wastewaters contain a small amount of biodegradable COD, which can be used to denitrify the produced  $NO_3^-$ .

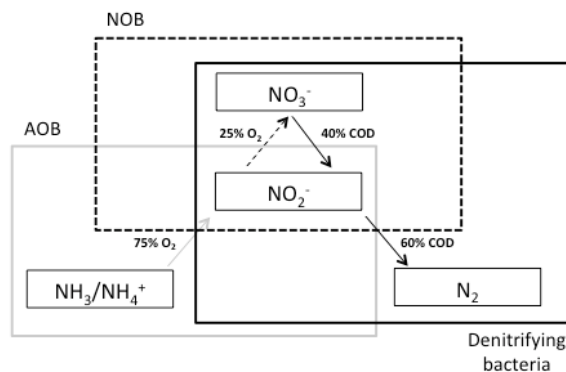


Figure 1.1 - Oxygen and COD requirements for traditional nitrification/denitrification.

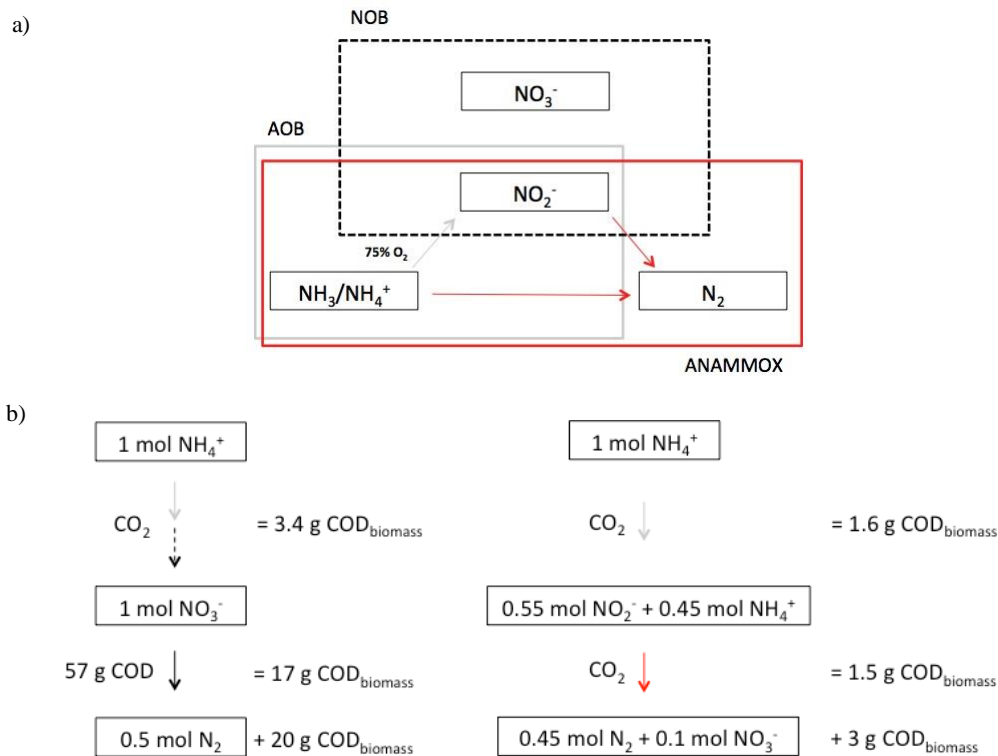


Figure 1.2 – a) Oxygen and COD requirements for PN/ANAMMOX and b) comparison of sludge production between traditional nitrification/denitrification and PN/ANAMMOX (Fux et al., 2002).

Table 1.2 - Process requirements for some of the main biological technologies used in WWTPs (Ahn, 2006, Van Hulle et al., 2010, Mulder, 2003, Lackner et al., 2014)

Process	Oxygen	Organic needed <sup>a</sup>	Alkalinity	Sludge production
	kg O <sub>2</sub> kg N <sup>-1</sup>	kg COD kg N <sup>-1</sup>	kg CaCO <sub>3</sub> kg N <sup>-1</sup>	kg d.w. kg N <sup>-1</sup>
Nitrification-denitrification	4.57	3.5	7.07	1-1.2
Nitritation-denitritation	3.43	2.1	7.07	0.8-0.9
Partial nitritation <sup>b</sup> -ANAMMOX	1.71-2.06	-	3.81	< 0.1
SNA	1.94	-	3.68	< 0.1

<sup>a</sup> calculations for methanol

<sup>b</sup> 50 to 60% partial nitritation

The main process requirements for biological technologies in WWTPs are given in Table 1.2. The buffering capacity for both PN/A and SNA processes (3.81 and 3.68 kg CaCO<sub>3</sub> kg<sup>-1</sup> NH<sub>4</sub>-N, respectively) results lower than N/DN and PN (7.07 kg CaCO<sub>3</sub> kg<sup>-1</sup> NH<sub>4</sub>-N); moreover, for PN/A and SNA when treating some waste streams, e.g. reject water, further alkalinity addition is not necessary, resulting in significant pH control costs savings (Vlaeminck, 2009). The sludge production decreases from 1-1.2 kg d.w. kg N<sup>-1</sup> (d.w. = dry weight) for N/DN, to

0.8-0.9 and to <0.1 kg d.w. kg N<sup>-1</sup> for PN-denitrification and PN/A, respectively (Mulder, 2003). As a consequence, sludge treatment and disposal costs significantly decrease.

High nitrite concentrations in oxygen limited environments are a major cause of N<sub>2</sub>O emissions through the nitrification process (Kampschreur et al., 2009). The amount of N<sub>2</sub>O emissions from the PN/A system are slightly higher than from an N/DN system but much higher than in SNA. In Table 1.3 are reported the energy requirements for some of the main processes used for nitrogen removal in WWTW; the data have been taken from a previous survey on energy estimation for one type of waste stream, reject water. The values are mainly accounting the chemicals, the electricity and the fuel used during the processes. The costs for transporting are not taken into account since it is considered similar to all processes. According to what the survey states, for air stripping operation, a great amount of sulphuric acid (H<sub>2</sub>SO<sub>4</sub>) is required for each kg of N treated to absorb the gaseous NH<sub>3</sub> (H<sub>2</sub>SO<sub>4</sub>:NH<sub>3</sub> molar ratio of 1.1:2). The process requires, in addition, calcium oxide (CaO) to increase the pH above 10. High energy is also needed considering the heat provided to the air/steam used in this technology. Struvite precipitation requires a molar Mg:P:N ratio of 1.3:1:1 that can be considered as adding 2.3 kg Mg and 2.2 kg P for each kg of NH<sub>4</sub>-N treated. The presence of competitive cations (e.g. calcium) can produce some sort of influence on the process performance, resulting in the formation of other phosphate salts rather than struvite and arising the costs for further chemicals utilisation. During the concentration for vacuum evaporation great amount of energy is used to reach the right temperatures and pressures used during the process. In reverse osmosis systems, the retention of NH<sub>4</sub><sup>+</sup> is better than that of the uncharged NH<sub>3</sub>, therefore acid addition to the supernatant enhances the separation performance, but at the same time increases the costs for chemicals. The energy for replacement of membranes should also be taken into account to calculate the costs of this technology.

Table 1.3 - Estimation of running energy demand for digester supernatant treatment, N content in the supernatant assumed to be 2.3 g NH<sub>4</sub>-NL<sup>-1</sup>; source:(Magrí et al., 2013).

Process	Primary energy consumption (MJ m <sup>-3</sup> )	
	per volume unit of supernatant processed	per mass unit N processed (specific energy)
PN/A	43	19
Nitritation-denitritation	130	57
Air stripping	114	50
Struvite precipitation	136	59
Concentration by vacuum evaporation	319	139
Concentration by reverse osmosis	124	54

Based on the results of the cited survey, it is possible to understand how the biological partial nitrification/ANAMMOX technology represents a very promising and cost-effective technology in the wastewater treatment. The costs for investment in this technology are very site-specific since existing reactors and machinery of the WWTW could be used, instead of building new ones. These results show how PN/A and SNA are very promising technologies for nitrogen wastewater treatment by overcoming the high costs of operation and chemicals for both previous traditional biological processes and physicochemical technologies.

## **1.2. Research objectives**

### **1.2.1. Fast start-up of partial nitrifying granules reactor and its long-term stable operation**

Due to the importance of applying partial nitrifying technology to the removal of ammonium from high and middle strength wastewater, it is necessary to implement strategies that could shorten the time needed for the process start-up. In addition, compared to the previous research done on this topic, certain autonomy of WWTWs is needed and reduction of external inocula purchasing is essential.

For these reasons, a novel strategy will be proposed in which partial nitrifying granules are quickly produced by using heterotrophic granules as biomass retention factor. Conventional activated sludge will be inoculated into an SBR reactor to quickly produce heterotrophic granules. A specific operational strategy will be used to accumulate nitrifying bacteria and avoid starvation of heterotrophic bacteria, granules structure disintegration and AOB inhibition. This will be done by adjusting the COD/N ratio during the first part of the experiment. In addition, since this strategy could be applied for typical anaerobic digesters effluent, the temperature effects on the fast heterotrophic granulation and formation of partial nitrifying granules will be investigated.

### **1.2.2. Physical, chemical and biological characteristics of partial nitrifying granules treating middle strength ammonium wastewater with high water hardness**

Precipitation of calcium phosphate as hydroxyapatite within granular sludge represents an interesting way to remove and at the same time recover P from wastewater. The bio-precipitation mechanism is still not quite understood and most of all, no description of such process was described before in a partial nitrifying system with a AOBs-dominant community.

Therefore, since minerals precipitation was observed within the granules produced in the first objective, the characterisation of different size partial nitrifying granules will be done. Hence, physical features, morphology and bioactivity will be investigated and the factors inducing bio-precipitation and the crystalline architecture of the precipitates discussed.

### **1.2.3. Study on EPS extraction from sludge with high mineral content and relevant factors for reliable protein measurement**

EPS plays a fundamental role in wastewater treatment by biological systems and mostly in granular sludge processes. Due to the contradictory results from literature on the EPS composition, a further improvement of the extraction methodologies and analytical protocols is needed. The modified Lowry method determination is widely used for measuring the proteins content analysis in wastewater treatment; however, it is known that soluble cations could interact with its reagents and create erroneous measurements. When EPS is extracted by chemical procedures such as formaldehyde plus NaOH from granular sludge that shows mineral precipitation (i.e. calcium carbonate or calcium phosphate), it is thought that both minerals and soluble calcium could be found in the final extracted solution and interfere with the Lowry method.

Since there is no mention of a possible interference of this kind in literature, a series of experiments will be done. The chemical formaldehyde/NaOH procedure will be first compared to a physical extraction, i.e. heat; then, the influence of calcium concentration on Lowry method will be investigated. From these studies, an optimised procedure to measure PN from EPS extracted from high ash content granular sludge will be produced.

#### **1.2.4. Reactivating ammonium removal activity of nitrifying biomass after inhibition using external electrostatic field**

The inhibition by chemicals contained in the wastewater is, together with the bacteria slow growing metabolism, another factor that explains the long time needed for nitrifying systems start-up. The positive effects of electric field application on the enhancement of activity and growth rate in different biological systems have been reported. However, no literature was found on the possible effect of this technology to recover the  $\text{NH}_4^+$  removal activity of nitrifying biomass after inhibition. Therefore, by using batch tests, the effects of duration and intensity of static electric field on activity will be investigated; then, the biomass will be fed with synthetic wastewater with two different inhibitors (i.e. NaCl and phenol) and the ammonium removal activity will be measured. Finally, the biomass will be treated by electric field technology and the activity will be analysed again. A possible novel application of electric field technology for enhancement of nitrifying biomass activity will be described.

The present study investigated the effects of the electric field application on inhibited nitrifying biomass by a series of batch tests. First, preliminary tests will be done to find the optimal duration and intensity of the EF; then, the biomass will be fed with different concentrations of known inhibitors (i.e. salinity and phenol) and the ammonium removal will be controlled. Finally, the EF will be implemented and the effects on the inhibited nitrifying biomasses will be described by measuring the ammonium removal once more.



**FAST START-UP OF PARTIAL NITRIFYING GRANULES REACTOR AND  
ITS LONG-TERM STABLE OPERATION AT HIGH CALCIUM  
CONCENTRATION**





## 2.1. Introduction

For the two-stages nitrogen removal processes such as partial nitrification followed by denitrification or partial nitrification followed by ANAMMOX, the enrichment of ammonia oxidising bacteria (AOBs) and the inhibition or elimination of nitrite oxidising bacteria (NOBs) in the first stage, are of main importance (Lackner et al., 2014, Agrawal et al., 2018). AOBs are slow growing bacteria (Wiesmann, 1994), sensitive to many environmental conditions such as pH, free ammonia (FA), free nitrous acid (FNA), and other toxic compounds (Anthonisen et al., 1976). Therefore, how to retain AOBs in the reactor and to overcome their inhibition by the environment, have been extensively investigated (Soliman and Eldyasti, 2018). Compared with biomass retention technology (i.e. biofilm and membrane bioreactor), aerobic granular sludge is relatively new; anyhow, it shows considerable potential to replace activated sludge technology due to the process simplicity, great settling skills, high biomass retention and tolerance to inhibition (Sarma and Tay, 2018a).

A few studies have been done on partial nitrification with aerobic granules technology and positive results have been obtained for real application in the practice. Due to the slow growth rate of AOBs and the combined requirement of both granulation and only enrichment of AOBs, however, the granulation of suspended activated sludge still takes long time; this was usually described as 3 - 5 months in lab-scale reactors and might take longer in pilot- and full-scale systems (Song et al., 2013, Wei et al., 2014). When nitrifying sludge is used as inoculum, the time taken to form nitrifying granules can go down to 70 days (Kim and Seo, 2006). To ensure a short granulation period for full scale application, different strategies were studied during the last decade. For instance, static magnetic field was applied to shorten nitrifying granulation period from 41 to 25 days, due to the enhancement of settling skills and production of extracellular polymeric substances (EPS) content in the granules (Wang et al., 2012). Tsuneda et al. (2004) observed a quicker nitrifying granules formation after metals addition; the precipitating minerals worked as nucleation sites for the bacteria to attach and the granules to develop. Both these two strategies are effective but need accessory approaches such as magnetic field or chemical dosage to accelerate nitrifying granulation, resulting in extra costs of operation. On the other hand, manipulating the reactor operation would involve lower costs and would be thus preferred. By stepwise increase of nitrogen (N) loading rate and applying short settling time, Chen et al. (2015) could reduce the nitrifying granulation period to 55 days. The inoculation of heterotrophic granules could specifically enhance the retention of AOBs present in wastewater, while NOBs were washed out (Wang et al., 2016); however, also to form heterotrophic granules takes time and, if considering both the heterotrophic granules formation and their enrichment with AOBs, the final time to achieve partially nitrifying granules would still be too long. It has been reported that combined short settling time and high organic loading rate (OLR) can form heterotrophic granules within 24 hours and the reactor can reach steady state within one week (Liu and Tay, 2015) by seeding activated sludge with a wide range of settling ability (i.e. from poor to good). Thus, if the short settling time and high OLR strategy was used to form heterotrophic granules and then they were enriched by AOBs, the total start-up period for the formation of partial nitrifying granules could be shortened. A strong selection pressure strategy was adopted in this study and it is believed that the slow growing bacteria would be easily washed out of the reactors. Thus, converting quickly formed heterotrophic granules to partial nitrifying granules might still take some time and some operational strategies have to be optimized to accelerate the enrichment process, as well as maintaining the structure of the formed granules.

Therefore, this study aims to shorten the overall formation period of partial nitrifying granules by quickly forming heterotrophic granules first; then, they will be transformed into nitrifying granules with a specific operational strategy, which is mainly a step-wise decrease of COD/N, to avoid sudden starvation of heterotrophic granules, disintegration of granules and AOB inhibition. Since side streams after anaerobic digestion usually have

high temperatures (35 °C and above), this study will also investigate temperature effects on the fast formation of partial nitrifying granules. Furthermore, the produced partial nitrifying granules will be characterized to investigate the effects of the proposed strategy on their properties.

## 2.2. Materials and methods

### 2.2.1. Reactors operation and inoculum

Four Perspex columns (R1, R2, R3 and R4) with a working volume of 2.6 L and a column height to diameter ratio of 20 ( $\varnothing$  60 mm) were operated sequentially with a cycle time of 4 hour (Figure 2.1). The cycle consisted of 10-min feeding, 227-199 min aeration, 2-30 min settling time and 1-min discharging. The effluent was discharged from the middle port of the reactors, corresponding to a volumetric exchange ratio of 50%. The air was provided from the reactor bottom with a flow rate of  $5 \text{ L min}^{-1}$  (superficial velocity =  $2.948 \text{ cm s}^{-1}$ ).

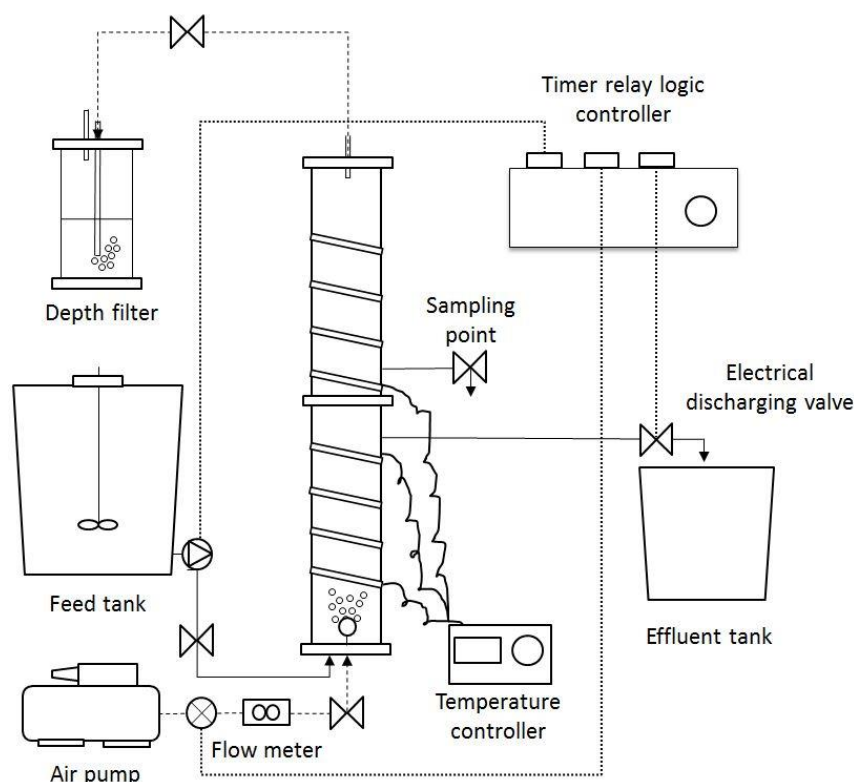


Figure 2.1– SBR configuration of reactors used in the experiment.

The reactors were started up by inoculating  $3.2 \text{ g L}^{-1}$  conventional activated sludge from Portswood Municipal WWTP, Southampton, UK. The reactor operation was divided into four phases: phase 1, the inoculated activated sludge was converted into heterotrophic granules by providing high OLR and short settling time; phase 2, the nitrifying bacteria were enriched within heterotrophic granules by decreasing COD/N ratio until no organic carbon was provided; phase 3,  $\text{NH}_4^+$  concentration was quickly elevated to speed-up the AOBs enrichment; phase 4, long-term stability of nitrification system with constant parameters. The operational conditions are also listed in Table 2.1. The reactors were maintained at the specific temperatures for at least three months, after which they had a slight increase due to summer days, i.e. 25-27 and 34-35, within R1/R3 and R2/R4, respectively.

Table 2.1 – Operational conditions of experiment.

	Units		R1	R2	R3	R4
	Temperature	°C	18-23	30-33	18-23	30-33
Phase 1 (0-21)	COD	mg L <sup>-1</sup>	1000	1000	1000	1000
	NH <sub>4</sub> <sup>+</sup>	mg N L <sup>-1</sup>	50	50	200	200
	COD/N		20	20	5	5
Phase 2 (22-37/49 <sup>a</sup> )	COD	mg L <sup>-1</sup>	1000 to 0	1000 to 0	1000 to 0	1000 to 0
	NH <sub>4</sub> <sup>+</sup>	mg N L <sup>-1</sup>	50 to 400	50 to 850	200 to 150	200 to 750
Phase 3 (38/50 <sup>a</sup> -107)	NH <sub>4</sub> <sup>+</sup>	mg N L <sup>-1</sup>	Varied influent ammonium concentration <sup>b</sup>			
Phase 4 (108-171)	NH <sub>4</sub> <sup>+</sup>	mg N L <sup>-1</sup>	500	65	650	850

<sup>a</sup> Phase 2 lasted till day 37 for R2 and R4 and till day 49 for R1 and R3.

<sup>b</sup> The NH<sub>4</sub><sup>+</sup> concentration was fluctuating until the values in phase 4 (R2 collapsed so the NH<sub>4</sub><sup>+</sup> needed to be reduced).

### 2.2.2. Medium

The nitrogen, carbon and phosphorous sources were provided by addition of ammonium sulphate, sodium acetate and mono-potassium phosphate (15 mg PO<sub>4</sub><sup>3-</sup>-P L<sup>-1</sup>), respectively. For nitrifying bacteria enrichment during phase 2, the organic carbon concentration was stepwise reduced together with ammonium and inorganic carbon increase (14 mg NaHCO<sub>3</sub> mg<sup>-1</sup> NH<sub>4</sub><sup>+</sup>-N L<sup>-1</sup> or 7.14 mg CaCO<sub>3</sub> mg<sup>-1</sup> NH<sub>4</sub><sup>+</sup>-N L<sup>-1</sup>); the bicarbonate was representing both the carbon source for autotrophic biomass growth and the buffer solution for neutralisation of protons produced by nitrification process. During phase 4, the ammonium concentrations were kept constant since the nitrifying granules had reached the process stability.

Apart from carbon, nitrogen and phosphorus sources, micronutrients to the synthetic wastewater were added as (per litre prepared): 25 mg CaCl<sub>2</sub>•2H<sub>2</sub>O, 20 mg MgSO<sub>4</sub>•7H<sub>2</sub>O, 10 mg FeSO<sub>4</sub>•7H<sub>2</sub>O. The trace elements were (per litre prepared): 0.12 mg MnCl<sub>2</sub>•4H<sub>2</sub>O, 0.12 mg ZnSO<sub>4</sub>•7H<sub>2</sub>O, 0.03 mg CuSO<sub>4</sub>•5H<sub>2</sub>O, 0.05 mg (NH<sub>4</sub>)<sub>6</sub>Mo<sub>7</sub>O<sub>24</sub>•4H<sub>2</sub>O, 0.1 mg CoCl<sub>2</sub>•6H<sub>2</sub>O, 0.1 mg NiCl<sub>2</sub>•6H<sub>2</sub>O, 0.05 mg AlCl<sub>3</sub>•6H<sub>2</sub>O, 0.05 mg H<sub>3</sub>BO<sub>3</sub>. Tap water was used to prepare the synthetic wastewater with a total Ca<sup>2+</sup> concentration of around 100-150 mg Ca<sup>2+</sup> L<sup>-1</sup>. From phase 3 (day 47), both CaCl<sub>2</sub> and MgSO<sub>4</sub> were removed from feedstock, since an excessive inorganic carbonate precipitation within the granules occurred. The synthetic wastewater pH was not adjusted but it was around 7.2-7.4.

### 2.2.3. Analytical methods

The pH in the columns (during aeration) and from the effluent, was daily monitored by using a bench pH meter (Mettler Toledo). Sludge volume index (SVI), ash content, mixed liquor volatile suspended solids (MLVSS) and mixed liquor suspended solids (MLSS) and COD were measured by using standard methods (APHA, 2012); the settled sludge volumes were recorded after 5 and 30 minutes within a 100-mL graduated cylinder (SVI<sub>5</sub> and SVI<sub>30</sub>, respectively). After granules formed, the standard method for MLVSS and MLSS analysis was replaced by the density method used by Beun et al. (1999) due to difficulty for homogenous sampling. Ammonium was measured spectrophotometrically by following the procedure in accordance with that in the manual BSI (1984), and using the UV-Visible spectrophotometer Cecil 3000 series (Cecil Instruments Ltd., UK). The concentration in solution of free ammonia and free nitrous acid (FA and FNA) was calculated by Equation 2.1 and Equation 2.2 (Ford et al., 1980):

$$NH_3 = \frac{[NH_4 - N] * 10^{pH}}{K + 10^{pH}} \quad (2.1)$$

$$HNO_2 = \frac{[NO_2 - N] * 10^{-pH}}{Y + 10^{-pH}} \quad (2.2)$$

Where

$$K = e^{\frac{6334}{273+T}} \quad (2.3)$$

$$Y = e^{-\frac{2300}{273+T}} \quad (2.4)$$

Anions ( $NO_2^-$ ,  $NO_3^-$ ,  $PO_4^{3-}$ ) and cations ( $Ca^{2+}$  and  $Na^+$ ) were measured by the ionic chromatographer 882 Compact IC plus (Metrohm, Switzerland). For the anions a Metrosep A Supp 5 - 150/4.0 column was used and the eluent was a solution of 1 mM  $NaHCO_3$  and 3.2 mM  $Na_2CO_3$ . For cations the Metrosep C4 250/4.0 column was used with the eluent containing 1.7 mM  $HNO_3$  and 0.7 mM  $C_7H_5NO_4$  (dipicolinic acid or Pyridin-2,6-dicarboxylic acid). The nitrite accumulation rate (NAR) was evaluated by using Equation 2.5, in which  $NO_2^-$  and  $NO_3^-$  are the concentrations of effluent nitrite and nitrate.

$$NAR (\%) = \left( \frac{NO_2^-}{NO_2^- + NO_3^-} \right) \times 100 \quad (2.5)$$

#### 2.2.4. Granules physical characteristics

The morphology of granule external and internal surfaces was observed by halving the particle and using the Quanta 250 scanning electron microscopy (SEM) (FEI, Oregon, USA). Samples were first fixed overnight with a solution of 3% glutaraldehyde + 4% formaldehyde in 0.1 M PIPES buffer with a pH of 7.2 (even if one-hour incubation would be still enough for this kind of samples). Then, the specimens were washed twice for 10 minutes with 0.1 M PIPES buffer with pH of 7.2, followed by a series of dehydration steps of 10 minutes' washes with ethanol 30%, 50%, 70% and 95%; finally, two rinses with absolute ethanol lasting 20 minutes each were done. The samples were then dried by a Balzers CPD 030 Critical Point Drier, before being carbon coated by a high resolution sputter and high vacuum carbon coater (Quorum, Q150T ES, West Sussex, UK). In addition, the coupled energy dispersive X-ray spectroscopy (EDX) was used with SEM (EDAX, New Jersey, USA) to analyse qualitatively the chemical elements present in the granule.

When particle size was smaller than 2000  $\mu m$ , it was measured by a laser particle size analyser system (PSA, Malvern Mastersizer 2000); for particle size over 2000  $\mu m$ , photos of sludge taken by Leica MZ16F stereomicroscope were analysed by ImageJ software.

### 2.2.5. Elemental and mineralogical analyses

The samples were lyophilised and then ground into fine powder for qualitative element analysis by X-ray diffraction (XRD), using a Bruker D2 phaser (Bruker AXS Gmgh, Karlsruhe, Germany).

Quantitative elemental composition within the granules was obtained by using a multi collector inductively coupled plasma emission spectrometer (X-SERIES 2 ICP-MS, Thermo Fisher Scientific, Bremen, Germany). Before the analysis, the sample was dried overnight at 105 °C and then ground into powder. The sample (50 mg) was then digested by adding 2 mL of aqua regia (a 1:3 mixture of 68% nitric acid and 36% hydrochloric acid) and 0.5 mL perchloric acid (68%) in a Teflon digestion vessel on a hotplate (150 °C) overnight. After digestion, the sample went completely dry and the vessel was opened to add 10 mL of concentrated hydrochloric acid (36%); after evaporation of the acid, prior to ICP-MS analysis, 3% nitric acid was added to the sample. The elements investigated were mainly the ones contained in the synthetic feedstock solution (e.g. Na, Mg, P, K, Ca and Fe). Since the analyses were sensitive to minimal amounts of metals, the all procedure was done by avoiding any source of metals and glass (e.g. spatulas, aluminium crucibles, glass vials, etc.). The data processing was done using the Plasmalab software.

The software Statistical Package for Social Science (SPSS V24, Inc., USA) was used to run a one-way ANOVA test to determine if the difference of ash content within the 4 reactors from day 100 to 150 was significant.

### 2.2.6. Saturation index

The saturation index (SI) of different minerals was calculated by using the software Visual MINTEQ (version 3.3), which uses the Davies equation to calculate the activity coefficients based on the chemicals contained in the feedstock (Mullin, 2001). The SI for each mineral was calculated as:

$$SI = \log \frac{IAP_a}{K_{sp_a}} \quad (2.6)$$

Where  $IAP_a$  is the ion activity product of the elements in a and  $K_{sp}$  is the solubility product constant of a; at values of SI above the zero, the compound was considered oversaturated, which means that the conditions in the system could favour its precipitation; on the other hand, under saturation was considered when the calculated values of SI were below zero. The SIs were calculated separately for R1, R2, R3 and R4 during phase 1, due to the different ammonium sulphate concentrations and temperatures in each. Then saturation index was also measured for R3 and R4 on day 70, when sodium bicarbonate and ammonium sulphate concentrations in the feedstock were highest. The SIs were calculated only within two reactors due to the similarity in chemicals concentration and pH values reported in both R1 and R2. The parameters used for SI calculations were temperature, pH and alkalinity and the concentrations of acetate,  $NH_4^+$ -N,  $PO_4^{3-}$ -P,  $Ca^{2+}$ ,  $Mg^{2+}$ ,  $Fe^{2+}$ ,  $Na^+$ ,  $Mn^{2+}$ ,  $K^+$ ,  $Zn^{2+}$ ,  $Cu^{2+}$ ,  $Co^{2+}$ ,  $Ni^{2+}$ ,  $Al^{3+}$ ,  $H^+$ ,  $SO_4^{2-}$ ,  $Cl^-$ ,  $Mo^-$  and  $BO_3^-$ .

## 2.3. Results

### 2.3.1. The fast formation of heterotrophic granules at different temperatures and COD/N ratios

Temperature effects on granulation were studied at two different influent COD/N ratios, i.e. 5 and 20. It was found that the effects of COD/N ratios on granulation were similar at two different temperatures. In this case, only results with COD/N ratio of 5 from R3 and R4 were discussed. Figure 2.2 shows the profiles of SVI<sub>5</sub>, MLVSS, sludge volume percentage with particle size smaller than 200 μm (volume <200 μm) and sludge mean size in R3 at 18-23 °C and R4 at 30-33 °C, during the granulation period from day 0 to day 21 (phase 1). It can be seen that SVI<sub>5</sub> increased sharply in both reactors in the first 3 days and then decreased quickly to less than 100 mL g<sup>-1</sup> after day 7. This phenomenon is in agreement with Liu et al. (2010b) and Liu et al. (2011), indicating a typical change of SVI<sub>5</sub> for fast granulation. Once SVI reduced to less than 100 mL g<sup>-1</sup>, the average sludge size started to increase quickly (Figure 2.2d) along with the decrease in sludge volume percentage with particle size smaller than 200 μm (Figure 2.2c). Although SVI<sub>5</sub> in both reactors are similar, sludge size increased more quickly in R3 at 18-23 °C (Figure 2.2d), resulting in higher biomass concentration in R3 (Figure 2.2b). On day 21, MLVSS in R3 at ambient temperature reached 4.6 g L<sup>-1</sup> while it was only 3.0 g L<sup>-1</sup> in R4 at 30-33 °C. Based on the definition of granulation by Liu and Tay (2007) that sludge volume percentage with particle size smaller than 200 μm below 50% represents the formation of granule dominant sludge, granular sludge formed on day 9 in R3 at 18-23 °C while it was on day 11 in R4 at 30-33 °C.

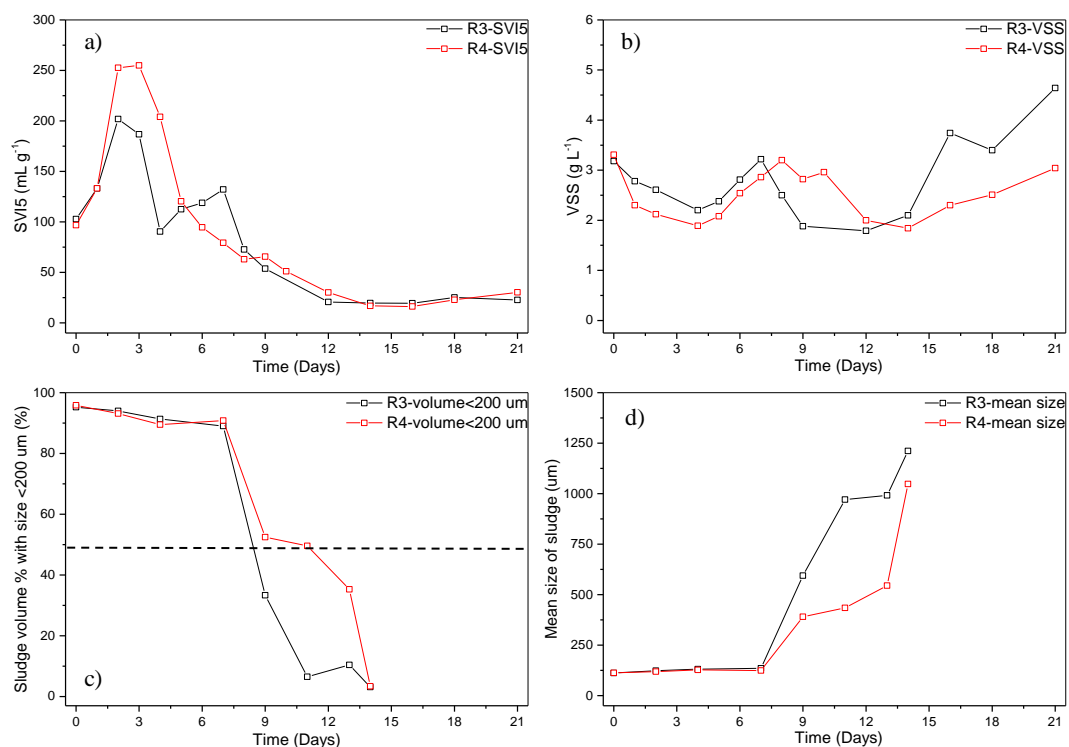


Figure 2.2 - a) profiles of SVI<sub>5</sub>, b) MLVSS, c) sludge volume percentages with size smaller than 200 μm and d) sludge mean size over time during phase 1 in R3 (18-23 °C) and R4 (30-33 °C) with 200 mg NH<sub>4</sub><sup>+</sup>-N L<sup>-1</sup> of influent N and COD/N of 5.

This suggests that higher temperature has a slightly negative effect on granulation in the lab-scale reactors, but this effect might be magnified in larger scale reactors because larger scale reactors took longer time to form granules (Ni et al., 2009, Liu et al., 2010b). If side-stream from digester was directly used to start up a granular sludge reactor, it is expected that granulation would be slower.

For real wastewater treatment in the practice, it is less likely to adjust COD/N ratio by reducing N concentration. Thus, it is necessary to study if high influent ammonium nitrogen concentration affects the rapid formation of granules. Since effects of COD/N ratio on granulation were not affected by temperature, only the results from reactors run at 30-33 °C were shown in Figure 2.3. Both SVI<sub>5</sub> values increased within the first 3 days with a following quick decrease to less than 100 mL g<sup>-1</sup> within a week. The sludge in R4 with influent ammonium at 200 mg NH<sub>4</sub><sup>+</sup>-N L<sup>-1</sup> showed a quicker increment in size, reaching 1000 μm on day 14. Based on the definition of granule dominant sludge mentioned above, granular sludge formed on day 11 in R4, while after day 13 in R2 run with influent ammonium concentration of 50 mg L<sup>-1</sup>. Because of faster granulation, R4 achieved higher biomass accumulation with a concentration of 3.0 g MLVSS L<sup>-1</sup>, whereas it was 1.8 g MLVSS L<sup>-1</sup> in R2 on day 21. These results suggest that 200 mg NH<sub>4</sub><sup>+</sup>-N L<sup>-1</sup> in influent and a lower carbon to nitrogen ratio facilitate a slightly quicker granulation. This is good for the start-up of such systems because it means that the variable ammonium concentration range, especially a high influent ammonium concentration and a low COD/N ratio, will not limit the process applicability.

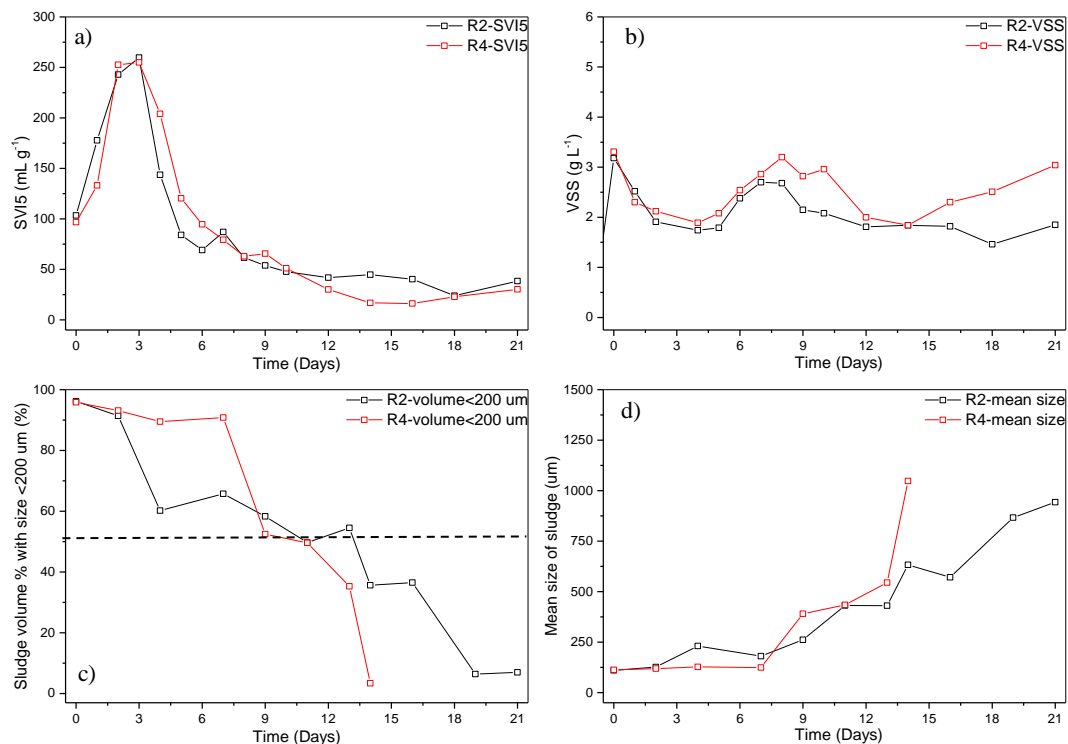


Figure 2.3 - a) profiles of SVI<sub>5</sub>, b) MLVSS, c) sludge volume percentages with size smaller than 200 μm and d) sludge mean size over time during phase 1 in R2 (COD/N at 20 and 50 mg NH<sub>4</sub><sup>+</sup>-N L<sup>-1</sup>) and R4 (COD/N at 5 and 200 mg NH<sub>4</sub><sup>+</sup>-N L<sup>-1</sup>) at operational temperature of 30-33 °C.



In these four reactors with different operation temperatures and influent ammonium concentrations, only heterotrophic bacteria grew dominantly as short settling time was adopted for the rapid granulation without ammonia oxidizing bacteria accumulating. The growth rate of heterotrophic bacteria at higher temperature and high COD/N ratio (low ammonium concentration without inhibition from ammonium) is higher than that at lower temperature and low COD/N ratio. The higher growth rate of heterotrophic bacteria in the study range resulted in slower granulation. Therefore, ambient temperature and higher ammonium concentration are favourable to the formation of heterotrophic granules.

### 2.3.2. Transforming heterotrophic granules into nitrifying granules by enriching nitrifying bacteria in rapidly formed heterotrophic granular sludge during phase 2

On day 14, both R3 and R4 showed pure granules, whereas sludge in R1 and R2 was a mixture of granules and suspended sludge. On day 20, all sludge in 4 reactors was almost pure granules. To transform heterotrophic granules to nitrifying granules, a step-wise increase in influent  $\text{NH}_4^+\text{-N}$  and decrease in COD were carried out from day 21. The influent ammonium concentration was increased from  $100 \text{ mg NH}_4^+\text{-N L}^{-1}$  step wisely with COD decreased concurrently over the time (Figure 2.4). COD supply to R2 and R4 was completely stopped in the synthetic wastewater from day 38, and from day 47 and 49 for R1 and R3, respectively. By the end of phase 2, heterotrophic granules were completely transformed into autotrophic nitrifying granules with 400, 850, 150 and  $750 \text{ mg L}^{-1}$  influent  $\text{NH}_4^+\text{-N}$  in R1, R2, R3 and R4, respectively.

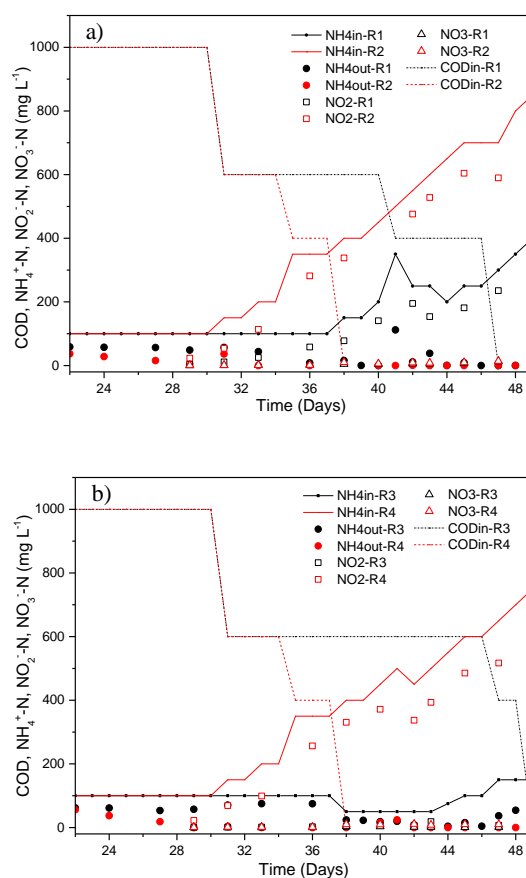


Figure 2.4 - Profiles of nitrogen species and COD over the time during phase 2 in a) R1 and R2 and b) R3 and R4.

On day 21, the removed COD over the removed N ratios for R1 and R2 were 23.19 and 19.19, respectively, which are very close to the typical COD/N ratio, i.e. 20, for assimilation of heterotrophic sludge (Metcalf and Eddy, 2003). However, the removed COD/N ratios were around 10 in both R3 and R4 from day 0, suggesting that ammonium oxidizing bacteria were already present in the inoculum and quickly accumulated within the systems with influent  $\text{NH}_4^+$  concentration of  $200 \text{ mg NH}_4^+-\text{N L}^{-1}$ . The nitrifying bacteria were able to enrich quickly in granules once granules formed due to the retention of granular sludge and long sludge retention time. Nitrification activity was observed on day 27 and 35 in R2 and R1, respectively.

On day 58,  $\text{NH}_4^+$  removal efficiency was 92.15, 96.19, 95.87 and 99.14% for R1, R2, R3 and R4, respectively, with influent  $\text{NH}_4^+$  concentrations of 700, 900, 600 and  $1000 \text{ mg NH}_4^+-\text{N L}^{-1}$ , corresponding to 1.89, 2.45, 1.61 and  $2.72 \text{ g NH}_4^+-\text{N L}^{-1} \text{ d}^{-1}$  nitrogen loading rates (NLRs). This indicates that higher temperature in R2 and R4 is beneficial for the rapid enrichment of nitrifying bacteria due to the higher specific growth rate of nitrifying bacteria at higher temperature. In all reactors, ammonium was mainly oxidized to nitrite with negligible nitrate production (less than  $10 \text{ mg L}^{-1}$ ). Within 37 days, heterotrophic granules were completely transformed into partial nitrifying granules to treat nitrogen rich wastewater with influent  $\text{NH}_4^+-\text{N}$  concentration as high as  $950 \text{ mg L}^{-1}$  at  $30\text{-}33 \text{ }^\circ\text{C}$  and  $650 \text{ mg L}^{-1}$  at ambient temperature. Similar results were also reported by Chen et al. (2015) where nitrifying granules could treat  $1000 \text{ mg NH}_4^+-\text{N L}^{-1}$  in less than 55 days from reactor start-up. However, nitrifying sludge was inoculated in their reactors while activated sludge was inoculated in our study. The strategy used in this study to form heterotrophic granules rapidly first and then transform heterotrophic granules to nitrifying granules, results in the quicker formation of partial nitrifying granules compared with 70 and 146 days reported in other studies (Kim and Seo, 2006, Song et al., 2013, Wei et al., 2014).

After day 58, influent  $\text{NH}_4^+$  concentration was further increased (Figure 2.5) but all reactors gradually showed reduced ammonium removal efficiency with high effluent ammonium concentration (even  $>400 \text{ mg NH}_4^+-\text{N L}^{-1}$ ). The reactors instability was explained by the concomitant increase of free ammonia (FA) concentration, as showed in Figure 2.6a; the reached FA in R2 and R4 was higher than  $120 \text{ mg N L}^{-1}$  on day 52, which was previously described in literature as the highest concentration at which AOB activity could be inhibited (Anthonisen et al., 1976). On the contrary, the free nitrous acid (FNA) was shown not to be a reason for the partial nitrification inhibition, as showed by the lower concentration in Figure 2.6b. Most seriously, R2 almost collapsed and the influent ammonium concentration had to be reduced to  $50 \text{ mg NH}_4^+-\text{N L}^{-1}$ . From day 70, influent  $\text{NH}_4^+$  concentrations in other reactors were decreased to get low effluent ammonium concentration, and from day 107, influent  $\text{NH}_4^+-\text{N}$  concentrations were supplied stably at 500, 50, 650 and  $850 \text{ mg L}^{-1}$  in 4 reactors, respectively, with stable performance. These performances are comparable to similar granular systems from previous research (Kim and Seo, 2006, Vázquez-Padín et al., 2010, Song et al., 2013, Shi et al., 2011), although unlike the mixed metabolisms in those studies a pure nitrifying community was achieved in our experiment.

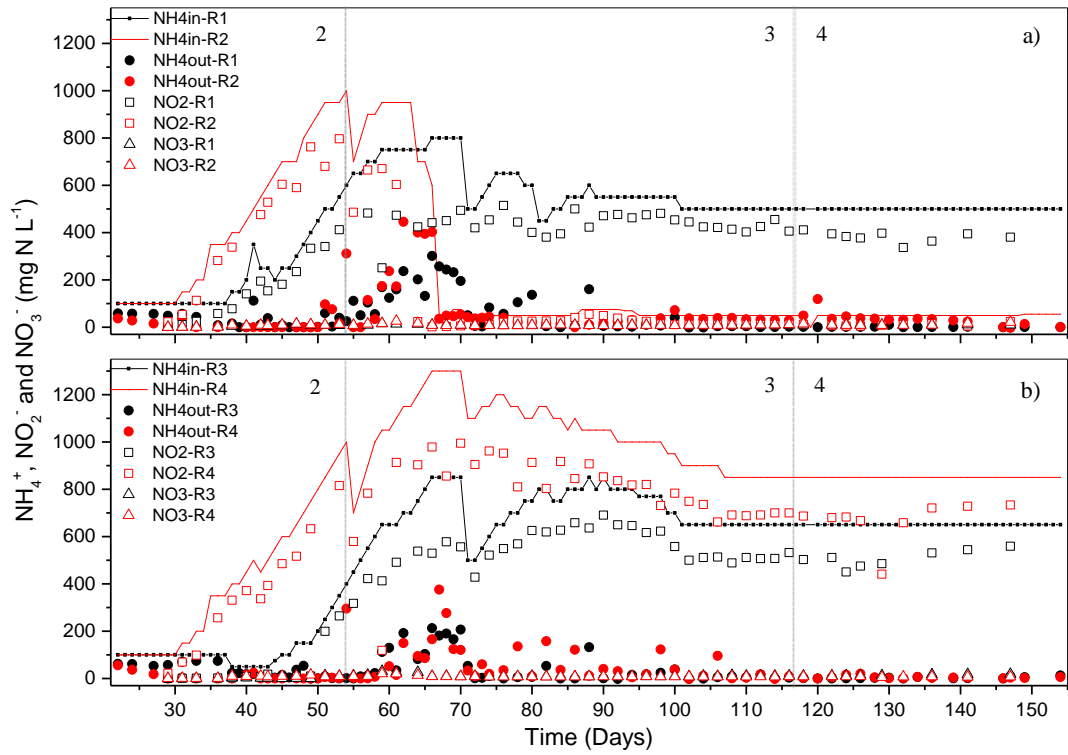


Figure 2.5 - Profiles of nitrogen species over the time during phases 2-4 with COD reduced quickly to 0 and  $\text{NH}_4^+\text{-N}$  increased to certain values in a) R1 and R2 and b) R3 and R4.

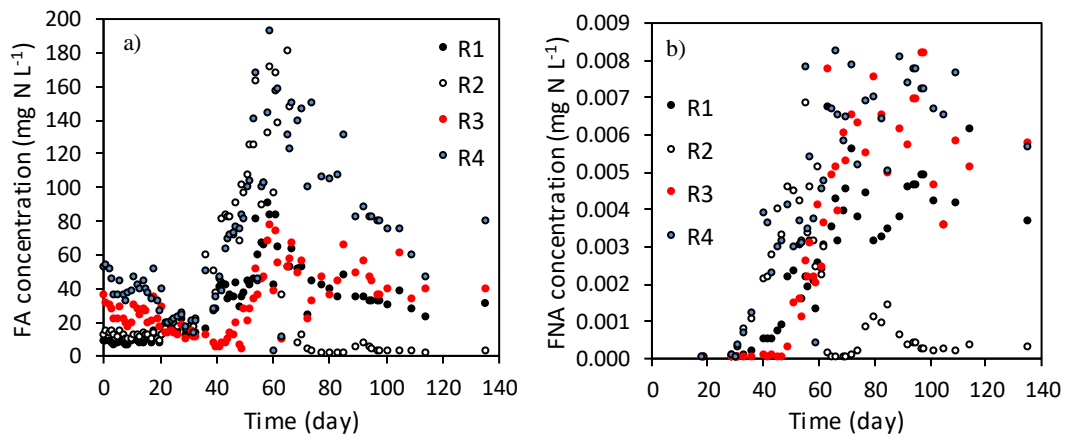


Figure 2.6 – Concentrations of a) free ammonia (FA) and b) free nitrous acid (FNA) over the operation time with the increased influent  $\text{NH}_4^+\text{-N}$  concentration.

### 2.3.3. Mineral accumulation in partial nitrifying granules over the operation time

During the long-term operational period, it was found that mineral was accumulated in granular sludge, leading to high ash content of granules. As shown in Figure 2.7, the sludge in four reactors showed excellent settleability with  $SVI_5$  lower than  $70 \text{ mL g}^{-1}$  during granules formation. At the same time, the ash percentage in all reactors increased slightly from an average value of  $17.86 \pm 0.32 \%$  on day 0 to 19.16-35.31 % in 4 reactors on day 21, i.e. the end of phase 1 for graduation (Figure 2.7a). Once granules formed, ash contents of granules increased steeply during phase 2, resulting in dense granules with  $SVI_5$  of 14, 5, 23 and  $8 \text{ mL g}^{-1}$ , respectively, on day 59 (Figure 2.7b). A similar high ash accumulation within aerobic granules coupled with such low  $SVI_5$  was also described by other research in literature (Liu et al., 2015). Ash content remained constant from this moment until the end of the experiment. It is to note that partial nitrifying granules in R2 and R4 at temperature of  $30\text{-}33 \text{ }^\circ\text{C}$  showed the lower  $SVI_5$  and the higher ash content compared with those at ambient temperature. Since  $\text{Ca}^{2+}$  concentration in tap water is around  $100 \text{ mg L}^{-1}$ , additional dose of  $\text{Ca}^{2+}$  and  $\text{Mg}^{2+}$  for the preparation of synthetic wastewater were removed from day 47. But ash content kept rising till day 70-90 with ash content of 52.0, 79.9, 45.4 and

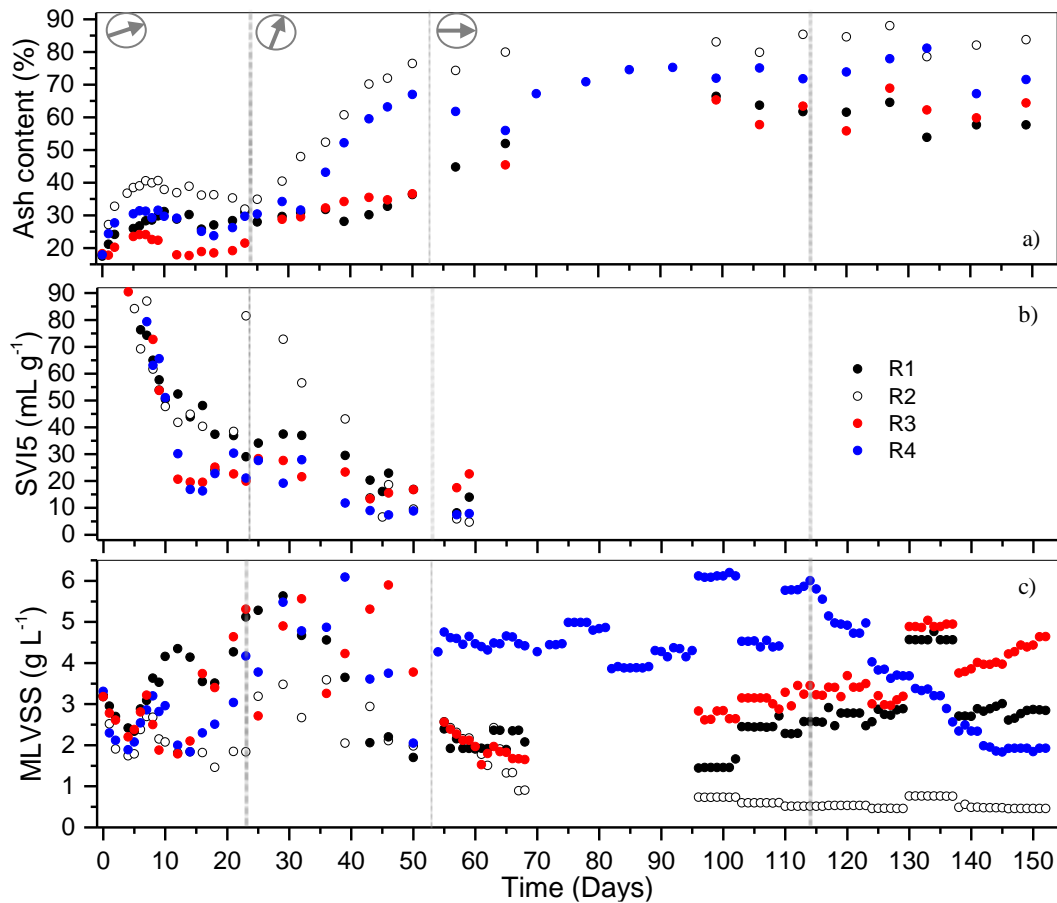


Figure 2.7 – a) ash content, b)  $SVI_5$  and c) MLSS-MLVSS along the whole experiment in the four reactors; in the first plot the three distinct stages, from left to right, of ash generation are shown (slight, high and negligible ash increase rate, respectively).

67.2 % in R1, R2, R3 and R4, respectively. One-way ANOVA test showed there was statistically significant difference ( $p < 0.05$ ) between the ash content in the four reactors during phase 4.

Since granules ash content, reactor operation and performance were stable after day 106 during phase 4, nitrogen removal performance of the four reactors on days 58 (the end of phase 2), 106 (the end of phase 3) and 121 (a typical day during phase 4) were compared. As shown in Table 2.2, specific ammonium oxidation rate (sAOR) in all reactors dropped from day 58 to day 106, suggesting reduced nitrifying activities. During this period, ash content increase in partial nitrifying granules was noticed. From day 106 to day 121, sAOR in all reactors were relatively stable although there was still a slight decrease. That the increased ash content in granules led to the reduced microbial activities was already reported in continuous reactor operation with heterotrophic granules by Liu et al. (2015b). There is great possibility that the reduced nitrifying activity in this study was also due to the high ash content in granules.

Table 2.2 - Ammonia removal performances and nitrite accumulation before and after biomass instability during phase 3 and after stable conditions were achieved during phase 4.

Unit	Day	R1			R2			R3			R4		
		58	106	121	58	106	121	58	106	121	58	106	121
<b>NLR</b>	mgNH <sub>4</sub> <sup>+</sup> -NL <sup>-1</sup> d <sup>-1</sup>	1889	1318	-	2454	134	-	1614	1726	-	2719	2438	-
<b>AOR</b>	mgNH <sub>4</sub> <sup>+</sup> -NL <sup>-1</sup> d <sup>-1</sup>	1615	1307	1280	2114	29.00	156	1449	1710	2040	2450	2178	1638
<b>sAOR</b>	mgNH <sub>4</sub> <sup>+</sup> -N mg <sup>-1</sup> VSS d <sup>-1</sup>	0.906	0.537	0.460	1.095	0.049	0.293	0.733	0.543	0.598	0.606	0.478	0.346
<b>NH<sub>4</sub><sup>+</sup> removal</b>	%	92.15	99.19	99.88	96.19	22.00	11.68	95.87	99.10	99.87	99.14	98.69	99.84
<b>NAR</b>	%	98.09	97.98	95.58	97.94	54.14	29.72	96.60	98.22	94.32	98.68	98.87	94.87

R1 and R3: 18-23 °C; R2 and R4: 30-33 °C. NLR = Nitrogen Loading Rate, AOR = Ammonium Oxidation Rate, sAOR = specific Ammonium Oxidation Rate, NAR = Nitrite Accumulation Rate. Day 121 corresponds to a cycle analysis.

Table 2.3 - ICP-MS analysis. Preliminary results on the concentration of main elements within R3 and R4 granules ash on day 107, at the end of phase 3.

Unit	Na	Mg	P	K	Ca	Fe	
<b>R3</b>	mg g <sup>-1</sup> TSS	12.79	0.59	76.80	0.94	172.30	2.94
<b>R4</b>	mg g <sup>-1</sup> TSS	11.42	0.91	40.86	0.36	254.40	3.05
<b>Tap water</b>	mg L <sup>-1</sup>	13.95	2.18	0.10	1.70	102.70	0.027
<b>Feedstock elements</b>	mg L <sup>-1</sup>	7210.00-3285.71	1.97	15.20	19.28	7.76	2.00

### 2.3.4. Characterization of partial nitrifying granules

To investigate the ash in nitrifying granules and possible reasons for the excessive ash accumulation, ICP-MS analyses were carried out for granules from R3 and R4, and mineral results are shown in Table 2.3. It was found that contents of elements Na, Mg, K, and Fe in granules are comparable to those reported in aerobic granules (Liu

et al., 2015b, Liu et al., 2016a), but elements P and Ca are extremely high. A typical P content in activated sludge is usually less than 1% (Metcalf and Eddy, 2003), but in this study, P content in granules from R3 and R4 reached 7.7% and 4.1%, respectively, which are comparable to those in the sludge from EBPR with the accumulation of poly-phosphate (Mañas et al., 2012b). From P and Ca content in nitrifying granules, it is reasonable to speculate that CaP precipitates might be accumulated. According to Ca/P molar ratio of 1.74 in granules from R3 and 4.83 from granules from R4, it can be speculated that hydroxyapatite could be the main calcium precipitate as 1.74 is very close to 1.67, the theoretical Ca/P ratio of hydroxyapatite. In contrast, Ca/P molar ratio in granules from R4 was as high as 4.83, indicating other calcium precipitate such as calcium carbonate might be formed together with CaP. The main difference between R3 and R4 is reactor operation temperature, which could affect the precipitate species in nitrifying granules with higher temperature facilitating other calcium precipitates. To identify the calcium source, tap water was also analysed, and it was found that calcium concentration in the tap water was as high as 102.70 mg L<sup>-1</sup>, because of chalk aquifer in Southampton, UK.

The saturation indexes calculated at the specific reactors' conditions confirmed the high calcium and phosphorus concentrations measured by ICP analyses. Table 2.4 shows that calcium phosphate as hydroxyapatite was the main mineral expected to precipitate in all reactors and during all experiment phases (SI higher than 9). Accumulation of calcium carbonate under the forms of calcite, aragonite and vaterite were also expected but in much lower extent. The high SI for hydroxyapatite was previously described in a similar autotrophic system without COD and with a pH higher than 8 (Johansson et al., 2017). On the other hand, much lower SIs were achieved in mixed bacteria systems (Mañas, 2011, Cunha et al., 2018a, Cunha et al., 2018b) where pH was lower than 8 and COD was provided.

To understand the element distribution in granules, they were halved and both exterior surface and core part were analysed by SEM/EDX. It can be seen from Figure 2.8 that the main element on the exterior surface in granules from R3 and R4 is carbon, followed by sulphur, oxygen, nitrogen, phosphorus and other metals but with very little calcium content. This indicates that the exterior surface is mainly composed of organic matters which could be biomass. However, the element distribution in the core part is quite different from that exterior surface. It was found that calcium and phosphorus were the main elements, which are much more than others, indicating the

Table 2.4 – Saturation index results

Day		HYDROXYAPATITE	CALCITE	ARAGONITE	VATERITE
		Ca <sub>5</sub> (PO <sub>4</sub> ) <sub>3</sub> (OH)	CaCO <sub>3</sub>		
21 <sup>a</sup>	R1	12.494	0.215	0.068	
	R2	12.626	0.314	0.173	
	R3	11.939	0.015		
	R4	12.070			
70 <sup>b</sup>	R3	9.913	1.569	1.422	0.99
	R4	9.508	1.712	1.572	1.159
108	R1	10.491	2.152	2.005	1.573
	R2	12.619	1.555	1.414	1.001
	R3	9.894	2.148	2.000	1.568
	R4	8.941	2.209	2.071	1.663

<sup>a</sup> pH considered for calculations was 8.7 and temperature was 20 °C for R1/R3 and 30 °C for R2/R4.

<sup>b</sup> pH considered for calculations was 8.65 and temperature was 20 °C for R3 and 30 °C for R4.

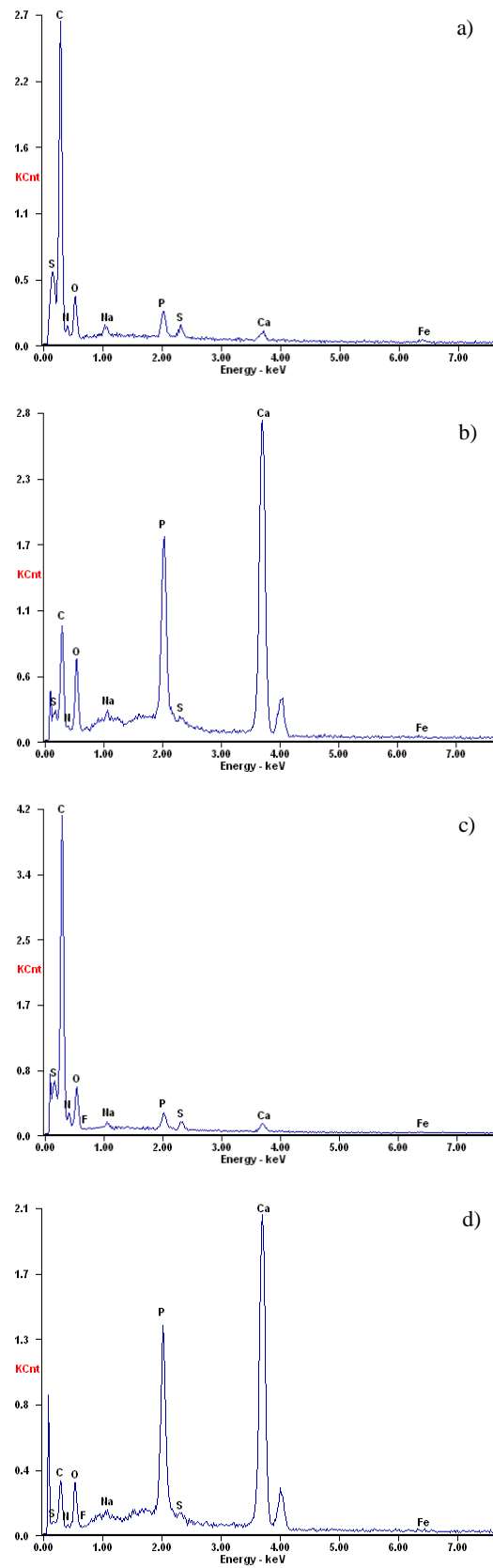


Figure 2.8 – EDX analysis; preliminary elemental composition of the a) external and b) internal surfaces of R3 granules and c) external and d) internal surfaces of R4 granule during phase 4 (day 126).

dominance of CaP precipitates. The similar element distribution was previously described for both heterotrophic aerobic granules (Ren et al., 2008) and EBPR granules with 30-35% of ash contents by other researchers (Mañas, 2011), who reported that external layers of granules were mainly composed of microorganisms with high contents of C, N and O, whereas inorganic matter such as Ca and P elements were much higher towards the core of the particles. There are two assumptions to explain this phenomenon. One is that inorganic precipitates form in the wastewater first, which then act as carriers for bacteria to attach and form granules. The other possibility is that granule structure and high EPS content in granules could provide favourable micro-environment for biomineralization. No matter which assumption is tenable, the bacteria tend to grow on the surface due to easy access to nutrients and oxygen in water without mass transfer resistance.

Although XRD is not able to detect amorphous precipitates, it is a good way to study which crystals could be in the ash. From Figure 2.9 it can be seen that mainly hydroxyapatite ( $\text{Ca}_{10}(\text{PO}_4)_6(\text{OH})_2$ ) and calcite ( $\text{CaCO}_3$ ) were identified in granules from R3 and R4. XRD results in Figure 2.9 are highly in agreement with ICP results, showing more calcite than hydroxyapatite in R4 granules but much less calcite in R3 granules. This further confirms that CaP is the main precipitate in R3 granules while both  $\text{CaCO}_3$  and  $\text{CaPO}_4$  are dominant precipitates in R4 granules.

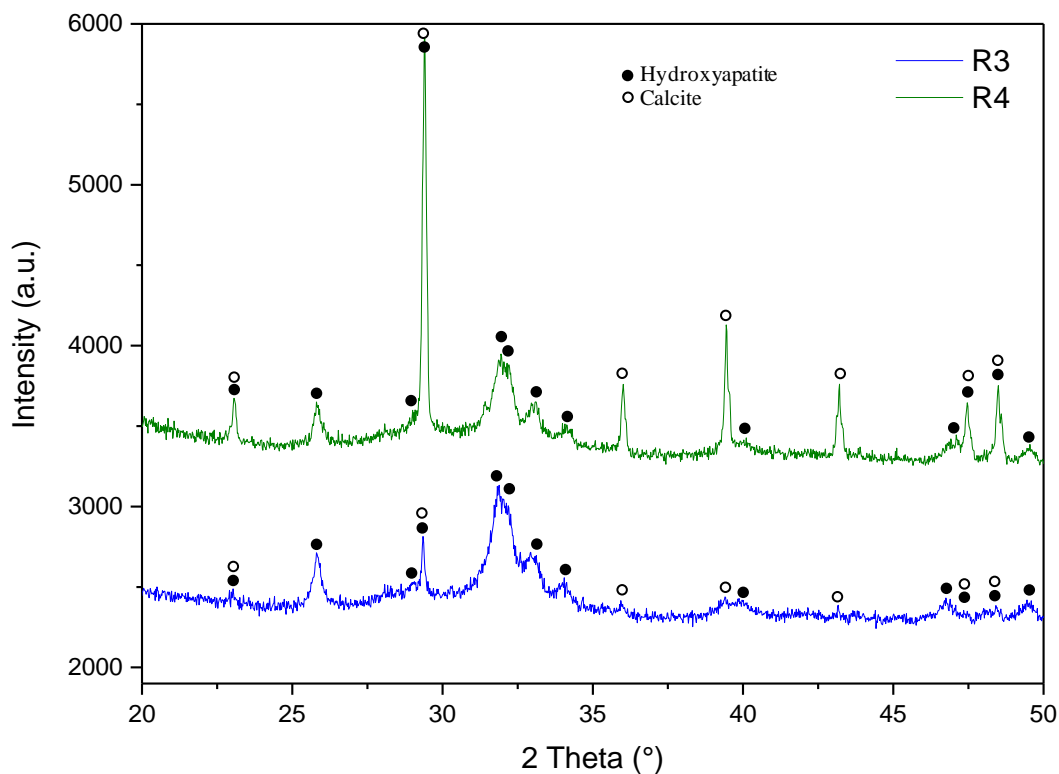


Figure 2.9 - XRD analysis; the inorganic solid phases present within granules ash from R3 and R4 (day 121).



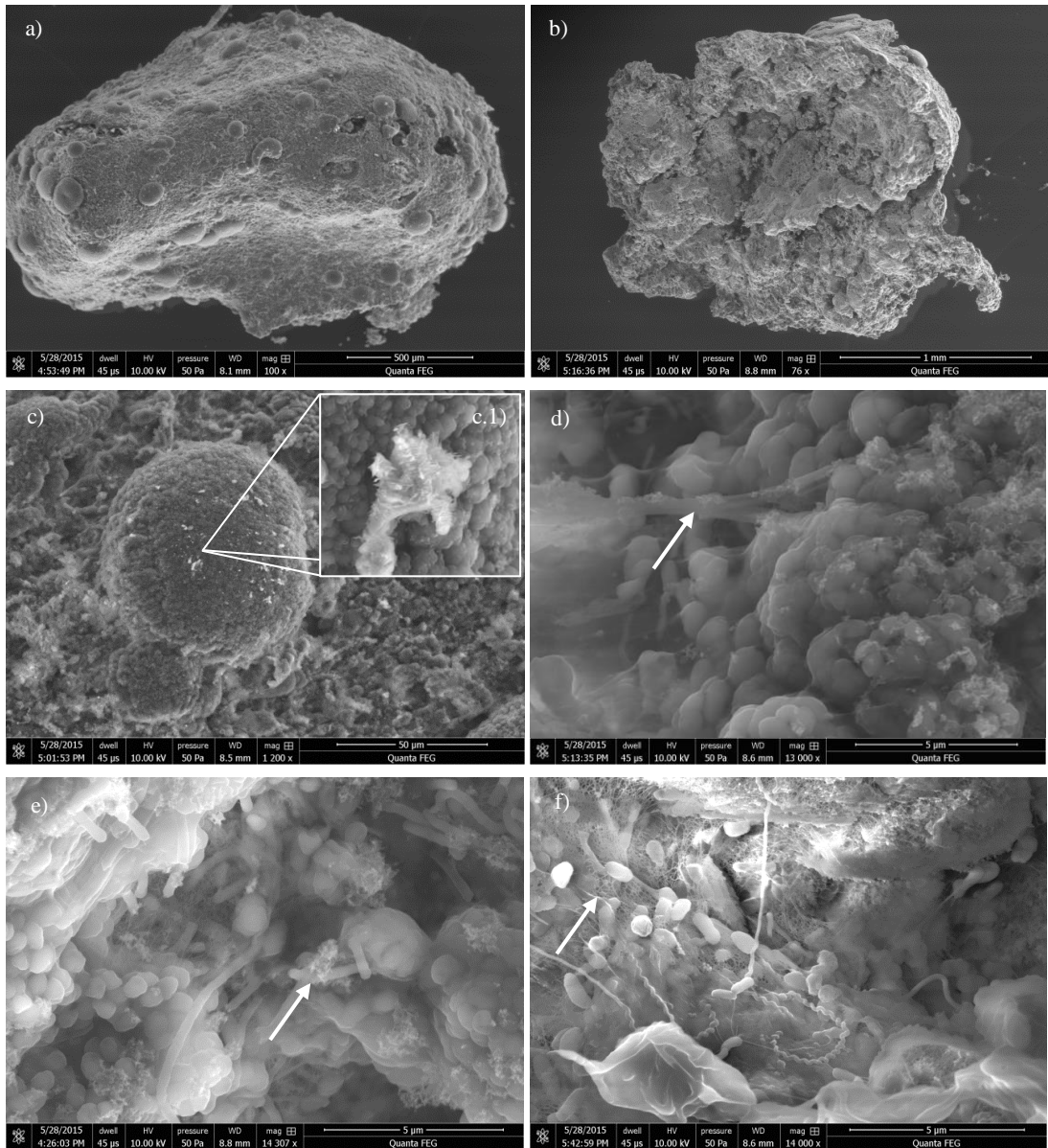


Figure 2.10 - SEM microscopy of R4 granules on day 113. a) External and b) internal surface of half cut granule, c) detail of a spherical structure on the granule external surface, c.1) crystal agglomeration on top of spherical structure, d) detail of external surface around the spherical structure on granule, e) details of bacillus and coccoid bacteria surrounded by an unknown clear material (arrow) and f) other bacteria embedded in EPS (white arrows).

In Figure 2.10a and b, SEM photos are shown of the external and internal surface of half cut granules. A granule from R4 on day 113 shows similar cauliflower structures on the surface with curds as reported by others (Liu et al., 2004a, Lemaire et al., 2008, Gonzalez-Gil and Holliger, 2014), although they look sparser (Figure 2.10a). These curds (Figure 2.10c) are mainly composed of tightly aggregated bacteria, with some inorganic precipitate-like substance scattered on the surface (Figure 2.10c.1). This indicates that some precipitation could occur in the bulk solution and then deposit on the surface of granules by some forces. Also, in the area surrounding the curds

the bacteria showed precipitate-like substance, but the cells looked less compact (Figure 2.10d). Meanwhile, it was noted that bacteria were embedded in EPS substances with scattered clusters of amorphous precipitates (arrows). It is still unclear, but it is speculated that these precipitates were facilitated to form by EPS and bacteria by creating favourable local conditions such as high pH, high calcium, phosphate and carbonate concentrations (Lin et al., 2012, Sarma and Tay, 2018a). The clusters were also observed in the core of granules as shown in Figure 2.10e (arrow), and the precipitates size was around 1-2  $\mu\text{m}$ . It has been verified by other experiments in our laboratory that organic molecule such as EPS can enhance precipitation (data not shown). Therefore, there is still possibility for precipitates form inside of granules as well.

For the morphology of granules from different reactors on day 142 with the average ash content of 82.0 and 67.2% in R2 and R4, and 57.7 and 59.8 in R1 and R3, respectively, stereoscopy observations were done (Figure 2.11). Although influent  $\text{NH}_4^+\text{-N}$  to R2 was just 50  $\text{mg L}^{-1}$ , but 850  $\text{mg L}^{-1}$  to R4, it was observed that granular sludge looked like similar with lighter colour at 30-33  $^\circ\text{C}$  compared with granules from R1 and R3 at ambient temperature. In addition, more fragments were observed in R2 and R4. The calcified granules usually exhibit lighter colour (Liu et al., 2015b, Johansson et al., 2017). Also, there is possibility that calcified granules at high temperature are easier to break into pieces for the growth of new granules; granules structure instability due to reduced nutrients mass transfer was already described in literature (Lemaire et al., 2008, Yuan et al., 2017).

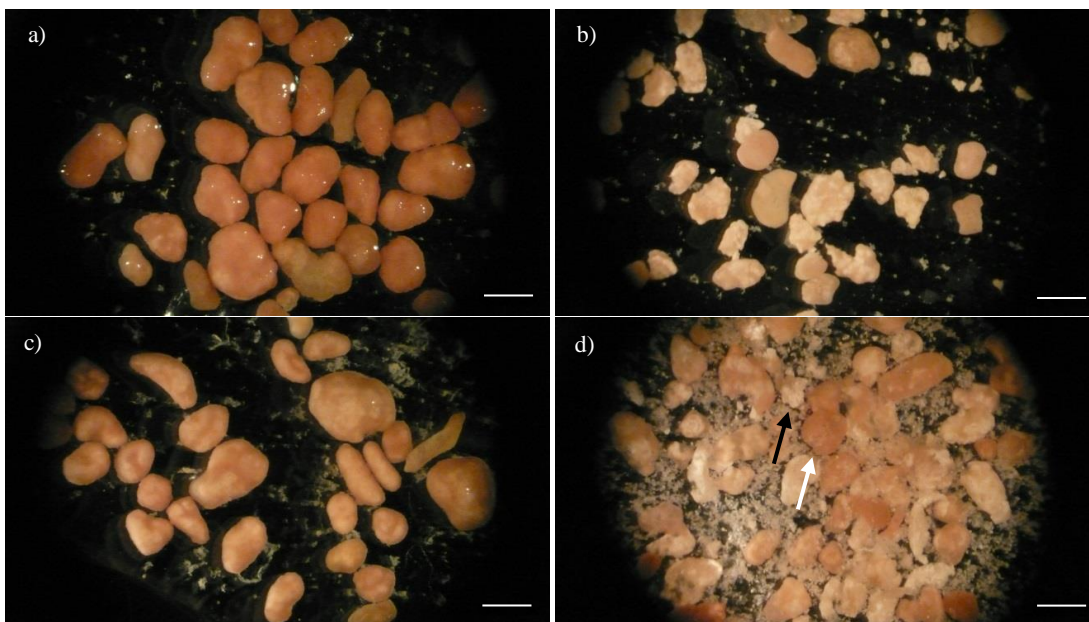


Figure 2.11 - Stereomicroscopy images; granular biomass from a) R1, b) R2, c) R3 and d) R4, during stable operation on day 142. Black and white arrows represent a granule fragment and a normal entire granule, respectively. Bar = 1000  $\mu\text{m}$ .

## 2.4. Discussion

### 2.4.1. Temperature and COD/N ratio effects on quick granulation

Since granulation is a gradual process in which suspended sludge turns into granular one, it may be hard to find a common rule in literature to describe the exact moment when this change takes place; anyhow, in this study three main requirements were selected to describe achieved granulation: (a) SVI<sub>15</sub> and SVI<sub>30</sub> lower than 80 mL g<sup>-1</sup> and difference between them lower than 10%; (b) 50% or more of biomass within the reactor represented by particle size greater than 200 µm; (c) well defined and clear particles outline, visible by microscope or naked eye (Dangcong et al., 1999, de Kreuk et al., 2007a, Liu and Tay, 2007, Liu et al., 2010b). The SVI pattern showed by all reactors during phase 1 was well in agreement with the ones reported by Liu et al. (2010b) and Liu et al. (2011), indicating that SVI increase followed by a decrease is a kind of adaption behaviour of sludge under selection pressure for granulation.

#### 2.4.1.1. Temperature

From our study, a higher temperature influenced negatively the granulation process, as shown by the slower rate of R4 to reach 90% of sludge volume of particles with size greater than 200 µm; at the same time, R4 was described by both smaller granules mean size and slower size increase rate than R3, with a lower biomass concentration at the end of phase 1 compared to the reactors run at lower temperature. The failure of granulation in systems run at higher temperatures was already described in literature. For instance, stable granules were obtained in Ebrahimi et al. (2010) in a SBR column with a starting temperature of 20 °C and a stepwise increase up to 30 °C; on the other hand, the reactor run at 30 °C from the beginning produced fluffy granules with poor settling skills. In Syutsubo et al. (1997) it was cited an experiment in which a thermophilic UASB system run for 300 days produced granules with a delay of 200 days due to the poor settleability of sludge which remarkably deteriorated during the first 100 days. To overcome this problem, mesophilic sludge was used instead as seeding material and then transformed to thermophilic by increasing the temperature stepwise. It has been described by van Loosdrecht et al. (1995) that an efficient way to enhance the stability of granules, or biofilm in general, is to slow down the growth rate of the microorganisms within it. de Kreuk and van Loosdrecht (2004) choose to select slow growing phosphate accumulating organisms (PAO) to achieve a smooth, dense and more stable granular sludge, while studying the effects of both high and low oxygen concentrations on the process. This would also be confirmed by Picioreanu et al. (1998) in which biofilm's stability was negatively affected by biomass at maximum density in biofilm, maximum specific microbial growth rate and granule radius or biofilm thickness. The slower growing bacteria in the reactors run at lower temperature in the present study could generate more stable granules, which consequently could shorten the granular sludge formation period.

During phase 4 at stable conditions, although R4 was run at 33 °C, a higher sAOR was observed in R3 which was kept at room temperature for the entire experiment. The main reason that explains this discrepancy may be the greater amount of inorganic matter accumulated in the former, as also described by ICP results; the presence of precipitates in aerobic granules was already described in Liu et al. (2016a) to reduce the bacteria activity. In addition, the replacement of the microorganisms with inorganic matter increased the nutrients mass transfer limitations in the granule internals, which consequently reduced its structure stability. It was reported that the excessive precipitation in both aerobic granules (Liu et al., 2015b) and in lithified layers of natural marine stromatolites (Kawaguchi and Decho, 2002), could induce the bacteria to start degrading polysaccharides. These were described in literature as a possible organic source for biomass growth in case of nutrients scarcity (Wang et al., 2010, Sadri Moghaddam and Alavi Moghaddam, 2015). Therefore, their removal could produce empty spaces

in the granules and reduce the whole particle structure strength. This would explain the reduced stability observed in R4 during granulation at higher temperature and consequently the particles fragmentation in phase 4, which generated a further lower ammonium activity.

#### **2.4.1.2. COD/N ratio**

The reactors run at lower COD/N ratio showed a quicker increase of the amount of sludge with a size greater than 200  $\mu\text{m}$ , with both biomass concentration and granule mean size reaching higher values and in a shorter time than the reactors fed with higher COD/N ratio. As already described by Liu et al. (2004a), lowering the COD/N ratio could enhance the nitrifying bacteria population at the expenses of the heterotrophic community within activated granular sludge treating synthetic wastewater. Since the maximum growth rate of nitrifying microorganisms was described ten times lower than the one for heterotrophic bacteria (Wiesmann, 1994), it could be confirmed that the enrichment of slow growing nitrifying bacteria within the system could achieve a quicker granulation due to the higher granules stability (van Loosdrecht et al., 1995, Picioreanu et al., 1998).

#### **2.4.2. Novel strategy to quickly produce nitrifying granular sludge**

To maximise the slow growing nitrifying biomass enrichment in the system, in our study good biomass retention was provided; the heterotrophic granules were produced in short time by using stringent reactor operations (i.e. settling time and high OLR) as previously described (Liu and Tay, 2015). This strategy selected only the bacteria able of creating cells-to-cells connections, which formed heavier particles able to settle quickly and to be retained within the reactor (Liu and Tay, 2002); then, the high OLR provided the feed to allow fast heterotrophic bacteria growth and consequently the formation of mature granules (Moy et al., 2002). The special structure of the granules could act to retain the bacteria and avoid the washout of the slow growing AOBs. Then, COD/N was quickly decreased to enrich the granules with autotrophic bacteria as also reported by Liu et al. (2004a), but this was possible also thanks to the step-by-step  $\text{NH}_4^+$  increase in the influent whenever its concentration in effluent was negligible, which could avoid the inhibition of the sensitive AOBs by free ammonia (Chen et al., 2015). The maximum or max FA concentration within the reactors was measured as high as 70.90  $\text{mg L}^{-1}$  during granulation, which has been previously described as inhibiting either the bacteria activity and/or the granulation process (Yang et al., 2004b, Wang et al., 2007a, Peyong et al., 2012). However, the obtained quick granulation demonstrated that no inhibition was observed at the present study's conditions, showing the strength of the strategy. From literature, the shortest time nitrifying granules were produced from common activated sludge were described in the range of 80-150 days. Specifically, nitrifying activity was detected after 80 days and partial nitrifying granules were produced after 146 days in a SBR treating synthetic wastewater (Wei et al., 2014). Partial nitrifying suspended biomass and partial nitrifying granules were observed in a sequencing batch air-lift reactor after 60 and 83 days from start-up, respectively (Song et al., 2013). Shorter times, i.e. 70 days, were described when a sequencing batch airlift reactor (SBAR) was inoculated directly with nitrifying sludge (Kim and Seo, 2006). When stepwise NLR increase (from 0.4 to 2  $\text{g L}^{-1} \text{d}^{-1}$ ) and short settling time (from 10 to 7 min) were applied to a nitrifying sludge SBR, quicker granulation of nitrifying biomass was achieved in 55 days (Chen et al., 2015). In the present study, in which the heterotrophic granules acted as a biomass retaining factor, the start-up time of granular nitrifying system was reduced as never described before in literature and complete nitrification could be confirmed in around 29 days in R2 and R4, 36 and 46 days within R1 and R3, respectively. All reactors showed mainly production of nitrite and the achieved biomass activity at the different conditions resulted in agreement with the ones found in literature for  $\text{NO}_2^-$  production (Kim and Seo, 2006, Vázquez-Padín et al., 2010, Shi et al., 2011, Song et al., 2013).

The presented strategy showed to produce a nitrifying system in very short time, which could be helpful to achieve fast start-ups of failed systems treating high-N loaded waste streams. In addition, this strategy could be applicable in most of WWTPs, since the autotrophic granules could be easily formed by using general activated sludge from the aeration tank, without a nitrifying biomass source; finally, there was no need to use expensive reactors setups or synthetic carriers or complicated equipment (e.g. magnetic field), or adding chemicals (e.g. lime, calcium or iron).

### 2.4.3. Mineral precipitation

Bulk precipitation is induced by specific conditions, generally ruled by factors such as pH, ions concentration (e.g.  $\text{Ca}^{2+}$ ,  $\text{PO}_4^{3-}$ ,  $\text{CO}_3^{2-}$ ,  $\text{Mg}^{2+}$  and  $\text{Fe}^{2+}$ ), temperature and the presence of nucleation sites (Hammes and Verstraete, 2002, Dupraz et al., 2009, Mañas, 2011, Peng et al., 2018). As explained by Maurer et al. (1999), solubility of calcium phosphate is lower than  $15 \text{ mg P L}^{-1}$  at pH between 7.4 and 7.5 ( $T=20 \text{ }^\circ\text{C}$  and  $\text{Ca}=60 \text{ mg L}^{-1}$ ); whereas, the solubility of calcium carbonate is around  $13 \text{ mg L}^{-1}$  in pure water, but at ambient  $\text{CO}_2$  pressure ( $p\text{CO}_2 = 3.5 \times 10^{-4} \text{ atm}$ ) it increases up to around  $47 \text{ mg L}^{-1}$  ( $19 \text{ mg Ca L}^{-1}$ ) (Geysant et al., 2001). Therefore, it is expected that at the conditions studied in the present research and in most common WWTP processes, bulk precipitation could occur.

In literature, both calcium carbonate precipitation (Ren et al., 2008, Juang et al., 2010, Liu et al., 2016a) and phosphorous accumulation as hydroxyapatite (HAP) (Mañas, 2011, Huang et al., 2015, Mañas et al., 2012a, Johansson et al., 2017) within granular sludge due to microorganisms-induced precipitation (MIP) have been described. Although a clear mechanism has not yet been illustrated in literature, five main factors were considered in the present study to induce or modulate MIP within the granular sludge instead of in the bulk solution: a) temperature, b) activity of specific microorganisms, c) mass transfer resistance, d) granules retention time and e) EPS structure.

It is to notice that the inorganic material accumulated much more quickly at higher temperature in R2 and R4 at  $33 \text{ }^\circ\text{C}$  than in R1 and R3. For what concerns  $\text{CaCO}_3$ , this can be justified by the increased  $\text{CO}_2$  stripping through evaporation (Castanier et al., 1999). A decreased  $p\text{CO}_2$  would indeed lower the  $\text{CaCO}_3$  solubility, whereas at constant  $\text{CO}_2$  pressure the  $\text{CaCO}_3$  solubility is reduced with a higher temperature (Miller, 1952). In addition, greater mineral accumulation would be emphasised by the increased AOBs activity that could further deplete  $p\text{CO}_2$  within the granules. On the other hand,  $\text{CaPO}_4$  minerals solubility generally increases with temperature, but for some forms like HAP and octacalcium phosphate the solubility decreases at higher temperatures (House, 1999). A higher temperature would also mean faster heterotrophic metabolism of acetate-consuming bacteria which would produce alkalinity, as previously described by Ren et al. (2008) and Liu et al. (2016). COD was removed from all reactors at the end of phase 2, therefore a consequent increase of bicarbonate and carbonate concentration would be expected. Beside the amount of precipitation, different temperatures induced different speciation of precipitates in our study. Although the medium for R3 and R4 in phase 4 were almost the same, hydroxyapatite was mainly found in the former, whereas a mixture of HAP and calcite was found in R4 run at higher temperature. In a similar way, precipitation of mainly hydroxyapatite was described in a granular simultaneous partial nitrification/ANAMMOX system run at  $25 \text{ }^\circ\text{C}$  (Johansson et al., 2017). When the temperature of the autotrophic process was then increased to  $35 \text{ }^\circ\text{C}$  both hydroxyapatite and calcite were encountered (Gonzalez-Martinez et al., 2017). In addition, it was showed that the increased process temperature from  $25$  to  $50 \text{ }^\circ\text{C}$  could raise the chemical precipitation of calcite over other minerals of around 90 % (Weiss et al., 2014). Therefore, the present study outcomes suggest that temperature plays an important role for

precipitation in granules and the higher temperature facilitates both more precipitation and more diverse species accumulation.

From the EDX analyses (Figure 2.8) we could confirm previous investigations results, showing that it is within the core of granules that the conditions are perfect for the minerals to accumulate (Mañas et al., 2012b, Huang et al., 2015). It has been described indeed that due to both activity of microorganisms and mass transfer resistance, the pH and the concentration of specific ions can be different from the bulk solution, showing a gradient pattern. Gieseke et al. (2006) measured that the pH within a biofilm could reach lower values compared to the bulk solution due to the bacteria proton release. Ren et al. (2008) and Liu et al. (2016a) showed that the acetate metabolism of heterotrophs producing carbon dioxide, could shift the equilibrium  $\text{CO}_2/\text{CO}_3^{2-}$  to the carbonate production; then, because of the granule mass transfer resistance, carbonate concentration would show higher values within the granule's core than in the bulk solution. Higher phosphate concentrations and/or pH values within the granule interior were reported also in EBPR (Mañas, 2011, Mañas et al., 2012a, Winkler et al., 2013a), and partial nitrification/ANAMMOX processes (Gonzalez-Martinez et al., 2017, Johansson et al., 2017); in the former, the PAOs would be releasing phosphate and at the same time increasing the pH after the acetate utilization, whereas in the latter the ANAMMOX activity would be the main factor increasing the hydroxide ions concentration within the granules, which would produce a subsequent pH increase. During phase 1, the pH values at the beginning of cycle within all reactors were recorded continuously as close to 9, due to the heterotrophic metabolism of acetate-consuming bacteria producing alkalinity (Ren et al., 2008, Liu et al., 2016a). At the same time, the calcium concentration of tap water provided for the feedstock preparation was in the range 100-150 mg  $\text{Ca}^{2+} \text{L}^{-1}$ . Therefore, as stated before, the pH and concentration of calcium and carbonate would be higher within the granule core than in the bulk solution, explaining why precipitation would be expected within the granules. Although calcite accumulation was expected at the studied conditions, for hydroxyapatite precipitation a further explanation is needed. Even though many natural water environments are oversaturated and should show HAP precipitation, this does not happen very often; because of the quite slow kinetics of hydroxyapatite precipitation, precursors of it are generally the first to form (Moutin et al., 1992, House, 1993). As also described by Ostwald's law of stages, it is not the most thermodynamically stable phase that forms first, but the more soluble in water instead (Nývlt, 1995). Since the hydroxyapatite precursors (i.e. amorphous calcium phosphate and octacalcium phosphate) have higher solubility product constants than HAP (Cunha et al., 2018a), they will accumulate first within the granules; then, because of the long retention time of granules within the system (Winkler et al., 2012a), the more stable and least soluble HAP will form. Therefore, even with high pH and calcium concentration within the granules, the main limiting factor for the hydroxyapatite accumulation in the systems stays in the long retention time that granular sludge can provide.

Different pHs in the same system have showed in literature to generate different precipitation of HAP and calcite. For a process with pH between 9 and 10, in presence of carbonate, calcium phosphate was the only mineral found to precipitate, whereas at lower pH than 8 or higher than 10 the two minerals would co-precipitate (Song et al., 2002). During phase 4, when stable conditions were provided, R4 granules showed an average particle size smaller than the one in R3 of 1 mm (data not shown). It could be speculated that the different sizes could generate different pHs within the granules. This could eventually explain the precipitation of solely hydroxyapatite within a larger particle where pH ranged 9-10. Although the cycle analyses showed a pH of at least 8.6, a higher granule internal pH due to mass transfer limitations and to dissolution of minerals as a protons consuming process (Plant and House, 2002) would be expected. In addition, it is also speculated that nitrifier denitrification activity was present in all reactors, since part of the  $\text{NH}_4^+$  in the influent was not converted to  $\text{NO}_2^-$ , but to  $\text{N}_2\text{O}$  instead (Colliver and Stephenson, 2000, Desloover et al., 2011). The AOBs can indeed switch to this pathway, especially

with conditions of low O<sub>2</sub> concentrations. Due to the larger diameter in R3, the granules generated a higher mass transfer limitation for O<sub>2</sub>, which would increase the nitrifier denitrification activity and consequently explain the higher pH within larger size granules. On the other hand, the smaller particles in R4 would show lower nitrifier denitrification and therefore a lower pH due to the normal proton generating nitrification pathway of AOBs. Therefore, different precipitates species could be generated due to the different granules size and consequently pH values within the particles. CaCO<sub>3</sub> precipitation would take place together with calcium phosphate within the smaller particles in R4, whereas only CaPO<sub>4</sub> would be found within larger granules.

It has been described in literature how Ca<sup>2+</sup> plays an important role in the granular structure adjustments (Yu et al., 2001, Jiang et al., 2003, Li et al., 2009, Huang et al., 2015); the alginate-like exopolysaccharides (ALE) contained in EPS have negative groups that can bind bulk cations (e.g. Ca<sup>2+</sup>, Mg<sup>2+</sup>, Na<sup>+</sup>, K<sup>+</sup>). ALEs find the highest affinity with Ca<sup>2+</sup>, which can create bridges among other ALE chains. These crosslinks act as the granules backbone and are the reason of the gel-like conformation of granular sludge (Lin et al., 2012, Wang et al., 2014b). The present study showed that the precipitating material was well in contact with the EPS surrounding the bacteria. It is possible that a very strong connection could be formed between the EPS molecules and precipitating deposits, as also shown by their persistent presence after several washes with ethanol and the whole SEM samples preparation. Sarma and Tay (2018b) hypothesised that an increasing cations amount, the absence of bulk chelating agents (e.g. VFAs as acetate) and an increase of pH, could together change the bridge conformation to a more suitable one able to host a molecule of phosphate; Huang et al. (2015) found that 17.6% of total removed P was actually accumulating in the EPS. In Sarma and Tay (2018b) there is no mention about carbonate as molecule binding to the calcium bridges at the above-mentioned conditions; anyhow, carbonate anions could behave as phosphate in reacting with Ca<sup>2+</sup> and producing the calcium carbonate precipitates due to the atomic structure similarity (two negative charged oxygen). It is therefore confirmed once again in the present study the fundamental importance that EPS structure and composition may play in mineral precipitation.

Calcium phosphate precipitation as HAP due to MIP was previously described mainly in EBPR granular systems, where a high concentration of phosphorus was present due to PAOs release in anaerobic conditions (Mañas, 2011, Filali et al., 2012, Mañas et al., 2012a, Winkler et al., 2013a); the only studies describing this precipitate in an autotrophic system were done by Gonzalez-Martinez et al. (2017) and Johansson et al. (2017) in a one-step partial nitrification/ANAMMOX process. MIP was also described in a pure ANAMMOX full-scale reactor, where HAP and whitlockite were found to accumulate within the granules which gained a stronger structure and good settleability (Lin et al., 2013a). Investigations on precipitation within pure partial nitrifying granular systems are missing now in literature, which explains why the present study can be of importance to the scientific community. Preliminary results from ICP-MS analyses showed molar Ca/P ratio for R3 granules as high as 1.73, which is close to the literature value 1.67 for hydroxyapatite (Mañas et al., 2012b, Peng et al., 2018); this could also confirm the results obtained from the XRD analyses (Figure 2.9), in which the best matching phase for R3 granules was indeed almost pure HAP. The concentration of P used in the synthetic wastewater in our study (15 mg P L<sup>-1</sup>) was much lower than the literature values, which are ranging between 30 and 50 mg P L<sup>-1</sup> (Lin et al., 2003, Mañas, 2011, Li et al., 2014b, Cunha et al., 2018a). Anyhow, the total inorganic P accumulated (41 and 77 mg P L<sup>-1</sup> in R3 and R4, respectively) was similar to the other studies, confirming that the specific process was able to accumulate a fair amount of P even though it was fed with low P-content wastewaters.

These are still preliminary results but it can be speculated that the production of HAP granules would be convenient as it could be a suitable substitute of phosphate rock in the already present industrial market (e.g. implants filling and coating, synthetic bones, corrosion resistant materials, drug delivery, etc.) (Peng et al., 2018, Tervahauta et al., 2014). The production of hydroxyapatite by aerobic granules would show convenient

advantages over previous technologies (i.e. struvite precipitation by MIP), since no pH adjustment or need of chemicals addition (e.g.  $MgCl_2$ , lime, etc.) or carbon dioxide degassing would be needed, with obvious reduction of the WWTP costs (De-Bashan and Bashan, 2004, Desmidt et al., 2015, Nancharaiah et al., 2016, Peng et al., 2018, Sarma and Tay, 2018b). Although HAP is considered a slightly soluble compound in soil, it has been suggested as a *slow releasing fertiliser* for direct application to land (Singh and Agrawal, 2008); indeed, there are acidic soils where solubilisation could be enhanced (Qiu et al., 2015) or HAP could be pre-treated with a slightly acid solution before application, or even phosphate-solubilizing bacteria or fungi (PSB or PSF) could be used to overcome the solubility problem (De-Bashan and Bashan, 2004).

## 2.5. Conclusions

The results described in Chapter 2 showed the possibility of cultivating partial nitrifying granules in a lab-scale SBR in the remarkable short time of 30 days. In addition, compared to other previous research, conventional activated sludge from the aeration tank of urban wastewater treatment works was used as inoculum. This showed basically that operation costs for starting-up a partial nitrifying granular system can be radically reduced since no chemicals nor special biofilm carriers nor expensive equipment were used. NOB activity was efficiently inhibited for more than three months, but it is speculated that a different strategy be used to keep nitrate production low. This was also confirmed by the results obtained in Chapter 5, where partial nitrifying granules stored for 6 months at 4 °C showed that NOB activity had recovered. However, those granules were cultivated for only 2 months and stored for 6, whereas the granules in Chapter 2 were cultivated for 5 months and stored for three, which are quite different and difficult to be compared.

Literature about the granulation process at different temperatures is missing at the moment but interesting results were found during the experiment described in Chapter 2; it can be affirmed that aerobic granules stability could be enhanced in systems run at lower temperature 18-23 °C and COD/N ratio=5, compared to the ones from the reactor at 30-33 °C with higher organic carbon. This could be justified by the general bacterial reduced growth rate induced by the lower temperature and enrichment of slow growing nitrifying bacteria, which could produce granules in shorter time and with a denser structure. An important consequence of these findings is the possibility to use this technology at reduced operational costs since milder temperatures would be implemented. In addition, lower temperatures could ensure a more stable long-term granular sludge system able to recover to loading stress.

## 2.6. Experimental weaknesses

During phase 2, when N load was step-wise incremented, the slow increasing concentration of ammonium (and most importantly ammonia) measured in the effluent was underestimated. For this reason, the nitrifying bacteria faced a load shock that likely generated the granules instability and ended with their fragmentation. A slower ammonium increase in the feedstock and the continuous measurement of ammonia in the effluent would be advisable for future application of the presented quick granulation strategy.

Although the controlled lab-scale experiment revealed interesting outcomes about temperature and COD/N influence over granulation, it would have been useful to compare the synthetic feedstock to real wastewater streams or in presence of specific contaminants and toxins. Also, a synthetic wastewater with diluted calcium content or a different pH range, could have clearly shown their role played during granulation.

The decision of removing completely the COD from the synthetic feedstock at the end of the experiment was due to the need to use the autotrophic granules for the following ANAMMOX bacteria accumulation. Unfortunately, resources and time were insufficient and ANAMMOX activity within the systems could never be detected.

However, after more literature review, it was understood that low amount of COD in the anaerobic environment



could have actually helped the accumulation of ANAMMOX. Therefore, the complete removal of COD only at the end of the experiment from the synthetic wastewater was considered a misjudgement.

The experiment lasted 5 months but this period appeared to be not enough to confirm the stability of the just produced granules. This was also seen with the fragmentation of R4 granules and the increase of biomass concentration in R1 and R3 at the end of experiment. A longer trial would have probably shown more stable granules.

During SEM and EDX analyses, only a small number of granules were analysed. Unfortunately, the resources and the time were not enough, but it would have been advisable to test a larger number of samples for a reliable comparison. In addition, elemental analysis was performed essentially after the granules have matured in the system. The continuous monitoring and the mass balance of elements like calcium, phosphorus and bicarbonate during the experiment early stages would have likely helped understanding their involvement in the granulation time and in the stability of the process.



**PHYSICAL, CHEMICAL AND BIOLOGICAL CHARACTERISTICS OF  
PARTIAL NITRIFYING GRANULES TREATING MIDDLE STRENGTH  
AMMONIUM WASTEWATER WITH HIGH WATER HARDNESS LEVEL**



### 3.1. Introduction

Compared with conventional oxidation of ammonium to nitrate by full nitrification, partial nitrification is able to save costs on aeration, sludge management and the provision of external organic carbon source (Lackner et al., 2014, Agrawal et al., 2018). Nitrifying bacteria are sensitive to environmental stresses such as toxic compounds, temperature and extreme pH; however, this can be reduced when granular sludge technology is applied, due to mass transfer resistance resulted by large size and high density (Sarma and Tay, 2018a). Granules have played an important role in the wastewater treatment during the last decade thanks to great settling properties, the high tolerance to shock loadings and the possibility to contain different microenvironments (aerobic and anaerobic).

Bacteria induced precipitation of inorganic matter within granular sludge has been controversially described in literature. The uncontrolled precipitation within the granules could on one hand represent a disadvantage for the wastewater treatment, since it may cause decreased biological activity (Ren et al., 2008, Liu et al., 2016a) and increased costs of energy for mixing (Van Langerak et al., 1998). On the other hand, in synergy with nutrients removal from wastewater, controlled biological precipitation within granular sludge would serve as a new technology to remove and collect those minerals that otherwise would generate scaling issues in pipes and reactors (Rathinam et al., 2018). Scaling is normally linked to the presence of soluble salts like calcium phosphate and calcium carbonate in the waste streams; recovery of calcium phosphate within the granules could be convenient since they could be suitable substitutes of phosphate rock in the already present industrial market (e.g. implants filling and coating, synthetic bones, corrosion resistant materials, drug delivery, etc.) and been processed using the existing infrastructures (Tervahauta et al., 2014, Peng et al., 2018).

It is common understanding that the main factors promoting bulk precipitation are pH, ions concentration (e.g.  $\text{Ca}^{2+}$ ,  $\text{PO}_4^{3-}$ ,  $\text{CO}_3^{2-}$ , etc.), temperature and the presence of nucleation sites (Hammes and Verstraete, 2002, Dupraz et al., 2009, Mañas, 2011, Peng et al., 2018). The biological processes for wastewater treatment in which bacteria-induced precipitation was previously described are quite various; accumulation of calcium phosphate minerals was observed in enhanced biological phosphorus removal (EBPR) (Mañas, 2011, Mañas et al., 2012b), one-step partial nitrification/ANAMMOX (Gonzalez-Martinez et al., 2017, Johansson et al., 2017) and ANAMMOX (Lin et al., 2013a). Calcium carbonate precipitation was reported among the others in aerobic granular sludge processes (Ren et al., 2008, Liu et al., 2016a). It is speculated that bio-precipitation is mainly caused by bacteria activity, micro-environments created within the granules due to mass transfer resistance and the extracellular polymeric substance (EPS) composition.

Recent studies have reported precipitation of both calcium phosphate and calcium carbonate in anaerobic granules treating black water (Cunha et al., 2018a) and partial nitrifying granules treating high ammonium strength synthetic wastewater (Chapter 2). In both these studies, high calcium content in the influent was provided; hence, it is thought that the cation concentration could also play an important role in the precipitation within granular sludge.

Although much research was done on bio-precipitation, its mechanism remains as yet, not completely clear; in addition, to the best of our knowledge, no study was described before on the relationship between excessive inorganic accumulation and granule size in a partial nitrifying system with an ammonia oxidising bacteria (AOB)-dominant community. Therefore, this study aims to investigate the minerals precipitation within AOB-dominant partial nitrifying granules treating middle strength ammonium wastewater with high water hardness; in addition, the physical features, morphology and bioactivity of different size granules will be described. The factors inducing bio-precipitation and the crystalline architecture of the precipitates will be also discussed.



## 3.2. Materials and methods

### 3.2.1. Medium

The synthetic wastewater was made every day and it was composed by ammonium sulphate ( $400 \text{ mg NH}_4^+\text{-NL}^{-1}$ ) and di-potassium phosphate ( $15 \text{ mg PO}_4\text{-PL}^{-1}$ ) as nitrogen and phosphorus sources, respectively. Slightly lower sodium bicarbonate than the theoretical one ( $10.8 \text{ g NaHCO}_3 \text{ g}^{-1} \text{ NH}_4^+\text{-NL}^{-1}$ ) was provided as explained in Chapter 2 to provide both the carbon source for biomass growth and the buffer solution. The metals were added as (per L wastewater prepared):  $0.02 \text{ g MgSO}_4\cdot 7\text{H}_2\text{O}$ ,  $0.01 \text{ g FeSO}_4\cdot 7\text{H}_2\text{O}$ ; whereas the trace elements were (per L wastewater prepared):  $0.12 \text{ mg MnCl}_2\cdot 4\text{H}_2\text{O}$ ,  $0.12 \text{ mg ZnSO}_4\cdot 7\text{H}_2\text{O}$ ,  $0.03 \text{ mg CuSO}_4\cdot 5\text{H}_2\text{O}$ ,  $0.05 \text{ mg (NH}_4)_6\text{Mo}_7\text{O}_{24}\cdot 4\text{H}_2\text{O}$ ,  $0.1 \text{ mg CoCl}_2\cdot 6\text{H}_2\text{O}$ ,  $0.1 \text{ mg NiCl}_2\cdot 6\text{H}_2\text{O}$ ,  $0.05 \text{ mg AlCl}_3\cdot 6\text{H}_2\text{O}$ ,  $0.05 \text{ mg H}_3\text{BO}_3$ . The synthetic wastewater was made by using tap water in which  $\text{Ca}^{2+}$  concentration ranged between 100 and  $150 \text{ mg L}^{-1}$ , whereas other main elements (i.e. Na, Mg, P, K and Fe) content was only negligible; the pH was not adjusted but it was constant at around 7.2-7.4.

### 3.2.2. Inoculum and granules reactor operation

Two Perspex columns with a working volume of 2.6 L and a column height to diameter ratio of 20 ( $\varnothing 60 \text{ mm}$ ) were operated sequentially with a cycle time of 4 hours including 10 minutes feeding, 227 minutes aeration, 2 minutes settling time and 1 minute discharging. The effluent was discharged from the middle port of the reactor, corresponding to a volumetric exchange ratio of 50%. The air was provided from the bottom of the reactor with a flow rate of  $5 \text{ L min}^{-1}$  and the temperature was kept constant at  $30 \text{ }^\circ\text{C}$ .

The partial nitrifying granules had been stored at  $4 \text{ }^\circ\text{C}$  for 3 months, from a previous experiment (Chapter 2). Then, they were left for 5 hours at room temperature and placed back into the SBR reactors for reactivation with an initial MLSS concentration of  $1.79 \pm 0.15 \text{ g L}^{-1}$  (MLVSS/MLSS=0.45); the granules were left overnight with wastewater containing  $100 \text{ mg NH}_4^+\text{-NL}^{-1}$  and the day after ammonium was increased as above. After two-month operation the partial nitrifying granules were still efficiently oxidising ammonium to nitrite only, when they were sorted into different size ranges and characterized.

### 3.2.3. Sorting of granules

The granules were washed thrice with tap water to remove residual chemicals before the wet sieving was employed for granule sorting by size. Granules with a diameter range of 150-250, 250-300, 300-425, 425-500, 500-600, 600-710, 710-1180, 1180-1400, 1400-2000, 2000-2800 and  $>2800 \text{ }\mu\text{m}$ , with an average size of 200, 275, 362.5, 462.5, 550, 655, 945, 1290, 1700, 2400 and  $>2800 \text{ }\mu\text{m}$ , respectively, were sorted using metal sieves with a corresponding pore size in diameter.

### 3.2.4. Biological batch tests of granules with different sizes for wastewater treatment performance

After sorting, to recover the activity, granules of four different size ranges were cultivated in 300 mL-flasks for overnight with synthetic wastewater as explained above, except for ammonium concentration that was changed to  $100 \text{ mg NH}_4^+\text{-NL}^{-1}$ . Lowering the ammonium concentration avoided the bacteria inhibition by FA which could limit the activity during the batch test. This was run within the same flasks at  $30 \text{ }^\circ\text{C}$ , with final biomass concentration of 0.93, 2.01, 2.01 and  $1.58 \text{ g MLVSS L}^{-1}$  for  $<600 \text{ }\mu\text{m}$ , 710-1180  $\mu\text{m}$ , 1400-2800  $\mu\text{m}$  and  $>2800$

$\mu\text{m}$ , respectively. The air was supplied via air stones placed at the bottom of the flasks with an aeration rate of  $2 \text{ L min}^{-1}$ . During the batch test period, 1 ml of liquid sample was taken from each flask every 30 minutes for the analysis of  $\text{NH}_4^+$ ,  $\text{NO}_2^-$ ,  $\text{NO}_3^-$ ,  $\text{PO}_4^{3-}$ ,  $\text{Ca}^{2+}$  and  $\text{Na}^+$  to evaluate nutrients removal. The specific ammonia oxidation rate (sAOR) was calculated based on ammonium removed divided by the time spent to remove it over the biomass concentration. For all size ranges investigated, the time used for calculations was 120 minutes, just before the ammonium removal rate was slowing down.

### 3.2.5. Analytical methods

Sludge volume index (SVI), mixed liquor suspended solids (MLSS) and mixed liquor volatile suspended solids (MLVSS) and the specific oxygen utilization rate (SOUR) were analysed by standard methods (APHA, 2012). Granule density was measured according to the method reported by Beun et al. (1999). Ammonium was analysed spectrophotometrically by following the procedure described in BSI (1984). Anions ( $\text{NO}_2^-$ ,  $\text{NO}_3^-$  and  $\text{PO}_4^{3-}$ ) and cations ( $\text{Ca}^{2+}$  and  $\text{Na}^+$ ) were measured by the ion chromatogram 882 Compact IC plus (Metrohm, Switzerland). A Metrosep A Supp 5 - 150/4.0 column and the eluent  $1 \text{ mM NaHCO}_3/3.2 \text{ mM Na}_2\text{CO}_3$  were used for anion analysis; whereas a Metrosep C4 250/4.0 column and the eluent  $1.7 \text{ mM HNO}_3/0.7 \text{ mM C}_7\text{H}_5\text{NO}_4$  (dipicolinic acid or Pyridin-2,6-dicarboxylic acid) were used for cation measurement instead.

To describe the NOB activity inhibition, the nitrite accumulation rate (NAR) was evaluated by using Equation 3.1 in which  $\text{NO}_2^-$  and  $\text{NO}_3^-$  are the concentrations of effluent nitrite and nitrate; a higher NAR value means a higher activity of AOBs over the NOBs.

$$\text{NAR (\%)} = \left( \frac{\text{NO}_2^- + \text{NO}_3^-}{\text{NO}_2^-} \right) \times 100 \quad (3.1)$$

The images of granules were taken by Leica MZ16F stereomicroscope for more detailed morphology observation. In addition, the granule images were uploaded to the software ImageJ for size analysis.

### 3.2.6. Morphology analysis with Scanning electron microscopy (SEM)

Bacteria composition within the granules and possible inorganic precipitates were qualitatively observed by the Quanta 250 SEM (FEI, Oregon, USA); samples were first fixed overnight with a solution of 3% glutaraldehyde + 4% formaldehyde in 0.1 M PIPES buffer pH 7.2. The specimens were then rinsed twice for 10 minutes with 0.1 M PIPES buffer pH 7.2 and a dehydration step by serial washes with ethanol followed; each wash lasted 10 minutes (30%, 50%, 70% and 95%), whereas at the end two rinses with absolute ethanol lasting 20 each were done. The samples were then dried by a Balzers CPD 030 Critical Point Drier, before being gold/palladium coated by a high-resolution sputter and high vacuum coater (Quorum, Q150T ES, West Sussex, UK). For particle sizes  $1400\text{-}2000 \mu\text{m}$  and  $>2800 \mu\text{m}$ , the granules were cut in halves by using a sharp scalpel before going through the fixing process.



### 3.2.7. Elemental and mineralogical analyses

#### 3.2.7.1. Saturation index

The software Visual Minteq 3.1 (KTH, Sweden) was used to estimate the saturation index (SI) by using Davies model for activity coefficients calculation (Mullin, 2001). Values below zero were considered as undersaturation conditions, whereas they were considered oversaturated when a value above the zero was calculated, which meant that the conditions in the system were favourable for precipitation of the specific mineral. The inputs used for the calculations are showed in Table 3.1 and correspond to the values measured during two months of granule cultivation, before the characterisation experiment.

Table 3.1 – Saturation index calculation parameters

Chemical	mg L <sup>-1</sup>
(NH <sub>4</sub> ) <sub>2</sub> SO <sub>4</sub>	1884 (400 mg N L <sup>-1</sup> )
NaHCO <sub>3</sub>	4320 (10.8 mg mg <sup>-1</sup> N L <sup>-1</sup> )
KH <sub>2</sub> PO <sub>4</sub>	67 (15.23 mg P L <sup>-1</sup> )
MgSO <sub>4</sub> •7H <sub>2</sub> O	20.00
FeSO <sub>4</sub> •7H <sub>2</sub> O	10.00
MnCl <sub>2</sub> •4H <sub>2</sub> O	0.12
ZnSO <sub>4</sub> •7H <sub>2</sub> O	0.12
CuSO <sub>4</sub> •5H <sub>2</sub> O	0.03
NH <sub>4</sub> ) <sub>6</sub> Mo <sub>7</sub> O <sub>24</sub> •4H <sub>2</sub> O	0.05
CoCl <sub>2</sub> •6H <sub>2</sub> O	0.10
NiCl <sub>2</sub> •6H <sub>2</sub> O	0.10
AlCl <sub>3</sub> •6H <sub>2</sub> O	0.05
H <sub>3</sub> BO <sub>3</sub>	0.05
Ca <sup>2+</sup> (from tap water)	102.70
pH (cycle begin)	8.01
Temperature	30 °C

#### 3.2.7.2. Energy dispersive X-ray spectroscopy (EDX)

Qualitative analysis of elements within and on surface of particles was done by Quanta 200 SEM (FEI, Oregon, USA) coupled with EDX (EDAX, New Jersey, USA); the samples were first treated as previously described for SEM image analysis but being coated with carbon instead of gold/palladium. For sizes 1400-2000 µm and >2800 µm, the mass percentage of elements was analysed along the granule thickness (5 points: outer layer, core and three more points in between, as shown in Figure 3.6), whereas for the smaller granules the analysis was done basically on the surface only.

### **3.2.7.3. X-ray diffraction (XRD)**

Mineralogical composition of nitrating granules has been studied by XRD technology and by using a Bruker D2 phaser (Bruker AXS Gmgh, Karlsruhe, Germany); the samples were first washed thoroughly with deionised water, to remove any soluble chemical from the feedstock or any biomass by-product, then kept at -20 °C overnight before being freeze dried (lyophilised) for a couple of days. Before the analysis, the dry granules were ground in a mortar to a fine powder, but unfortunately the amount of sample available could not be similar for all specimens. The resulting phases were finally compared with the database phases containing elements such as carbon, oxygen, calcium and phosphorus.

### **3.2.7.4. Inductively coupled plasma (ICP)**

Quantitative elemental composition within the granules was obtained by using a multi collector ICP emission spectrometer (X-SERIES 2 ICP-MS, Thermo Fisher Scientific, Bremen, Germany). Before the analysis, the sample needed to be dried overnight at 105 °C and then ground in a mortar; 50 mg of it were digested in a Teflon digestion vessel on a hotplate overnight with 2 mL of aqua regia (nitric acid and hydrochloric acid) and 0.5 mL perchloric acid. After the digestion, 10 mL of concentrated HCl were added to the completely dry sample; after this solution went dry, it was rediluted in 3% nitric acid and analysed by ICP-MS. The elements investigated were mainly the ones contained in the synthetic feedstock solution (e.g. Na, Mg, P, K, Ca and Fe). Since the analysis was interfered by presence of metals, the all procedure was done by avoiding any source of metals and glass (e.g. spatulas, aluminium crucibles, glass vials, etc.). The data processing was done using the Plasmalab software. Raw data were blanked and internally corrected and then calibrated against matrix matched synthetic standards.

### **3.2.7.5. Extracellular Polymeric Substance (EPS) analysis with formaldehyde/NaOH extraction**

For the extraction of extracellular polymeric substance (EPS) from partial nitrifying granules, the sample was first washed with tap water, then frozen overnight and finally dried for a couple of days by freeze drier (lyophilisation). Part of the sample was used to measure ash content and total solids, whereas the rest was weighed in a 15 mL centrifuge tube; to which 10 mL of PBS were then added and the sample was incubated on a shaker (150 RPM) for 1 h at 4 °C with 0.06 mL of formaldehyde (36.5 %) and then for 3 h at 4 °C with 4 mL of sodium hydroxide (1 M). After the first incubation, the sample was centrifuged for 10 minutes at 10000 g (4 °C) and the supernatant obtained was regarded as loosely bound-EPS (LB-EPS); after the second incubation the centrifuge was instead set for 20 minutes at 20000 g (4 °C) and the supernatant this time was considered as tightly bound-EPS (TB-EPS). After each centrifuge, the supernatant was analysed or discharged and the sample resuspended with a PBS solution to the starting volume. Both LB-EPS and TB-EPS extracted solutions were first filtered with a 0.22 µm syringe filter, and then placed at -20 °C until analyses for proteins (PNs) and polysaccharides (PS) content were done. PNs were analysed by Lowry's method (Lowry et al., 1951, Shen et al., 2013), whereas the PSs were measured by phenol-sulfuric acid method (Dubois et al., 1956). Phosphate Buffer Saline (PBS): 8 g L<sup>-1</sup> sodium chloride, 0.2 g L<sup>-1</sup> potassium chloride, 1.15 g L<sup>-1</sup> di-sodium hydrogen phosphate, 0.2 g L<sup>-1</sup> potassium di-hydrogen phosphate, pH 7.3 ± 0.2 at 25 °C, using HCl to adjust.

### **3.2.7.6. Extracellular Polymeric Substance (EPS) analysis with Excitation and emission matrix (EEM)**

EPS content was also analysed qualitatively by measurement of EEM spectra, using a Cary Eclipse Fluorescence Spectrophotometer (Agilent Technologies, USA); in this study, the spectra were collected with subsequent scanning emission spectra from 280 to 700 nm at 2 nm increments, by varying the excitation wavelength from

200 to 600 nm at 5 nm sampling intervals. The excitation and emission slits were maintained at 5 nm. The EEM data were processed as described by Chen et al. (2003b) and Guo et al. (2017). The X and Y axes represent the emission and excitation spectra, respectively; the contour lines represent the fluorescence intensity, which is the third dimension. The six main EPS components found within the samples are listed in Table 3.2. A UV1800 spectrophotometer (Shimadzu, Japan) was used to detect the dilution needed for EEM analyses; the scanning range used was from 200 nm to 700 nm, with 2 nm interval between each scan.

Table 3.2 - Excitation and emission ranges detected with EEM for EPS analysis (Chen et al., 2003b, Wang and Zhang, 2010, Wang et al., 2014a).

<b>Excitation/Emission (nm)</b>					
Region I <sup>a</sup>	Region II <sup>a</sup>	Region III	Region IV	Region V	Region VI
220-240/ 280-360	220-290/ 280-360	300-330/ 360-390	220-240/ 410-450	260-290/ 420-460	330-370/ 420-460
Tyrosine and tryptophan amino acid	Tyrosine and tryptophan protein	Polysaccharides	Fulvic acid- like substances	Polyaromatic- type humic acid	Polycarboxylate- type humic acid

<sup>a</sup> The regions I and II can be further divided by a vertical line on  $E_m = 320$  nm. For  $E_m < 320$  nm mainly tyrosine is detected, whereas for  $E_m > 320$  nm is mainly tryptophan.

### 3.3. Results

The stored partial nitrifying granules were reactivated in SBRs and operated for 2 months. Before the characterisation experiment, a batch analysis was done on the reactivated mixed partial nitrifying granules; the granules activity as specific ammonia oxidation rate (sAOR) decreased during storage from 2.21 to  $1.58 \pm 0.04 \text{ g g}^{-1} \text{ MLVSS d}^{-1}$ , yet showing a complete removal of  $\text{NH}_4^+$ . The nitrite shunt was efficiently maintained, and negligible amount of nitrate was detected in the SBR effluent, with pH decrease from  $8.04 \pm 0.05$  to  $7.69 \pm 0.17$ . The MLSS increased marginally from 2.20 to  $2.27 \pm 0.46 \text{ g L}^{-1}$  ( $\text{MLVSS}/\text{MLSS}=0.40 \pm 0.06$ ) during the two-month operation. As showed later, the ash content of some particle size ranges reached values higher than 80%, which may contradict the 40% of organic matter measured at beginning of experiment. This was explained by the fact that most of heavier granules with great ash content would be located under the sampling valve, for which the  $\text{MLVSS}/\text{MLSS}$  was likely overestimated.

#### 3.3.1. Biological activity of nitrating granules with different sizes

The SOUR test showed that the bacteria activity, described as oxygen depletion together with  $\text{NH}_4^+$  substrate utilisation, was inversely proportional to granules size and that the highest bacteria activity was measured within the smaller size range (Figure 3.1), with over  $150 \text{ mg O}_2 \text{ g}^{-1} \text{ MLVSS h}^{-1}$ ; a similar finding was previously observed by Ren et al. (2008) and Liu et al. (2016a), with the latter describing particles of size 106-212  $\mu\text{m}$  showing  $\text{SOUR}=120 \text{ mg O}_2 \text{ g}^{-1} \text{ MLVSS h}^{-1}$ . The SOUR results were also confirmed by the batch test, where the specific ammonium oxidation rate (sAOR) was described to be closely related to the particles size (Figure 3.2a). The highest activity was observed in the  $<600 \mu\text{m}$  range granules, whereas a lower ammonium removal activity was detected within particles with greater size. The  $<600 \mu\text{m}$  granules were able to reduce  $\text{NH}_4^+$  to a negligible concentration within 180 minutes, whereas it took 210, 257 and 407 minutes for ranges 710-1180  $\mu\text{m}$ , 1400-2000 and  $>2800 \mu\text{m}$ , respectively (Figure 3.17). The corresponding sAOR were 0.843, 0.328, 0.299 and  $0.236 \text{ g NH}_4^+-\text{N g}^{-1} \text{ MLVSS d}^{-1}$ . In a similar way,  $\text{NO}_2^-$  production was quicker within smaller granules, with specific nitrite

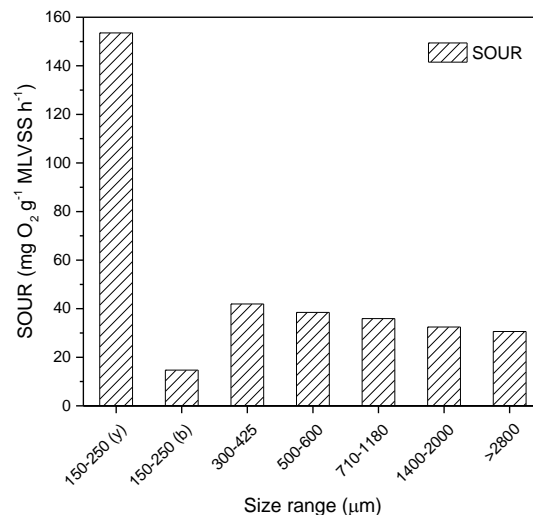


Figure 3.1 – Specific oxygen utilization rate (SOUR) of granules with different size ranges (y: yellow, b: brown).

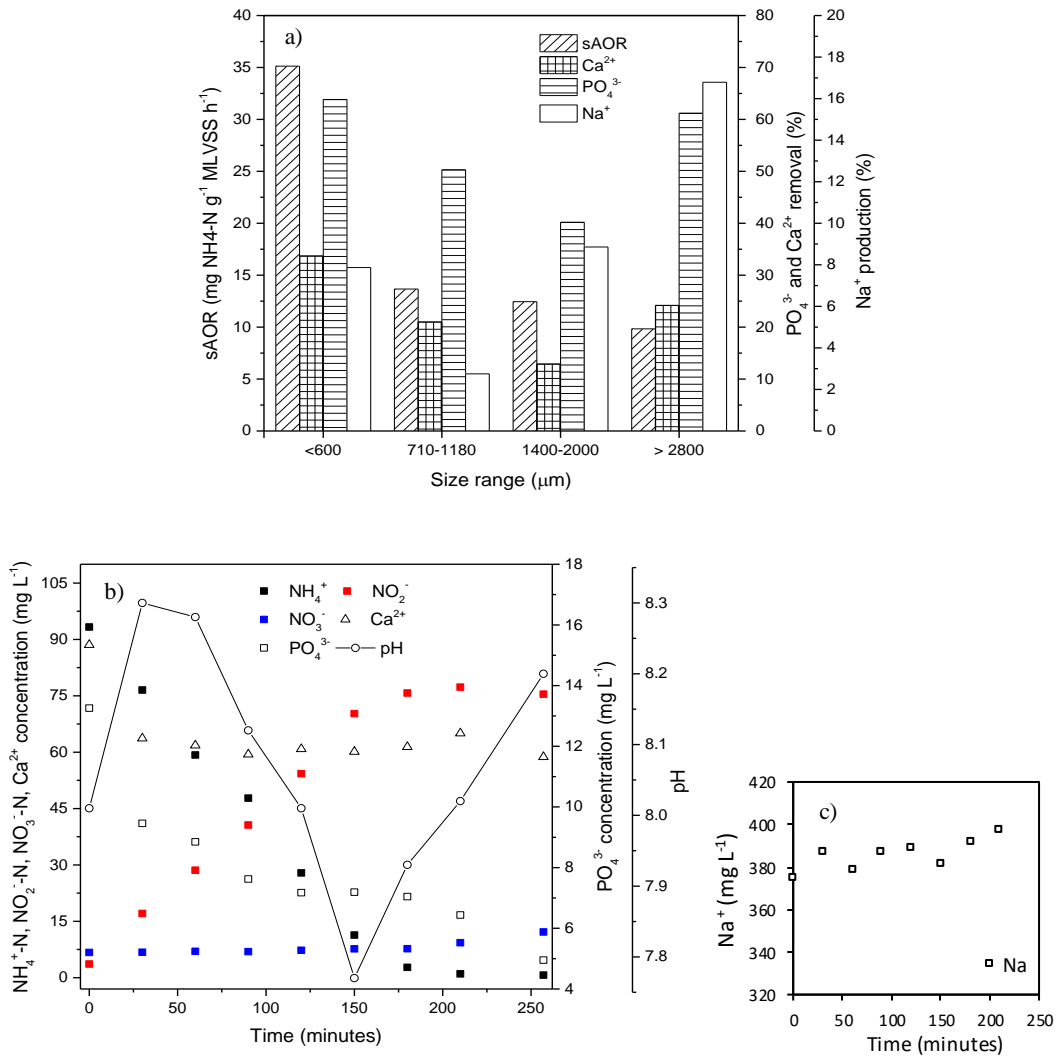


Figure 3.2 – a) sAOR, PO<sub>4</sub><sup>3-</sup> and Ca<sup>2+</sup> removal and Na<sup>+</sup> production in different sizes granules during batch tests; b)c) examples of batch test results from <600 μm.

production rate (sNPR) as high as 0.652, 0.232, 0.149 and 0.130 g NO<sub>2</sub><sup>-</sup>-N g<sup>-1</sup> MLVSS d<sup>-1</sup>, respectively. On the other hand, 150-250 μm showed almost negligible bacteria activity, which could be explained by the fact that mainly inorganic material was represented by that range. These results suggest that the bacteria activity will be reduced in larger diameter particles and the possible cause may be linked to the mass transfer limitation of substrate and oxygen. In addition, also the inorganic precipitation could somehow interfere with the activity, although this could not be confirmed by the PO<sub>4</sub><sup>3-</sup> and Ca<sup>2+</sup> removal rates. The ranges <600 μm, 710-1180 μm, 1400-2000 μm and >2800 μm showed 62.4, 50, 40 and 61.2% PO<sub>4</sub><sup>3-</sup> removal and 33.7, 21, 12.9 and 24.1% Ca<sup>2+</sup> removal, respectively. This means that the nitrating granules fed with inorganic synthetic wastewater were able to remove P and Ca by internal accumulation or by transforming them into insoluble form. However, to

understand the effect of particles size on  $\text{PO}_4^{3-}$  and  $\text{Ca}^{2+}$  removal further investigation elsewhere would be needed, since a clear trend was not observed.

Since the batch test showed a similar pattern in the four size ranges, only  $<600 \mu\text{m}$  results are illustrated (Figure 3.2b and Figure 3.2c). While  $\text{NH}_4^+$ ,  $\text{NO}_2^-$  and  $\text{NO}_3^-$  changes are typical for a nitrating system, it is interesting to observe the  $\text{PO}_4^{3-}$  and  $\text{Ca}^{2+}$  trends. All batches showed a quick decrease of both elements during the first 30-60 minutes of experiment, which is closely related to the rapid increase of pH due to  $\text{CO}_2$  degassing; then, as soon as the pH starts lowering, due to nitrification activity and production of protons, both  $\text{PO}_4^{3-}$  and  $\text{Ca}^{2+}$  stop decreasing and they remain stable until again a quick pH change is observed (Figure 3.18). These results suggest that the bulk concentration of the two elements could be strongly influenced by changes in protons concentration (Maurer et al., 1999). On the other hand,  $\text{Na}^+$  showed a slow and constant increase until the end of test, especially with larger size granules (Figure 3.2a and Figure 3.18).

### **3.3.2. Physical characteristics of nitrifying granules with different sizes**

#### ***3.3.2.1. Density, ash content, elemental contents and their distribution***

Two distinct types of granules with different colours were found within range  $150\text{-}250 \mu\text{m}$  during the sorting process; one type showed yellow/light brown colour and settled relatively slowly, while the other had deep brown colour and could settle quickly. Based on experience, the former were newly formed biomass while the latter were old granules with long sludge retention time (Gao et al., 2011a, Yuan et al., 2017). They were carefully separated and annotated as  $150\text{-}250(\text{y}) \mu\text{m}$  and  $150\text{-}250(\text{b}) \mu\text{m}$ , respectively. The average density for size ranges  $<600 \mu\text{m}$ ,  $710\text{-}1180 \mu\text{m}$ ,  $1400\text{-}2000 \mu\text{m}$  and  $>2800 \mu\text{m}$  is shown in Table 3.3; as also previously reported, it was found that granules density increased linearly with the particles diameter up to size  $2000 \mu\text{m}$ , then it started slowing down until size range  $>2800 \mu\text{m}$  (Toh et al., 2003). This suggests that the accumulation of heavy matter was somehow depending on the particles size and the specific conditions within. In between the ranges  $150\text{-}250(\text{b}) \mu\text{m}$  and  $600\text{-}710 \mu\text{m}$ , granules achieved ash contents of around 90%, whereas granules of ranges between  $710\text{-}1180 \mu\text{m}$  and  $>2800 \mu\text{m}$  described a slightly decreased inorganic material percentage, with a mean value of around 72%. Interestingly,  $150\text{-}250(\text{y}) \mu\text{m}$  described a completely different pattern, with only 3% of inorganic matter. This last result suggests that mainly organic matter, therefore biomass, would be included in that range size. On the other hand, high inorganic matter would be present in the other ranges. This was also confirmed by ICP-MS analyses, which showed that calcium and phosphorus were in excess within most of the size ranges except for the smallest  $150\text{-}250(\text{y}) \mu\text{m}$  (Table 3.3). The other analysed elements seemed to have no obvious difference among the size ranges, except for iron, which showed a higher concentration within  $150\text{-}250(\text{y}) \mu\text{m}$ , probably explained by the fact that the element may be a common factor in enzymes and biological systems.

Table 3.3 – Density, ash content and ICP-MS results of main elements concentrations within different size granules.

		Size range ( $\mu\text{m}$ )												
		150-250(y)	150-250(b)	250-300	300-425	425-500	500-600	All granules <600	600-710	710-1180	1180-1400	1400-2000	2000-2800	>2800
<b>Density</b>	$\text{g L}^{-1}$	-	-	-	-	-	-	172.3	-	264.7	-	358.0	-	402.3
<b>Ash content</b>	%	2.9	91.0	91.2	88.7	90.3	87.1	75.2	89.2	70.6	75.4	70.5	66.4	80.0
<b>Ca</b>		71.4	309.4	317.1	323.5	315.5	324.9	276.9	316.4	269.4	282.3	216.5	253.7	244.1
<b>P</b>	MLSS	34.9	68.15	63.9	64.6	67.8	67.7	61.20	72.2	84.5	91.8	83.4	95.3	95.7
<b>Na</b>		0.9	2.4	2.2	2.4	2.4	2.5	2.15	2.6	2.8	2.9	2.5	2.9	2.6
<b>Mg</b>	$\text{mg g}^{-1}$	0.9	1.0	1.0	1.0	1.0	1.0	1.01	1.0	0.9	0.9	0.8	0.9	0.9
<b>K</b>		1.2	0.2	<0.1	<0.1	<0.1	<0.1	0.27	<0.1	<0.1	<0.1	<0.1	<0.1	<0.1
<b>Fe</b>		9.9	2.7	1.5	0.8	0.9	0.7	2.76	0.7	0.9	0.9	1.9	0.9	0.9
<b>Ca/P molar ratio</b>		1.58	3.51	3.83	3.87	3.59	3.71	3.50	3.39	2.46	2.38	2.01	2.06	1.97

### **3.3.2.2. Granules morphology by stereomicroscopy**

From stereomicroscopy analyses, different size granules showed a quite diverse appearance. Figure 3.3a and b represent the yellow portion of 150-250  $\mu\text{m}$ , which is mainly formed by light brown flocs (blue arrows) and two types of rounded particles, one with a darker brown centre (white arrows) and one with a lighter brown colour (grey arrows) (also see Figure 3.20, Figure 3.21 and Figure 3.22). These were described later in the Discussion paragraph as to be mature and young granules, respectively. In addition, also another particle is visible in Figure 3.3b (red arrow), which shows a cauliflower-like shape. Figure 3.3c and d show the granules found in the brown portion of 150-250  $\mu\text{m}$ ; in this picture less rounded particles could be identified that can likely be granules fragments, which were either dark or light brown colour. Also a transparent type of particle with bright appearance was encountered, which resembles a crystal (green arrows). Before separation by size, the mixture of granules investigated in the present study looked like in Figure 3.23. Due to instability of some granules, fragmentation of the larger particles was observed and smaller and lighter brown particles were formed. The stereomicroscopy pictures would explain how flocs and little granules represent young and active biomass, whereas the fragments could be either dead granules formed by little bacteria activity or de novo inorganic precipitates formed at the system conditions. This also explains the high difference in activity between the two portions encountered in this size range. The size range 600-710  $\mu\text{m}$  was described by not-rounded particles of dark and light brown colour (Figure 3.3e and f); also these granules look similar to fragments of greater size granules, some of which showing dark surfaces. Finally, Figure 3.3g, h and Figure 3.3i, j show 1400-2000  $\mu\text{m}$  and >2800  $\mu\text{m}$  granules, respectively; the particles from the two sizes look similar except for the diameter, they are light brown colour and the surface is covered by light (orange arrows) and dark (yellow arrows) brown spots. In the Discussion paragraphs they were described as attached cauliflower-like particles or buds and the cracks left from their detachment from the granule, respectively. Further details of these structures can be seen in Figure 3.19, Figure 3.20, Figure 3.21, Figure 3.22 and Figure 3.23.



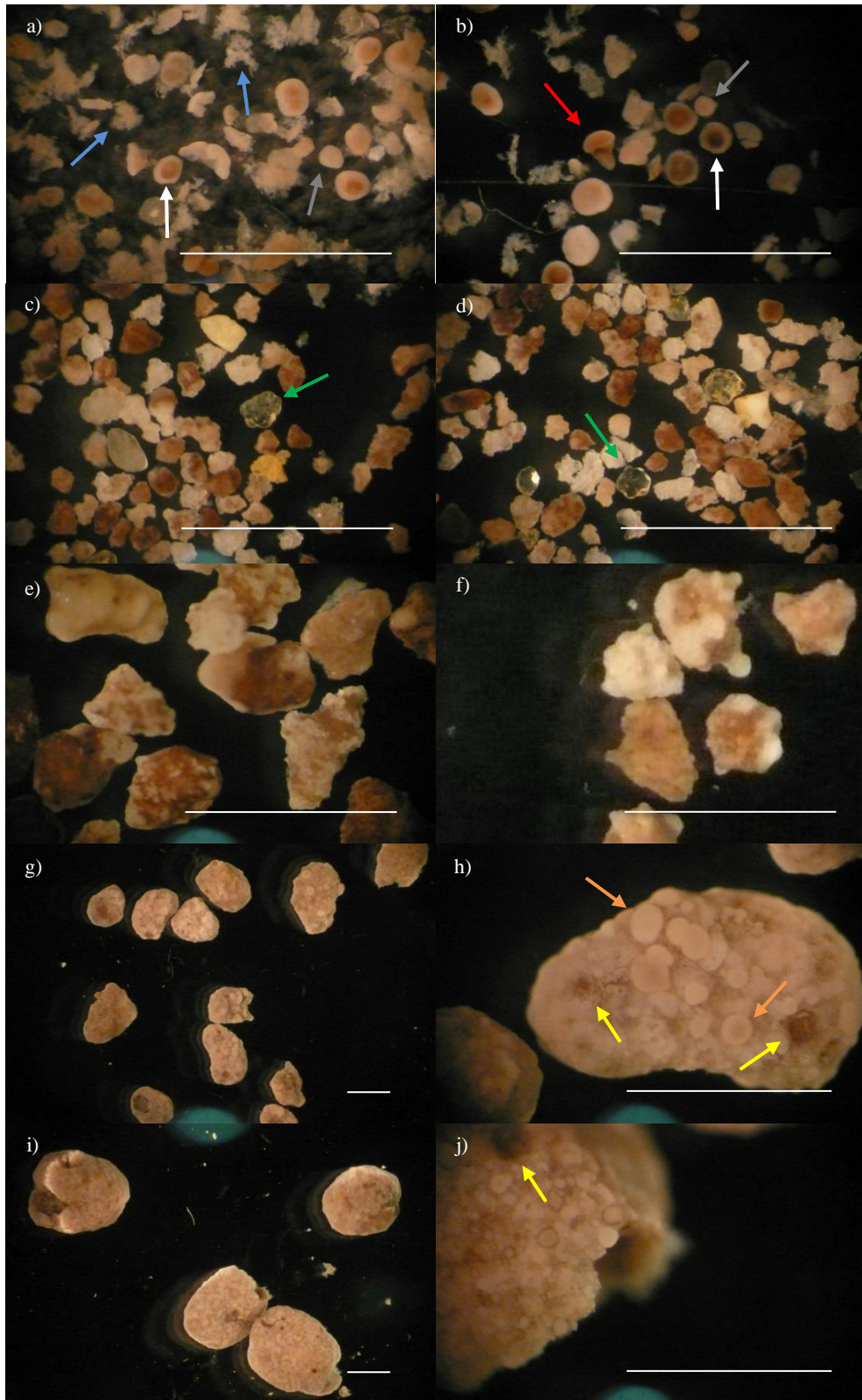


Figure 3.3 - Stereomicroscopy images of different sizes granules. a)b) 150-250(y)  $\mu\text{m}$ , c)d) 150-250(b)  $\mu\text{m}$ , e)f) 600-710  $\mu\text{m}$ , g)h) 1400-2000  $\mu\text{m}$  and i)j)  $>2800$   $\mu\text{m}$  granules. Blue, white, red, grey, green, orange and yellow arrows are floccs, mature granules, cauliflower-like particle, young granules, crystals, buds and cracks respectively. Bar = 1000  $\mu\text{m}$ .

### 3.3.2.3. Saturation index and inorganic crystalline phases

From the SI calculations the most probable minerals precipitating at the specific conditions were predicted to be calcium phosphate in the form of hydroxyapatite (HAP, 14.761), calcium carbonate as calcite (3.667) and aragonite (3.265). To confirm the ICP and SI previsions, the crystalline composition of the granules was analysed by XRD. Figure 3.4a shows no particular phase in 150-250(y), which suggests the presence of amorphous matter only. On the other hand, in a similar way for all the other size ranges, the granules showed a clear crystalline composition, mainly formed by hydroxyapatite ( $\text{Ca}_{10}(\text{PO}_4)_6(\text{OH})_2$ ) and in lower extent by calcite ( $\text{CaCO}_3$ ) (Figure 3.4b-d and Figure 3.5 a-c). The intensity of each phase is described by an arbitrary unit (a.u.) since the methodology is rather qualitative than quantitative; however, it is possible to notice how a higher amount of crystalline inorganic phase was present within the granules larger than 500  $\mu\text{m}$  (6000 a.u.). This suggests that, as was also revealed by the density results, it was within larger particles that heavier crystalline matter had accumulated as hydroxyapatite.

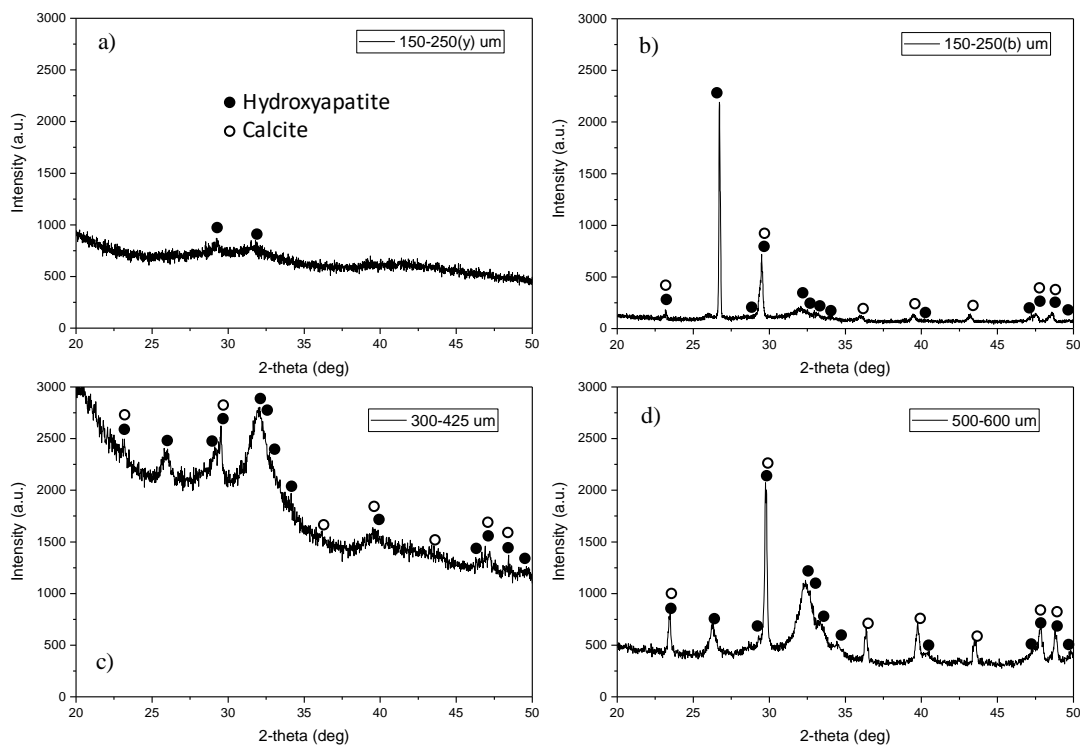


Figure 3.4 - XRD results of different sizes granules; a) 150-250(y)  $\mu\text{m}$ , b) 150-250(b)  $\mu\text{m}$ , c) 300-425  $\mu\text{m}$  and d) 500-600  $\mu\text{m}$ .

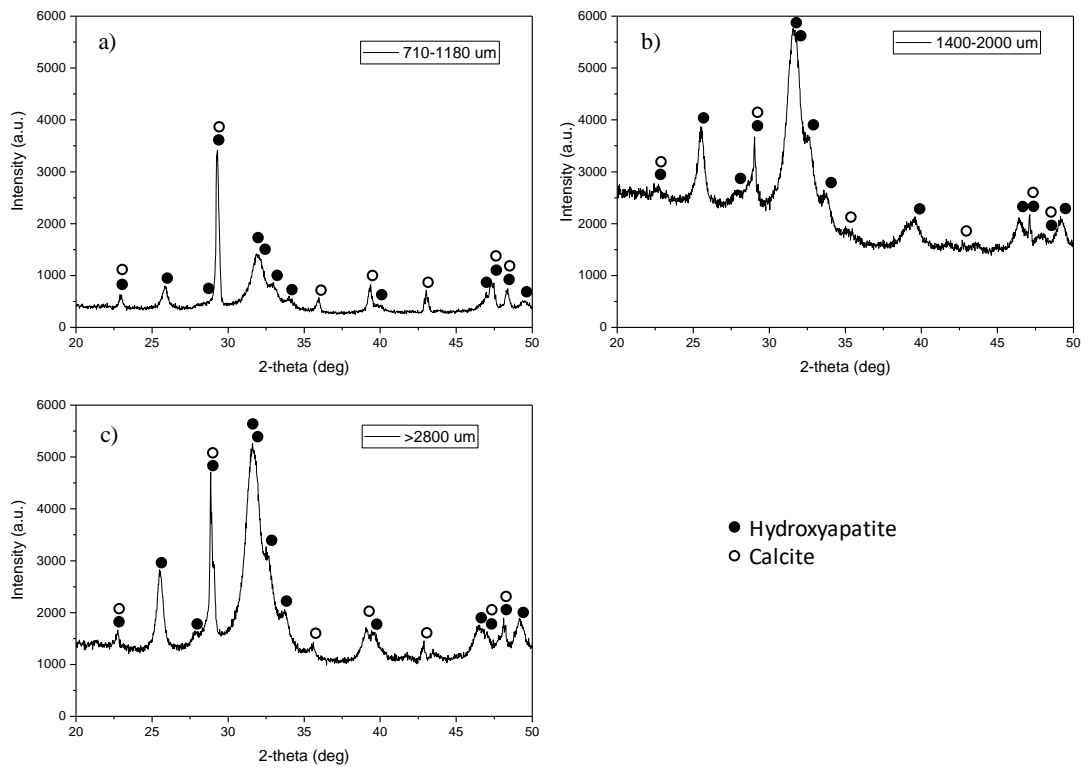


Figure 3.5 – XRD results of different sizes granules; a) 710-1180 μm, b) 1400-2000 μm and c) >2800 μm.

### 3.3.2.4. Granules morphology by SEM

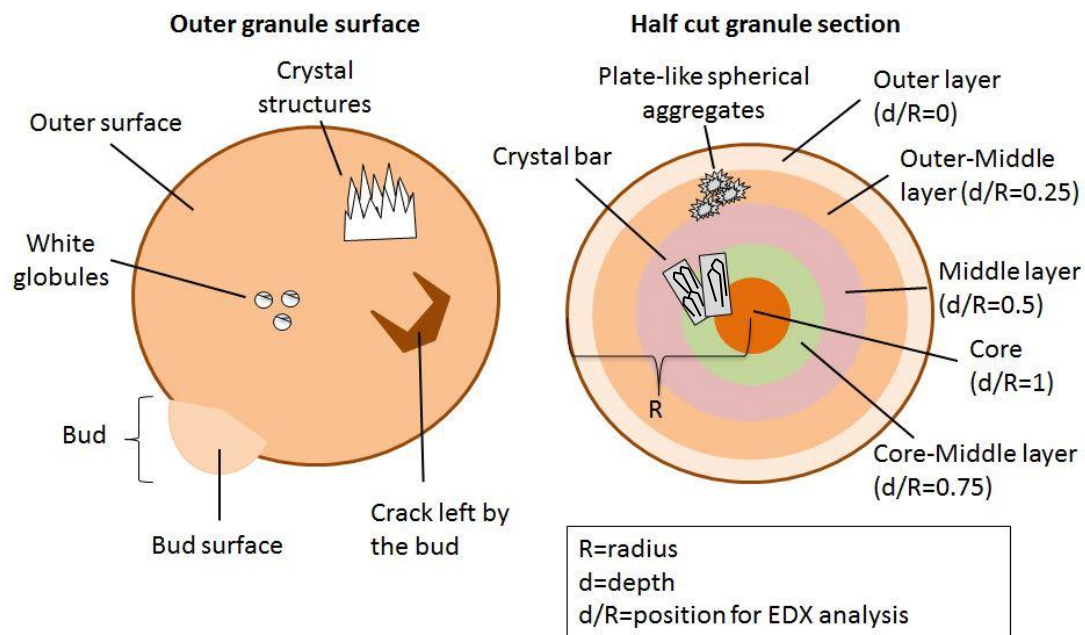


Figure 3.6 – Hypothetical description of granule’s surface (left) and internal layers (right) from SEM and SEM-EDX results; the different structures found within samples are illustrated just for convenience and to make the following pictures clearer.

In Figure 3.6 the outline of the proposed structures found within and on the surface of SEM analysed granules is presented; the microscope was directed to different areas which are described on the figure and that will be recalled during the next paragraphs. The terms used to name the layers (e.g. core, outer-middle, etc.) or the peculiar structures (e.g. *crystal bar*, *bud*, *crack*, etc.) and their representations are used in this description for the sake of clearness. Figure 3.7a and b show an almost cubic particle and its surface, respectively, from the 150-250(y)  $\mu\text{m}$  specimen; it is possible that one of the crystal-like granules seen by stereomicroscopy analysis within 150-250(b)  $\mu\text{m}$  (Figure 3.3c and d, green arrows) had accidentally mixed with the 150-250(y)  $\mu\text{m}$ , since sampling was hard with the naked eye. Unfortunately, there is no proof whether this was ever an active granule or if it was created by inorganic precipitation, but as noted in the EDX analyses (see later), it was concluded that it was likely something else. On Figure 3.7c and d are shown what possibly could be a granule fragment and the granule fragment surface, respectively. It is still not clear why the surface of the granule showed such appearances, but it is plausible that the low pressure during the pre-treatment for SEM analyses could have caused such behaviour. However, few bacteria cells were visible on the surface of the granule’s fragment in Figure 3.7d. Unfortunately, since it was quite hard to manage so little particles, a better picture of a floc or an entire round granule was not available from this specimen. More interestingly, in Figure 3.8 is shown sample 150-250(b)  $\mu\text{m}$ , in which three of the structures suggested in Figure 3.6 could be found. As Figure 3.8a shows, the analysed granule had a peculiar not-round shape (similarly to some particles noticed in stereomicroscopy, Figure 3.8 a.1), formed by visible fingers-like arrangements of material which are named for convenience as *crystal structure* in this text, and of which a detailed picture is visible in Figure 3.8b.

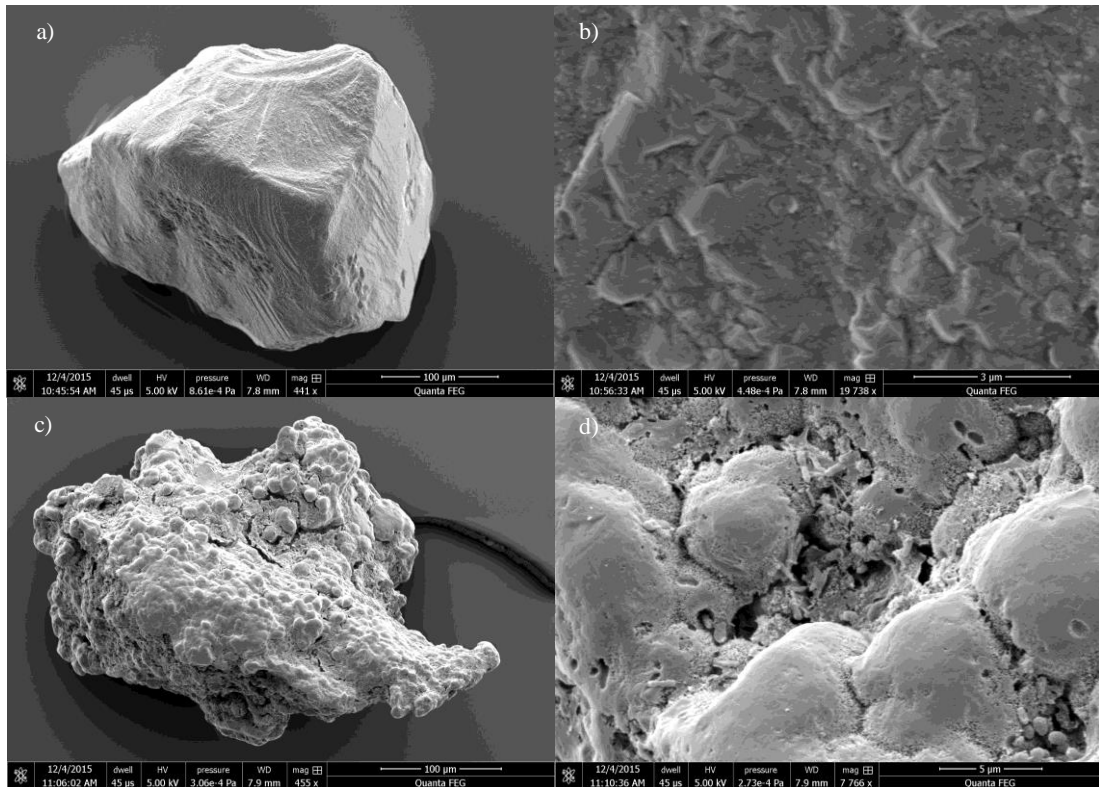


Figure 3.7 – SEM morphology of 150-250(y)  $\mu\text{m}$  granules; a) crystal-like particle overview and b) its surface, c) granule fragment overview and d) its surface.

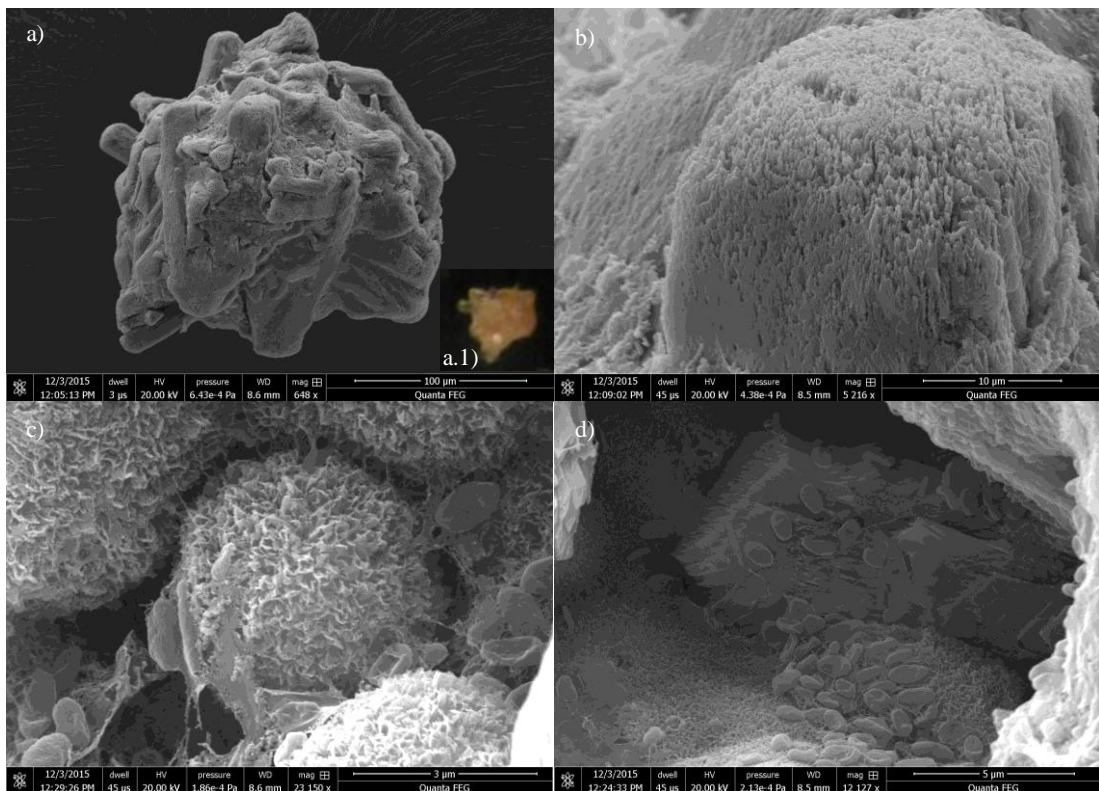


Figure 3.8 – SEM morphology of 150-250(b)  $\mu\text{m}$  granules; a) granule overview, a.1) granule with stereomicroscopy for comparison, b) crystal structure, c) plate-like spherical aggregate and d) crystal bar.

In the picture no microorganisms are visible and the solid organisation suggests a possible inorganic composition. In Figure 3.8c, from the same particle, a *plate-like spherical aggregate* is shown, surrounded by bacteria and extracellular polymeric substance; this special structure was also previously described in a partial nitrification/ANAMMOX system (Johansson et al., 2017) and other studies (He et al., 2003, Han and Louhi-Kultanen, 2018), which may suggest that it is not produced by a single type of microorganism or environmental conditions. Finally, in Figure 3.8d, it was observed a *crystal bar*, which was covered and surrounded by bacilli and EPS. A similar structure was also identified in a study where calcite precipitation was encountered in presence of organic matrixes (Mann et al., 1990). On Figure 3.9a is illustrated a normal granule from the 300-425  $\mu\text{m}$  range, on which again *crystal structures* were observed (not shown); from the same size range but quite different from the other granules it was found what is shown in Figure 3.9b, which in the present research is considered a *bud*, as it will be described later. The bud is described by two portions, the base (left side of picture) and the external surface or dome (right side of picture). The composition of the base is shown in Figure 3.9c, where a surprisingly high amount of microorganisms was found and no amorphous or inorganic structure were observed. On the other hand, in Figure 3.9d the bud external surface is illustrated, where many bacteria covered with both a film and a great amount of little clumps of not-identified matter are shown. For the range 500-600  $\mu\text{m}$  more granules could be analysed, as shown in Figure 3.10a, and two quite different kinds of particles were detected: one with a not-round shape (Figure 3.10b), characterised by several *cracks* and *crystal structures* (Figure 3.10c) spread all over the surface; the other one displayed in Figure 3.10d, with a much spherical form and a peculiar surface architecture.

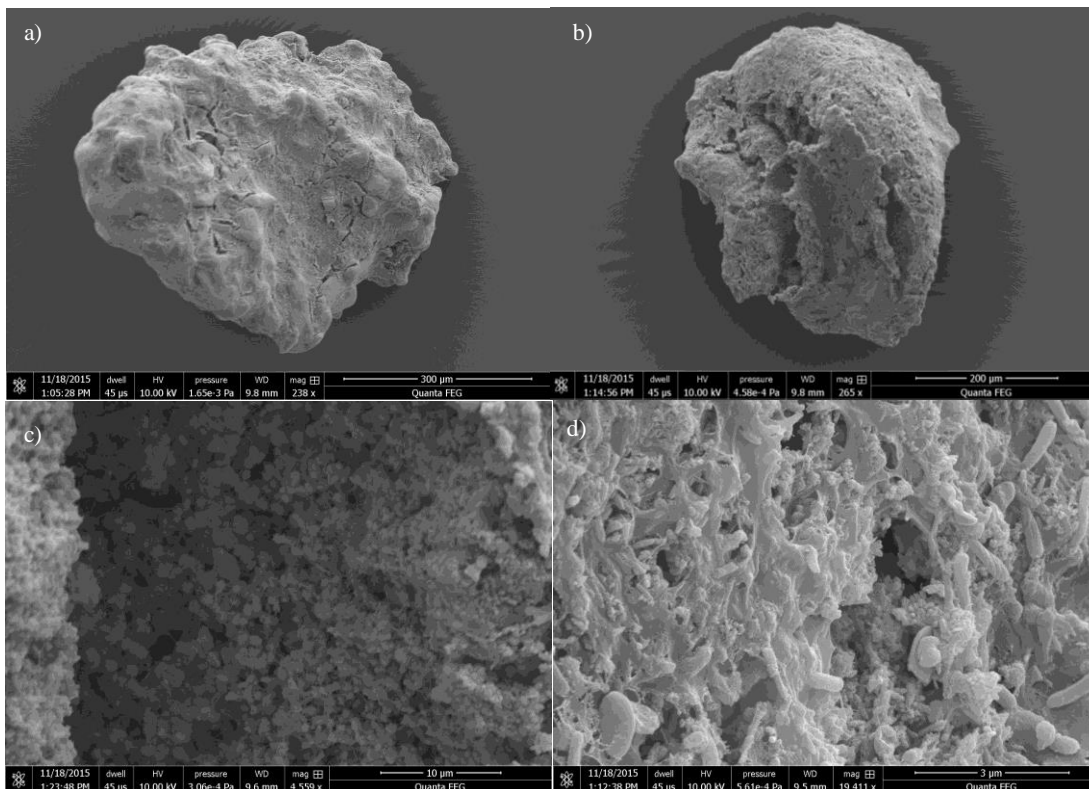


Figure 3.9 – SEM morphology of 300-425  $\mu\text{m}$  granules; a) granule overview, b) bud overview, c) left and d) right portion of the bud.

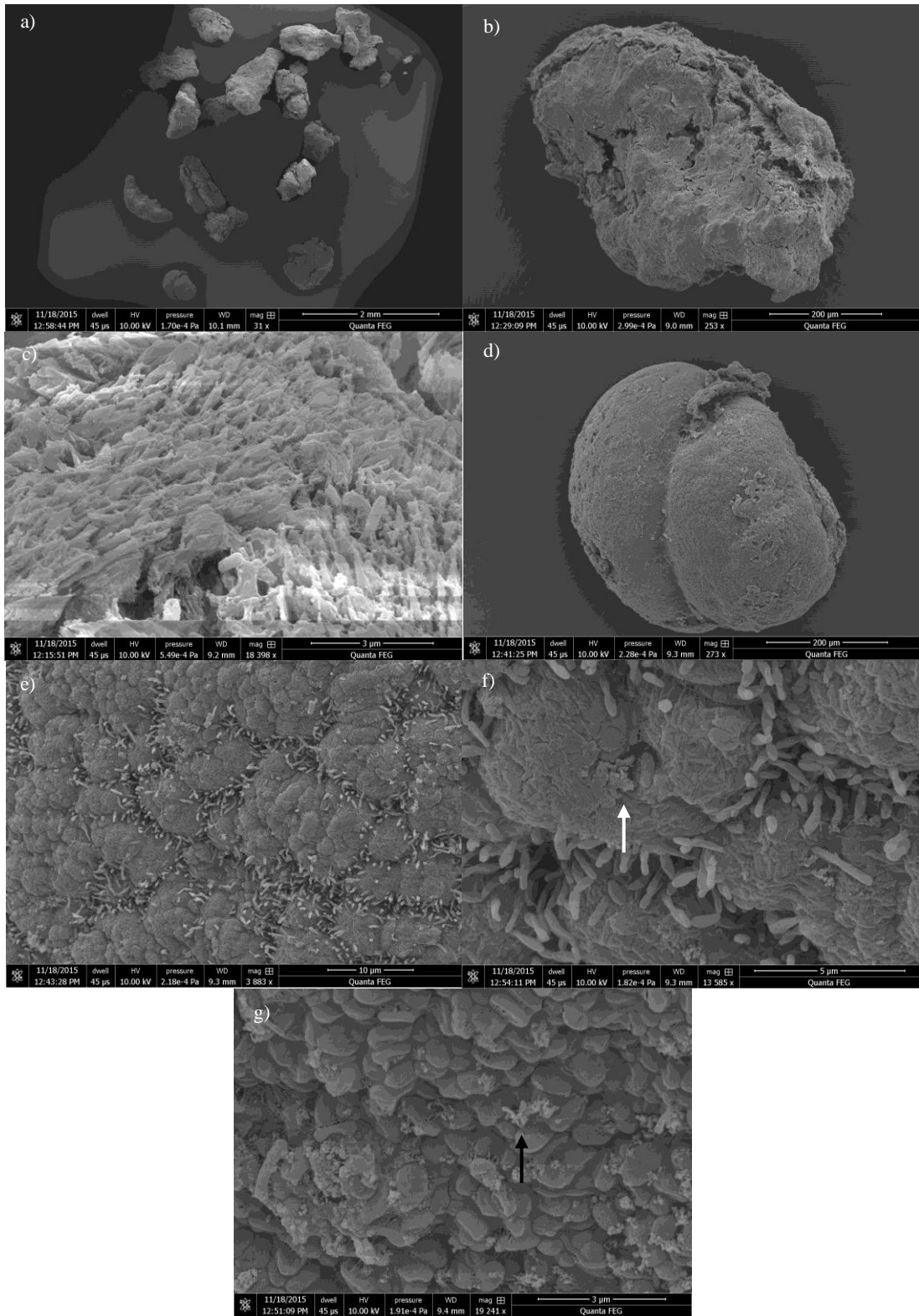


Figure 3.10 – SEM morphology of 500-600 μm granules; a) group of granules, b) mature granule overview and c) crystal structure on its surface, d) young granule overview and e)f) its right portion and g) left portion. White and black arrows indicate the inorganic layer and clumps, respectively, formed on top of bacteria cells.

Indeed, the granule looked almost split in two portions, the right one formed by bacilli surrounding globular structures (Figure 3.10e and f), and the left one formed by coccoid bacteria on which a not recognised clear matter is visible (Figure 3.10g). Figure 3.11a represents a not-spherical granule from size range 710-1180  $\mu\text{m}$ , in which some cracks can be seen; when the microscope was pointed to the internal of the cracks, a surprising great amount of bacteria was found surrounding globular structures (Figure 3.11b and c), as also seen previously in Figure 3.10e and f. In Figure 3.11d and e are shown a still attached bud and its surface, respectively, where several bacteria are visible; the surface in this picture can be easily compared to the one of the bud shown in Figure 3.9d. Furthermore, crystal structures were found at the base of this bud and they were covered by EPS Figure 3.11f.

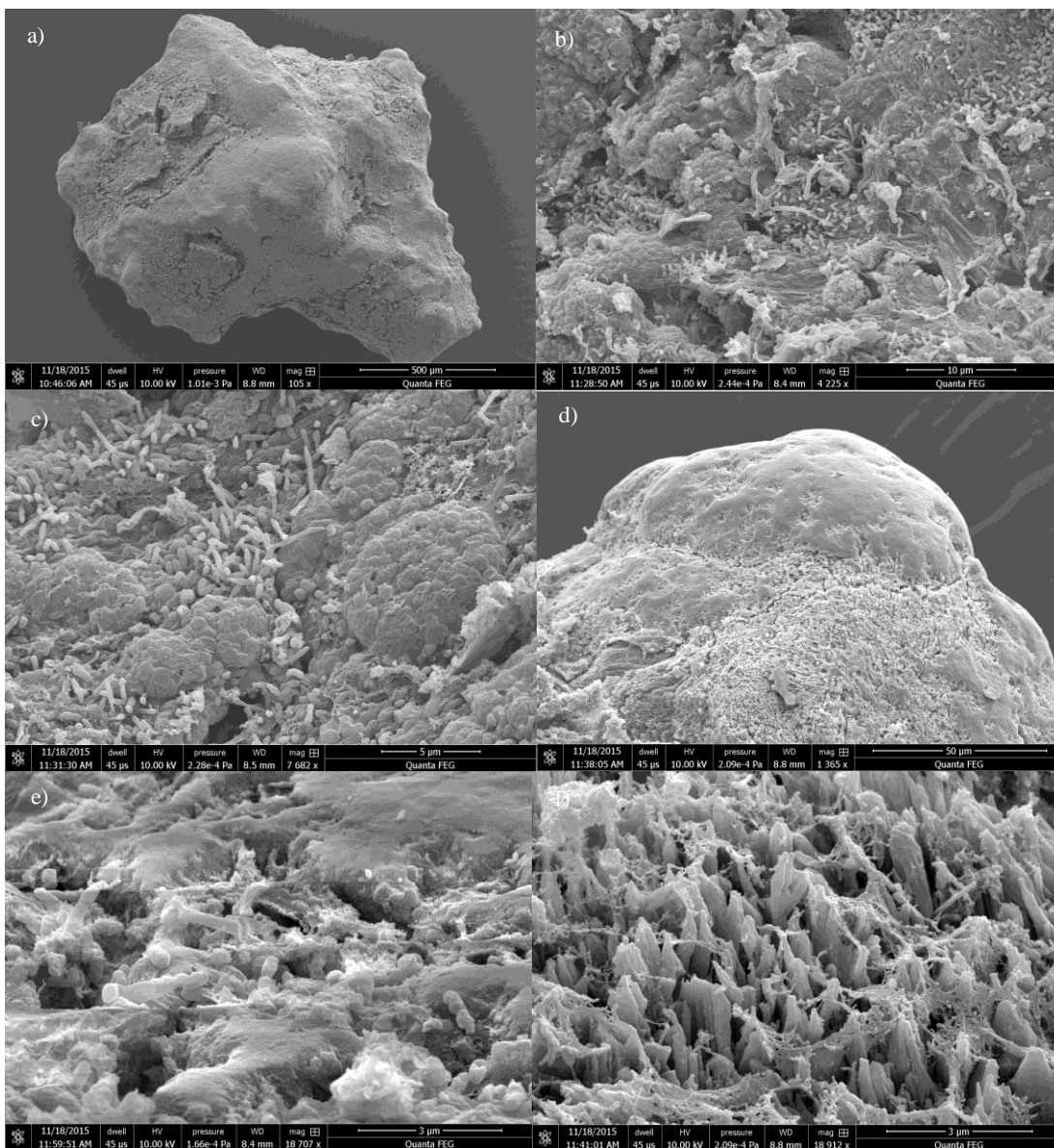


Figure 3.11 – SEM morphology of 710-1180  $\mu\text{m}$  granules; a) granule overview, b)c) bacteria and globular structures in a crack, d) bud and e) its surface, f) crystal structure at the bud base covered with EPS.



As explained before, 1400-2000  $\mu\text{m}$  granules could be cut in halves and SEM analyses were carried out on both external and internal surface; Figure 3.12a and b show, respectively, the entire external surface granule half, with visible buds, and the internal one with the core. SEM pictures were taken in three different points on the internal surface: outer layer, where compact amorphous material-formed globes were dominant (Figure 3.12c); middle layer, where less compact forms of globes were present (Figure 3.12d); and core, where the globes became even sparser and left space to the solid crystal bars already found within 150-250(b)  $\mu\text{m}$  and to dense agglomerations of not-recognised clumps (Figure 3.12e and f). In Figure 3.12f.1 is a detail of a smooth-steps appearance on the lateral face of the crystal bar.

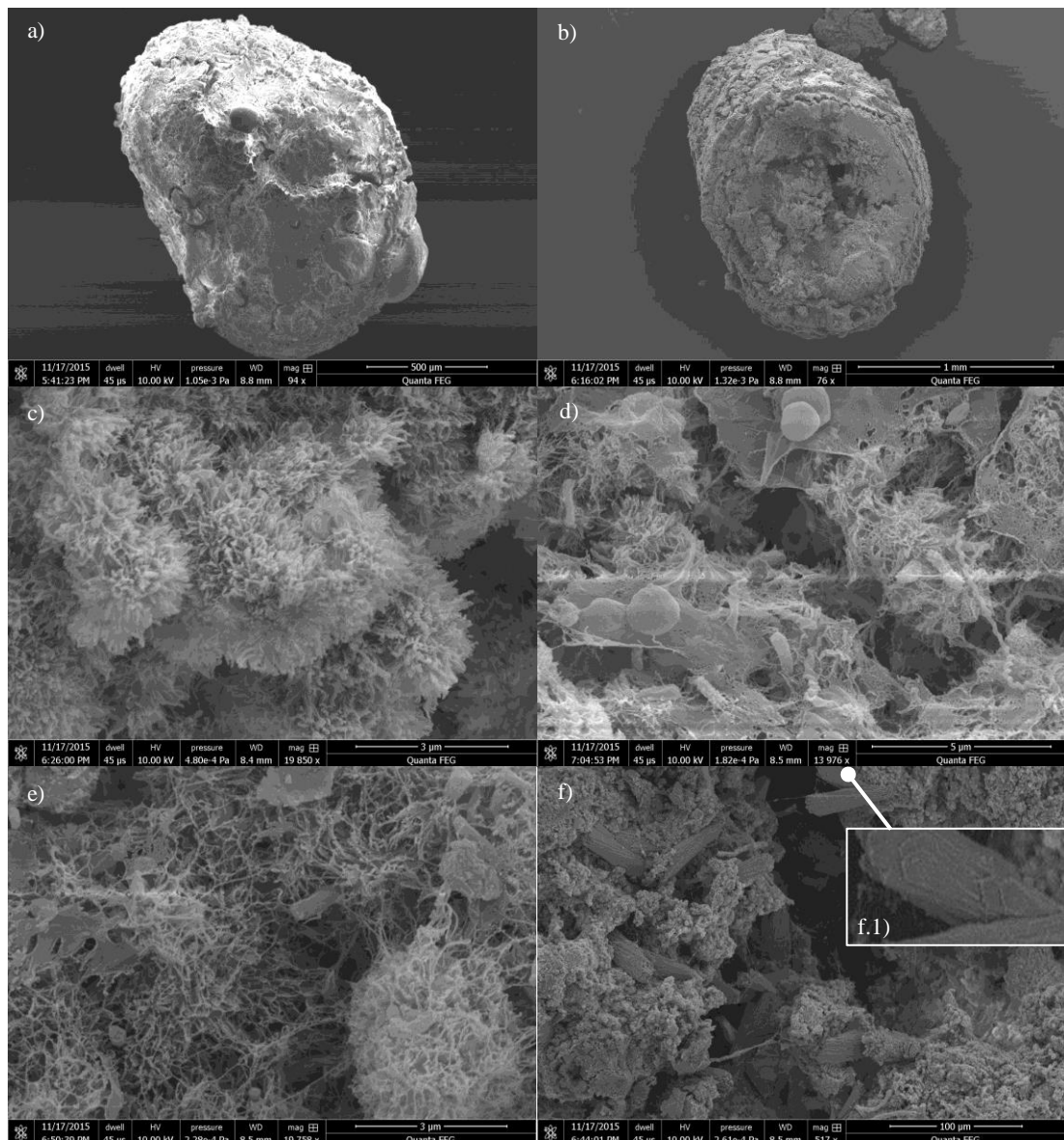


Figure 3.12 – SEM morphology of 1400-2000  $\mu\text{m}$  granules; a) entire granule overview, b) halved granule overview, c) external layer of the granule half, d) middle layer of the granule half and e)f) core of the granule half. f.1) shows a zoomed in of the inorganic crystal bar present in the granule half core.

Figure 3.13a is showing the external surface of a half granule with a size  $>2800\ \mu\text{m}$ ; it seems that the structure could not resist the fixing and drying procedures and eventually got flat. Anyhow, buds could still be observed on the surface and in Figure 3.13b a *white globule* on top of one of these buds was described. The external surface was also analysed by SEM and a dense concentration of bacilli surrounded by EPS and a not-recognised clear matter were observed (Figure 3.13c). Unfortunately, during the drying procedure, which preceded the SEM analyses, the  $>2800\ \mu\text{m}$  granule half that was supposed to be analysed for the internal surface, got completely shattered and high-quality images could not be taken. On the other hand, the granule half used for EDX analyses did not break and eventually a couple of pictures could be taken (Figure 3.13d and e); in the first picture is shown the entire half granule, whereas from the second one, even though the quality is not optimal, it is easy to detect the solid crystal bars already seen within previous specimens.

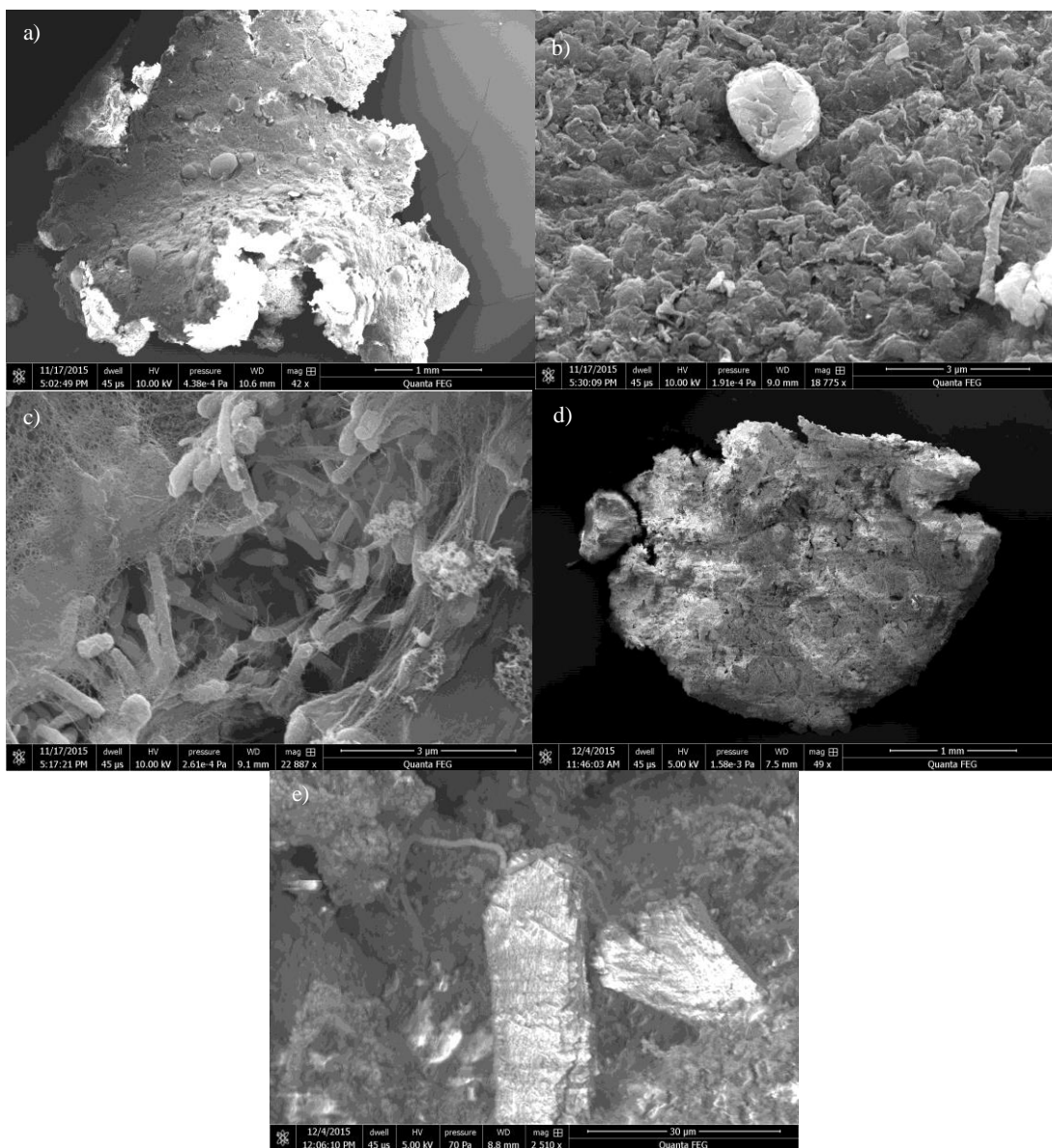


Figure 3.13 – SEM morphology of  $>2800\ \mu\text{m}$  granules; a) granule overview, b) a white globule and c) bacilli on the granule surface, d) halved granule overview and e) crystal bars in its core.

### 3.3.3. EPS of partial nitrifying granules with different sizes

#### 3.3.3.1. Proteins and polysaccharides

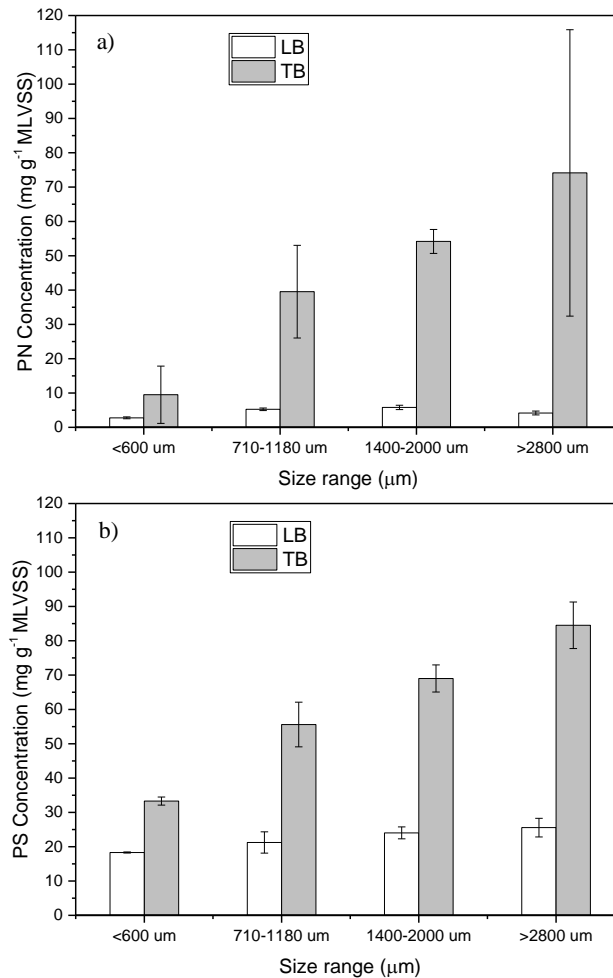


Figure 3.14 – EPS content from different sizes granules of a) proteins and b) polysaccharides. Extraction with formaldehyde/NaOH method; Lowry's and Dubois's procedures used for PNs and PSs determination, respectively. LB=loosely bound-EPS, TB=tightly bound-EPS.

The amount of proteins (PNs) and polysaccharides (PS) extracted from the EPS of each size range are shown in Figure 3.14a and b, respectively; they are assembled in the subgroups loosely- and tightly-bound EPS (i.e. LB and TB), depending on the strength of their binding to the granular structure. The extracted TB-EPS resulted in greater amount than the LB-EPS, describing a more important role of the former in the granules architecture. A gradual decrease of both PNs and PS in parallel with the reduction in particle size was described. The PS were observed (Figure 3.14a and b) in higher amounts compared to PNs, with PN/PS ratio of 0.29, 0.71, 0.78 and 0.88; at the same time, with increasing particles diameter the PN/PS ratio showed an increase, showing less PS in larger granules. This was previously described as a response of the bacteria community within the granules to the increasing mass transfer limitation (Liu et al., 2015b), where the PS present in EPS could be used as nutrients

(Wang et al., 2010, Sadri Moghaddam and Alavi Moghaddam, 2015). Anyway, the two EPS components resulted almost similar in amount and they showed a trend that is contradictory to literature. This result could be linked to two main reasons: the excessive precipitation described within the granules and the inefficacy of extracting EPS from the granules. For proteins measurement, the samples were incubated with sodium carbonate and sodium hydroxide present in the Lowry's protocol reagents. The presence of carbonate and the alkaline pH could likely facilitate the precipitation of Ca contained in the granule during the test; this was likely the reason why the standard deviation encountered in PNs analyses of TB samples was a bit high. Besides, interference of proteins measurement due to the presence of cations was already described in literature (Lucarini and Kilikian, 1999, Shen et al., 2013). A strong interior structure within the granules could be the reason for a not complete EPS release by the formaldehyde plus NaOH procedure; Adav and Lee (2008) showed a more efficient EPS extraction by treating the sludge with a physical method (sonication) prior to the chemicals incubation.

### ***3.3.3.2. Excitation and emission matrix (EEM) spectra***

The composition of granular sludge LB- and TB-EPS was monitored by EEM spectroscopy and representative spectra are shown in Figure 3.15. Two main patterns could be described that were formed by two peaks each for both LB and TB: peak I and II were mainly found in LB samples, whereas peak III and IV were present in TB samples. Peak I is generally related in literature (see Table 3.2) to the tyrosine aminoacids, whereas peak II represents the tryptophan aminoacids; peak IV is commonly described as fulvic acid-like substances, whereas peak III was described as polysaccharides (Chen et al., 2003b, Yamashita and Tanoue, 2003, Wang and Zhang, 2010, Wang et al., 2014a). Although EEM was used as a non-quantitative analysis in this study, it can still provide information on approximate extent of a certain fluorophore in contrast to the other size ranges. Among different granules sizes, it can be observed that for both LB- and TB-EPS there is a quite high fluorescence from sample 1400-2000  $\mu\text{m}$ , whereas a lower intensity was found in 710-1180  $\mu\text{m}$  and  $>2800 \mu\text{m}$ , which were similar to each other; on the other hand, very limited fluorescence was detected into sample  $<600 \mu\text{m}$ , which was also the sample with lower dilution compared to the others.

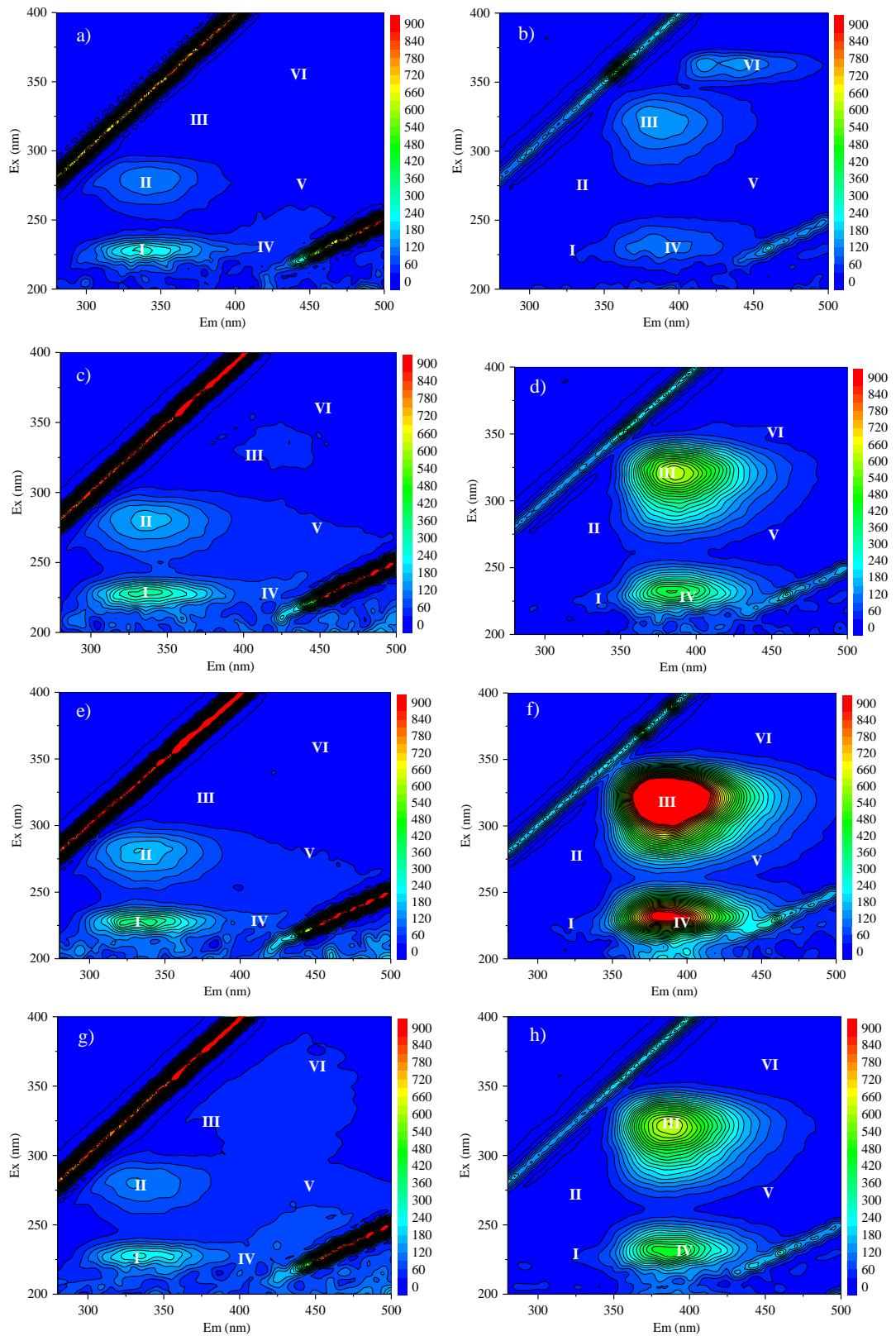


Figure 3.15 – EEM results from a) LB-EPS and b) TB-EPS in  $<600 \mu\text{m}$ , c) LB-EPS and d) TB-EPS in  $710\text{-}1180 \mu\text{m}$ , e) LB-EPS and f) TB-EPS in  $1400\text{-}2000 \mu\text{m}$ , g) LB-EPS and h) TB-EPS in  $> 2800 \mu\text{m}$ . Except for TB in  $<600 \mu\text{m}$ , which was diluted 16 times before analysis, all TB samples were diluted 64 times. The different regions encountered are described in Table 3.2.

### 3.3.4. Elements disposition

The EDX measurements done for the different size ranges are described in Figure 3.16; In the case of the granules with a diameter greater than 1400  $\mu\text{m}$  the inner layers were also analysed, since the particles could be cut in halves. As described in Figure 3.16a and b, in both 150-250(y)  $\mu\text{m}$  and 150-250(b)  $\mu\text{m}$  two types of granules were found, a squared-shape granule (similar to the one found in SEM picture) and a common spherical one. The outer surface of the former showed a peculiar signal for silicon and oxygen, with low or absent carbon and nitrogen, and also negligible calcium and phosphorus; they could be coming from the fiberglass air stones used for aeration of the SBRs and they could have detached and be retained in the system because of their weight. On the contrary, the analysed rounded-shape granules in both size ranges showed presence of carbon, nitrogen and oxygen; interesting, also phosphorous and calcium were present, even though, in different percentage from the 150-250(y)  $\mu\text{m}$ , calcium percentage weight was higher than the carbon, nitrogen and oxygen within 150-250(b)  $\mu\text{m}$ . Furthermore, within 150-250(y)  $\mu\text{m}$  range a floc was described and it showed no granular structure and low calcium and phosphorus, but high percentage of carbon, nitrogen and oxygen. Similarly to 150-250(y)  $\mu\text{m}$ , 300-425  $\mu\text{m}$  (Figure 3.16c) and 710-1180  $\mu\text{m}$  (Figure 3.16e) showed carbon, nitrogen and oxygen with higher percentage than phosphorus and calcium; instead, 500-600  $\mu\text{m}$  (Figure 3.16d) had a pattern closely related to 150-250(b)  $\mu\text{m}$ , with more calcium than any of the other elements present (i.e. carbon, nitrogen, oxygen and phosphorus). Figure 3.16f shows the size range 1400-2000  $\mu\text{m}$ , of which the internal surface could be analysed as well as the outer one; the core was basically represented by a rather high percentage of calcium and in little extent phosphorus. By moving the laser towards the external layers, carbon, nitrogen and oxygen concentrations seemed to slowly increase, until the outer layer where phosphorous and calcium were almost negligible. A quite similar pattern was shown within the outer layers, the outer surface and the bud surface, where almost only carbon, nitrogen and oxygen were present. The analyses of >2800  $\mu\text{m}$  interior layers showed similar pattern to the previous range, but this time calcium percentage showed a much higher value compared to the other elements in almost all layers (Figure 3.16g). The crystal bar, also described by SEM analyses as crystal bar, was analysed within the core and it was described mainly by calcium and, in lower extent, carbon and oxygen. When analysing the outer surface of the greater size granules, a great percentage of carbon, nitrogen and oxygen was detected, whereas only little phosphorous and calcium were present. A similar pattern was also found both on the outer surface and on a couple of buds of the same granule; finally, also a white globule was analysed and appeared constituted by carbon, nitrogen, oxygen, phosphorous and calcium.

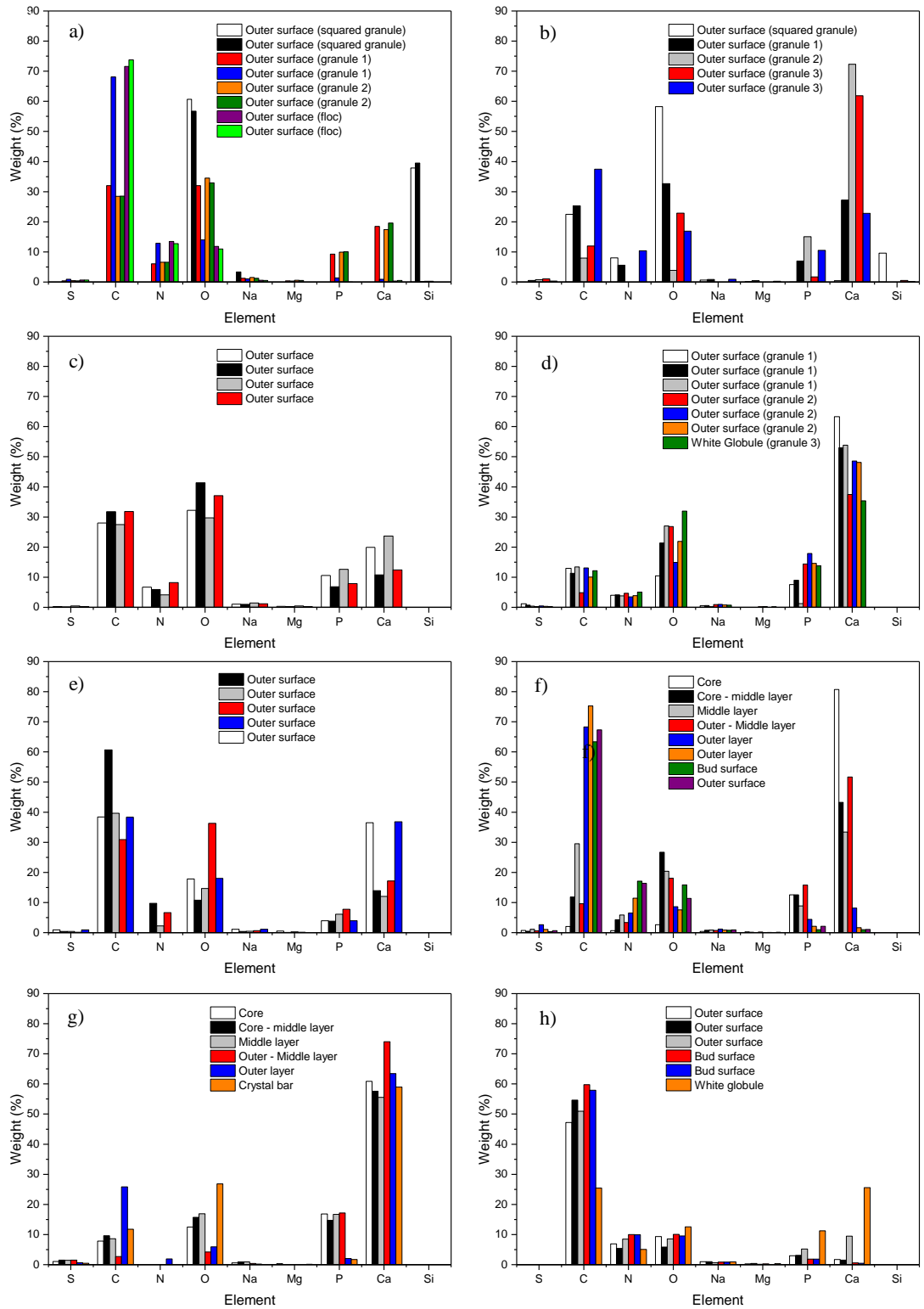


Figure 3.16 – SEM-EDX spectroscopy results of the elements weight percentage of external and internal granule surface in a) 150-250(y) μm, b) 150-250(b) μm, c) 300-425 μm; d) 500-600 μm, e) 710-1180 μm, f) 1400-2000 μm and g)h) >2800 μm granules. For reference of the analysed granule portions see Figure 3.6.

## 3.4. Discussion

### 3.4.1. Biological activity of partial nitrifying granules with different sizes and excessive precipitation

In this study the characterisation of different size partial nitrifying granules cultivated using hard water ( $100\text{-}150\text{ mg Ca}^{2+}\text{ L}^{-1}$ ) was described. The activity of nutrients removal measured for these particles was described as sAOR and SOUR, which were inversely proportional to the granule size and ash content; similar results were previously reported in Liu et al. (2016a) and Ren et al. (2008), where the higher mass transfer limitations within the larger granules limited the diffusion of  $\text{O}_2$  and nutrients (Li and Liu, 2005, Liu et al., 2005b). In addition, also the presence of precipitates, although in lower extent, could induce a lower removal activity (Liu et al., 2016a). Generally, a mixed bacterial community was used in those studies, whereas the granules in the present investigation were mainly formed by autotrophic partial nitrifying bacteria, as also confirmed by cycle analyses; this means that, despite the found similarity in activity, a thorough comparison with previous literature is not possible. However, before the characterisation experiment, the mixed granules showed a fair ammonium removal activity (sAOR) of  $1.58 \pm 0.04\text{ g g}^{-1}\text{ MLVSS d}^{-1}$ , but it is well established that the activity of high ash content granules will likely be reduced compared to granules with lower inorganic matter (Liu et al., 2015b). High AOB activity was observed by the complete oxidation of  $\text{NH}_4^+$  to  $\text{NO}_2^-$  (absent NOBs); however, the produced  $\text{NO}_2^-$  was lower than the oxidised  $\text{NH}_4^+$  and this was more emphasised within larger granules (Figure 3.17).  $\text{NH}_4^+$  for assimilation in similar processes was described to be around 8% (Bassin et al., 2012), therefore another metabolism was using  $\text{NO}_2^-$ ; it is known that in presence of high  $\text{NO}_2^-$  and  $\text{NH}_4^+$ , a low COD/N ratio and limiting  $\text{O}_2$ , AOBs are able to oxidise  $\text{NH}_4^+$  using  $\text{NO}_2^-$ , instead of  $\text{O}_2$ . This process is generally called *nitrifier denitrification* (Colliver and Stephenson, 2000, Desloover et al., 2011) and causes the  $\text{N}_2\text{O}$  release. This metabolism was observed mainly in larger granules due to the more stringent  $\text{O}_2$  mass transfer limitations (Li and Liu, 2005, Liu et al., 2005b). In addition, the transfer limitation also explained the slower activity of those larger particles, which needed a longer time to completely remove  $\text{NH}_4^+$  during the test. At the same time, this could help the NOBs activity inhibition in larger granules, as visible from negligible  $\text{NO}_3^-$  production; by contrast, as soon as all  $\text{NH}_4^+$  was oxidised in the smaller granules, nitrate was observed (Volcke et al., 2010, Isanta et al., 2012).

From the batch tests, both P and Ca accumulation within different size partial nitrifying granules could be described. The quick  $\text{PO}_4^{3-}$  and  $\text{Ca}^{2+}$  depletion in the first 30 minutes and the further decrease in the last part of test confirmed that precipitation took place in those very moments; these also coincide with a pH increase due to  $\text{CO}_2$  stripping. After partial nitrification started, pH was reduced due to proton production, which counteracted the  $\text{CO}_2$  stripping effect. In agreement with Maurer et al. (1999), the decrease of pH generates minerals dissolution, which is described by the slower rate of both  $\text{PO}_4^{3-}$  and  $\text{Ca}^{2+}$  decrease. At this point  $\text{Ca}^{2+}$  remains stable, whereas  $\text{PO}_4^{3-}$  keeps decreasing, likely due to bacteria assimilation. P removal in systems similar to the one presented was already described in literature (Gonzalez-Martinez et al., 2017); polyphosphate accumulating organisms (PAOs) *Accumulibacter*-like bacteria were observed in those systems, where both ammonium and phosphorus were removed with no COD provided (i.e. CANON process). Although EPS as main carbon source for bacteria growth in starvation conditions was previously observed (Zhang and Bishop, 2003, Wang et al., 2006), the possibility that denitrification or accumulation of phosphate by those metabolisms could take place in the nitrifying granules could not be confirmed, but it was thought to be unlikely or quantitatively negligible. Therefore, the main reason for P removal in the investigated system is to be related to precipitation with Ca. This is interesting since previous reports on inorganic precipitation in systems like the one presented are missing at the moment in literature.



### 3.4.2. Excessive precipitation in different sizes partial nitrifying granules

#### 3.4.2.1. Inorganic precipitation, P accumulation as HAP and segregation of different sizes granules

The granules described a density increase in parallel to their size increment, with linearity up to around 2000  $\mu\text{m}$ , after which density increase rate plateaued (Toh et al., 2003). This is generally due to prevention of biomass growth by higher substrate mass transfer limitation within larger granules, which consequently creates void spaces (SEM pictures) due to bacteria decay (Lemaire et al., 2008, Gonzalez-Gil and Holliger, 2014). Similar density increase within granules with bacteria-induced precipitation was also reported in anaerobic (Van Langerak et al., 1998) and aerobic (Liu et al., 2015b) systems; a parallel ash content increase to extraordinary high values (>80%), as in this study, was described. The ash content for characterised particles between 150-250(b)  $\mu\text{m}$  and 600-710  $\mu\text{m}$  was as high as 90%, which disagrees with most previous research, which showed 30-35% inorganic matter for such sizes (Li et al., 2014a, Liu et al., 2016a, Cunha et al., 2018a). In 150-250(b)  $\mu\text{m}$  the high content of Ca and P and the XRD crystalline phases reveal that what was observed by SEM were not common granules nor suspended sludge (Metcalf and Eddy, 2003). Indeed, they could be either pure inorganic particles, as previously reported in wastewater treatment processes with high Ca-content feedstock (Van Langerak et al., 1998, Cunha et al., 2018a), or fragments produced from breakage of large granules, which would explain the not-round shape. This would explain the peculiar crystal-like appearance of some particles under the stereomicroscope and the almost absent bacteria removal activity in 150-250(b)  $\mu\text{m}$ . The fragments could be due to both stability and strength reduction of structure in large sizes granules (Toh et al., 2003, Wu et al., 2012). The lower stability was also confirmed by higher PN/PS detected within the larger particles, which would be justified by degradation of EPS polysaccharides as a substrate, due to nutrient scarcity in inner layers (Wang et al., 2010, Sadri Moghaddam and Alavi Moghaddam, 2015). The low biomass content within these fragments could be explained by the consequent bacteria wash-out. For these reasons, because of the presence of both inorganic particles and fragments, the proportionality between granules ash content and diameter increment could not be compared to other research in literature (Ren et al., 2008, Liu et al., 2016a). However, since 3% ash was found in 150-250(y)  $\mu\text{m}$  and around 70-80% from size 710  $\mu\text{m}$  and up, it is plausible that a similar trend was present also in the present study. In addition, ash content was constant in diameters greater than 710  $\mu\text{m}$ , confirming that higher inorganic matter would mean granules instability. Minor fluctuation of ash content in larger particles was due to re-population of void spaces and channels by bacteria, to overcome the increasing mass transfer limitations (Ivanov et al., 2005). This was also observed on EEM results, where 710-1180  $\mu\text{m}$  and 1400-2000  $\mu\text{m}$  showed proportional fluorescence intensity to granules size, whereas >2800  $\mu\text{m}$  showed a similar signal to 710-1180  $\mu\text{m}$ . Similarly to ash content, both Ca and P increased in parallel with size raise except for sizes 150-250(b)  $\mu\text{m}$  to 600-710  $\mu\text{m}$ . It is reasonable that ash accumulation was due to precipitation of the two elements only, since the other elements were negligible in ICP results. The higher Ca in larger granules can be explained by the greater EPS produced by the bacteria; alginate-like exopolysaccharides (ALEs) contained in EPS have negative groups that bind  $\text{Ca}^{2+}$  (Lin et al., 2012, Sarma and Tay, 2018a), which can subsequently create bridges among other ALE chains. The greater P within larger diameters can be expected as a result of the presence of biological complexes (i.e. cell membrane, DNA, etc.) (Longnecker et al., 2010, Huang et al., 2015); in addition, ALE-Ca-ALE bridge conformations can chelate a molecule of phosphate if the right conditions are provided (Sarma and Tay, 2018b).

The conditions described in literature to generate bulk precipitation are mainly pH, temperature, ions concentration (e.g.  $\text{Ca}^{2+}$ ,  $\text{PO}_4^{3-}$ ,  $\text{CO}_3^{2-}$ ) and the presence of nucleation sites (Hammes and Verstraete, 2002, Dupraz et al., 2009, Mañas, 2011, Peng et al., 2018). Calcium phosphate solubility at pH 7.4-7.5 and  $\text{Ca} = 60 \text{ mg L}^{-1}$  ( $T = 20^\circ \text{C}$ ) is around  $15 \text{ mg PL}^{-1}$  (Maurer et al., 1999) and the calcium carbonate solubility at ambient  $\text{CO}_2$  pressure ( $p\text{CO}_2 = 3.5 \times 10^{-4} \text{ atm}$ ) is around  $47 \text{ mg L}^{-1}$  ( $19 \text{ mg Ca L}^{-1}$ ) (Geysant et al., 2001). This means that in

most wastewater treatment processes and especially at the conditions studied in the present research, bulk precipitation will occur. However, the precipitation observed within the characterised granules needs a more thorough explanation. Calcium carbonate can precipitate as different polymorphs, but calcite crystals need relatively short time to form (Simkiss, 1964, Besselink et al., 2017). On the other hand, HAP generally needs longer retention time to form because of the intermediate polymorphs (Boskey and Posner, 1973, Maurer et al., 1999, Mañas, 2011). The most soluble one in water will be the first to form, followed by the most thermodynamically stable phases (Nývlt, 1995). Therefore, only the precursors will accumulate at first within the partial nitrifying granules, but thanks to the granules long retention in the system (Winkler et al., 2012a), the least soluble and more stable HAP will form. This was also confirmed by the XRD and ICP results and by other research (Lin et al., 2013a), in which the older (and larger) granules showed higher HAP signal with no other precursor and a Ca/P ratio = 2 close to theoretical (1.67).

To explain further why a preferential precipitation within the particles was observed, it is necessary to look at the specific conditions created by the bacteria activity within the granules. It is plausible that AOBs uptake of inorganic carbon for cellular growth could deplete the  $p\text{CO}_2$  within the particle and consequently reduce the  $\text{CaCO}_3$  solubility. At the same time, although slowly, the already precipitated minerals in the granule could dissolve and by doing this, the protons would be consumed and consequently the pH increased (Plant and House, 2002). This was also showed by the batch test pH (7.9-8.0), slightly higher than the prepared synthetic wastewater (7.2-7.4), and which is likely to be higher within the granule, due to mass transfer limitations. The mass transfer limitations for  $\text{O}_2$  would also increase nitrifier denitrification activity, which generated an even higher bulk pH in the larger granules batch (8.6) (Figure 3.17).

The strong hydroxyapatite phase encountered within larger size granules is to be related to the pH conditions. Song et al. (2002) reported that at pH higher or equal to 9, in presence of  $\text{CO}_3^{2-}$ ,  $\text{CaPO}_4$  precipitation would be preferred to  $\text{CaCO}_3$ ; whereas at pH lower than 8 or higher than 10 the two minerals would interfere or co-precipitate, respectively. Hence, the  $\text{CaCO}_3$  precipitation would be favourable within the smaller particles mainly because of the reduced mineral solubility and the lower measured pH; on the other hand, more  $\text{CaPO}_4$  would be described within larger granules due to a slightly alkaline pH. For an improved  $\text{CaPO}_4$  precipitation over  $\text{CaCO}_3$  in presence of carbonate, a higher influent Ca/P ratio would be needed, but only up to a limit of 5 (Cunha et al., 2018a). This would agree with the results obtained in this study, where the influent Ca/P ratio was slightly higher than 5, hence justifying the presence of little  $\text{CaCO}_3$ . Therefore, lower influent calcium content would probably reduce the  $\text{CaCO}_3$  precipitation for a better P recovery as HAP.

#### **3.4.2.2. Characterisation of HAP and calcite precipitates**

The precipitates of both HAP and calcite were recognised by this research within different sizes granules and were characterised by distinct shapes and dispositions. As previously observed in partial nitrification/ANAMMOX (Johansson et al., 2017) and other research fields (He et al., 2003, Han and Louhi-Kultanen, 2018), crystallisation of calcium phosphate was identified as a sequential process and mainly under the plate-like form. No distinct shape but only clumps of amorphous calcium phosphate were present during nucleation (Figure 3.10g, black arrow); then, more mineral would accumulate in layers over the bacteria (Figure 3.10f, white arrow), after which some sort of ridge could form from which the plate-like shape becomes visible (Figure 3.8c). At this stage, HAP could grow into the very crystalline structures found on the external granules surface (Figure 3.8b and

Figure 3.11f). On the other hand, calcium carbonate was found in lower amount and mainly as crystal bars and white globules. The former were similar to the ones encountered in a study on calcite precipitation in presence of

organic matrixes (Mann et al., 1990); a smooth-steps pattern was found in common to the structures in SEM pictures (Figure 3.12f.1). EDX mineral composition also confirmed that C, O and Ca were the main elements found on both crystal bars and white globules; in addition, their Ca/O weight ratio resulted 0.29 and 0.30, respectively, which are quite close to the calcite one (0.33) (Mañas, 2011). Although formation of visible crystals within anaerobic and aerobic granular sludge was described in literature (Van Langerak et al., 1998, Liu et al., 2016a), the report of crystalline structures within partial nitrifying granules was still missing. These results could demonstrate how the same crystals could be encountered in much different biological systems, which confirms how their shapes would be species-independent. At the same time, the importance of this research is represented by the opportunity to expand the knowledge on the bacteria-induced precipitation mechanism, by which the abiotic precipitation can be distinguished.

#### **3.4.2.3. Budding theory**

In 150-250(y)  $\mu\text{m}$ , in addition to flocs, light and dark brown granules, also rooted particles were found; these are also described in literature as a portion (called bud in this study) of a cluster-like granule (also known mushroom-like or cauliflower-like). They were reported in different biological processes: anaerobic digestion (Gonzalez-Gil et al., 2001), aerobic granular system for COD and N removal (Liu et al., 2004a), simultaneous nitrification, denitrification and phosphorus removal systems (Lemaire et al., 2008), OLAND (Vlaeminck et al., 2010) and EBPR (Barr et al., 2010, Gonzalez-Gil and Holliger, 2014). The special biofilm growth, although slightly different to what was observed in 1400-2000  $\mu\text{m}$  and  $>2800 \mu\text{m}$ , has been reported to be caused by specific environmental stresses, among which nutrients and  $\text{O}_2$  were the most common (Picioreanu et al., 1998). In our partial nitrifying granules, the vast accumulation of inorganics could represent a stress that eventually forced the bacteria to start growing out radially, in order to have access to food. Due to impacts with other particles or because of the fluid shear force, or even for general instability of the whole arrangement, the bud detached from the granule; this would reveal a dark spot (crack) on the particle surface, visible on both SEM and stereomicroscopy. The mechanism of detachment from granules was already described in literature as budding theory (Vlaeminck et al., 2010). The size of the buds that featured a peculiar darker interior (Figure 3.20 to Figure 3.22), were in agreement with other research. This mechanism could justify the observation of crystal structures essentially in every point of the granules, contrasting with opinions in literature where precipitation could only take place in the core (Ren et al., 2008, Mañas, 2011). On the one hand, it is possible that a specific metabolism in the outer layers could produce the right environment for inorganic precipitation, as also described by Mañas et al. (2012b) and Yuan et al. (2017). On the other hand, it is also plausible that the extent of precipitation could be too high to be contained only within the granule core, which would confirm the bacteria displacement and the budding observation. To the best of our knowledge, this special mechanism of granules formation was only hypothesised previously in literature, but never described as in this study; the results could reveal that not only conventional operating parameters could have an impact on the granule size but also the specific conditions within the granules (i.e. inorganic matter).

### **3.5. Conclusions**

This is the first time that precipitation of both calcium phosphate (hydroxyapatite) and calcium carbonate (calcite) was observed in AOB-dominant partial nitrifying granules. The findings showed in Chapter 3 are of great importance because P removal from wastewater is a hot topic at the moment. In addition, the possibility to apply the partial nitrifying granules for both ammonium and P removal from waste streams and to recover the latter seem an appealing opportunity.

The granules characterisation revealed that no chemical or pH control was needed for the precipitation to take place. The mass transfer limitation within the larger granules was the main factor to create the suitable conditions for the minerals accumulation. This is interesting since further reduction of operation costs would be advantageous. The presence of little calcite was likely due to an unbalanced Ca/P in the influent synthetic wastewater, which was explained by the high hardness tap water used to make it. It is thought that either a higher concentration of P or lower content of Ca in the influent could improve the hydroxyapatite accumulation and reduce the calcite content. However, further investigation would be needed to disclose if the alkaline pH within the granules could generate a long-term accumulation although no chemicals are used. Indeed, the results presented here are referred to batch tests, whereas a continuous operation of this system would confirm its applicability. The direct application of hydroxyapatite granules as fertiliser is not yet approved, due to the presence of heavy metals, pathogens and recalcitrant organics; however, its recycling as a substitute of  $\text{PO}_4^{3-}$  rock in industrial applications represents a real opportunity.

The precipitation within AOBs-dominant partial nitrifying granules was mainly observed under the plate-like spheres of hydroxyapatite and the smooth-steps bars for calcite. These results could confirm previous research that specific crystal shapes were not bacteria-dependent, but could be found in biological systems quite different from each other. At the same time, the importance of these results is represented by the increased knowledge about the bio-precipitation mechanism and the possibility to help distinguish it from the abiotic processes. Due to the excessive minerals precipitation, it was possible to observe in this study a bacteria behaviour that was previously only hypothesised in literature, the budding theory. This could be confirmed by the presence of buds both attached to the larger granules and in solution; therefore, the great inorganic precipitation played an important role in this investigation on influencing the particles size in the system.

### **3.6. Experimental weaknesses**

The characterisation was done on granules that were produced from different reactors at different operation conditions (Chapter 2). Then, they were mixed together and separated based on their different sizes. Although meaningful results were obtained in the study, it would have been similarly helpful to characterise the granules based on the different operation conditions at which they were produced. It is speculated indeed, as also confirmed by results in Chapter 2, that precipitation would be specific at different temperatures and wastewater composition.

In addition, the ash, Ca and P content within most size ranges were not comparable to most literature. The reason for this is ascribable to the presence of granules fragments from the previous experiment. If those fragments were removed before the size separation and characterisation, for instance by not mixing the particles from the unstable reactors, it is likely that more explanatory results would have been obtained.

As for Chapter 2, replicability of SEM and EDX results was not confirmed due to the analysis of only few granules. More resources would have been needed to do the tests again, but this was not possible for this experiment.

### **3.7. Appendix**

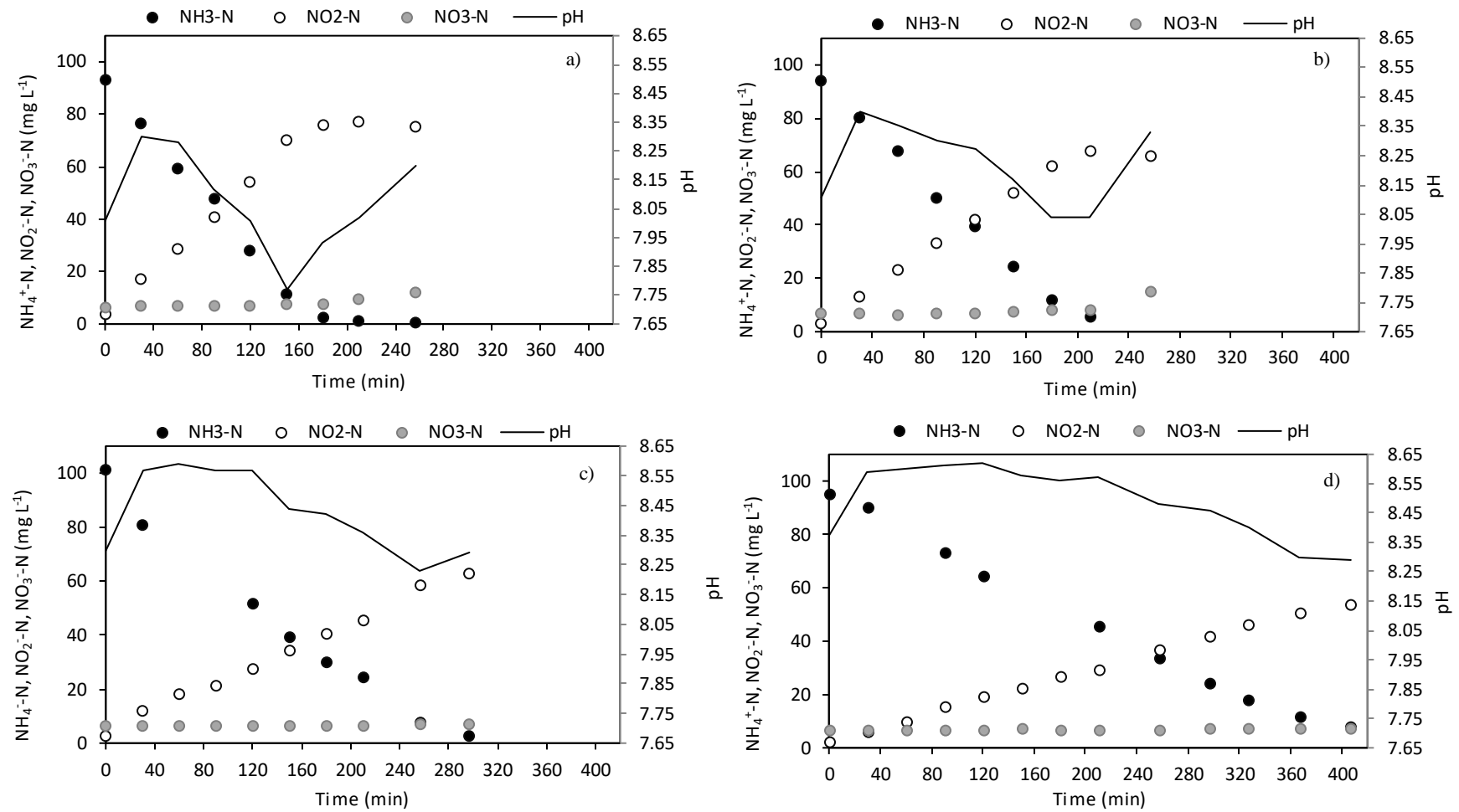


Figure 3.17 – Ammonium, nitrite and nitrate concentrations along with pH during batch test of a)  $<600 \mu\text{m}$ , b)  $710\text{-}1180 \mu\text{m}$ , c)  $2000\text{-}2400 \mu\text{m}$  and d)  $>2800 \mu\text{m}$  granules.

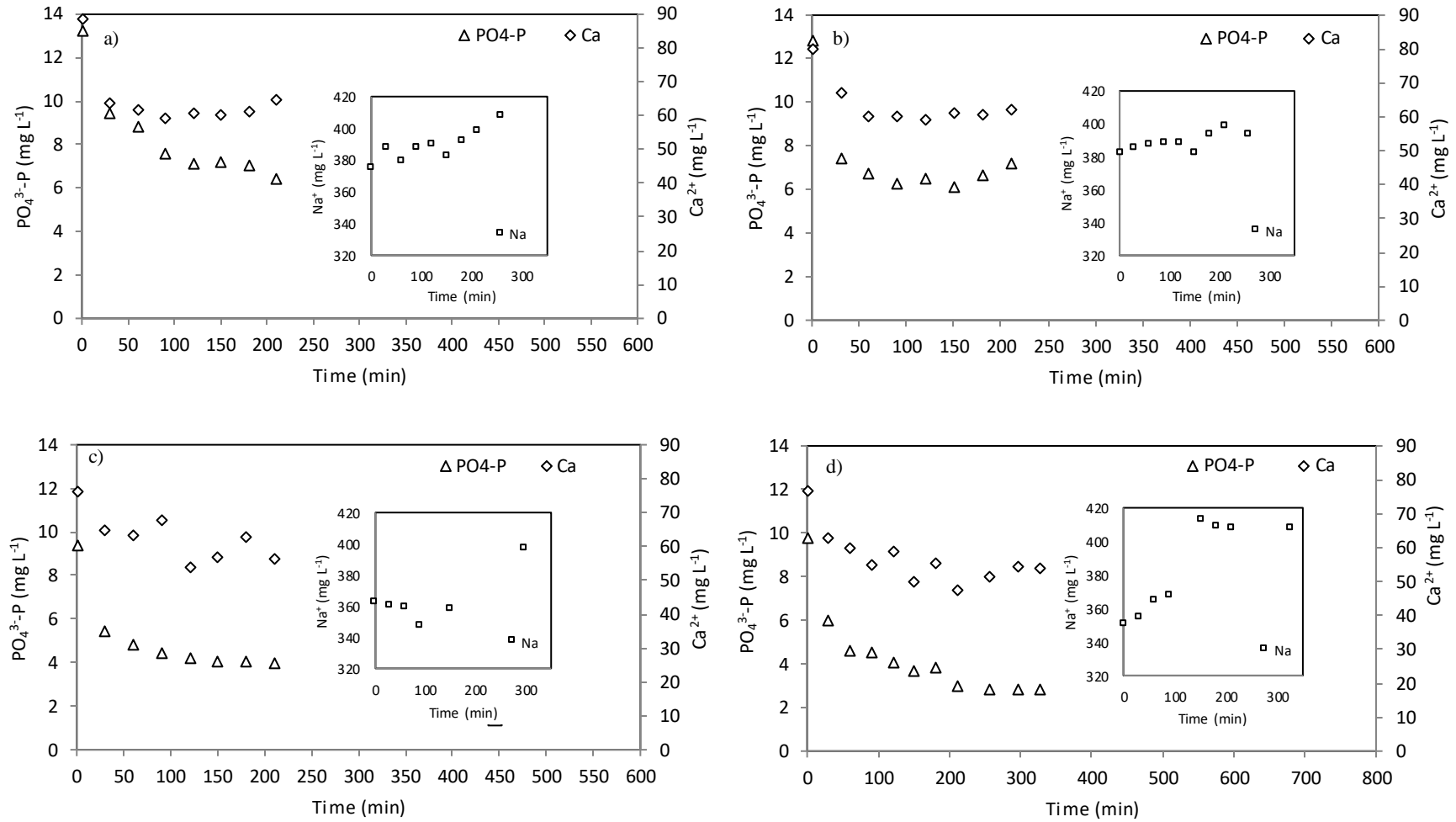


Figure 3.18 –  $\text{Ca}^{2+}$  and  $\text{PO}_4^{3-}$  concentrations during batch test of a) <600  $\mu\text{m}$ , b) 710-1180  $\mu\text{m}$ , c) 2000-2400  $\mu\text{m}$  and d) >2800  $\mu\text{m}$  granules.

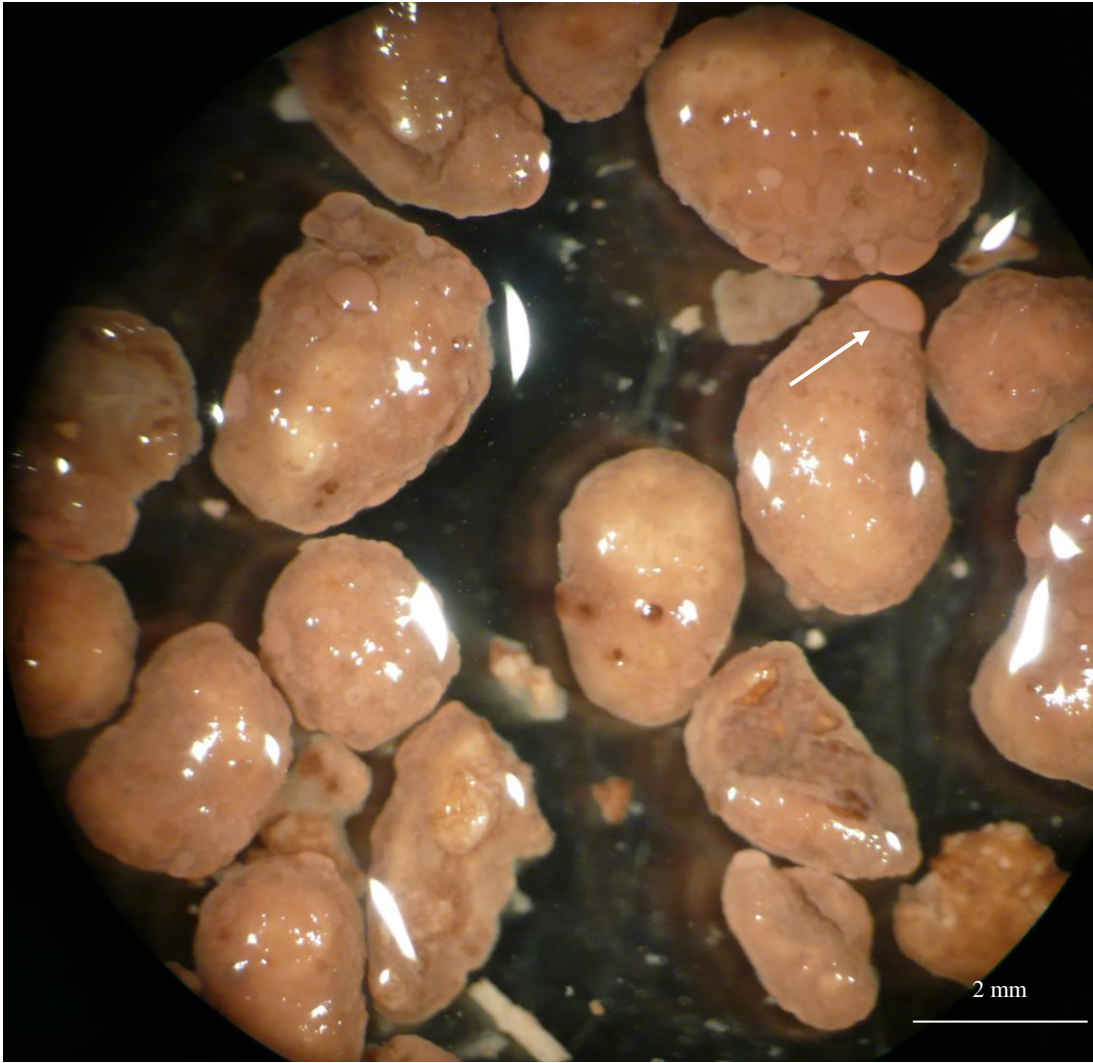


Figure 3.19 – Mixture of different sizes granules before characterisation study. The arrow indicates a bud.





Figure 3.20 - Mixture of different sizes granules before characterisation study. The arrow indicates a bud.

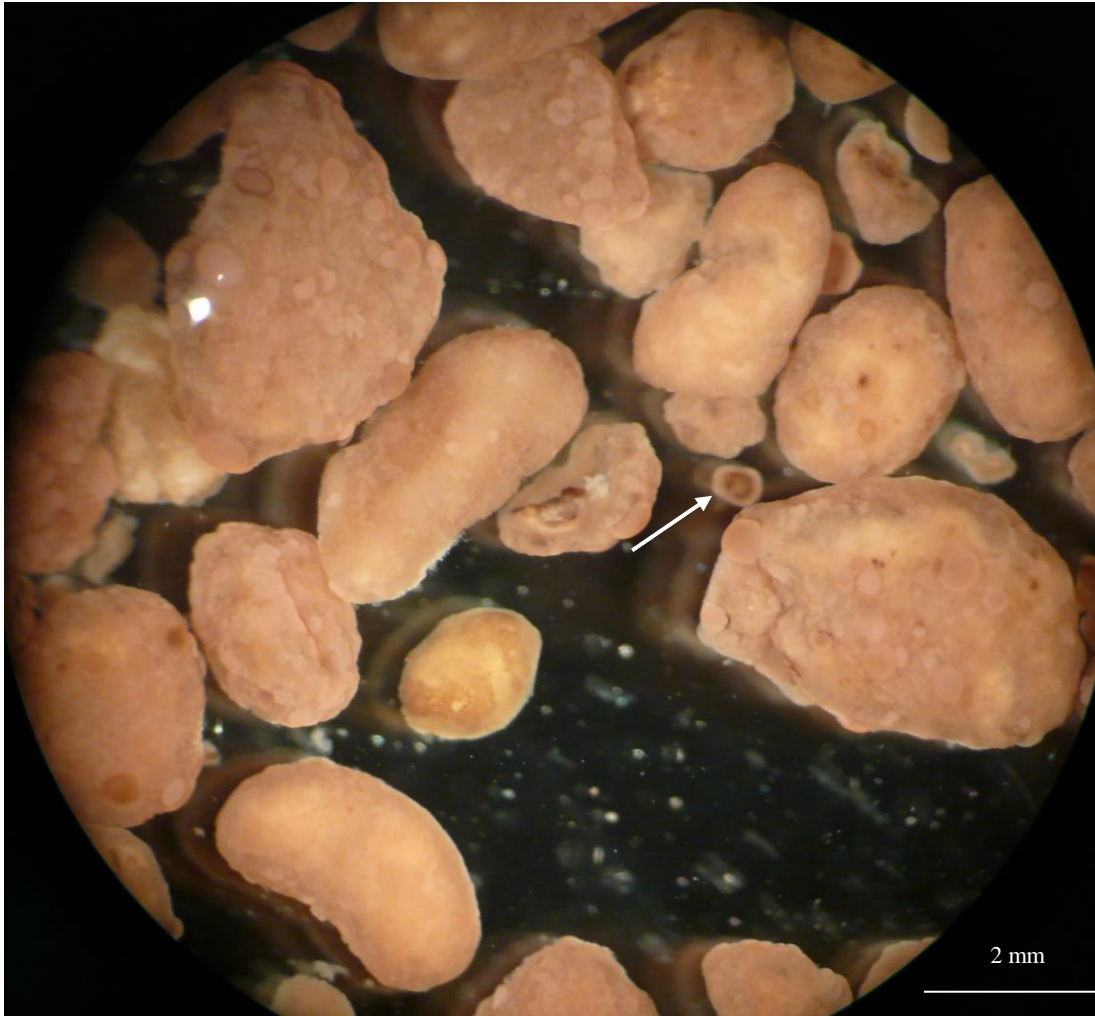


Figure 3.21 - Mixture of different sizes granules before characterisation study. The arrow indicates a bud.

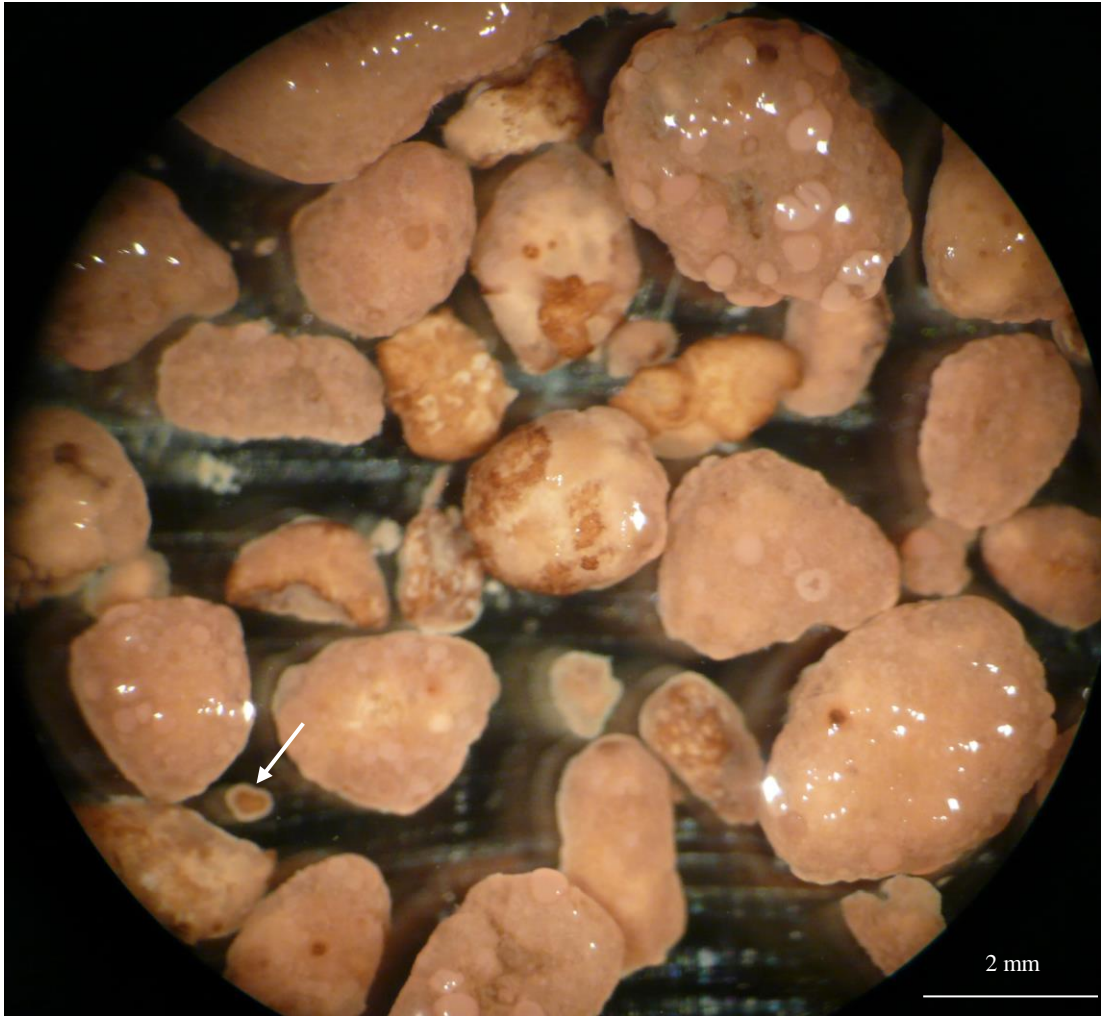


Figure 3.22 - Mixture of different sizes granules before characterisation study. The arrow indicates a bud.

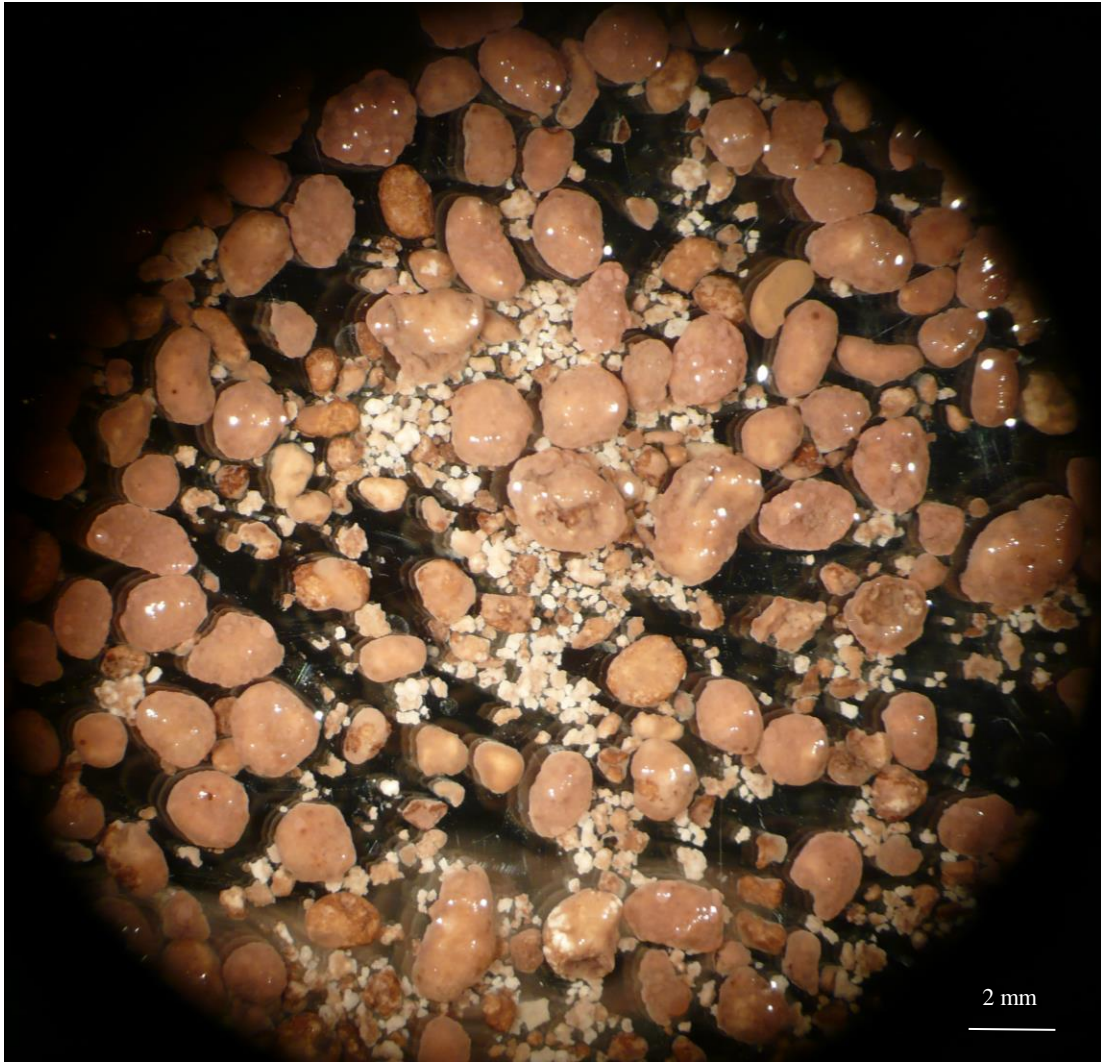


Figure 3.23 – Mixture of different sizes granules before characterisation study.

**STUDY ON EPS EXTRACTION FROM SLUDGE WITH HIGH MINERAL  
CONTENT AND RELEVANT ACTORS FOR RELIABLE PROTEIN  
MEASUREMENTS**



## 4.1. Introduction

It has been widely reported that EPS content in biofilm including granular sludge, is much higher than that in suspended sludge (Tay et al., 2001c). EPS plays an important role in the stimulation of bacteria aggregation and maintains the compact structure of biofilm (Adav and Lee, 2008). It is mainly composed of polysaccharides, proteins, humic-like molecules, lipids and nucleic acids. The procedures described in literature to extract these molecules include physical and chemical methods. The physical protocols normally used are centrifugation (Villain et al., 2010), heating (Wingender et al., 1999), cation exchange resin (Xie et al., 2012) and ultrasonication (Ramesh et al., 2006). The chemical ones instead are formaldehyde plus NaOH (Liu and Fang, 2002), formamide plus NaOH (Adav and Lee, 2008), EDTA (Comte et al., 2006), ethanol (Adav and Lee, 2008) and glutaraldehyde (Comte et al., 2006). Each method has its advantages and disadvantages. In general, formaldehyde/NaOH extraction was reported to produce the highest extraction yield compared with the other physical and chemical methods (Comte et al., 2006, D'Abzac et al., 2010, Keithley and Kirisits, 2018). In the literature, the analytical methods used to measure polysaccharides, or carbohydrates, in EPS are mainly colorimetric and chromatographic. The most widely used methods due to their simplicity are the colorimetric Anthrone method (Gaudy, 1962) and Phenol-Sulfuric Acid protocol (Dubois et al., 1956, Kunacheva and Stuckey, 2014). For the proteins determination, the modified Lowry method (Frølund et al., 1995, Lowry et al., 1951) represents one of the most preferred protocols. Although other colorimetric methods like Bradford (Bradford, 1976) and bicinchoninic (Smith et al., 1985) are also used. The Lowry method is preferred because the results are more accurate, with less interference by many compounds contained in wastewater and the possibility to measure, at the same time, the humic acid (Lucarini and Kilikian, 1999). However, there are studies that reported a certain extent of interference on proteins determination when the samples concentration of cations such as  $\text{Ca}^{2+}$  and  $\text{Mg}^{2+}$  was higher than 0.5 and 0.9  $\text{mmol L}^{-1}$ , respectively (Xie and Burnell, 1994) or even negative amount of proteins in the waste streams analysed (Westgate and Park, 2010). Alkaline conditions are created when using Lowry's method reagents (5.7  $\text{g L}^{-1}$  of NaOH and 28.6  $\text{g L}^{-1}$  of  $\text{Na}_2\text{CO}_3$ ,  $\text{pH} > 12$ ), hence generating cations precipitation. The pre-treatment of samples containing 3  $\text{mmol L}^{-1}$  of  $\text{Ca}^{2+}$  and  $\text{Mg}^{2+}$  with technologies like dialysis and cation exchange resin proved to be useful to completely eliminate interference of Lowry method by cations removal over 90% (Shen et al., 2013). Basically, the cations were physically removed through the dialysis membrane pores (3.5 kDa), whereas the larger proteins to be measured were retained. The negatively charged ions in the cation exchange resin could bind the cations, hence leaving mainly the proteins in the treated sample.

Dupraz et al. (2009) reported that EPS compositions could reduce the energy needed for the nucleation of inorganic matter and thus enhance the precipitation within biological systems. This was later confirmed by reporting the possibility of cations binding to alginate-like exopolysaccharides (ALEs) in EPS, due to interactions with their negative groups (Lin et al., 2012, Sarma and Tay, 2018a). High calcium concentration in the influent to granular sludge systems have been shown to induce excessive precipitation of minerals like calcium carbonate and calcium phosphate (Cunha et al., 2018a) (Chapter 2). It is thought that when EPS is extracted from this kind of biofilms, the bound Ca with EPS or dissolved Ca ion due to strong extraction solution such as formaldehyde/NaOH (F/NaOH) could also be found in the final extracted solution. In Chapter 3, EPS was extracted from high ash content, partial nitrifying granules by the chemical F/NaOH procedure (Liu and Fang, 2002); during proteins determination by the Lowry method, a cloud of precipitates at the bottom of spectrophotometric cuvettes was observed that lowered the results reproducibility. For this reason, in this chapter a physical EPS extraction procedure, i.e. heat, will be compared to F/NaOH. The study aims to investigate the factors that could interfere in protein measurement by the Lowry method after EPS extraction from granular sludge by formaldehyde/NaOH or heat with high minerals content.

## 4.2. Materials and methods

### 4.2.1. Extracellular polymeric substance (EPS) extraction

In this study, suspended activated sludge (AS) and granular sludge with ash content of 20 and 47%, respectively, were used to extract EPS. For both F/NaOH and heat extractions, both granules and AS were first washed with tap water, then, after overnight storage at -20 °C, they were dried by freeze drying technology (lyophilisation). Ash content and total solids (TS) were measured for each sample and a portion of the biomass was weighted and placed in a 15 mL tube; 10 mL of phosphate buffer saline solution (PBS) were then added and the sample was centrifuged at 5000 g at 4 °C for 10 minutes. The saline solution was used in this experiment to avoid any stress to the bacteria that could produce unwanted cellular lysis. The only difference between the two methods at this stage was that PBS was heated up to 50 °C before the centrifuge in the physical extraction; the supernatant obtained after the first centrifuge was considered the lightly bound (LB) portion of EPS. At this point, for the chemical method, the pellet was resuspended with 10 mL of PBS and incubated on a shaker (150 rpm) for 1 h at 4 °C with 0.06 mL of formaldehyde (36.5 %) and subsequently for 3 h at 4 °C with 4 mL of sodium hydroxide (1 M). For the physical procedure, the pellet was resuspended with PBS and incubated for 30 minutes at 60 °C. For both methods, the sample was centrifuged for 20 minutes at 10000g at 4 °C, after which the supernatant was collected and considered as the tightly bound (TB) portion of EPS. The PBS solution, was composed of 8 g L<sup>-1</sup> sodium chloride, 0.2 g L<sup>-1</sup> potassium chloride, 1.15 g L<sup>-1</sup> di-sodium hydrogen phosphate, 0.2 g L<sup>-1</sup> potassium di-hydrogen phosphate, pH 7.3 ± 0.2 at 25 °C. Both LB- and TB-EPS extracted solutions were filtered with a 0.22 µm syringe filter before being stored at -20 °C, until analyses for proteins (PN), humic acid (HA) and polysaccharides (PS) content were done as described below. A portion of both LB and TB-EPS extracted solutions was dialysed overnight at 4 °C in a SnakeSkin Dialysis regenerated-cellulose membrane, 3.5kDa MWCO-22 mm (ThermoFisher Scientific, USA). All samples were analysed in triplicates.

### 4.2.2. PN, HA and PS analysis

PN and HA were analysed by the modified Lowry method (Lowry et al., 1951, Frølund et al., 1995, Shen et al., 2013). In this method, protein is pre-treated with copper (II) in a modified biuret reagent (alkaline copper solution stabilized with sodium potassium tartrate). In the absence of copper, colour intensity is determined primarily by the tyrosine and tryptophan content of the protein, and to a lesser extent by cysteine and histidine. Copper (II) has no effect on colour formation by tyrosine, tryptophan, or histidine, but reduces colour formation due to cysteine. Addition of the Folin reagent generates chromogens that give increasing absorbance between 550-750 nm. Normally, absorbance of 660 nm is used to quantify protein concentrations between 1-100 mg mL<sup>-1</sup>, while absorbance at 550 nm is used to quantify higher protein concentrations.

For the analyses four reagents are prepared: reagent A: 28.6 g L<sup>-1</sup> Na<sub>2</sub>CO<sub>3</sub> (2.86%), 5.7 g L<sup>-1</sup> NaOH (0.57%), reagent B: 9.1 g L<sup>-1</sup> CuSO<sub>4</sub> (0.91%) or 14.3 g L<sup>-1</sup> CuSO<sub>4</sub>.5H<sub>2</sub>O (1.43%), reagent C: 35 g L<sup>-1</sup> KNaC<sub>4</sub>H<sub>4</sub>O<sub>6</sub>.4H<sub>2</sub>O (Potassium sodium tartrate) (3.5%), reagent D: Folin reagent (2N) diluted 5:6 with distilled water. B and C are mixed and then added to A in order to prevent copper from precipitating in a 100:1:1 ratio (A:B:C) (Cu-solution). Reagent A is mixed with distilled water and reagent C with a 100:1:1 ratio A:H<sub>2</sub>O:C (noCu-solution). For PN analysis, 2 centrifuge tubes (2 mL) for each sample are prepared by placing 0.5 mL of sample (or blank or standard solution) in each tube. 0.7 mL of Cu-solution is added to one testing tube and 0.7 mL of non-Cu-solution (for humic compounds) is added to the other test tube. The tubes are well mixed by vortex stirrer, then 0.1 mL of diluted Folin reagent is added to each tube and quickly the tubes are mixed by vortex and incubated for 45 min in



the dark. After this time, the solutions can be transferred in 10 mm-cuvette to read absorption at 750 nm. The calculations used are:

$$ABS_{total} = ABS_{Protein} + ABS_{Humic}$$

$$ABS_{Blind} = 0.2 * ABS_{Protein} + ABS_{Humic} \text{ (only 20\% coloration with non-Cu-solution)}$$

$$ABS_{Protein} = 1.25 * (ABS_{total} - ABS_{Blind})$$

$$ABS_{Humic} = ABS_{total} - ABS_{Protein}$$

Where:  $ABS_{total}$  = Total absorbance for sample with Cu-solution

$ABS_{Blind}$  = Total absorbance for sample with non Cu-solution.

$ABS_{Humic}$  = Absorbance from Humic compounds. Calculated.

$ABS_{Protein}$  = Absorbance from protein. Calculated.

Three calibration curves are needed, with Cu-solution and with no Cu-solution for PN, with non Cu-solution for HA. Bovine Serum Albumin (BSA) and Na-humic acid were used as standard stock solutions ( $2 \text{ g L}^{-1}$ ) for PN and HA, respectively. Linearity of calibration curves for both proteins and humic acid is up to  $80\text{-}100 \text{ mg L}^{-1}$ . The developed colour is stable for several hours before changing (not less than 5).

PS were measured by phenol-sulfuric acid method (Dubois et al., 1956). Concentrated sulfuric acid is used to convert all non-reducing polysaccharides to reducing polysaccharides, and phenol reacts with reducing polysaccharides and develops a yellow-orange color which can be used to quantify the sugar concentration. To analyze the sample, phenol (5%) and sulphuric acid (95%, concentrated) are needed. 1 mL of sample (or blank or standard solution) are placed in 10-mL testing tubes (Round-bottom borosilicate tubes, 16 x 100-mm, with TFE-lined screw caps). 1 mL of phenol is added into each tube and then 5 mL of concentrated sulphuric acid are rapidly poured into each tube (the stream of acid should be directed against the liquid surface rather than against the side of the test tube in order to obtain good mixing). The tube is lidded and left to stand 10 minutes, after which it is shaken for 10 to 20 minutes in an incubator at  $25 \text{ }^{\circ}\text{C}$  to  $30 \text{ }^{\circ}\text{C}$ . Finally, the solution is transferred to a 10 mm cuvette and absorbance at 490 nm is read. The calibration curve is made by using glucose as standard and linearity is up to  $16 \text{ mg glucose L}^{-1}$ .

The absorbance of PN, HA and PS was measured by UV-Visible Scanning spectrophotometer (Cecil 3000 series, Cecil Instruments Ltd., UK).

#### **4.2.3. EPS content by Excitation and Emission Matrix (EEM)**

The EPS content was also analysed in a 1-cm quartz cuvette by measurement of excitation and emission matrix spectra, using a Cary Eclipse Fluorescence Spectrophotometer (Agilent Technologies, USA); the spectra were collected with subsequent scanning emission spectra from 280 to 500 nm at 5 nm increments by varying the excitation wavelength from 200 to 400 nm at 5 nm sampling intervals. The excitation and emission slits were maintained at 5 nm. The EEM data were processed as described by Chen et al. (2003b) and Guo et al. (2017) by using the fluorescence regional integration (FRI) technique. The peaks from EEM were divided in 5 regions ‘i’ as in Chapter 3. The area beneath each EEM spectra was integrated as explained below:

$$\Phi_{1,n} = MF_i \Phi_i = MF_i \sum_{ex} \sum_{em} I(\lambda_{ex} \lambda_{em}) \Delta \lambda_{ex} \lambda_{em} \quad (4.1)$$

$$\Phi_{T,n} = \sum \Phi_{1,n} \quad (4.2)$$

$$P_{1,n} = \frac{\Phi_{1,n}}{\Phi_{T,n} \times 100} \% \quad (4.3)$$

Where:

$\Phi_i$  = volume beneath the region

$\Phi_{i,n}$ ,  $\Phi_{T,n}$  = normalised ex/em area volumes

$\Delta \lambda_{em}$  = excitation wavelength interval (5nm)

$\Delta \lambda_{ex}$  emission wavelength interval (5nm)

$I(\lambda_{em} \lambda_{ex})$  = intensity of fluorescence (au) at each excitation-emission wavelength pair

$MF_i$  = multiplication factor, or the inverse of fractional projected excitation-emission area

$P_{i,n,\%}$  = percent fluorescence response

A UV1800 spectrophotometer (Shimadzu, Japan) was used to detect whether dilution was needed for EEM analyses and TB-EPS samples were diluted 1:5; the scanning range used was from 200 nm to 700 nm, with 2 nm interval between each scan.

### 4.3. Results

Three hypotheses were formulated: (a) erroneous colouration of samples when PN amount is too high due to as unreliable dilution procedure, (b) sample reaction with F/NaOH reagents or (c) sample reaction with Lowry method reagents. To investigate which of the above hypotheses could be true, different trials followed.

#### 4.3.1. BSA calibration curve and dilution test

A series of different dilutions of EPS extracted from partial nitrifying granules were tried to see whether this could interfere with the results (Table 4.1); it was found that the lower dilutions of sample corresponded with an unexpectedly higher PN concentration in the range of dilutions 1 to 10; but when the dilution factor was greater than 10 a decrease and even negative concentrations were observed, as if a certain interference component could be diluted. Therefore, the standard curve made by using the standard protein bovine serum albumin (BSA) was extended to a concentration higher than suggested in the methodology; this was done to investigate whether the high concentration of proteins could somehow interfere with the colorimetric analysis and generate fluctuating results. Above 100 mg BSA L<sup>-1</sup>, the curve started plateauing, as shown in Figure 4.1, reaching an obvious too high absorbance for a reliable spectrophotometric analysis (normally < 1.0); however, no peculiar trend was observed for high BSA amount and fluctuations of absorbance was not observed.

Table 4.1 –EPS extraction sample with different dilutions and relative PN amount measured by Lowry's method.

Absorbance	Dilution factor	PN (mg L <sup>-1</sup> )
0.157	1	14.49
0.184	5	136.74
0.145	10	325.42
0.12	100	-80.00
0.119	1000	-1213.33

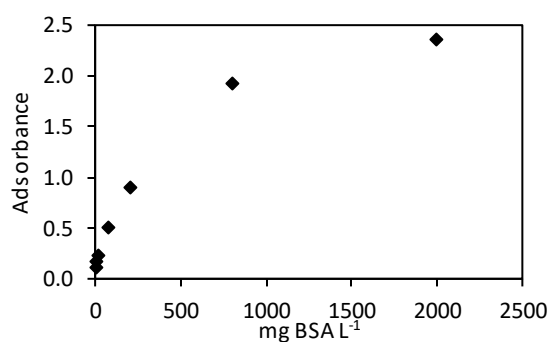


Figure 4.1 – Extended calibration curve for proteins detection by Lowry's method.

#### 4.3.2. EPS extraction by physical heat method

Once the first hypothesis was discharged, the possibility that the F/NaOH extraction procedure could interfere on the PN analysis was investigated. In Lowry method, alkaline reagents (i.e.  $\text{Na}_2\text{CO}_3$  and NaOH) are used that could eventually react or have cumulative effects with either formaldehyde and/or NaOH; therefore, the chemical protocol was substituted with physical heat extraction. Once the extraction was completed and the filtered samples were analysed for PN content, interestingly no precipitation within the spectrophotometric cuvettes was found. This fact could show that interference could take place by using F/NaOH; in addition, since NaOH was already present within Lowry method, this means that the base presence could not explain the interference. From Figure 4.2a, b and Figure 4.2e and f the extracted EPS by heat protocol is shown as PN, HA and PS content in granules and AS, respectively. Similarly to previous results on partial nitrifying granules (Chapter 3), the EPS components showed higher amount in the TB-EPS portion compared to the LB-EPS one, which justifies the main importance of the latter in the granular structure. To confirm that the interference was removed or reduced by using the physical protocol, a higher concentration of PN than reported in Chapter 3 was observed, however, the PS was much lower than what was described in the previous Chapter 3. The EEM data (Figure 4.2c, d and Figure 4.2g, h) confirmed the absence of PS, showing peaks I (tyrosine/tryptophan amino acids) and II (tyrosine/tryptophan proteins) well visible in both granules and AS, whereas peak III, representing the polysaccharides, was not present. Also peaks V (polyaromatic-type humic acids) and VI (polycarboxylate-type humic acid) were clear in the plots, although only a little amount of HA was shown by the chemical analyses. The literature behind the organic matter correspondence to each peak can also be read elsewhere (Chen et al., 2003b, Wang and Zhang, 2010, Wang et al., 2014a). Even though EEM results are considered qualitative, they showed that peaks I and II were found in larger amounts in TB-EPS than in LB-EPS, confirming the chemical analyses of EPS components; on the other hand, peaks V and VI showed an opposite trend, with lower amounts of TB-EPS and higher in LB-EPS. These findings could not be confirmed by the chemical analysis since only little HA could be measured in either LB- and TB-EPS. These results showed that replacing the chemical F/NaOH procedure could efficiently remove the cloud precipitation observation during proteins analysis; and this was also confirmed by the greater amount of extracted PN compared to that in Chapter 3. However, the low HA and PS concentrations in the extracted solution suggests that heat protocol extraction yield with regard to the two components was poor; this was also described by Adav and Lee (2008), where extracted PN were much higher than HA and PS in both heat treated sludge and granules samples.

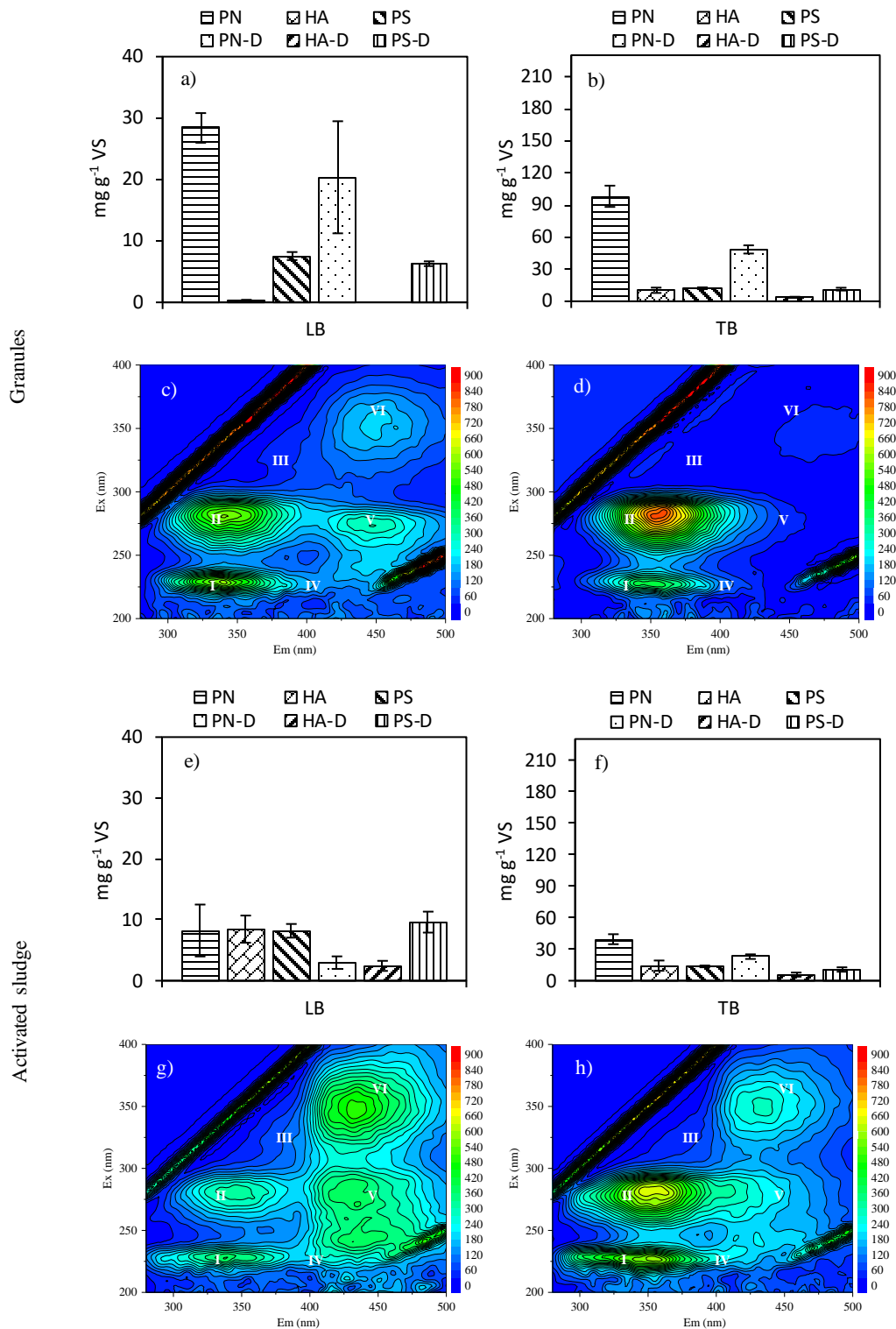


Figure 4.2 – Profile of EPS extracted with heat procedure; proteins and polysaccharides amount with and without dialysis in a) LB and b) TB-EPS of granules. EEM spectra from granules in c) LB and d) TB-EPS. Proteins and polysaccharides amount with and without dialysis in e) LB and f) TB-EPS of sludge. EEM spectra from sludge in g) LB and h) TB-EPS.

### 4.3.3. Calcium ion effect on PN analysis with Lowry method

The results in Chapter 2 and Chapter 3 showed more than 200 mg Ca g<sup>-1</sup> MLSS in nitrifying granular sludge, which is much higher than that in typical suspended and granular sludge (Metcalf and Eddy, 2003). Thus, it is speculated that because of the bonds with negative charged groups in EPS (Lin et al., 2012, Sarma and Tay, 2018a), high Ca<sup>2+</sup> could be extracted too. To verify whether Ca<sup>2+</sup> could be one of the factors to cause precipitation during PN determination, some tests on the effects of calcium addition to PN analysis were done. 3 mmol L<sup>-1</sup> of Ca<sup>2+</sup> (120 mg L<sup>-1</sup>) were added to the BSA standard solution for the PN calibration curve. After all Lowry's reagents were added, the samples were well mixed by vortex and 45 minutes incubation at room temperature in the dark followed, before spectrophotometric analysis. During the incubation of the calibration samples, clear precipitates were visible at the bottom of the spectrophotometric cuvettes (Figure 4.3a and b), as also described in Chapter 3. These results, especially the precipitates within the blank (deionised water plus 3 mmol L<sup>-1</sup> of Ca<sup>2+</sup>), could justify that, although F/NaOH was not used, also the reagents from Lowry method could likely react with calcium. Figure 4.4a and b show the results of two calibration curves made without and with addition of calcium, respectively. The presence of the metal shifts the curve to a higher absorbance, with a consequent increase of the intercept (Table 4.2); the spectrophotometric readings were underestimating the real proteins amount. These results could also explain why in the previous test the final PN concentration result was higher when diluted; possibly by reducing the calcium concentration in solution, which consequently lowered the interference effect on the spectrophotometric readings. The greater the concentration of the calcium (Figure 4.4c), corresponded a greater reading error in the PN analysis; this is shown in the correlation plot in Figure 4.4c, where increasing concentrations of Ca<sup>2+</sup> were added to an extracted sample and added up to 60 mg Ca<sup>2+</sup> L<sup>-1</sup> and a proportional curve was generated.

After the calcium role in the interference of the Lowry proteins determination was confirmed, a pre-treatment dialysis was used to reduce the element's concentration within the samples. The removal of Ca<sup>2+</sup> by dialysis was successfully described to eliminate interference of Lowry method in previous literature (Shen et al., 2013). Therefore, both LB- and TB-EPS samples were pre-treated by being left in the dialysis membrane overnight to allow mineral ions such as Ca<sup>2+</sup> to pass through the membrane and be removed from the sample, which was supposed to reduce the interference on PN analysis. The results of the pre-treatment are described in Figure 4.2a, b and Figure 4.2e, f; contrary to what was expected, the PN content showed reduced concentrations of both LB- and TB-EPS, with a similar trend between granules and AS, hence dialysis could not eliminate the interference. In addition, these results indicate that great amount of proteins smaller than 3.5kDa could be present in the EPS sample and pass through the membrane during dialysis, which underestimated the protein contents by 50%.

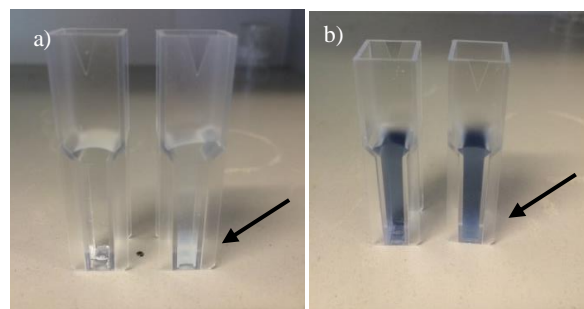


Figure 4.3 - Precipitates cloud observed during Lowry method incubation of a) blank (without and with Ca<sup>2+</sup>) and b) last point (without and with Ca<sup>2+</sup>) of BSA calibration curve.

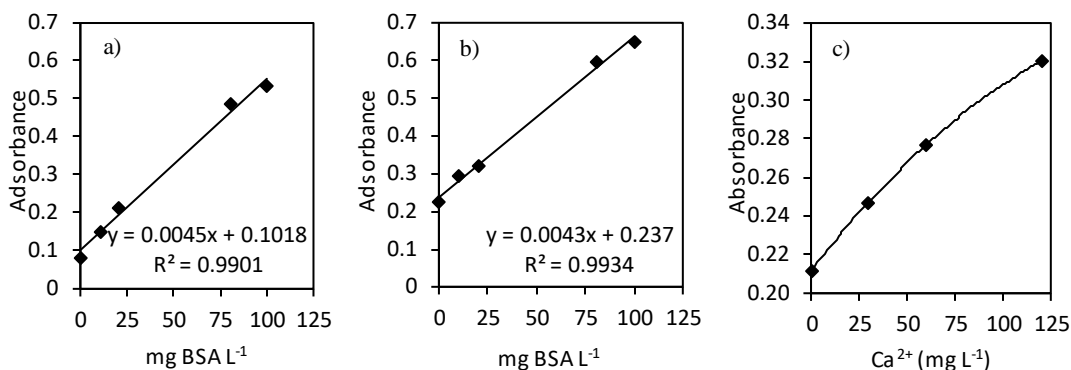


Figure 4.4 – Proteins calibration curves done a) without and b) with 120 mg Ca<sup>2+</sup> L<sup>-1</sup> addition, c) correlation between added Ca<sup>2+</sup> concentration and absorbance after 1 h incubation.

Table 4.2 – Proteins calibration curves with and without calcium addition.

BSA mg L <sup>-1</sup>	Absorbance	
	No Ca <sup>2+</sup>	120 mg Ca <sup>2+</sup> L <sup>-1</sup>
0	0.081	0.223
10	0.148	0.293
20	0.212	0.320
80	0.483	0.596
100	0.533	0.647

After these results, cation chromatography analysis was done on the EPS extraction solutions following heat procedure; in this way the content of soluble Ca<sup>2+</sup> in both LB- and TB-EPS could be measured. What those analyses revealed was that the cation, which was thought to be the main factor causing the precipitation during Lowry determination, was not present in any sample. Therefore, this could imply that the calcium interfering with the spectrophotometric proteins determination could not be present as cation in solution, but bound to EPS.

#### 4.3.4. Effect of incubation duration on PN measurement with Lowry method

At this point, since the poor reliability of colorimetric readings was probably due to the shielding effect from the precipitate cloud on the spectrophotometer, the incubation time in Lowry method was extended to first 2 hours and then to 3 hours, instead of one hour as suggested by the standard method. After this change was applied, comparable results were achieved for the calibration curve of protein with and without calcium addition; as shown in Figure 4.5a and b and Table 4.3, after 2 hours the interference extent was lowered but still visible, whereas after 3 hours the results were quite close to the control calibration curve. These results explain how calcium could be found bound to large organic molecules rather than in its cation form in solution when EPS was extracted, which would explain why it would be retained in the dialysis membrane. Changing the incubation time from 1 to 3 hours during Lowry determination could almost completely remove the interference and obtain reliable measurements.

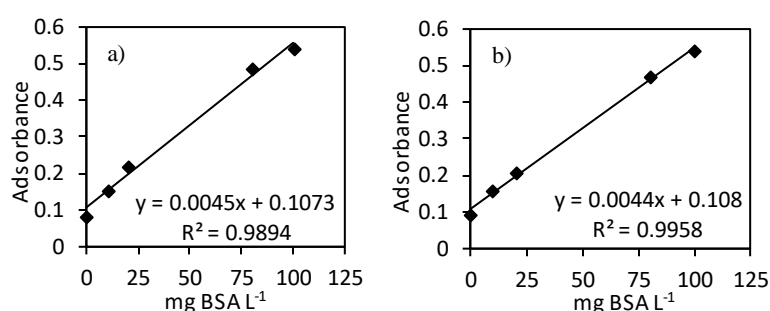


Figure 4.5 – Spectrophotometric results of calibration curve a) without  $\text{Ca}^{2+}$  addition (1 hour incubation) and b) with addition of  $\text{Ca}^{2+}$  (3 hours incubation).

Table 4.3 – Comparison between calibration curves after different incubation times.

BSA mg L <sup>-1</sup>	Absorbance			
	control	1 h	2 h	3 h
0	0.081	0.223	0.090	0.082
10	0.148	0.293	0.160	0.150
20	0.212	0.320	0.208	0.201
80	0.483	0.596	0.468	0.454
100	0.533	0.647	0.540	0.533

#### 4.3.5. Optimisation of EPS extraction and PN analysis by Lowry method

After the results obtained by the tests described in the previous paragraphs, 3 hours of incubation were applied to lower the interference of calcium on PN analyses, since precipitation was still visible during the incubation time; differently, no precipitation was observed during incubation of AS, due to the lower  $\text{Ca}^{2+}$  content. The results obtained by implementing this simple step are shown in Figure 4.6a, b and Figure 4.6e and f, where the extracted



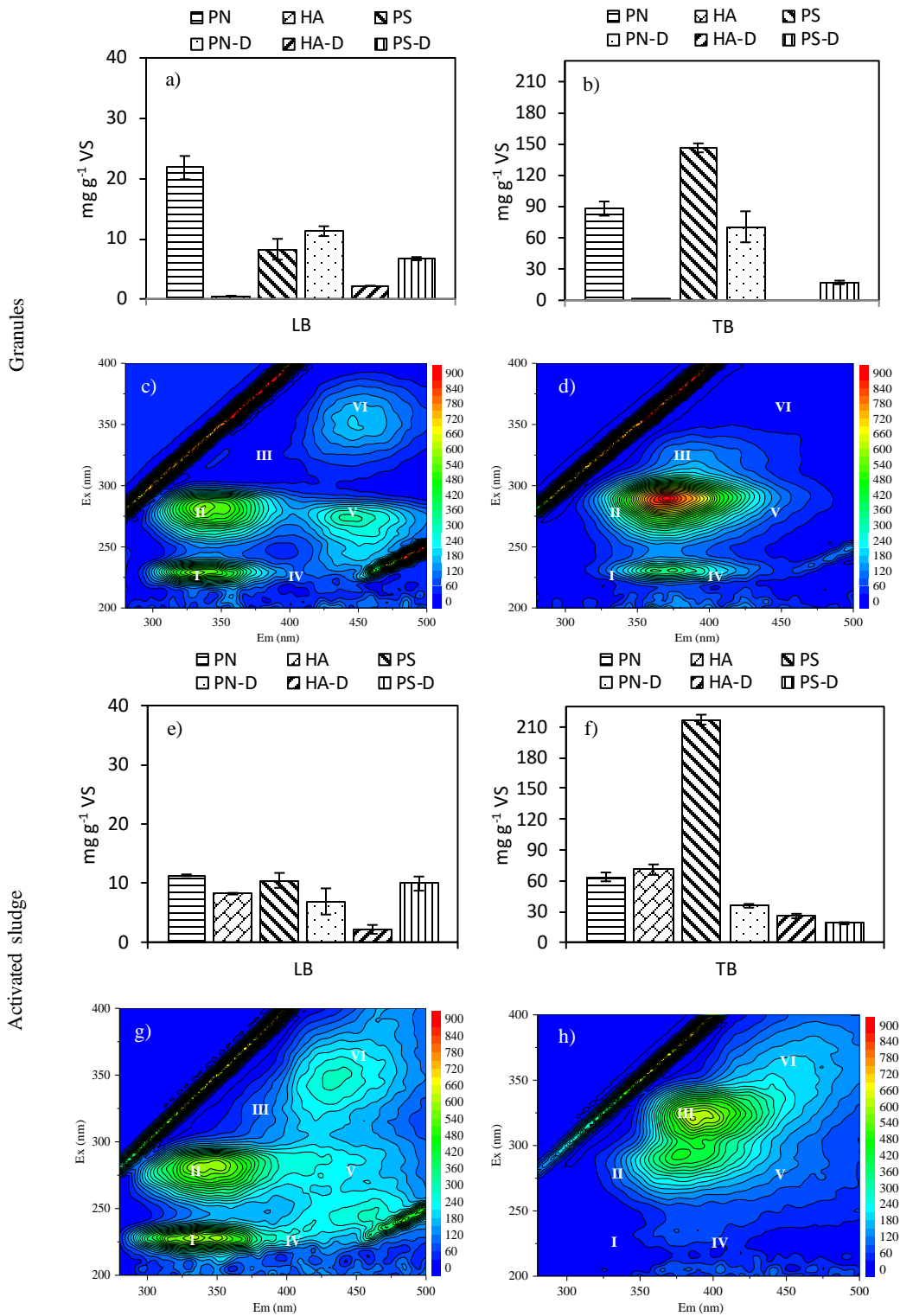


Figure 4.6 – Profile of EPS extracted with formaldehyde/NaOH procedure; proteins and polysaccharides amount with and without dialysis in a) LB and b) TB-EPS of granules. EEM spectra from granules in c) LB and d) TB-EPS. Proteins and polysaccharides amount with and without dialysis in e) LB and f) TB-EPS of sludge. EEM spectra from sludge in g) LB and h) TB-EPS.

EPS by F/NaOH are shown as PN, HA and PS content in granules and AS, respectively. The PN concentrations showed a similar trend to when physical extraction was used, except for a slightly lower amount; PN content in granules and AS resulted 88 and 64 mg g<sup>-1</sup> MLSS, respectively, compared to 98 and 40 mg g<sup>-1</sup> MLSS, respectively, measured after heat extraction. On the other hand, a great difference could be encountered between the PS extracted with the two methods; the amount was much higher this time and it resulted even greater than previously reported in Chapter 3. Also this time both PN and PS were shown to be mainly present in the TB-EPS portion compared to the LB-EPS. The EEM spectra confirmed the presence of the three components in the samples, especially PS in TB-EPS; as described for the heat extraction, the PN were represented by peaks I and II in Figure 4.6c, d, g and h. PS were described by peak III in both Figure 4.6d and h, which were expected since a stronger signal was measured by the chemical analysis. Also peak V was clearly described in Figure 4.6c and g, whereas its presence could not be certified in Figure 4.6d and h. Finally, peak VI was shown in Figure 4.6c, g and h but it absent in Figure 4.6d. In addition, between the two extraction procedures there could be a visible difference that made peaks I and II to move towards higher emission length in F/NaOH; this could imply that a different conformation of proteins contained in those two peaks could take place, possibly due to an increase of pH. To double check this, a sample was measured by EEM with and without first adjusting the pH to a neutral value. After NaOH is added for the extraction process, the pH increases up to 12-13; therefore, once pH was reduced to around 7.2-7.5, it was observed that both peak I and II were shifted to a lower emission wavelength, i.e. from 350-400 to 325-375.

#### 4.4. Discussion

The EPS extraction by chemical method F/NaOH was described in literature as to show the highest extraction yield among several other physical and chemical methods (Keithley and Kirisits, 2018). In addition, it was shown to be the most reliable technique for leaving microbial cells undamaged, avoiding therefore the interference of intracellular molecules with following analyses. The role of formaldehyde is to fix the cells, binding to amino, hydroxyl, carbonyl and sulfhydryl groups of proteins and nucleic acids of the cell membrane, therefore preventing cell lysis. The EPS extraction is then possible due to the increase of pH after the addition of NaOH; the acidic groups contained in EPS dissociate creating many negative charges that repulse from each other, with a consequent crumbling of the EPS. The NaOH makes EPS more soluble to water. From the results described above it could be confirmed what other studies have previously reported, that the EPS extraction procedure F/NaOH could achieve better yields than the heat extraction (Comte et al., 2006, D'Abzac et al., 2010); similar results could be previously reported by Adav and Lee (2008), where the three components extracted by heat were found in lower amounts than in both AS and granules extracted with F/NaOH. Therefore, the poor extraction of both HA and PS means that the procedure would likely be underestimating their concentration, making the heat extraction as a not advisable procedure for both granular and activated sludge. In addition, it could be speculated that the inefficient extraction could result in lower calcium in the extraction solution. Indeed, no precipitation during the Lowry method incubation was observed when heat procedure was used.

Compared to Chapter 3, the PN content in EPS in the present study was higher since Lowry method was optimised by using a 3 hours incubation time. A thorough comparison with the other experiment was not possible since the EPS was analysed for different size granules in that study; however, the average amount of PN for different diameters was roughly 50 mg g<sup>-1</sup> MLSS, which is 35% lower than in the present study. In addition, the standard error between the triplicates achieved in the optimised procedure is visibly reduced compared to the one for the largest size, for instance.

The PN and HA contents after F/NaOH extraction were similar in AS, whereas the humic material was much lower than PN in the granules. Adav and Lee (2008) described that the reason for generating a low concentration

of HA by solely F/NaOH extraction, could be due to the humic material to be contained mostly in the internal layers of granular sludge. In addition, HA within AS could be higher using the same chemical procedure since the material could be better extracted from the loose flocs structure. Similarly, the HA in the present study was almost absent in granules when F/NaOH was used, whereas much higher amounts were measured in the AS. In Adav and Lee (2008) study the ultrasound technology could eventually increase the extraction by a deterioration of the compact granular structure before F/NaOH were used. This could justify that a more efficient extraction yield in the granules be investigated in this research could be achieved by using synergically both chemical and physical procedures, especially when inorganic material is expected to be present in the granules.

The lower PS content in granules compared to AS could be explained by the PS degradation by the bacteria. A parallel decrease of PS and an ash content increase was previously described in a granular system with excessive inorganic precipitation (Liu et al., 2015b) and in lithified layers of natural marine stromatolites (Kawaguchi and Decho, 2002). PS are considered to be an organic carbon source for bacteria growth (Sadri Moghaddam and Alavi Moghaddam, 2015) and their reduction in these studies could be justified by high nutrients mass transfer limitations due to the accumulation of inorganic matter, as also reported in Chapter 3. Therefore, the lower PS in the granules in the present study could be due to the high ash content (47%), which was almost half in the AS (20%). The presence of inorganic matter could also justify the difficulties in extracting PS which would be strongly bound to calcium due to the ALE-Ca-ALE bridges. It is also interesting to notice that the dialysis pre-treatment could drastically reduce the concentration of PS in both granules and AS. It was reported in literature that when using chemical extraction procedures, some of the used reagents could either interfere with the following analyses (i.e. Lowry, Dubois, etc.) or react with the extracted EPS components, producing misleading EPS characterisation (Comte et al., 2006, D'Abzac et al., 2010). Since formaldehyde can bind amine groups of proteins or amino sugars, the dialysis pre-treatment was used in some study to reduce its effects (Keithley and Kirisits, 2018). On one hand, it is possible that in this study a great amount of PS smaller than 3.5kDa could be part of the extracted EPS and could be lost through the membrane; but on the other hand, it could also be due to the depletion of chemical residues from extraction. This could not be confirmed in the study, but it should be further investigated because it means that the measured PS amount could be actually overestimated.

However, these results are promising since the optimised Lowry method could improve the EPS characterisation in granular systems with high inorganic precipitation; in addition, synergic use of physical extraction procedures and F/NaOH may be further investigated, to have a deeper understanding on the EPS composition within biofilms with high ash content. It could not be confirmed in this study whether interactions between EPS and formaldehyde could result in interference on PS analyses, but in the future this should be addressed.

In Chapter 2, the accumulation of high content of calcium in partial nitrifying granules was described. EPS contained in biofilm can facilitate inorganic matter precipitation (Dupraz et al., 2009) due to the  $\text{Ca}^{2+}$  bonds with negatively charged molecules in EPS (Lin et al., 2012, Sarma and Tay, 2018a). It could be speculated that once EPS is extracted, also the minerals will be found in the final extraction solution. Therefore, the presence of calcium and bicarbonate at  $\text{pH} > 13$  (because of NaOH) during the Lowry proteins determination would likely generate inorganic calcium precipitation. Importantly, since precipitation was not observed after heat extraction, although NaOH was still present in Lowry's reagents, this means that it is not the concentration of the base that causes the precipitation, but the amount of calcium from the extraction instead. It is possible that the heat extraction yield does not release enough Ca-EPS to generate the precipitation. At these alkaline conditions the concentration of  $\text{CO}_3^{2-}$  in Lowry reagents is roughly 4.5 mM, which in theory could react with around 180 mg  $\text{Ca}^{2+} \text{L}^{-1}$ . However, if calcium in the extracted sample is low, no precipitation would take place or would be visible. The interference of Lowry method for proteins determination by  $\text{Ca}^{2+}$  and  $\text{Mg}^{2+}$  was already described in literature (Shen et al., 2013); they reported that the cations could precipitate after reacting with bicarbonate

present in Lowry reagents at alkaline conditions and interfere with the colorimetric analysis. However, by using a dialysis pre-treatment they could remove the cations from the sample, hence eliminating the interference.

Similarly, the membrane was tried also in the present study, but the pre-treatment could not remove the interference, instead it generated a further decrease of proteins due to their loss through the membrane. For heat extraction, roughly 50% of the proteins extracted were smaller than the 3.5kDa membrane pore size, whereas only 20% were dialysed after F/NaOH. Heat extraction is a quite strong method that could destroy the bacteria cellular membranes with a following lysis (Comte et al., 2006), explaining the possibility to create a great amount of small proteins encountered with the chemical procedure.

Therefore, in the present study calcium was described to be bound to organic molecules in the EPS extraction solutions; this result confirms the importance of  $\text{Ca}^{2+}$  bonds to EPS of granular sludge. In addition, this could also justify the absence of precipitation during Lowry method incubation after heat extraction. The poor efficiency of the physical method indeed resulted in lower calcium concentration due to less extracted EPS to which the cation would be bound.

#### **4.5. Conclusions**

The calcium present in EPS extracted from aerobic granules showing high minerals precipitation ( $200 \text{ mg g}^{-1}$  MLSS) was found to be the main factor to generate interference of proteins determination through Lowry's method. Its reaction with the carbonate reagent and the alkaline pH could indeed induce the precipitation of  $\text{CaCO}_3$  within the cuvettes used for the spectrophotometric proteins measurement. However, the interference could be partially eliminated by extending the incubation time during Lowry's method from 1 hour to 3 hours. Differently from previous research, chromatography analyses could not confirm the presence of the cation in the extracted solution; it is thought that calcium could be present bound to large organic molecules contained in EPS, under which form it cannot be detected. This would also justify the fact that dialysis pre-treatment inefficiently removed the interference, as it was instead reported possible in previous literature. In addition, by changing the chemical formaldehyde/NaOH procedure to extract EPS with the heat protocol, prevented this precipitation. It is possible that the less efficient physical extraction could free a lower amount of calcium; this would be justified by the fact that the chemical procedure could also show a greater amount of extracted proteins and polysaccharides. Further investigation in this way would be needed to understand precisely what could induce precipitation in samples extracted from high ash content granules.

#### **4.6. Experimental weaknesses**

A physical pre-treatment could have helped to facilitate the opening of the complex EPS structure in the granular sludge. For instance, sonication coupled with a chemical extraction could have been a possible candidate procedure to try dissolving the EPS.

The absence of calcium from the solution of extraction as a free cation may be due to the element agglomeration with organic molecules. However, a mass balance of the element was missing in the study and elemental analysis by ICP-MS or element analyser would have been useful for clarifying this.

In addition, a morphological aspect of the granules by SEM or also simple stereomicroscopy before and after the different extraction methodologies, would have been useful to compare their efficiencies in releasing the EPS structure. At the same time, DNA and lipids analyses were missing that could confirm if bacteria lysis was happening, which consequently could explain the measured low amount of proteins and polysaccharides.

To confirm the specificity of the inorganic matter interference on both Lowry and Dubois methods, different methodologies should have been tested in parallel.

**REACTIVATING AMMONIUM REMOVAL ACTIVITY OF NITRIFYING  
BIOMASS AFTER INHIBITION USING EXTERNAL ELECTROSTATIC  
FIELD**



## 5.1. Introduction

The efficient application of partial nitrification granules at full-scale depends mostly on the stable activity of ammonium oxidising bacteria (AOBs) (Agrawal et al., 2018). They are slow growing bacteria and sensitive to a great number of compounds, such as free ammonia (FA), free nitrous acid (FNA), toxic compounds (Anthonisen et al., 1976) and some environmental conditions like variations of pH, salinity and temperature. The granular sludge is represented by a much stronger and resistant structure than flocculent activated sludge and can reduce the extent of inhibition (Sarma and Tay, 2018a); anyhow, a sudden variation in stream quality and the increase of a specific toxic compound concentration could still generate the process failure of partial nitrification. In this situation the reactor could be augmented with new nitrifying granules, but their cultivation would not be quick since it took a month in a lab-scale SBR reactor (Chapter 2) and it could take much longer in a full-scale. In addition, the AOBs activity should be strongly enhanced over the nitrite oxidising bacteria (NOBs), to keep the partial nitrification shunt. Another option would be to augment the system with new purchased granules, which means higher costs for the plant and uncertainty on the fact that the new granules could still go back to complete nitrification (Turk and Mavinic, 1989, Peng and Zhu, 2006). These are only some of the reasons why further research would be needed on novel technologies able to avoid or to quickly reduce the nitrifying biomass inhibition effects. In literature, some studies have reported interesting results by using magnetic and ultrasound fields and published evidence of effects on the biomass activity (Filipič et al., 2015, Zheng et al., 2015). However, the complex theory behind them and special equipment needed would still make these technologies difficult to be implemented in most systems. On the other hand, the application of an electrostatic field was shown in the past to be simple enough and to represent a non-invasive technology. Most research on electric field (EF) applications was done on enhancement of bacteria activity in nitrifying (Qian et al., 2017), activated sludge (Alshawabkeh et al., 2004) and ANAMMOX (Yin et al., 2016) systems, among the others; on the other hand, to the best of our knowledge, EF application on the reactivation and enhancement of inhibited microorganisms activity by a toxic compound is still missing in literature. The recovery of nitrifying granules activity without the need of an external biomass source would obviously represent an interesting and cost-effective advantage; therefore, it is believed that EF application could be a promising treatment to improve nitrifying granular sludge activity after inhibition.

The present study investigated the effects of the electric field application on inhibited nitrifying biomass by a series of batch tests. First, preliminary tests were done to find the optimal duration and intensity of the EF; then, the biomass was fed with different concentrations of known inhibitors (i.e. salinity and phenol) and the ammonium removal was evaluated. Finally, the EF was implemented and the effects on the inhibited nitrifying biomasses were described by measuring the ammonium removal once more.





## 5.2. Materials and methods

### 5.2.1. Reactor operation

A column reactor (Perspex) with a 2.6 L working volume and a column height to diameter ratio of 20 ( $\varnothing$  60 mm) was operated in a sequencing batch mode, including 10 minutes feeding, 227 minutes aeration, 2 minutes settling time and 1 minute discharging, with a total cycle time of 4 hours. The volumetric exchange ratio was kept at 50% with the effluent discharged from the middle port of the reactor. Air was continuously provided with a flow rate of  $5 \text{ L min}^{-1}$  through an air stone at the bottom of the reactor; the temperature within the system was kept constant at  $30 \text{ }^\circ\text{C}$ .

### 5.2.2. Synthetic wastewater and inoculum

The synthetic wastewater was prepared following the procedure explained in previous research (Chapter 2); briefly, organic carbon ( $1200 \text{ mg COD L}^{-1}$ ) was provided during the first part of sludge cultivation to achieve a quick granulation and it was then substituted by inorganic sodium bicarbonate ( $10.8 \text{ g NaHCO}_3 \text{ g}^{-1} \text{ NH}_4^+ \text{-N L}^{-1}$ ) to provide both carbon source for nitrifying biomass growth and buffer solution to the newly formed granules. Ammonium was increased step by step from 50 to  $500 \text{ mg NH}_4^+ \text{-N L}^{-1}$ , in order to enhance nitrifying bacteria accumulation. Phosphorus was provided as  $15 \text{ mg PO}_4\text{-P L}^{-1}$  and the metals were added as (per L prepared):  $0.02 \text{ g MgSO}_4\cdot 7\text{H}_2\text{O}$ ,  $0.01 \text{ g FeSO}_4\cdot 7\text{H}_2\text{O}$ ; whereas the trace elements were (per L prepared):  $0.12 \text{ mg MnCl}_2\cdot 4\text{H}_2\text{O}$ ,  $0.12 \text{ mg ZnSO}_4\cdot 7\text{H}_2\text{O}$ ,  $0.03 \text{ mg CuSO}_4\cdot 5\text{H}_2\text{O}$ ,  $0.05 \text{ mg (NH}_4)_6\text{Mo}_7\text{O}_{24}\cdot 4\text{H}_2\text{O}$ ,  $0.1 \text{ CoCl}_2\cdot 6\text{H}_2\text{O}$ ,  $0.1 \text{ mg NiCl}_2\cdot 6\text{H}_2\text{O}$ ,  $0.05 \text{ mg AlCl}_3\cdot 6\text{H}_2\text{O}$ ,  $0.05 \text{ mg H}_3\text{BO}_3$ . The synthetic wastewater pH was not adjusted and was constant at 7.2-7.4.

The reactor was inoculated with conventional activated sludge from Portswood Municipal WWTP (Southampton, UK) for a final solids concentration of  $3 \text{ g SS L}^{-1}$  and 25% of ash content. After one month of cultivation, partial nitrifying granules were produced and the system was run for a further month at stable conditions. Then, the particles were washed with tap water to remove remaining feedstock and were stored at  $4 \text{ }^\circ\text{C}$  for around 6 months; after this time, the granules were placed back to the SBR with  $200 \text{ mg NH}_4\text{-N L}^{-1}$  synthetic wastewater and during the next week the feedstock ammonium was increased up to  $500 \text{ mg NH}_4\text{-N L}^{-1}$  and nitrate was still absent from effluent. The batch tests started after 45 days from reactivation of granules.

### 5.2.3. Batch tests

Part of the granules were ground and tested at the same time as intact particles; this would show whether the treatment could have a different influence in suspended rather than granular sludge. A first batch test with toxic chemicals was done and the sludge activity measured; then, the biomass was washed with tap water and by centrifugation, fresh inhibitor free-synthetic wastewater was added and the electric field treatment was implemented. Then, granules and sludge sAOR was analysed again during a second batch test, to investigate whether the treatment could recover or enhance the biomass activity. The batch tests were run within 0.25 L Erlenmeyer flasks and the final biomass concentration was between  $0.8$  and  $0.9 \text{ g VSS L}^{-1}$ . The medium provided was as for the SBR during reactivation but with  $45 \text{ mg NH}_4^+ \text{-N L}^{-1}$  initial ammonium concentration. The batch test was run at a constant temperature of  $30 \text{ }^\circ\text{C}$  by keeping the flasks in a water bath. Air was provided during the whole test with a flow of 1-2 LPM, which made the solution oxygen saturated. The bioactivity of the nitrifying biomass was measured by calculating the specific ammonium oxidation rate (sAOR) during the first hour of test, by measuring the ammonium concentration at intervals and dividing it by the time. The sludge inhibition was

provided by addition to the synthetic wastewater of different concentrations of either sodium chloride (2% and 4%) or phenol (50 and 100 mg L<sup>-1</sup>). During the salinity inhibition test, two flasks with granules and toxic chemicals-free synthetic wastewater were used as controls, i.e. C1 and C2, with the only difference that the latter would be treated with electric field. On the other hand, when investigating the phenol inhibition, 100 mg L<sup>-1</sup> of toxic chemical were added to a flask of granules that was not treated with electric field (G).

#### 5.2.4. Electric field treatment

The uniform electric field was provided by the power supplier EP-603 (Manson Engineering Industrial Ltd, Hong Kong) which generated an electric potential difference between two graphite plates (9 x 7, 0.1 cm thickness), applied on the external wall of a 200 mL- Pyrex beaker (0.2 cm thickness); the distance between the two plates was 7 cm. The uniform electric field intensity was calculated by the equation  $E: \Delta\phi/d$ , where  $\Delta\phi$  is the electric potential difference between one plate and the other and  $d$  is the distance at which they were kept. The power supplier was used with a constant voltage (CV) setup.

Preliminary tests without toxic chemicals inhibition were done on the biomass; these could tell which intensity of electric field and which duration of treatment would generate the maximum enhancement of bioactivity. In the first preliminary study, four durations of treatment were tried, i.e. 20, 60, 90 and 120 minutes, with a common electric field intensity of 2 V cm<sup>-1</sup> (14 V); in a second trial, the durations 60 and 90 minutes were tried with electric field intensities 2V cm<sup>-1</sup> and 3 V cm<sup>-1</sup> (21 V). All tests were run at room temperature and the biomass was simply stirred every 10 minutes with a glass bar. The electric field treatment setup is shown in Figure 5.1.



Figure 5.1 – Electric field setup showing power supplier and the samples containing beaker.

#### 5.2.5. Analytical Analyses

The supernatant (1 mL) from the batch test was taken from each flask, centrifuged and analysed for NH<sub>4</sub><sup>+</sup> concentration; then, the sample was kept at -20 °C, until next analyses for NO<sub>2</sub><sup>-</sup> and NO<sub>3</sub><sup>-</sup> could be done. Ammonium was measured spectrophotometrically by following the procedure described in BSI (1984) and using the UV-Visible spectrophotometer Cecil 3000 series (Cecil Instruments Ltd., UK). The anions NO<sub>2</sub><sup>-</sup> and NO<sub>3</sub><sup>-</sup> were measured by the ionic chromatographer 882 Compact IC plus (Metrohm, Switzerland); a Metrosep A Supp

5 - 150/4.0 column was used and the eluent was a solution of 1 mM NaHCO<sub>3</sub> and 3.2 mM Na<sub>2</sub>CO<sub>3</sub>. The mixed liquor suspended solids (MLSS) and mixed liquor volatile suspended solids (MLVSS) were analysed by standard methods (APHA, 2012). The granulation process was followed by microscopy observations by Leica MZ16F stereomicroscope; the images were then processed by ImageJ (version: 1.8) to analyse the biomass morphology and size.

## 5.3. Results

### 5.3.1. Formation of partial nitrifying granules and morphological characterisation

In Figure 5.2, the morphology of biomass during the granulation process previous to the batch test is shown; three days of acclimation were used and for this reason the inoculum sample was represented as Day -3. Mostly flocculent sludge was observed, which was how the sludge would look in the wastewater works from where it was collected. On day 0, the settling time was changed from 25 to 5 minutes, to speed up the process of granulation; anyhow, few granules with hairy edges were visible at this moment, showing how at those conditions granulation had already started during acclimation. During next days, flocs number reduced and more granules were observed; the edges of the particles became clearer and their size greater. On Day 7, almost pure granules were detectable in the stereomicroscopy sample, with clear edges and with a darker yellow colour appearance. After this moment, COD/N ratio was reduced quickly to enrich nitrifying biomass in the young granules. Nitrifying activity was observed on day 23, when the COD/NH<sub>4</sub><sup>+</sup> removed were clearly showing nitrification activity; the ammonium was completely oxidised to nitrite, meaning that partial nitrification was achieved. The specific ammonium oxidation rate of biomass ranged between 0.6 and 0.7 g NH<sub>4</sub><sup>+</sup>-N g<sup>-1</sup> VSS d<sup>-1</sup>. The MLVSS and size of partial nitrifying granules kept increasing till day 32, when a stable operation was achieved and the particles diameter averaged 2500 ± 560 µm. Before the partial nitrifying granules were stored (day 51), the ash content measured within the granules was between 40-50 %. These results are in agreement with previous research (Chapter 2), where slightly increased ash-content granules were achieved in short time in a sequencing batch system.

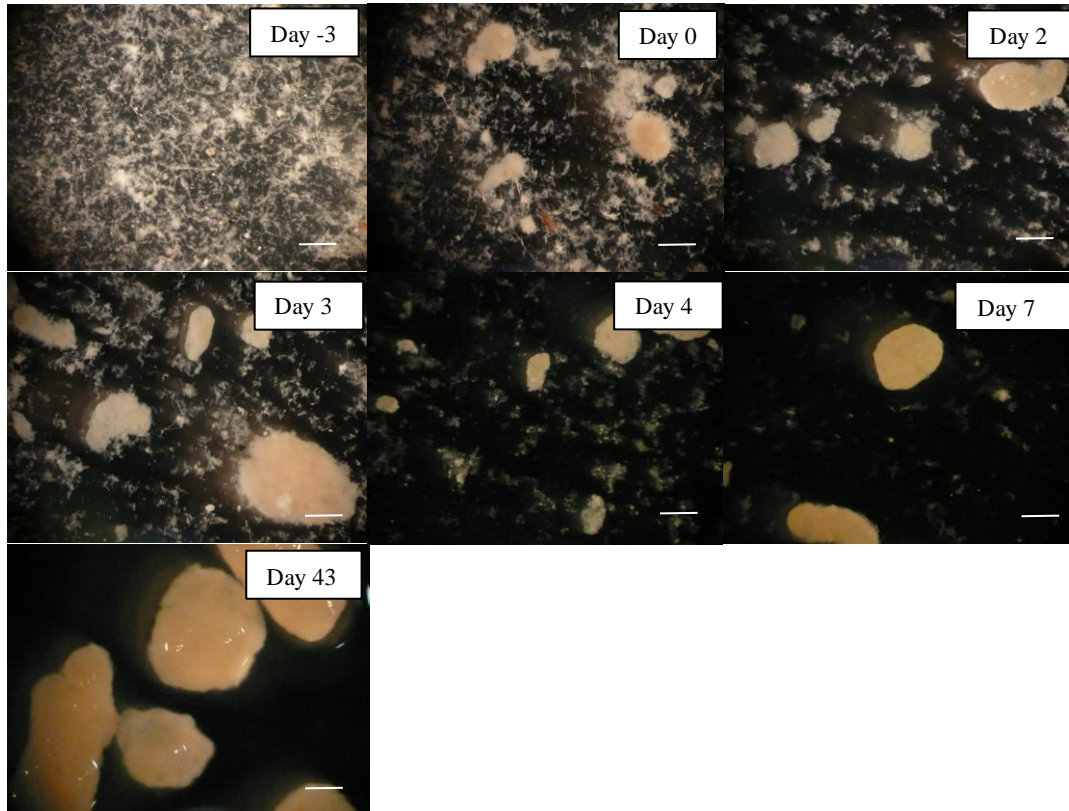


Figure 5.2 – Sludge morphology and granulation process showed by stereomicroscopy; bar = 1000 µm.

### 5.3.2. Electric field treatment

#### 5.3.2.1. Baseline experiment on the improvement of nitrifying activity using electric field

Before the electric field reactivation/enhancement tests, some trials were done to investigate the most suitable duration and intensity to use in the following experiments. The EF treatment showed, except for a negligible negative effect on the granules treated for 20 minutes, that all samples had an increased ammonium removal. The most satisfactory result was obtained for 90 minutes at  $2 \text{ V cm}^{-1}$  (Figure 5.3a and b), where the sAOR of nitrifying granules showed an increase of 44% compared to the not treated control; to a lesser extent, 120 and 60 minutes described an enhancement of 35 and 10%, respectively. After these results, the intensity of the EF to be used in the enhancement/reactivation test was investigated; in Figure 5.3c and d it is visible how the best EF intensity was encountered at  $2 \text{ V cm}^{-1}$  for 90 minutes, whereas the other granules showed a negligible increase if not a reduction of the activity. Both 60 and 90 minutes at  $2 \text{ V cm}^{-1}$  confirmed the previous tests results, whereas the effect of  $3 \text{ V cm}^{-1}$  for 60 minutes resulted almost negligible. On the other hand, treatment for a period of 90

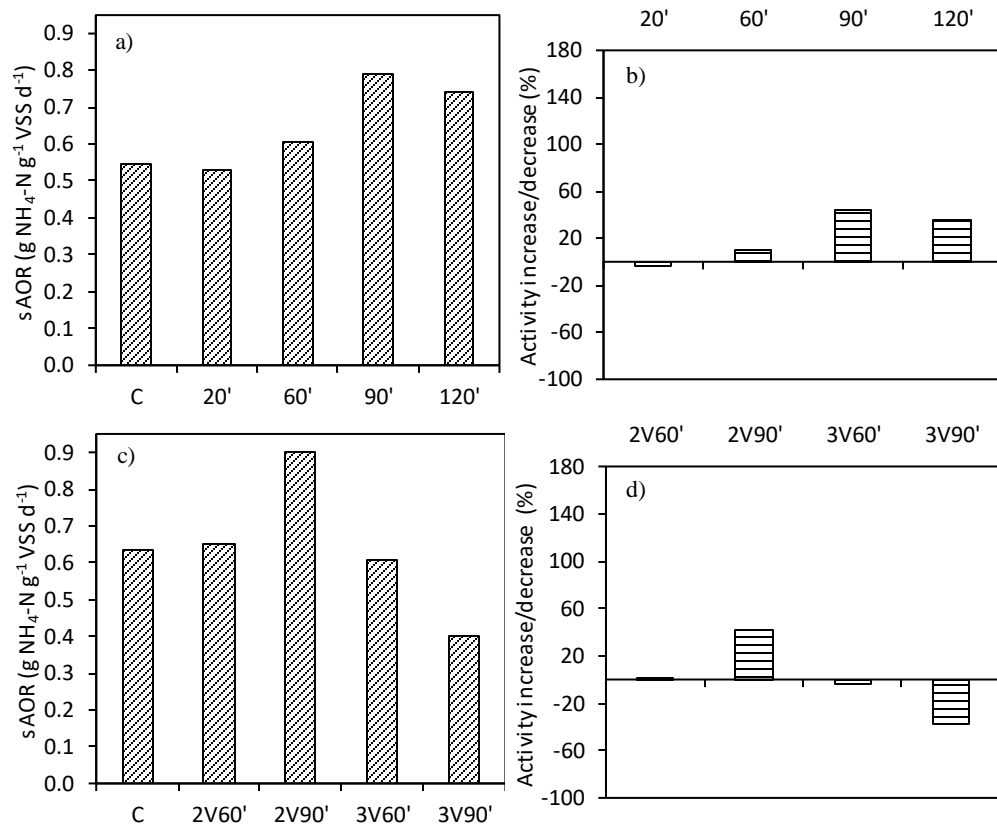


Figure 5.3 – Pre-trials to measure the most suitable duration and intensity for the electric field treatment. a) sAOR after different treatment durations (at  $2 \text{ V cm}^{-1}$ ), b) the percentage increase/decrease of activity at the investigated duration compared to control, c) sAOR at different electric field intensities and durations and d) the percentage increase/decrease of activity at the investigated intensities and durations compared to control.

minutes at  $3 \text{ V cm}^{-1}$  resulted excessive and the ammonium removal activity described a reduction of 37 % compared to the control. The reason for trying 60 instead of 120 minutes at  $3 \text{ V cm}^{-1}$  was due to uncertainty on the possible negative effects of a too long treatment at that high field intensity; this was eventually confirmed by the negligible effect on the sAOR of granules treated for 60 minutes at  $3 \text{ V cm}^{-1}$ . These results explain how an optimal EF treatment should be chosen in a specific *window* of intensities and durations to achieve a consistent improvement of bacteria activity; at the same time, a lower or higher voltage or duration than the optimal window could either produce no effects or reduce the bacteria activity. After the preliminary trials, batch tests with addition of toxic chemicals followed by EF treatment in both intact and ground granules were done; the effectiveness of the EF treatment to re-activate or enhance the sludge activity was going to be validated.

### 5.3.2.2. Using electric field to improve nitrifying activity of nitrifying granules inhibited by high salinity

Before the EF was used to investigate its effectiveness on reactivation of nitrifying sludge activity, two different NaCl concentrations were provided to the synthetic feed of both intact and ground granules, i.e. 2 and 4%, and the ammonium removal activity was measured during the batch test. Since all samples showed a similar pattern, only the control and G4% before and after electric field treatment were reported in Figure 5.4, where the changes of nitrogen species during the test are described. The first thing to notice is the loss of partial nitrifying activity of granules, described by the total  $\text{NH}_4^+$  oxidation to  $\text{NO}_3^-$  (Figure 5.4a). After the storage period, the granules were able to completely remove ammonium by production of nitrite only, with negligible concentrations of nitrate; unfortunately, it seems that during the 50 days before the batch tests, the nitrite oxidising bacteria could resume

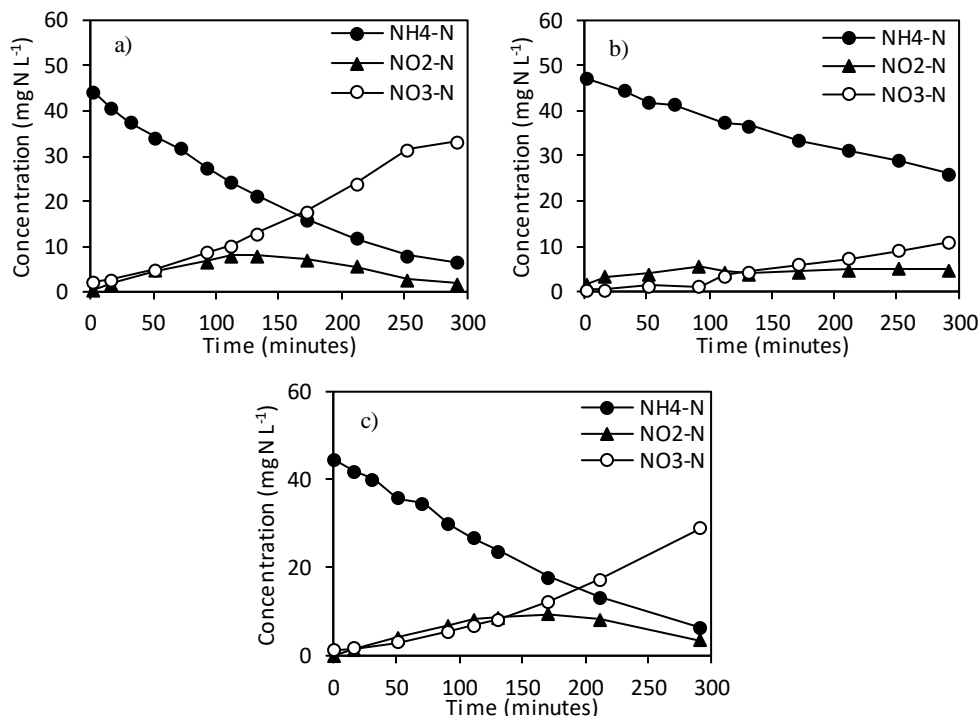


Figure 5.4 – Ammonium, nitrite and nitrate concentrations change during salinity batch test of a) the control, b) G4% after inhibition and c) G4% after electric field treatment.

their activity in the SBR and produce a complete nitrification. In Figure 5.4b both AOBs and NOBs activities are shown to be inhibited by the 4% salinity, as visible by the not complete removal of  $\text{NH}_4^+$  and the low concentrations of both  $\text{NO}_2^-$  and  $\text{NO}_3^-$ . On the other hand, a clear increase of both ammonium and nitrate concentrations in Figure 5.4c is visible, explaining the recovered granules activity.

In Figure 5.5a and b, the results of the salinity inhibition test are shown; the granules with addition of 2% and 4% of NaCl showed 15 and 61% less activity than the control, respectively; these results are in agreement with other studies on biofilm systems, where for higher concentrations of NaCl than 1%, nitrification could show inhibition (Bassin et al., 2011, Cortés-Lorenzo et al., 2015). A decrease in bioactivity was observed in all biomasses except for S2% that showed an activity 29% higher than the control; on the other hand, S4% showed a reduction of sAOR of 39%. 2% NaCl provided was likely not enough to cause any inhibition, as showed from these results. The controls C1 and C2 showed a close activity, with only 8.53% discrepancy. After the inhibition test, the sludge from different flasks were washed and treated with EF for 90 minutes and a batch test was run again to

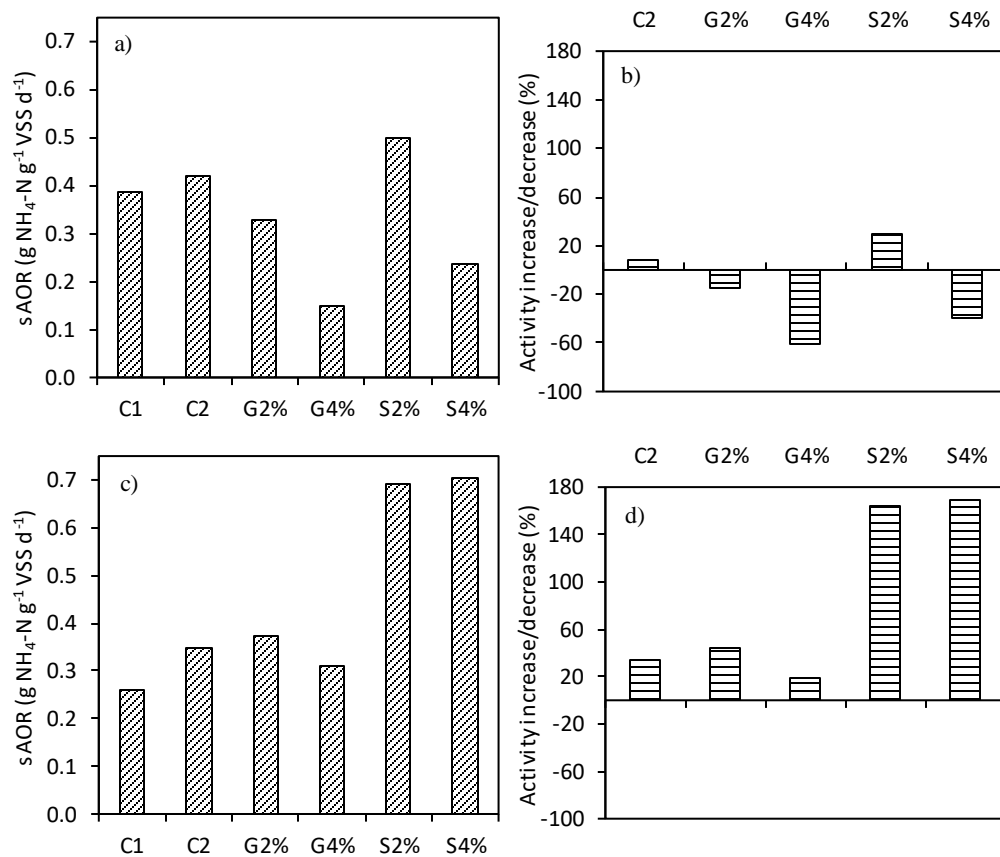


Figure 5.5 – Activity test after salt inhibition and electric field treatment. a) sAOR and b) the percentage of activity increase/decrease compared to control after salt inhibition. c) sAOR and d) the percentage of activity enhancement compared to control after electric field treatment.

check the possible effects; all biomasses showed a restored sAOR with some interesting results (Figure 5.5c and d); both ground granules could remove ammonium three times quicker than C1, which could be justified by the enhancement effect of the electric field on the suspended bacteria activity. C2, G2% and G4% showed a higher removal than the control, which is implying that, although no inhibition was provided (C2), the electric field could enhance the granules bioactivity compared to C1, as also shown previously in Figure 5.3c; in addition, G2% and G4% could efficiently recover from the inhibition. Specifically, C2, G2% and G4% activities were more than 33, 43 and 18% higher than control without treatment.

### 5.3.2.3. Using electric field to improve nitrifying activity of nitrifying granules inhibited by phenol

Similarly to the salinity test, fresh sludge was used to run an inhibition batch test with two different concentrations of phenol, i.e. 50 and 100 mg L<sup>-1</sup>. During the test all biomasses showed a considerable decrease of ammonium removal (Figure 5.6a and b). Also this time, the granules showed a slightly higher inhibition (82-90%) than the ground particles (76-84%); because of the greater phenol concentration, G100, G (also 100 mg L<sup>-1</sup>) and S100 showed a higher inhibition compared to respective similar sludge at lower phenol concentration. The

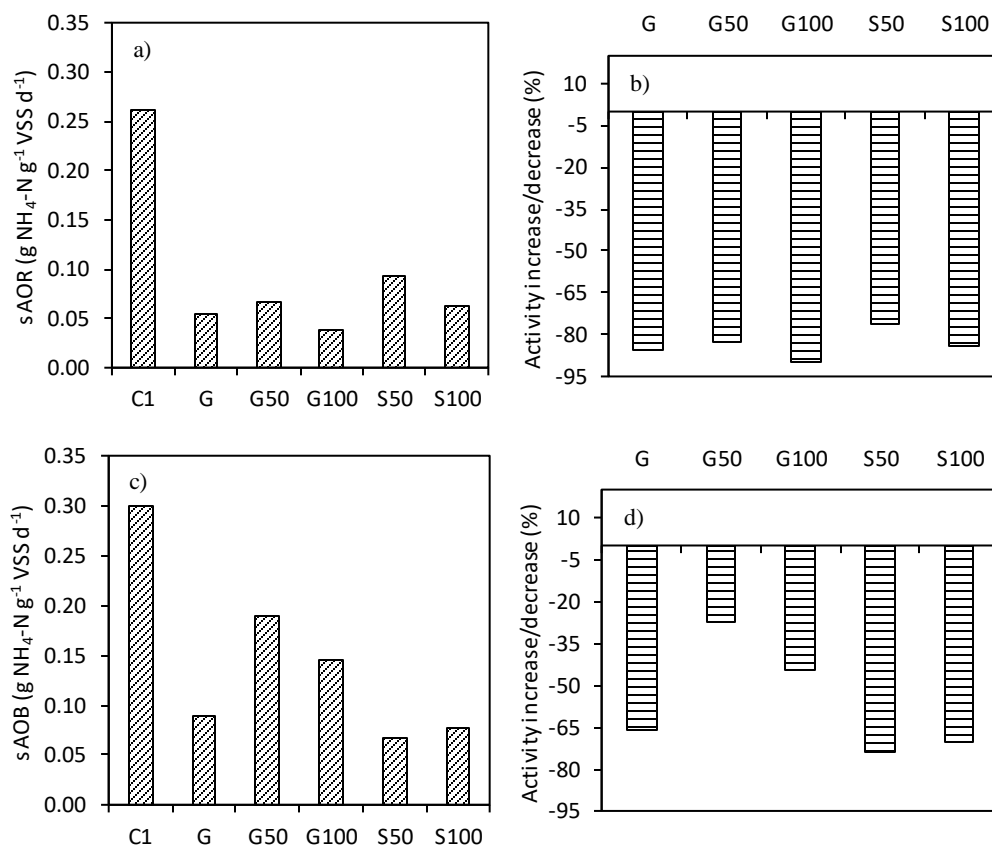


Figure 5.6 - Activity test after phenol inhibition and electric field treatment; a) sAOR and b) the percentage of activity decrease compared to control after phenol inhibition. c) sAOR and d) the percentage of activity enhancement compared to control after electric field treatment.



inhibitor amount used in this experiment was probably a bit too high, as also previously described (Liu et al., 2005c). This was also observed during the reactivation batch test when, after EF treatment was implemented, the biomasses could only partially resume their activity. It is interesting to notice that S50 showed almost no activity recovery (2%) and S100 could restore its activity only in lower extent (14%) than the intact granules; on the other hand, G50 and G100 could recover around 60 and 45%, respectively, of the activity previously lost. For what concerns G, which was inhibited by  $100 \text{ mg L}^{-1}$  of phenol but not treated with EF, the activity recovery was lower than G100; this would be justified by the enhancement effect of the electric field treatment in restoring the bioactivity of the inhibited granules.

## **5.4. Discussion**

### **5.4.1. Fast partial nitrifying granules production**

In our experiment, small granules were already observed during the first 3 days of acclimation time with 25 minutes settling time, agreeing with previous research where 30 minutes were used (Wan et al., 2011). A mild hydraulic selection pressure was used, by applying a step-wise decrease of settling time from 5 minutes on day 0 to 2 minutes on day 7; the portion of granules in the reactor was greater than the flocs on day 4. Previous research confirmed that stable heterotrophic granules could be achieved in 3 days from start-up by using strong hydraulic selection and high OLR (Liu and Tay, 2015); although a high OLR was used in our study, the granules were obtained slightly later (7 days), which is probably justified by the relatively slow decrease of settling time. After granulation, a quick decrease of COD/N ratio was used to quickly enrich the heterotrophic granules with nitrifying bacteria and at the same time avoiding free ammonia inhibition (Chen et al., 2015) and instability of the granules structure. Partial nitrifying granules were obtained after day 23, when the COD/N removed was lower than for typical heterotrophic sludge assimilation (Metcalf and Eddy, 2003). The granules nitrogen removal activity is in agreement with previous sAOR measured in similar systems (Vázquez-Padín et al., 2010, Shi et al., 2011, Song et al., 2013); however, a precise comparison cannot be done since those studies used mixed bacteria systems, whereas our granules contained mainly AOBs and NOBs nitrifying bacteria. The results are well in agreement with previous formation of stable partial nitrifying granules (Chapter 2).

Before the electric field treatment was implemented, it was noticed that partial nitrification activity was lost during the reactivation period. High ammonia and pH in the synthetic feed were used as strategy to produce the partial nitrifying granular sludge for the electric field treatment experiment; however, different cases in literature are known for describing the nitrite accumulation failure due to acclimation of NOBs biomass to the harsh conditions (Turk and Mavinic, 1989, Peng and Zhu, 2006). Similarly, it is possible that our granules lost the partial nitrifying activity during the storage and reactivation periods.

### **5.4.2. EF effects on granular sludge nitrifying activity**

From preliminary tests, the range of durations and electric field intensities tried in a previous ANAMMOX system (Qiao et al., 2014) were confirmed, resulting in the improvement of removal activity in nitrifying biomass. These results are probably to link to the similarities that the two bacteria species share (Agrawal et al., 2018). The tests have shown that both duration and intensity of EF need to be chosen carefully, since only a little window of appropriate parameters will affect positively the system. This was also described by Alshawabkeh et al. (2004), where a voltage of 16V generated a higher COD removal than at 4 V, but at the same time lower than at 8 V. On the other hand, the positive effect of the treatment was possible only within the 24 h, after which inhibition of bacteria was encountered. These results are due to harmful effects of too high or long-lasting EF; studies were

reported where bacteria activity was reduced due to oxygen radicals generation (She et al., 2006) or to irreversible permeabilisation of cell membrane (Drees et al., 2003).

#### **5.4.3. EF effects on salinity inhibition of nitrifying biomass**

The salinity inhibition observed for intact granules in the test was in agreement with other literature on salt effects on biofilm (Cortés-Lorenzo et al., 2015), where nitrifying activity was completely lost when nitrifying granules were exposed to NaCl solution with a concentration higher than 2.4%. Differently, S2% showed no inhibition compared to the rest of samples and together with S4% they showed higher activity than the intact granules. This was likely due to their lower mass transfer limitations compared to the particles (Liu and Joo-Hwa, 2012). In several studies in the literature, the presence of flocculent sludge within granular SBRs is common. This is mainly due to the lower mass transfer limitation that justifies the flocs greater specific growth rate, biomass yield and specific O<sub>2</sub> consumption rate. It is to note that the negligible inhibition of suspended sludge to 2% salt is in disagreement with previous research (Bassin et al., 2011), where higher NaCl concentration than 1% was already described to inhibit nitrification in suspended sludge. This could be due to the way ground granules and flocs are produced. Importantly, in the present study it was shown that full recovery of the nitrifying activity occurred. Previous research has described how nitrifying bacteria could not recover the removal activity as before NaCl was added to feedstock (Moussa et al., 2006); on the other hand, a complete recovery and, most interesting, even enhancement of ammonium removal activity in both intact and ground granules was observed in the present study, confirming the promising EF effects on inhibited nitrifying biomass.

#### **5.4.4. EF effects on phenol inhibition of nitrifying biomass**

The inhibition obtained in the test was in agreement with Liu et al. (2005c), where at concentrations of phenol higher than 15 mg L<sup>-1</sup>, there was a partial irreversible disruption of nitrification. However, in the present study the inhibition of the autotrophic biomass showed to be worse, likely due to the absence of heterotrophs able to degrade phenol (McCarty, 1999). As for the salinity test, the ground granules showed to be less inhibited by phenol compared to intact granules, which can be again justified by the lower mass transfer limitation than the thick structure of intact granules (Liu and Joo-Hwa, 2012). Differently, both S50 and S100 showed less or no recovery once the EF treatment was implemented compared to intact granules. Activated sludge was previously described as less tolerant to phenol in wastewater than granular sludge (Tay et al., 2005), which would explain why only the intact granules showed some recovery; the three-dimensional structure of the granules could generate a better protection of the bacteria from phenol toxicity. Although partially, it is clear that the effects of EF could speed-up the recovery in G100, showing a 46% recovery; differently, G that was fed with 100 mg phenol L<sup>-1</sup> and was not treated with EF showed only 20% recovery. Therefore, even after an almost complete inhibition by phenol, EF was shown to improve the rate of granular sludge recovery; this was not possible for the ground granules, which confirms the advantages of using the strong and dense granular sludge in wastewater treatment.

#### **5.4.5. Mechanism of electric field effect and its future application**

An electrical potential difference is constantly present between the internal and the external solution of every bacteria cytoplasmic membrane (transmembrane potential) and it is generated by the differential amount of contained charges; potential difference ranges between few mV mm<sup>-1</sup> to 100 mV mm<sup>-1</sup> and it generally changes due to transportation of charged ions between the two compartments through channels or ions pumps; however, sometimes, this happens because of external electric stimuli (Thrivikraman et al., 2018). It is thought that an

external EF can affect the bacteria activity by three main mechanisms: a) changing the space disposition of cytoplasmic charged molecules, b) perturbing the transmembrane potential and c) moving charged molecules on the cytoplasmic membrane; in a synergic way, they all start a reaction cascade that stimulates the bacteria activity.

In wastewater treatment and soil remediation literature, many studies have shown interesting effects of EF implementation; these effects are generally related to improvement of bacteria removal activity or to the increased growth rate. For instance, after an electrical stimulus was provided, the amount of adenosine triphosphate (ATP) was described to increase (Liu et al., 2015a, Ailijiang et al., 2016), whereas NAD/NADH ratio showed quick depletion (She et al., 2006). Both ATP and NADH are well-known energy molecules important for the bacterial activity; their increased production could therefore justify the reported higher microbial growth in those studies. In a nitrification system the activity of ammonia monooxygenase (AMO), hydroxylamine oxidoreductase (HAO) and nitrite oxidoreductase (NOR) were enhanced due to the EF applied (Qian et al., 2017). These enzymes catalyse the oxidation of  $\text{NH}_4^+$  to  $\text{NH}_2\text{OH}$ , of  $\text{NH}_2\text{OH}$  to  $\text{NO}_2^-$  and of  $\text{NO}_2^-$  to  $\text{NO}_3^-$ , respectively (Ge et al., 2015); their increased activity could eventually stimulate both bacteria's nitrogen removal activity and growth rate. Another example of electrically stimulated nitrification bacteria was described in Huang et al. (2014); in that experiment the biomass in the control reactor showed a typical switch from complete nitrification to partial nitrification, with a following nitrite accumulation, once the ammonium in the feedstock reached a concentration higher than  $300 \text{ mg N L}^{-1}$ . On the other hand, when applying the EF, a continuous NOBs activity was observed and partial nitrification was not achieved. It is known that high  $\text{NH}_4^+$  concentrations can inhibit the NOBs activity more than AOBs due to free ammonia toxicity (Anthonisen et al., 1976); on the contrary, the effect generated by the electric field could somehow improve the NOBs activity and avoid the free ammonia inhibition. In other research the change of structure of the organelle anammoxosome was described in ANAMMOX cells under effect of EF (Yin et al., 2016). The enlargement of the membrane surface of the anammoxosome was described in this study, with a consequent greater space for cytochrome c allocation; since this protein is essential for bacterial enzymatic activity (Jetten et al., 2009), the higher bacterial activity in nitrogen removal and consequently higher cells growth rate was justified. Also organic carbon removal was enhanced by using EF in a specific voltage window (Alshawabkeh et al., 2004) and a treatment longer than 24 h was described as inhibiting the removal in the activated sludge.

For most of these studies it is speculated that the effects of the electric field was closely related to modifications of the cell membrane characteristics, as also described by Luo et al. (2005); indeed an external electric field generated the change of transmembrane potential described by the increase of both zeta potential and hydrophobicity of phenol-degrading bacteria; this was justified by the generation of an increase of external negative charges. In addition, Chen et al. (2006b) confirmed that electro-stimulation could change the membrane structure by creating little pores; also called membrane permeabilisation or electroporation, it is thought that in this way the EF could improve the transportation of nutrients into the cells. This process is normally reversible at low electric field intensities, but it is also used as bactericide technique for food sterilisation at higher voltage, by producing an irreversible membrane permeabilisation and other drastic effects (Wang et al., 2018). Therefore, the EF most probably generates a perturbation of cellular stability, which consequently produces a response; these effects could somehow be interpreted as a reaction of the bacteria to a stressful condition as it could be the provided electric field/current. This is also confirmed from the fact that other research has described heat shock proteins (HSP) production (Thrivikraman et al., 2018) and increased 16S rRNA gene copies (Yin et al., 2016) following an EF treatment.

## 5.5. Conclusions

In Chapter 5 it was confirmed that the electric field application could improve the nitrifying granules ammonium removal activity of both intact and ground granules. This was justified by 33% increase in activity compared to the not treated control. More interestingly, the complete recovery of nitrifying biomass after inhibition by salinity (2% and 4% NaCl) was reported. All samples could show higher activity than the control after the electric field was applied and the ground granules could also measure a removal activity of roughly 164% more than the untreated control. When phenol was added to the feedstock, a stronger inhibition was induced and recovery was only partial in all biomasses. However, between two flasks of granules with the same concentration of phenol ( $100 \text{ mg L}^{-1}$ ), a faster recovery (45%) was observed in EF-treated granules compared to the untreated ones (20%); this means that the electric field could shorten the time needed for biomass to recover after inhibition. In this case the ground granules showed almost no recovery, which is probably due to the harsh conditions to which only a granular structure could resist. These are only preliminary results but they are promising for a future application of the electric field technology for reactivation of inhibited biomass activity. In addition, although it was not confirmed, it is plausible that the improvement of removal metabolism in nitrifying system could also increase the bacteria growth rate, which would be consequently advantageous for shortening the process start-up. Further investigation would be needed to confirm these results and to prove that the technology could be applied to a continuous system or to different biological processes. Although the plates used in this study were applied externally, the field effects were still visible, which defines the possibility to build less invasive systems biomass treatment.

## 5.6. Experimental weaknesses

The granules used for the experiment were showing complete nitrifying activity and, since partial nitrifying systems represent a more interesting and cost effective option over complete nitrification in wastewater treatment, it would have been interesting to investigate the EF effects on the partial nitrifying granules. This could not be possible since the granules were produced in a system where NOB activity was not efficiently inhibited.

Though the simplicity of the EF application, it was not possible to try the technology on a continuous system with or without biomass inhibition, whereas it was tried only on batch tests. For application at full scale, it would have been useful to also try the EF on a continuously run biological system.

In addition, the EF benefits on nitrifying granules presented in the experiment cannot be fully comparable to other technologies, like magnetic field or ultrasounds, since these techniques were not tested at the same time with the same conditions.

The electric field effects on real wastewater were not investigated. There are reasons to believe that the EF could act differently on the bacterial activity in presence of unidentified molecules in real streams.

Finally, after the first interesting results were discovered, more tests did not follow for lack of time. Because of this, the experiment replicability and accuracy may be criticised.

**OVERALL DISCUSSION, CONCLUSIONS AND RECOMMENDATIONS  
FOR FUTURE WORK**



## **6.1. Overall discussion**

### **6.1.1. Granulation mechanism and key factors**

The most critical factors described in literature for aerobic granulation were described as settling time, hydraulic retention time (HRT), hydraulic stress (shear stress), loading rate, periodic starvation time and height to diameter (H/D) ratio (Liu and Tay, 2002, Qin et al., 2004a, Qin et al., 2004b, Tay et al., 2004, Wang, 2005, Liu and Tay, 2008, Gao et al., 2011b). It is speculated that the fast granulation described in this thesis and the observed characteristics of the produced granules may be partially due to the specific conditions used in the lab-scale experiment.

#### ***6.1.1.1. Readily biodegradable organic source and water hardness***

Acetate is an easily degradable COD source chosen for heterotrophic biomass growth and added to the synthetic wastewater. Readily biodegradable organic substrates can generate an increase of hydrophobicity in the biomass, favouring the cell-to-cell interactions (Sarma et al., 2017). There are several reports showing that granulation could take place in a shorter time due to the readily biodegradable nature of the organic substrate (Sepúlveda-Mardones et al., 2019). However, when real wastewater is used, the biomass behaviour in generating granules can be more challenging. This is mainly due to presence of different organic sources, inorganic matter, xenobiotic chemicals and suspended material. The results from the characterisation of the PN granules in Chapter 3 showed that the provided acetate was the main reason for the high alkalinity observed in the system. This, at the same time, affected the pH of the system where, also due to the hardness of water and to the warmer temperatures used, compared to previous work, gave the right conditions for mineral precipitation (hydroxyapatite and calcite). It has been reported in literature that little concentrations of metal ions in the wastewater could improve the bacteria aggregation and the granule structure stability and settling rate (Jiang et al., 2003, Lin et al., 2013a). Furthermore, mineral crystals can potentially act as nucleation factors for the bacteria colonisation, which would consequently enhance the granulation process (Zhou et al., 2015, Liu et al., 2019). Therefore, it is possible that the presented granulation strategy and the feature of the PN granules could be specific for the conditions used in the lab-scale experiment. Following research is needed at this point to understand if granulation could take place differently with other organic sources, lower concentrations of calcium, or if real streams were to be used.

#### ***6.1.1.2. Solids-free synthetic wastewater***

Differently from real wastewater, the synthetic stream used in the experiments was containing no solids. It is reasonable that suspended matter may have an effect on the granulation process, however this may not represent a problem for the granules formation. It was observed in other studies that suspended material present in the influent was retained in the system after flocculating (Pronk, 2015). At the same time, particles entering the reactor were showed to be entrapped in the forming granules. As explained before, such flocs or particles may act as nucleation sites, enhancing the granulation process (Zhou et al., 2015, Liu et al., 2019). However, it is important to limit the proliferation of flocculent sludge in a granular system by carefully controlling the biomass settling skills. Flocs are basically present in most of the reported granular systems in literature, due to the physical friction on the granules surface, their fragmentation or simply due to de novo flocculation of particles present in the influent (Liu and Joo-Hwa, 2012). The mass transfer limitation of O<sub>2</sub> and nutrients within the granules allows the flocculent sludge to grow faster, leading to a possible granulation failure (Li and Liu, 2005, Liu et al., 2005b). Therefore, to apply the presented fast granulation strategy to real wastewater, further understanding of the role played by suspended matter on granules formation is still needed.

## **6.1.2. Considerations on scaling up**

### **6.1.2.1. Settling time and solids in the effluent**

Moving the granulation process investigated in this thesis from the laboratory to the full scale implies that special attention is placed on few points. The settling time is necessary to impose the right hydraulic selection pressure on the biomass for a quick granulation. In the sequencing batch reactor (SBR) configuration, the sludge unable to settle on time below the discharging point will be removed from the system, while the settling particles will be retained and will start the aerobic granulation (Qin et al., 2004a, Qin et al., 2004b). As shown from the experiments in the thesis, the time would be set at around 20 - 30 minutes at beginning of experiment, then it would be quickly reduced to 2 or 5 minutes when clear and well settling granules are detected. However, these short times remain challenging at full scale where sludge can only settle between 15 and 60 minutes (Pronk, 2015). Under this stringent selection pressure, a great part of the inoculum will be lost from the reactor during granulation. For example, after 24h from reactor start-up, only 10-36% of the biomass was retained in the system described by Liu and Tay (2015). Therefore, if the presented quick granulation strategy was to be used at full scale, during the first days further treatment of the reactor effluent from the solids would be necessary.

### **6.1.2.2. Reactor size and shear stress**

A very important factor to take into account when scaling-up a granular sludge system is reactor size. Despite using the same conditions at both laboratory and full scale, granules will show only partially comparable characteristics (Pishgar, 2019). The particles produced in larger reactors are characterised by a greater size but much looser structure compared to granules produced in smaller reactors. In addition, a longer time is generally needed by the larger reactor for the granulation to take place. These results are normally attributable to the lower shear stress generated by the wall in the larger diameter reactors (Liu, 2010) and to the composition of the real wastewater. Shear stress can influence the granules production and their stability by removing filamentous biomass, reducing porosity and increasing density (Liu and Tay, 2002, Adav and Lee, 2008). In the SBR systems it is generated by aeration and wastewater flow through the biomass and it relies on the reactor design. Therefore, aeration intensities and H/D ratio of the tank will need to be carefully chosen to generate the perfect biomass granulation. On the other hand, there is a limit for their increase, after which only negligible effects on shear stress and on granulation are observed (Zhou et al., 2019). Due to the viscous resistance of the liquid, the bubbles from the aeration eventually reach a constant up flow velocity of  $55.8 \text{ cm s}^{-1}$ . This needs to be taken into account when designing a granular sludge process because the high costs for the increased aeration or for the large size reactor may strongly affect the treatment plant economics.

### **6.1.2.3. SBR vs continuous**

In WWTW the application of continuous systems remains appealing due to the easy design and to the possibility to retrofit the already present tanks used for activated sludge. The SBR configuration is generally preferred in most studies for investigating the aerobic granulation (Sarma and Tay, 2018a). In addition, the easy control and real-time monitoring of several parameters (e.g. pH, dissolved  $\text{O}_2$ , settling time, etc.), make the SBR one of the most desirable systems for separate partial nitrification followed by denitrification or ANAMMOX (Nhat et al., 2017). In literature, continuous systems have been compared to SBR for granular sludge treatments (Jahn et al., 2019). To keep the selection pressure on the quick settling biomass, a following separation process needed to be added to the continuous reactors. However, the results showed that the granules produced in the SBR were still better settling than the ones in the continuous system, explaining the higher selection pressure in the former. Although some authors have tried to use a hydrocyclone in continuous systems to improve the selection pressure (Wett et al., 2015), the SBR still remains the preferred option for producing full scale aerobic granular processes.



#### **6.1.2.4. NOB inhibition**

In literature, many strategies were presented to develop a stable and efficient NOB activity inhibition, including the operation under limited oxygen concentrations, alternating oxic and anoxic conditions, short SRT, step feeding and use of real-time control of parameters like pH, O<sub>2</sub>, NH<sub>4</sub><sup>+</sup> (Winkler and Straka, 2019). In the presented thesis, NOB activity was inhibited during 5 months due to two main factors: step increase of ammonium in the feed and relatively high reactor temperature. At a certain pH and temperature, ammonium is present in solution together with the deprotonated form free ammonia (FA). A slightly alkaline pH would increase the amount of FA over the ammonium. Both bacteria groups are inhibited by different FA concentrations. AOB were described to be affected at FA values of 8 - 120 mg L<sup>-1</sup>, whereas NOB showed to be more sensitive and were inhibited at values of 0.08 - 0.82 mg L<sup>-1</sup>. In addition, the activation energy for AOB and NOB was reported in the range of 72-60 kJ mol<sup>-1</sup> and 43-47 kJ mol<sup>-1</sup>, respectively (studies run between 7 and 30 °C) (Van Hulle et al., 2010). This means that AOB would be more active than NOB at the same temperature. Therefore, both the high ammonium in the feed and the warmer temperatures used in the systems in the experiments would explain the stronger activity of ammonium oxidising bacteria over the nitrite oxidising bacteria, which were consequently washed out from the system. However, such a strategy has already been shown by the literature to be unsuitable for stable partial nitrification for long time (Turk and Mavinic, 1989, Peng and Zhu, 2006), as it was also confirmed by the experiment in Chapter 5. The acclimation of NOB biomass to the system conditions was reported as the increase of NO<sub>3</sub><sup>-</sup> in effluent and the nitrite accumulation failure. Intermittent aeration, on the other hand, would represent a practical solution at full scale to keep the NOB inhibition for long time (Lackner et al., 2014, Winkler and Straka, 2019). The NOB activity recovery after the anoxic period showed a delay of around 1.5 - 12 h (this time being function of the length of the anoxic stress) (Kornaros et al., 2010, Bournazou et al., 2013). The decay rate of AOB, on the other hand, resulted lower than that of NOB when exposed to anoxic conditions (Salem et al., 2006). In addition to this, whenever a simultaneous denitrification or ANAMMOX step was decided to be implemented in the partial nitrification granular system, the oxygen absence within the inner portion of the particles would induce the competition of a different metabolism for the same substrate. In case of denitrification, the COD provided would be degraded together with NO<sub>2</sub><sup>-</sup> by heterotrophic bacteria. In a similar way, ANAMMOX would remove NO<sub>2</sub><sup>-</sup> which would be no more available for NOB metabolism (Lemaire et al., 2008). Although this strategy was reported to be effective at full scale, the possibility of production of the greenhouse gas N<sub>2</sub>O at low dissolved oxygen and the necessity to remove it before discharging the effluent, should be carefully evaluated for the economics of the process (Massara et al., 2017).

#### **6.1.3. Real wastewater and examples of side-stream applications**

Compared to the conventional nitrification-denitrification process, that is widely used for middle and high ammonium strength wastewater treatment, the partial nitrification (PN), either followed by denitrification or ANAMMOX, can mitigate the costs for aeration energy and external carbon source addition (Cho et al., 2020). Application of PN has been reported for treating synthetic wastewater (Isanta et al., 2015, Poot et al., 2016), black water (De Graaff et al., 2011), digester liquor (Yamamoto et al., 2008, Qiao et al., 2010), reject water (Lackner et al., 2014) and landfill leachate (Ganigué et al., 2009, Nhat et al., 2017, Xu et al., 2020). The NH<sub>4</sub><sup>+</sup>-N content in these studies ranges between 500 and 4000 mg N L<sup>-1</sup>. The PN technology becomes preferable when a low COD/N ratio (generally < 2) is present in the stream to treat. In specific cases in literature, the digester liquors and reject water produced from sugar industries, paper recycling, bone processing and treatment of landfill leachates were also described to contain high Ca<sup>2+</sup> concentrations (Van Langerak et al., 1998, Hammes et al., 2003). The typical concentration of Ca<sup>2+</sup> reported in these streams was shown to range between 100 and 500 mg Ca<sup>2+</sup> L<sup>-1</sup>. At this calcium concentrations, uncontrolled inorganic precipitation can be problematic, leading to

scaling issues by clogging pipelines, boilers or heat exchangers (Rathinam et al., 2018). In addition, biological activity reduction was observed in aerobic granular systems (Ren et al., 2008, Liu et al., 2016a) and also the increase of energy costs for mixing were described (Van Langerak et al., 1998), due to solidification at the bottom of reactors. Nevertheless, there are reports in which the increased amount of minerals within the granular sludge could enhance the bacteria aggregation, showing faster settling rates and more stability of the granule structure (Jiang et al., 2003, Lin et al., 2013a). In addition, the simultaneous precipitation of phosphorus together with calcium has lately interested the scientific community, due to the possibility of recovering the elements in the solid form as a valuable product (i.e. struvite and hydroxyapatite) (Desmidt et al., 2015, Nancharaiah et al., 2016, Peng et al., 2018, Sarma and Tay, 2018b).

The fast granulation strategy and the PN system presented in the thesis would be possibly applicable on effluents coming from digesters treating streams like the ones described above, which show low COD/N ratio, high alkalinity, medium/high strength ammonium content and slightly high water hardness. It would be important to carefully adjust the COD/N ratio during the granulation, in order to achieve quick accumulation of nitrifying bacteria, but also without causing load stress on the ammonium oxidising bacteria and their washout. Adjusting the residence time of wastewater within the anaerobic tank would change the COD/N in the effluent. During the heterotrophic granulation, a shorter retention time should be used to produce an effluent with enough COD; after nitrifying bacteria are accumulating, the AD retention time should be step-wise extended, in order to reduce the COD/N ratio. However, further research should follow to understand if it would be economically feasible to use the PN reactor mainly for producing the right influent for a following denitrification or ANAMMOX reactor, or if calcium accumulation would be profitable. Calcification reactors were described in literature to accumulate  $\text{Ca}^{2+}$  in the biomass whenever they were fed with AD effluent; the alkalinity produced by the anaerobic reactor together with the specific biomass activity of the calcification reactor, helped establishing the right conditions for the  $\text{Ca}^{2+}$  removal from the wastewater (Van Langerak et al., 1997, Hammes et al., 2003). However, in these studies a following biological process was still needed for nitrogen removal before the stream was discharged. This is important because in the PN process investigated in the thesis, only one system would be needed after the anaerobic digester.

## 6.2. Overall conclusions

### 6.2.1. Fast start-up of partial nitrifying granules reactor and its long-term stable operation at high calcium concentration

- Our results demonstrate that partial nitrifying granules can be cultivated in a lab-scale SBR in a very short time of 30 days.
- The presented strategy shows how the operational costs for partial nitrifying granular systems start-up can be reduced. By using conventional activated sludge from aeration basins as inoculum, more autonomy of the WWTW from purchasing expensive inocula for partial nitrifying granules start-up can be achieved.
- To our knowledge, this is the first report that clearly shows enhanced granules stability during granulation at the temperature of 18-23 °C and COD/N ratio of 5, compared to when the process is run at 30-33 °C and higher organic carbon. In agreement with previous literature, it is confirmed that both the lower bacterial growth rate (lower T) and the enrichment of slow growing nitrifying bacteria (lower COD/N), produce granules in shorter time and with a denser structure.
- Partial nitrification over the complete nitrification was shown by the NOB activity inhibition during the 5 months the experiment lasted, due to the high ammonium in the influent.

### 6.2.2. Physical, chemical and biological characteristics of partial nitrifying granules treating middle strength ammonium wastewater with high water hardness level

- To our knowledge, this is the first time that the precipitation and accumulation of calcium phosphate (as hydroxyapatite) and calcium carbonate (as calcite) within AOB-dominant partial nitrifying granules is described.
- From the presented results, the mass transfer limitation within the larger particles and the slightly high water hardness (100-150 mg Ca<sup>2+</sup>) showed to be the main factors for the mineral precipitation to take place within the autotrophic granules.
- The direct application of hydroxyapatite as fertiliser and its use as a substitute of PO<sub>4</sub><sup>3-</sup> rock in industry represent an interesting opportunity.
- The AOBs-dominant partial nitrifying granules show precipitation under the plate-like spheres of hydroxyapatite and the smooth-steps bars for calcite. These specific appearances were found in very different biological systems from the one studied in this experiment, which explains they may not be bacteria-dependent.
- It is also described that the high accumulation of minerals within the granules showed a bacterial behaviour that in literature was only hypothesised before, the budding theory. The presence of buds both attached to the larger granules and in solution was confirmed by microscopy. This also shows that the great inorganic precipitation plays an important role in influencing the particles size in the system.

### **6.2.3. Study on EPS extraction from sludge with high mineral content and relevant factors for reliable protein measurements**

- High amount (200 mg g<sup>-1</sup> MLSS) of calcium content in partial nitrifying granules is shown to be the main factor interfering with proteins determination by Lowry's method. Alkaline pH and carbonate present in the method reagents induce precipitation during the analyses.
- The results from the chromatography analyses show that calcium is not present in the extraction solution. It is speculated that it could be bound to organic molecules contained in EPS, which is also confirmed by the impossibility to remove the precipitation by dialysis pre-treatment.
- The precipitation is reduced when a physical protocol for the extraction (heat method) is used. This can be explained by the lower extent of EPS extraction compared to the chemical procedure (formaldehyde/NaOH) and therefore to the lower amount of calcium released.

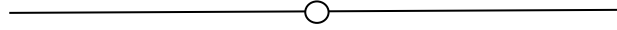
### **6.2.4. Reactivating ammonium removal activity of nitrifying biomass after inhibition using external electrostatic field**

- In this experiment preliminary positive effects of the electric field (EF) application on the activity of nitrifying granules are shown. For instance, the ammonium removal rate of the particles after 90 minutes of treatment at 2V is enhanced of 44% compared to the control.
- The treatment is also shown to be capable of reducing the granules ammonium removal activity inhibition after salinity shock at 2 and 4% of NaCl. The granules that show inhibition of 15 and 61% to the two salinity concentrations, are able to completely recover and to improve the ammonium removal activity of 43 and 18% compared to the control that was not EF treated.
- A stronger inhibition is shown by phenol addition to the granules and only partial biomass activity recovery is obtained. However, between two flasks of granules with the same concentration of phenol (100 mg L<sup>-1</sup>), a faster recovery of 45% of activity is observed if particles are EF-treated, whereas only 20% recovery is shown for untreated ones. Therefore, it can be concluded that the electric field can shorten the time needed for biomass to recover after inhibition.
- The difference in recovery rates between ground and intact granules shows how only the particles can stand harsh environmental conditions like high phenol concentrations in the feedstock and recover from the inhibition. On the other hand, the suspended biomass activity is not inhibited by NaCl, but on the contrary shows enhanced activity of 164%.

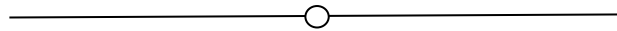
### **6.3. Recommendations for future work**

- Despite the importance of the results on fast granulation of PN biomass, it is suggested that in future experiments the synthetic feedstock is replaced by real wastewater, to confirm the strategy under real conditions. This also means that different pH ranges and calcium concentrations in the waste streams should be tested to understand if the mineral precipitation found during the experiment could affect granulation.
- The mass balance of nitrogen species and inorganic elements in the system would be advisable. It is speculated that nitrifier denitrification was taking place in the granules, together with calcium and phosphate accumulation. Being aware of the presence of specific bacterial systems or that some inorganic elements are consumed or generated, could help understanding if they play a role in the quick production of granules.

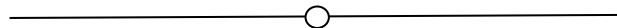
- For a longer NOB inhibition, it is recommended that a different strategy than high ammonium in influent, e.g. intermittent aeration and SRT control, is used to avoid the bacteria to accumulate again in the system. At the same time, for a stable process, it is advisable that the ammonium and ammonia concentrations in the effluent are continuously monitored, in order to avoid load stress on the bacterial community and a following system instability and failure.



- It is thought that recovery of both hydroxyapatite and calcite from granules would be beneficial for the WWTW and more research in this direction, as techniques of solubilisation or extraction from the biomass, are needed.
- Although no chemicals or pH control were necessary for mineral precipitation within PN granules, since these findings were observed in batch tests, it is recommended that further investigation be done to understand this behaviour in a continuous system.
- The use of real wastewater would be critical to understand the mineral accumulation under real conditions and it is also speculated that the control of Ca/P ratio in the waste stream would be needed to improve the minerals accumulation.
- Due to the short time available, only a limited amount of granules was analysed by SEM and EDX to describe the different mineral structures. In the future, a larger amount of granules should be tested for a more reliable description.



- Although the calcium interference with the Lowry's method can partially be removed if the incubation time during the procedure is extended from 1 to 3 hours, it is recommended that other methods be tried if high concentrations of calcium are expected.
- Unfortunately, there was no time to confirm the hypothesis that calcium could be bound to organic molecules contained in EPS and further research is still needed in this direction.



- It is speculated that electrostatic field (EF) results could be applied to other biological systems that are still missing, reason for which it would be interesting in the future to further understand the EF effects on partial nitrifying granules.
- Although the EF results seem very positive, it would be recommended that more tests are run on continuous systems and with real conditions to confirm the possibility of electric field application in wastewater treatment.



## LIST OF REFERENCES

- ABELING, U. & SEYFRIED, C. F. 1992. Anaerobic– aerobic treatment of high strength ammonium wastewater nitrogen removal via nitrite. *Water Science & Technology*, 26, 1007-15.
- ADAV, S. S. & LEE, D.-J. 2008. Extraction of extracellular polymeric substances from aerobic granule with compact interior structure. *Journal of hazardous materials*, 154, 1120-1126.
- AGRAWAL, S., SEUNTJENS, D., COCKER, P. D., LACKNER, S. & VLAEMINCK, S. E. 2018. Success of mainstream partial nitrification/anammox demands integration of engineering, microbiome and modeling insights. *Current Opinion in Biotechnology*, 50, 214-221.
- AHN, Y. H. 2006. Sustainable nitrogen elimination biotechnologies: A review. *Process Biochemistry*, 41, 1709-1721.
- AILJIANG, N., CHANG, J., LIANG, P., LI, P., WU, Q., ZHANG, X. & HUANG, X. 2016. Electrical stimulation on biodegradation of phenol and responses of microbial communities in conductive carriers supported biofilms of the bioelectrochemical reactor. *Bioresource Technology*, 201, 1-7.
- AKUNNA, J. C., BIZEAU, C. & MOLETTA, R. 1993. Nitrate and nitrite reductions with anaerobic sludge using various carbon sources: glucose, glycerol, acetic acid, lactic acid and methanol. *Water Research*, 27, 1303-1312.
- ALSHAWABKEH, A. N., SHEN, Y. & MAILLACHERUVU, K. Y. 2004. Effect of DC electric fields on COD in aerobic mixed sludge processes. *Environmental engineering science*, 21, 321-329.
- ANTHONISEN, A. C., LOEHR, R. C., PRAKASAM, T. B. S. & SRINATH, E. G. 1976. Inhibition of nitrification by ammonia and nitrous acid. *Journal of the Water Pollution Control Federation*, 48, 835-852.
- APHA 2012. *Standard Methods of Water and Wastewater*, Washington, DC, American Public Health Association, American Water Works Association, Water Environment Federation.
- BALOWS, A., TRUPER, H. G., DWORKIN, M., W., H. & SCHLEIFER, K. H. 1992. *The prokaryotes. A handbook on the biology of bacteria: ecophysiology isolation identification applications.*, New York, NY, Springer-Verlag.
- BARNES, D. & BLISS, P. J. 1983. *Biological Control of Nitrogen in Wastewater Treatment*, London, UK., E.&F.N. Spon.
- BARR, J. J., COOK, A. E. & BOND, P. L. 2010. Granule formation mechanisms within an aerobic wastewater system for phosphorus removal. *Applied and environmental microbiology*, 76, 7588-7597.
- BARTROLI, A., PEREZ, J. & CARRERA, J. 2010. Applying Ratio Control in a Continuous Granular Reactor to Achieve Full Nitrification under Stable Operating Conditions. *Environmental Science & Technology*, 44, 8930-8935.
- BASSIN, J., KLEEREBEZEM, R., MUYZER, G., ROSADO, A., VAN LOOSDRECHT, M. & DEZOTTI, M. 2011. *Effect of Different Salt Adaptation Strategies on the Microbial Diversity, Activity, and Settling of Nitrifying Sludge in Sequencing Batch Reactors.*
- BASSIN, J. P., KLEEREBEZEM, R., DEZOTTI, M. & VAN LOOSDRECHT, M. C. M. 2012. Measuring biomass specific ammonium, nitrite and phosphate uptake rates in aerobic granular sludge. *Chemosphere*, 89, 1161-1168.
- BERNAT, K., KULIKOWSKA, D., ZIELIŃSKA, M., CYDZIK-KWIATKOWSKA, A. & WOJNOWSKA-BARYŁA, I. 2012. The treatment of anaerobic digester supernatant by combined partial ammonium oxidation and denitrification. *Desalination and Water Treatment*, 37, 223–229.
- BESSELINK, R., RODRIGUEZ-BLANCO, J., STAWSKI, T., BENNING, L. & TOBLER, D. 2017. How Short-Lived Ikaite Affects Calcite Crystallization. *Crystal Growth & Design*, 17, 6224-6230.
- BEUN, J. J., HENDRIKS, A., VAN LOOSDRECHT, M. C. M., MORGENROTH, E., WILDERER, P. A. & HEIJNEN, J. J. 1999. Aerobic granulation in a sequencing batch reactor. *Water Research*, 33, 2283-2290.
- BEUN, J. J., VAN LOOSDRECHT, M. C. M. & HEIJNEN, J. J. 2000. Aerobic granulation. *Water Science and Technology*.
- BEUN, J. J., VAN LOOSDRECHT, M. C. M. & HEIJNEN, J. J. 2002. Aerobic granulation in a sequencing batch airlift reactor. *Water Research*, 36, 702-712.

- BOSKEY, A. L. & POSNER, A. S. 1973. Conversion of amorphous calcium phosphate to microcrystalline hydroxyapatite. A pH-dependent, solution-mediated, solid-solid conversion. *The Journal of Physical Chemistry*, 77, 2313-2317.
- BOSSIER, P. & VERSTRAETE, W. 1996. Triggers for microbial aggregation in activated sludge? *Applied Microbiology and Biotechnology*, 45, 1-6.
- BOURNAZOU, M. N. C., HOOSHIAR, K., ARELLANO-GARCIA, H., WOZNY, G. & LYBERATOS, G. 2013. Model based optimization of the intermittent aeration profile for SBRs under partial nitrification. *Water Research*, 47, 3399-3410.
- BRADFORD, M. 1976. A rapid and sensitive method for quantitation of microgram quantities of protein utilizing the principle of protein-dye binding. *Anal. Biochem.*, 72, 248-254.
- BROUWER, M., VAN LOOSDRECHT, M. C. M. & HEIJNEN, J. J. 1996. One reactor system for ammonium removal via nitrite. STOWA Report. 96-01. Utrecht (The Netherlands): STOWA, ISBN: 90 74476 55 4. Utrecht (The Netherlands): STOWA.
- BSI 1984. BS 6068-2.11:1984, ISO 7150-1:1984 *Water quality. Physical, chemical and biochemical methods. Determination of ammonium: manual spectrometric method*, British Standards Institution.
- CASTANIER, S., LE MÉTAYER-LEVREL, G. & PERTHUISOT, J.-P. 1999. Ca-carbonates precipitation and limestone genesis—the microbiogeologist point of view. *Sedimentary geology*, 126, 9-23.
- CHAI, L.-Y., ALI, M., MIN, X.-B., SONG, Y.-X., TANG, C.-J., WANG, H.-Y., YU, C. & YANG, Z.-H. 2015. Partial nitrification in an air-lift reactor with long-term feeding of increasing ammonium concentrations. *Bioresource Technology*, 185, 134-142.
- CHANG, X., LI, D., LIANG, Y., YANG, Z., CUI, S., LIU, T., ZENG, H. & ZHANG, J. 2013. Performance of a completely autotrophic nitrogen removal over nitrite process for treating wastewater with different substrates at ambient temperature. *Journal of Environmental Sciences*, 25, 688-697.
- CHEN, C., SMYE, S., ROBINSON, M. & EVANS, J. 2006a. Membrane electroporation theories: a review. *Medical and Biological Engineering and Computing*, 44, 5-14.
- CHEN, C., SMYE, S. W., ROBINSON, M. P. & EVANS, J. A. 2006b. Membrane electroporation theories: a review. *Medical and Biological Engineering and Computing*, 44, 5-14.
- CHEN, F.-Y., LIU, Y.-Q., TAY, J.-H. & NING, P. 2015. Rapid formation of nitrifying granules treating high-strength ammonium wastewater in a sequencing batch reactor. *Applied Microbiology and Biotechnology*, 99, 4445-4452.
- CHEN, G. & STREVEIT, K. A. 2003. Impact of carbon and nitrogen conditions on E. coli surface thermodynamics. *Colloids and Surfaces B: Biointerfaces*, 28, 135-146.
- CHEN, G. H., AN, K. J., SABY, S., BROIS, E. & DJAFER, M. 2003a. Possible cause of excess sludge reduction in an oxic-settling-anaerobic activated sludge process (OSA process). *Water research*, 37, 3855-3866.
- CHEN, W., WESTERHOFF, P., LEENHEER, J. A. & BOOKSH, K. 2003b. Fluorescence Excitation–Emission Matrix Regional Integration to Quantify Spectra for Dissolved Organic Matter. *Environmental Science & Technology*, 37, 5701-5710.
- CHO, S., KAMBEY, C. & NGUYEN, V. K. 2020. Performance of Anammox Processes for Wastewater Treatment: A Critical Review on Effects of Operational Conditions and Environmental Stresses. *Water*, 12, 20.
- CHUANG, H.-P., OHASHI, A., IMACHI, H., TANDUKAR, M. & HARADA, H. 2007. Effective partial nitrification to nitrite by down-flow hanging sponge reactor under limited oxygen condition. *Water Research*, 41, 295-302.
- COLLIVER, B. B. & STEPHENSON, T. 2000. Production of nitrogen oxide and dinitrogen oxide by autotrophic nitrifiers. *Biotechnology Advances*, 18, 219-232.
- COMTE, S., GUIBAUD, G. & BAUDU, M. 2006. Relations between extraction protocols for activated sludge extracellular polymeric substances (EPS) and EPS complexation properties: Part I. Comparison of the efficiency of eight EPS extraction methods. *Enzyme and Microbial Technology*, 38, 237-245.
- CORTÉS-LORENZO, C., RODRÍGUEZ-DÍAZ, M., SIPKEMA, D., JUÁREZ-JIMÉNEZ, B., RODELAS, B., SMIDT, H. & GONZÁLEZ-LÓPEZ, J. 2015. Effect of salinity on nitrification efficiency and structure of ammonia-oxidizing bacterial communities in a submerged fixed bed bioreactor. *Chemical Engineering Journal*, 266, 233-240.
- CUNHA, J. R., SCHOTT, C., VAN DER WEIJDEN, R. D., LEAL, L. H., ZEEMAN, G. & BUISMAN, C. 2018a. Calcium addition to increase the production of phosphate granules in anaerobic treatment of black water. *Water research*, 130, 333-342.



- CUNHA, J. R., TERVAHAUTA, T., VAN DER WEIJDEN, R. D., HERNÁNDEZ LEAL, L., ZEEMAN, G. & BUISMAN, C. J. N. 2018b. Simultaneous recovery of calcium phosphate granules and methane in anaerobic treatment of black water: Effect of bicarbonate and calcium fluctuations. *Journal of Environmental Management*, 216, 399-405.
- D'ABZAC, P., BORDAS, F., VAN HULLEBUSCH, E., LENS, P. N. & GUIBAUD, G. 2010. Extraction of extracellular polymeric substances (EPS) from anaerobic granular sludges: comparison of chemical and physical extraction protocols. *Applied microbiology and biotechnology*, 85, 1589-1599.
- DAALKHAIJAV, U. & NEMATI, M. 2013. Ammonia loading rate: an effective variable to control partial nitrification and generate the anaerobic ammonium oxidation influent. *Environmental Technology*, 34, 2907-2916.
- DANGCONG, P., BERNET, N., DELGENES, J.-P. & MOLETTA, R. 1999. Aerobic granular sludge—a case report. *Water Research*, 33, 890-893.
- DANGCONG, P., BERNET, N., DELGENES, J.P. AND MOLETTA, R. 1999. Aerobic granular sludge—a case report. *Water Research*, 33, 890-893.
- DAPENA-MORA, A., CAMPOS, J. L., MOSQUERA-CORRAL, A., JETTEN, M. S. M. & MENDEZ, R. 2004. Stability of the ANAMMOX process in a gas-lift reactor and a SBR. *Journal of Biotechnology*, 110, 159–170.
- DAVEREY, A., SU, S.-H., HUANG, Y.-T., CHEN, S.-S., SUNG, S. & LIN, J.-G. 2013. Partial nitrification and anammox process: A method for high strength optoelectronic industrial wastewater treatment. *Water Research*, 47, 2929-2937.
- DE-BASHAN, L. E. & BASHAN, Y. 2004. Recent advances in removing phosphorus from wastewater and its future use as fertilizer (1997–2003). *Water research*, 38, 4222-4246.
- DE CLIPPELEIR, H., VLAEMINCK, S. E., DE WILDE, F., DAENINCK, K., MOSQUERA, M., BOECKX, P., VERSTRAETE, W. & BOON, N. 2013. One-stage partial nitritation/anammox at 15 A degrees C on pretreated sewage: feasibility demonstration at lab-scale. *Applied Microbiology and Biotechnology*, 97, 10199-10210.
- DE CLIPPELEIR, H., YAN, X. G., VERSTRAETE, W. & VLAEMINCK, S. E. 2011. OLAND is feasible to treat sewage-like nitrogen concentrations at low hydraulic residence times. *Applied Microbiology and Biotechnology*, 90, 1537-1545.
- DE GRAAFF, M., TEMMINK, H., ZEEMAN, G., VAN LOOSDRECHT, M. & BUISMAN, C. 2011. Autotrophic nitrogen removal from black water: calcium addition as a requirement for settleability. *Water research*, 45, 63-74.
- DE KREUK, M. K., HEIJNEN, J. J. & VAN LOOSDRECHT, M. C. M. 2005. Simultaneous COD, nitrogen, and phosphate removal by aerobic granular sludge. *Biotechnology and Bioengineering*, 90, 761-769.
- DE KREUK, M. K., KISHIDA, N. & VAN LOOSDRECHT, M. C. M. 2007a. Aerobic granular sludge - state of the art. *Water Science and Technology*, 55, 75-81.
- DE KREUK, M. K., PICIOREANU, C., HOSSEINI, M., XAVIER, J. B. & VAN LOOSDRECHT, M. C. M. 2007b. Kinetic model of a granular sludge SBR: Influences on nutrient removal. *Biotechnology and Bioengineering*, 97, 801-815.
- DE KREUK, M. K. & VAN LOOSDRECHT, M. C. M. 2004. Selection of slow growing organisms as a means for improving aerobic granular sludge stability. *Water Science and Technology*, 49, 9-17.
- DE PRÁ, M. C., KUNZ, A., BORTOLI, M., PERONDI, T. & CHINI, A. 2012. Simultaneous removal of TOC and TSS in swine wastewater using the partial nitritation process. *J. Chem. Technol. Biotechnol.*, 87, 1641-1647.
- DESLOOVER, J., DE CLIPPELEIR, H., BOECKX, P., DU LAING, G., COLSEN, J., VERSTRAETE, W. & VLAEMINCK, S. E. 2011. Floc-based sequential partial nitritation and anammox at full scale with contrasting N<sub>2</sub>O emissions. *Water Research*, 45, 2811-2821.
- DESMIDT, E., GHYSELBRECHT, K., ZHANG, Y., PINOY, L., VAN DER BRUGGEN, B., VERSTRAETE, W., RABAEY, K. & MEESCHAERT, B. 2015. Global Phosphorus Scarcity and Full-Scale P-Recovery Techniques: A Review. *Critical Reviews in Environmental Science and Technology*, 45, 336-384.
- DREES, K. P., ABBASZADEGAN, M. & MAIER, R. M. 2003. Comparative electrochemical inactivation of bacteria and bacteriophage. *Water research*, 37, 2291-2300.
- DUBOIS, M., GILLES, K. A., HAMILTON, J. K., REBERS, P. & SMITH, F. 1956. Colorimetric method for determination of sugars and related substances. *Analytical chemistry*, 28, 350-356.

- DUPRAZ, C., REID, R. P., BRAISSANT, O., DECHO, A. W., NORMAN, R. S. & VISSCHER, P. T. 2009. Processes of carbonate precipitation in modern microbial mats. *Earth-Science Reviews*, 96, 141-162.
- EBRAHIMI, S., GABUS, S., ROHRBACH-BRANDT, E., HOSSEINI, M., ROSSI, P., MAILLARD, J. & HOLLIGER, C. 2010. Performance and microbial community composition dynamics of aerobic granular sludge from sequencing batch bubble column reactors operated at 20 C, 30 C, and 35 C. *Applied microbiology and biotechnology*, 87, 1555-1568.
- EPA, U. 1993. *Process design manual of nitrogen control*, Cincinnati, Ohio.
- FASSBENDER, A. G. 2001. ThermoEnergy Ammonia Recovery Process for Municipal and Agricultural Wastes. *TheScientificWorld*, 908-913.
- FILALI, A., MAÑAS, A., MERCADE, M., BESSIERE, Y., BISCANS, B. & SPÉRANDIO, M. 2012. *Stability and performance of two GSBP operated in alternating anoxic/aerobic or anaerobic/aerobic conditions for nutrient removal*.
- FILIPIČ, J., KRAIGHER, B., TEPUŠ, B., KOKOL, V. & MANDIĆ-MULEC, I. 2015. Effect of low-density static magnetic field on the oxidation of ammonium by *Nitrosomonas europaea* and by activated sludge in municipal wastewater. *Food technology and biotechnology*, 53, 201.
- FORD, D. L., CHURCHWELL, R. L. & KACHTICK, J. W. 1980. COMPREHENSIVE ANALYSIS OF NITRIFICATION OF CHEMICAL-PROCESSING WASTEWATERS. *Journal Water Pollution Control Federation*, 52, 2726-2746.
- FRANCA, R. D., PINHEIRO, H. M., VAN LOOSDRECHT, M. C. & LOURENÇO, N. D. 2018. Stability of aerobic granules during long-term bioreactor operation. *Biotechnology advances*.
- FRØLUND, B., GRIEBE, T. & NIELSEN, P. H. 1995. Enzymatic activity in the activated-sludge floc matrix. *Applied Microbiology and Biotechnology*, 43, 755-761.
- FURUKAWA, K., INATOMI, Y., QIAO, S., QUAN, L., YAMAMOTO, T., ISAKA, K. & SUMINO, T. 2009. Innovative treatment system for digester liquor using anammox process. *Bioresource Technology*, 100, 5437-5443.
- FUX, C., VELTEN, S., CAROZZI, V., SOLLEY, D. & KELLER, J. 2006. Efficient and stable nitrification and denitrification of ammonium-rich sludge dewatering liquor using an SBR with continuous loading. *Water Research*, 40, 2765-2775.
- GANIGUÉ, R., GABARRÓ, J., SÀNCHEZ-MELSIÓ, A., RUSCALLEDA, M., LÓPEZ, H., VILA, X., COLPRIM, J. & BALAGUER, M. D. 2009. Long-term operation of a partial nitrification pilot plant treating leachate with extremely high ammonium concentration prior to an anammox process. *Bioresource Technology* 100, 5624-5632.
- GAO, D., LIU, L., LIANG, H. & WU, W.-M. 2011a. Aerobic granular sludge: characterization, mechanism of granulation and application to wastewater treatment. *Critical reviews in biotechnology*, 31, 137-152.
- GAO, D., LIU, L. & WU, W. M. 2011b. Comparison of four enhancement strategies for aerobic granulation in sequencing batch reactors. *Journal of hazardous materials*, 186, 320-327.
- GAO, M., DIAO, M.-H., YUAN, S., WANG, Y.-K., XU, H. & WANG, X.-H. 2017. Effects of phenol on physicochemical properties and treatment performances of partial nitrifying granules in sequencing batch reactors. *Biotechnology Reports*, 13, 13-18.
- GAUDY, A. 1962. Colorimetric determination of protein and carbohydrate. *Ind. Water Wastes.*, 7, 17-22.
- GE, S., WANG, S., YANG, X., QIU, S., LI, B. & PENG, Y. 2015. Detection of nitrifiers and evaluation of partial nitrification for wastewater treatment: A review. *Chemosphere*.
- GEYSSANT, J., HUWALD, E. & STRAUCH, D. 2001. Calcium Carbonate: From the Cretaceous Period into the 21st Century. Birkhäuser Verlag, Basel, Boston.
- GIESEKE, A., TARRE, S., GREEN, M. & DE BEER, D. 2006. Nitrification in a Biofilm at Low pH Values: Role of In Situ Microenvironments and Acid Tolerance. *Applied and Environmental Microbiology*, 72, 4283-4292.
- GONÇALVES, A. L., PIRES, JOSÉ C. M. AND SIMÕES, MANUEL 2017. A review on the use of microalgal consortia for wastewater treatment. *Algal Research*, 24, 403-415.
- GONZALEZ-GIL, G. & HOLLIGER, C. 2014. Aerobic Granules: Microbial Landscape and Architecture, Stages, and Practical Implications. *Applied and environmental microbiology*, 80, 3433-3441.
- GONZALEZ-GIL, G., LENS, P., VAN AELST, A., VAN AS, H., VERSPRILLE, A. & LETTINGA, G. 2001. Cluster structure of anaerobic aggregates of an expanded granular sludge bed reactor. *Applied and environmental microbiology*, 67, 3683-3692.

- GONZALEZ-MARTINEZ, A., RODRIGUEZ-SANCHEZ, A., RIVADENEYRA, M. A., RIVADENEYRA, A., MARTIN-RAMOS, D., VAHALA, R. & GONZALEZ-LOPEZ, J. 2017. 16S rRNA gene-based characterization of bacteria potentially associated with phosphate and carbonate precipitation from a granular autotrophic nitrogen removal bioreactor. *Applied Microbiology and Biotechnology*, 101, 817-829.
- GONZALEZ-SILVA, B. M., JONASSEN, K. R., BAKKE, I., ØSTGAARD, K. & VADSTEIN, O. 2016. Nitrification at different salinities: Biofilm community composition and physiological plasticity. *Water research*, 95, 48-58.
- GRUNDITZ, C. & DALHAMMAR, G. 2001. Development of nitrification inhibition assays using pure cultures of Nitrosomonas and Nitrobacter. *Water Research*, 35, 433-440.
- GUILLEN, J. A. S., JAYAWARDANA, L. K. M. C. B., VAZQUEZ, C. M. L., CRUZ, L. M. D. O., BRDJANOVIC, D. & VAN LIER, J. B. 2015. Autotrophic nitrogen removal over nitrite in a sponge-bed trickling filter. *Bioresource Technology*, 187, 314-325.
- GUO, Y., GUO, L., SUN, M., ZHAO, Y., GAO, M. & SHE, Z. 2017. Effects of hydraulic retention time (HRT) on denitrification using waste activated sludge thermal hydrolysis liquid and acidogenic liquid as carbon sources. *Bioresource Technology*, 224, 147-156.
- HAMMES, F., SEKA, A., DE KNIFF, S. & VERSTRAETE, W. 2003. A novel approach to calcium removal from calcium-rich industrial wastewater. *Water Research*, 37, 699-704.
- HAMMES, F. & VERSTRAETE, W. 2002. Key roles of pH and calcium metabolism in microbial carbonate precipitation. *ReViews in Environmental Science and BioTechnology*, 1, 3-7.
- HAN, B. & LOUHI-KULTANEN, M. 2018. Real-Time Raman Monitoring of Calcium Phosphate Precipitation in a Semi-Batch Stirred Crystallizer. *Crystal Growth & Design*, 18, 1622-1628.
- HANAOKI, K., WANTAWIN, C. & OHGAKI, S. 1990. Nitrification at low-levels of dissolved oxygen with and without organic loading in a suspended-growth reactor. *Water Research*, 24, 297-302.
- HAO, O. J. & CHEN, J. M. 1994. FACTORS AFFECTING NITRITE BUILDUP IN SUBMERGED FILTER SYSTEM. *Journal of Environmental Engineering-Asce*, 120, 1298-1307.
- HAO, X. D., HEIJNEN, J. J. & VAN LOOSDRECHT, M. C. M. 2001. Sensitivity analysis of a biofilm model describing a one-stage completely autotrophic nitrogen removal (CANON) process. *Biotechnology & Bioengineering*, 77, 266-277.
- HAVUKAINEN, J., NGUYEN, M. T., HERMANN, L., HORTTANAINEN, M., MIKKILÄ, M., DEVIATKIN, I. & LINNANEN, L. 2016. Potential of phosphorus recovery from sewage sludge and manure ash by thermochemical treatment. *Waste Management*, 49, 221-229.
- HE, G., DAHL, T., VEIS, A. & GEORGE, A. 2003. Nucleation of apatite crystals in vitro by self-assembled dentin matrix protein 1. *Nature materials*, 2, 552.
- HEDSTRÖM, A. 2001. Ion exchange of ammonium in zeolites: a literature review. *Journal of Environmental Engineering*.
- HELLINGA, C., SCHELLEN, A., MULDER, J. W., VAN LOOSDRECHT, M. C. M. & HEIJNEN, J. J. 1998. The SHARON process: an innovative method for nitrogen removal from ammonium-rich wastewater. *Water Science & Technology*, 37, 135-142.
- HOUSE, W. 1993. Solid/liquid reactions of environmental significance. *Research in Chemical Kinetics, Volume 1*. Elsevier.
- HOUSE, W. A. 1999. The Physico-Chemical Conditions for the Precipitation of Phosphate with Calcium. *Environmental Technology*, 20, 727-733.
- HU, Z., CHANDRAN, K., GRASSO, D. & SMETS, B. F. 2003. Impact of metal sorption and internalization on nitrification inhibition. *Environmental science & technology*, 37, 728-734.
- HU, Z., LOTTI, T., DE KREUK, M., KLEEREBEZEM, R., VAN LOOSDRECHT, M., KRUIT, J., JETTEN, M. S. & KARTAL, B. 2013. Nitrogen removal by a nitrification-anammox bioreactor at low temperature. *Applied and environmental microbiology*, 79, 2807-2812.
- HUANG, W., CAI, W., HUANG, H., LEI, Z., ZHANG, Z., TAY, J. H. & LEE, D.-J. 2015. Identification of inorganic and organic species of phosphorus and its bio-availability in nitrifying aerobic granular sludge. *Water Research*, 68, 423-431.
- HUANG, W., WANG, W., SHI, W., LEI, Z., ZHANG, Z., CHEN, R. & ZHOU, B. 2014. Use low direct current electric field to augment nitrification and structural stability of aerobic granular sludge when treating low COD/NH<sub>4</sub>-N wastewater. *Bioresource technology*, 171, 139-144.

- HÜLSEN, T., BARRY, EDWARD M., LU, YANG, PUYOL, DANIEL, KELLER, JURG AND BATSTONE, DAMIEN J. 2016. Domestic wastewater treatment with purple phototrophic bacteria using a novel continuous photo anaerobic membrane bioreactor. *Water Research*, 100, 486-495.
- HÜLSEN, T., BATSTONE, D. J. & KELLER, J. 2014. Phototrophic bacteria for nutrient recovery from domestic wastewater. *Water Research*, 50, 18-26.
- HULSEN, T., BATSTONE, DAMIEN J. AND KELLER, JURG 2014. Phototrophic bacteria for nutrient recovery from domestic wastewater. *Water Research*, 50, 18-26.
- ISANTA, E., REINO, C., CARRERA, J. & PEREZ, J. 2015. Stable partial nitrification for low-strength wastewater at low temperature in an aerobic granular reactor. *Water Research*, 80, 149-158.
- ISANTA, E., SUÁREZ-OJEDA, M. E., DEL RÍO, Á. V., MORALES, N., PÉREZ, J. & CARRERA, J. 2012. Long term operation of a granular sequencing batch reactor at pilot scale treating a low-strength wastewater. *Chemical engineering journal*, 198, 163-170.
- IVANOV, V., TAY, S.-L., LIU, Q.-S., WANG, X.-H., WANG, Z.-W. & TAY, J.-H. 2005. Formation and structure of granulated microbial aggregates used in aerobic wastewater treatment. *Water science and technology*, 52, 13-19.
- JACKMAN, S. A., MAINI, G., SHARMAN, A. K. & KNOWLES, C. J. 1999. The effects of direct electric current on the viability and metabolism of acidophilic bacteria. *Enzyme and Microbial Technology*, 24, 316-324.
- JAHN, L., SVARDAL, K. & KRAMPE, J. 2019. Comparison of aerobic granulation in SBR and continuous-flow plants. *Journal of environmental management*, 231, 953-961.
- JAROSZYNSKI, L. W. & OLESZKIEWICZ, J. A. 2011. Autotrophic ammonium removal from reject water: partial nitrification and anammox in one-reactor versus two-reactor systems. *Environmental Technology*, 32, 289-294.
- JETTEN, M. S., NIFTRIK, L. V., STROUS, M., KARTAL, B., KELTJENS, J. T. & OP DEN CAMP, H. J. 2009. Biochemistry and molecular biology of anammox bacteria. *Critical reviews in biochemistry and molecular biology*, 44, 65-84.
- JIANG, H. L., TAY, J. H., LIU, Y. & TAY, S. T. L. 2003. Ca<sup>2+</sup> augmentation for enhancement of aerobically grown microbial granules in sludge blanket reactors. *Biotechnology letters*, 25, 95-99.
- JIN, R.-C., XING, B.-S. & NI, W.-M. 2013. Optimization of partial nitrification in a continuous flow internal loop airlift reactor. *Bioresource Technology*, 147, 516-524.
- JIN, R.-C., ZHENG, P., MAHMOOD, Q. & ZHANG, L. 2008. Performance of a nitrifying airlift reactor using granular sludge. *Separation and Purification Technology*, 63, 670-675.
- JOHANSSON, S., RUSCALLEDA, M. & COLPRIM, J. 2017. Phosphorus recovery through biologically induced precipitation by partial nitrification-anammox granular biomass. *Chemical Engineering Journal*, 327, 881-888.
- JOSS, A., DERLON, N., CYPRIEN, C., BURGER, S., SZIVAK, I., TRABER, J., SIEGRIST, H. & MORGENROTH, E. 2011. Combined nitrification–anammox: advances in understanding process stability. *Environmental science & technology*, 45, 9735-9742.
- JOSS, A., SALZGEBER, D., EUGSTER, J., KONIG, R., ROTTERMANN, K., BURGER, S., FABIJAN, P., LEUMANN, S., MOHN, J. & SIEGRIST, H. 2009. Full-scale nitrogen removal from digester liquid with partial nitrification and anammox in one SBR. *Environmental Science & Technology* 43, 5301-5306.
- JUANG, Y.-C., ADAV, S. S., LEE, D.-J. & TAY, J.-H. 2010. Stable aerobic granules for continuous-flow reactors: Precipitating calcium and iron salts in granular interiors. *Bioresource Technology*, 101, 8051-8057.
- KAMPSCHREUR, M. J., POLDERMANS, R., KLEEREBEZEM, R., VAN DER STAR, W. R. L., HAARHUIS, R., ABMA, W. R., JETTEN, M. S. M. & VAN LOOSDRECHT, M. C. M. 2009. Emission of nitrous oxide and nitric oxide from a full-scale single-stage nitrification-anammox reactor. *Water Science & Technology*, 60, 3211-3217.
- KAMPSCHREUR, M. J., VAN DER STAR, W. R. L., WIELDERS, H. A., MULDER, J. W., M.S.M., J. & VAN LOOSDRECHT, M. C. M. 2008. Dynamics of nitric oxide and nitrous oxide emission during full-scale reject water treatment. *Water Research*, 42, 812-826.
- KATSOU, E., ALVARINO, T., MALAMIS, S., SUAREZ, S., FRISON, N., OMIL, F. & FATONE, F. 2016. Effects of selected pharmaceuticals on nitrogen and phosphorus removal bioprocesses. *Chemical Engineering Journal*, 295, 509-517.
- KAWAGUCHI, T. & DECHO, A. W. 2002. A laboratory investigation of cyanobacterial extracellular polymeric secretions (EPS) in influencing CaCO<sub>3</sub> polymorphism. *Journal of Crystal Growth*, 240, 230-235.

- KEITHLEY, S. E. & KIRISITS, M. J. 2018. An improved protocol for extracting extracellular polymeric substances from granular filter media. *Water research*, 129, 419-427.
- KHIN, T. & ANNACHHATRE, A. P. 2004. Novel microbial nitrogen removal processes. *Biotechnology Advances*, 22, 519-32.
- KIM, D.-J. & SEO, D. 2006. Selective enrichment and granulation of ammonia oxidizers in a sequencing batch airlift reactor. *Process Biochemistry*, 41, 1055-1062.
- KORNAROS, M., DOKIANAKIS, S. N. & LYBERATOS, G. 2010. Partial Nitrification/Denitrification Can Be Attributed to the Slow Response of Nitrite Oxidizing Bacteria to Periodic Anoxic Disturbances. *Environmental Science & Technology*, 44, 7245-7253.
- KUNACHEVA, C. & STUCKEY, D. C. 2014. Analytical methods for soluble microbial products (SMP) and extracellular polymers (ECP) in wastewater treatment systems: A review. *Water Research*, 61, 1-18.
- KUNTKE, P., SLEUTELS, T. H. J. A., RODRÍGUEZ ARREDONDO, M., GEORG, S., BARBOSA, S. G., TER HEIJNE, A., HAMELERS, HUBERTUS V. M. AND BUISMAN, C. J. N. 2018. (Bio)electrochemical ammonia recovery: progress and perspectives. *Applied Microbiology and Biotechnology*, 102, 3865-3878.
- LACKNER, S., GILBERT, E. M., VLAEMINCK, S. E., JOSS, A., HORN, H. & VAN LOOSDRECHT, M. C. M. 2014. Full-scale partial nitrification/anammox experiences e An application survey. *Water Research*, 55, 292-303.
- LASPIDOU, C. S. & RITTMANN, B. E. 2002. A unified theory for extracellular polymeric substances, soluble microbial products, and active and inert biomass. *Water Research*, 36, 2711-2720.
- LAURENI, M., PALATSI, J., LLOVERA, M. & BONMATÍ, A. 2013. Influence of pig slurry characteristics on ammonia stripping efficiencies and quality of the recovered ammonium - sulfate solution. *Journal of Chemical Technology and Biotechnology*, 88, 1654-1662.
- LEMAIRE, R., MARCELINO, M. & YUAN, Z. 2008. Achieving the nitrite pathway using aeration phase length control and step - feed in an SBR removing nutrients from abattoir wastewater. *Biotechnology and bioengineering*, 100, 1228-1236.
- LI, H., ZHOU, S., HUANG, G. & XU, B. 2013. Partial nitrification of landfill leachate with varying influent composition under intermittent aeration conditions. *Process Safety and Environmental Protection*, 91, 285-294.
- LI, J., ELLIOTT, D., NIELSEN, M., HEALY, M. G. & ZHAN, X. 2011. Long-term partial nitrification in an intermittently aerated sequencing batch reactor (SBR) treating ammonium-rich wastewater under controlled oxygen-limited conditions. *Biochemical Engineering Journal*, 55, 215-222.
- LI, X.-M., LIU, Q.-Q., YANG, Q., GUO, L., ZENG, G.-M., HU, J.-M. & ZHENG, W. 2009. Enhanced aerobic sludge granulation in sequencing batch reactor by Mg<sup>2+</sup> augmentation. *Bioresour. Technol.*, 100, 64-67.
- LI, Y. & LIU, Y. 2005. Diffusion of substrate and oxygen in aerobic granule. *Biochemical Engineering Journal*, 27, 45-52.
- LI, Y., ZOU, J., ZHANG, L. & SUN, J. 2014a. Aerobic granular sludge for simultaneous accumulation of mineral phosphorus and removal of nitrogen via nitrite in wastewater. *Bioresour. Technol.*, 154, 178-184.
- LI, Y., ZOU, J., ZHANG, L. & SUN, J. 2014b. Aerobic granular sludge for simultaneous accumulation of mineral phosphorus and removal of nitrogen via nitrite in wastewater. *Bioresour. Technol.*, 154, 178-184.
- LIN, Y.-M., LIU, Y. & TAY, J.-H. 2003. Development and characteristics of phosphorus-accumulating microbial granules in sequencing batch reactors. *Applied Microbiology and Biotechnology*, 62, 430-435.
- LIN, Y. M., BASSIN, J. P. & VAN LOOSDRECHT, M. C. M. 2012. The contribution of exopolysaccharides induced struvites accumulation to ammonium adsorption in aerobic granular sludge. *Water Research*, 46, 986-992.
- LIN, Y. M., LOTTI, T., SHARMA, P. K. & VAN LOOSDRECHT, M. C. M. 2013a. Apatite accumulation enhances the mechanical property of anammox granules. *Water Research*, 47, 4556-4566.
- LIN, Y. M., SHARMA, P. K. & VAN LOOSDRECHT, M. C. M. 2013b. The chemical and mechanical differences between alginate-like exopolysaccharides isolated from aerobic flocculent sludge and aerobic granular sludge. *Water Research*, 47, 57-65.
- LIU, H. & FANG, H. H. P. 2002. Extraction of extracellular polymeric substances (EPS) of sludges. *Journal of Biotechnology*, 95, 249-256.

- LIU, H., TONG, S., CHEN, N., LIU, Y., FENG, C. & HU, Q. 2015a. Effect of electro-stimulation on activity of heterotrophic denitrifying bacteria and denitrification performance. *Bioresource Technology*, 196, 123-128.
- LIU, J., LI, J., XIE, K. & SELLAMUTHU, B. 2019. Role of adding dried sludge micropowder in aerobic granular sludge reactor with extended filamentous bacteria. *Bioresource Technology Reports*, 5, 51-58.
- LIU, L., LI, W.-W., SHENG, G.-P., LIU, Z.-F., ZENG, R. J., LIU, J.-X., YU, H.-Q. & LEE, D.-J. 2010a. Microscale Hydrodynamic Analysis of Aerobic Granules in the Mass Transfer Process. *Environmental Science & Technology*, 44, 7555-7560.
- LIU, Q. S., TAY, J. H. & LIU, Y. 2003. Substrate concentration - independent aerobic granulation in sequential aerobic sludge blanket reactor. *Environmental technology*, 24, 1235-1242.
- LIU, S., YANG, F., MENG, F., CHEN, H. & GONG, Z. 2008. Enhanced anammox consortium activity for nitrogen removal: Impacts of static magnetic field. *Journal of biotechnology*, 138, 96-102.
- LIU, Y.-Q. & JOO-HWA, T. 2012. The competition between flocculent sludge and aerobic granules during the long-term operation period of granular sludge sequencing batch reactor. *Environmental Technology*, 33, 2619-26.
- LIU, Y.-Q., KONG, Y., TAY, J.-H. & ZHU, J. 2011. Enhancement of start-up of pilot-scale granular SBR fed with real wastewater. *Separation and Purification Technology*, 82, 190-196.
- LIU, Y.-Q., LAN, G.-H. & ZENG, P. 2015b. Excessive precipitation of CaCO<sub>3</sub> as aragonite in a continuous aerobic granular sludge reactor. *Applied Microbiology and Biotechnology*, 1-10.
- LIU, Y.-Q., LAN, G.-H. & ZENG, P. 2016a. Size-dependent calcium carbonate precipitation induced microbiologically in aerobic granules. *Chemical Engineering Journal*, 285, 341-348.
- LIU, Y.-Q., MOY, B., KONG, Y.-H. & TAY, J.-H. 2010b. Formation, physical characteristics and microbial community structure of aerobic granules in a pilot-scale sequencing batch reactor for real wastewater treatment. *Enzyme and Microbial Technology*, 46, 520-525.
- LIU, Y.-Q. & TAY, J.-H. 2015. Fast formation of aerobic granules by combining strong hydraulic selection pressure with overstressed organic loading rate. *Water research*, 80, 256-266.
- LIU, Y., SUHARTINI, S., GUO, L. & XIONG, Y.-P. 2016b. *Improved biological wastewater treatment and sludge characteristics by applying magnetic field to aerobic granules.*
- LIU, Y. & TAY, J. H. 2002. The essential role of hydrodynamic shear force in the formation of biofilm and granular sludge. *Water Research*, 36, 1653-1665.
- LIU, Y. & TAY, J. H. 2004. State of the art of biogranulation technology for wastewater treatment. *Biotechnology Advances*, 22, 533-563.
- LIU, Y., WANG, Z. W., QIN, L., LIU, Y. Q. & TAY, J. H. 2005a. Selection pressure-driven aerobic granulation in a sequencing batch reactor. *Applied microbiology and biotechnology*, 67, 26-32.
- LIU, Y., YANG, S.-F. & TAY, J.-H. 2004a. Improved stability of aerobic granules by selecting slow-growing nitrifying bacteria. *Journal of Biotechnology*, 108, 161-169.
- LIU, Y., YANG, S. F., TAY, J. H., LIU, Q. S., QIN, L. & LI, Y. 2004b. Cell hydrophobicity is a triggering force of biogranulation. *Enzyme and Microbial Technology*, 34, 371-379.
- LIU, Y. Q., LIU, Y. & TAY, J. H. 2005b. Relationship between size and mass transfer resistance in aerobic granules. *Letters in Applied Microbiology*, 40, 312-315.
- LIU, Y. Q., MOY, B., KONG, Y. H. AND TAY, J. H. 2010. Formation, physical characteristics and microbial community structure of aerobic granules in a pilot-scale sequencing batch reactor for real wastewater treatment. *Enzyme and Microbial Technology*, 46, 520-525.
- LIU, Y. Q. & TAY, J. H. 2007. Characteristics and stability of aerobic granules cultivated with different starvation time. *Applied microbiology and biotechnology*, 75, 205-210.
- LIU, Y. Q. & TAY, J. H. 2008. Influence of starvation time on formation and stability of aerobic granules in sequencing batch reactors. *Bioresource technology*, 99, 980-985.
- LIU, Y. Q., TAY, J. H., IVANOV, V., MOY, B. Y. P., YU, L. & TAY, S. T. L. 2005c. Influence of phenol on nitrification by microbial granules. *Process Biochemistry*, 40, 3285-3289.
- LOCHMATTER, S. & HOLLIGER, C. 2014. Optimization of operation conditions for the startup of aerobic granular sludge reactors biologically removing carbon, nitrogen, and phosphorous. *Water Research*, 59, 58-70.

- LOCHMATTER, S., MAILLARD, J. & HOLLIGER, C. 2014. Nitrogen Removal over Nitrite by Aeration Control in Aerobic Granular Sludge Sequencing Batch Reactors. *International Journal of Environmental Research and Public Health*, 11, 6955-6978.
- LONGNECKER, K., LOMAS, M. W. & VAN MOOY, B. A. S. 2010. Abundance and diversity of heterotrophic bacterial cells assimilating phosphate in the subtropical North Atlantic Ocean. *Environmental Microbiology*, 12, 2773-2782.
- LÓPEZ - PALAU, S., DOSTA, J., PERICAS, A. & MATA - ÁLVAREZ, J. 2011. Partial nitrification of sludge reject water using suspended and granular biomass. *Journal of Chemical Technology and Biotechnology*, 86, 1480-1487.
- LÓPEZ, H., PUIG, S., GANIGUÉ, R., RUSCALLEDA, M., BALAGUER, M. D. & COLPRIM, J. 2008. Start-up and enrichment of a granular anammox SBR to treat high nitrogen load wastewaters. *Journal of Chemical Technology and Biotechnology* 83, 233-241.
- LOWRY, O. H., ROSEBROUGH, N. J., FARR, A. L. & RANDALL, R. J. 1951. Protein measurement with the Folin phenol reagent. *J Biol Chem*, 193, 265-275.
- LUCARINI, A. C. & KILIKIAN, B. V. 1999. Comparative study of Lowry and Bradford methods: interfering substances. *Biotechnology Techniques*, 13, 149-154.
- LUO, Q., WANG, H., ZHANG, X. & QIAN, Y. 2005. Effect of direct electric current on the cell surface properties of phenol-degrading bacteria. *Applied and environmental microbiology*, 71, 423-427.
- MA, Y., PENG, Y., WANG, S., YUAN, Z. & WANG, X. 2009. Achieving nitrogen removal via nitrite in a pilot-scale continuous pre-denitrification plant. *Water Research*, 43, 563-572.
- MAGRÍ, A., BÉLINE, F. & DABERT, P. 2013. Feasibility and interest of the anammox process as treatment alternative for anaerobic digester supernatants in manure processing—An overview. *Journal of environmental management*, 131, 170-184.
- MAÑAS, A., BISCANS, B., SPERANDIO, S. 2011. Biologically induced phosphorus precipitation in aerobic granular sludge process. *Water Research*, 45, 3776-3786.
- MAÑAS, A., POCQUET, M., BISCANS, B. & SPERANDIO, M. 2012a. Parameters influencing calcium phosphate precipitation in granular sludge sequencing batch reactor. *Chemical Engineering Science*, 77, 165-175.
- MAÑAS, A., SPÉRANDIO, M., DECKER, F. & BISCANS, B. 2012b. Location and chemical composition of microbially induced phosphorus precipitates in anaerobic and aerobic granular sludge. *Environmental Technology*, 33, 2195-2209.
- MANN, S., DIDYMUS, J. M., SANDERSON, N. P., HEYWOOD, B. R. & SAMPER, E. J. A. 1990. Morphological influence of functionalized and non-functionalized [small alpha],[small omega]-dicarboxylates on calcite crystallization. *Journal of the Chemical Society, Faraday Transactions*, 86, 1873-1880.
- MASSARA, T. M., MALAMIS, S., GUIASOLA, A., BAEZA, J. A., NOUTSOPOULOS, C. & KATSOU, E. 2017. A review on nitrous oxide (N<sub>2</sub>O) emissions during biological nutrient removal from municipal wastewater and sludge reject water. *Science of The Total Environment*, 596-597, 106-123.
- MASSE, L., MASSE, D. I. & PELLERIN, Y. 2007. The use of membranes for the treatment of manure: a critical literature review. *Biosystems engineering*, 98, 371-380.
- MASZENAN, A. M., LIU, Y. & NG, W. J. 2011. Bioremediation of wastewaters with recalcitrant organic compounds and metals by aerobic granules. *Biotechnology Advances*, 29, 111-123.
- MAURER, M., ABRAMOVICH, D., SIEGRIST, H. & GUJER, W. 1999. Kinetics of biologically induced phosphorus precipitation in waste-water treatment. *Water Research*, 33, 484-493.
- MCCARTY, G. 1999. Modes of action of nitrification inhibitors. *Biology and Fertility of Soils*, 29, 1-9.
- METCALF & EDDY 2003. *Wastewater engineering: treatment, disposal and reuse*, New York, USA.
- MEYER, R. L., ZENG, R. J. X., GIUGLIANO, V. & BLACKALL, L. L. 2005. Challenges for simultaneous nitrification, denitrification, and phosphorus removal in microbial aggregates: mass transfer limitation and nitrous oxide production. *Fems Microbiology Ecology*, 52, 329-338.
- MILLER, J. P. 1952. A portion of the system calcium carbonate-carbon dioxide-water, with geological implications. *American Journal of Science*, 250, 161-203.
- MORALES, N., VAL DEL RÍO, Á., VÁZQUEZ-PADÍN, J. R., MÉNDEZ, R., MOSQUERA-CORRAL, A. & CAMPOS, J. L. 2015. Integration of the Anammox process to the rejection water and main stream lines of WWTPs. *Chemosphere*, 140, 99-105.

- MORGENROTH, E., SHERDEN, T., VAN LOOSDRECHT, M., HEIJNEN, J. & WILDERER, P. 1997. Aerobic granular sludge in a sequencing batch reactor. *Water Research*, 31, 3191-3194.
- MOUSSA, M. S., SUMANASEKERA, D. U., IBRAHIM, S. H., LUBBERDING, H. J., HOOIJMANS, C. M., GIJZEN, H. J. & VAN LOOSDRECHT, M. C. M. 2006. Long term effects of salt on activity, population structure and floc characteristics in enriched bacterial cultures of nitrifiers. *Water Research*, 40, 1377-1388.
- MOUTIN, T., GAL, J. Y., EL HALOUANI, H., PICOT, B. & BONTUOX, J. 1992. Decrease of phosphate concentration in a high rate pond by precipitation of calcium phosphate: Theoretical and experimental results. *Water Research*, 26, 1445-1450.
- MOY, B. Y. P., TAY, J. H., TOH, S. K., LIU, Y. & TAY, S. T. L. 2002. High organic loading influences the physical characteristics of aerobic sludge granules. *Letters in Applied Microbiology*, 34, 407-412.
- MULDER, A. 2003. The quest for sustainable nitrogen removal technologies. *Water Science & Technology*, 48, 67-75.
- MULLIN, J. W. 2001. *Crystallization*, Elsevier.
- NANCHARAI, Y., MOHAN, S. V. & LENS, P. 2016. Recent advances in nutrient removal and recovery in biological and bioelectrochemical systems. *Bioresour. Technol.*, 215, 173-185.
- NHAT, P. T., BIEC, H. N., VAN, T. T. T., VAN TUAN, D., TRUNG, N. L. H., NGHI, V. T. K. & DAN, N. P. 2017. Stability of partial nitritation in a sequencing batch reactor fed with high ammonium strength old urban landfill leachate. *International Biodeterioration & Biodegradation*, 124, 56-61.
- NI, B. J., XIE, W. M., LIU, S. G., YU, H. Q., WANG, Y. Z., WANG, G. & DAI, X. L. 2009. Granulation of activated sludge in a pilot-scale sequencing batch reactor for the treatment of low-strength municipal wastewater. *Water research*, 43, 751-761.
- NIELSEN, M., BOLLMANN, A., SLIEKERS, O., JETTEN, M., SCHMID, M., STROUS, M., SCHMIDT, I., LARSEN, L. H., NIELSEN, L. P. & REVSBECH, N. P. 2005. Kinetics, diffusional limitation and microscale distribution of chemistry and organisms in a CANON reactor. *FEMS Microbiol. Ecol.*, 51, 247-256.
- NÝVL, J. 1995. The Ostwald rule of stages. *Crystal Research and Technology*, 30, 443-449.
- OHASHI, A. & HARADA, H. 1994. Adhesion strength of biofilm developed in an attached-growth reactor. *Water Science and Technology*, 29, 281-288.
- OKABE, S., OSHIKI, M., TAKAHASHI, Y. & SATOH, H. 2011. Development of long-term stable partial nitrification and subsequent anammox process. *Bioresour. Technol.*, 102, 6801-6807.
- PAN, M., HENRY, L. G., LIU, R., HUANG, X. & ZHAN, X. 2014. Nitrogen removal from slaughterhouse wastewater through partial nitrification followed by denitrification in intermittently aerated sequencing batch reactors at 11 degrees C. *Environmental Technology*, 35, 470-477.
- PAN, S., TAY, J. H., HE, Y. X. & TAY, S. T. L. 2004. The effect of hydraulic retention time on the stability of aerobically grown microbial granules. *Letters in applied microbiology*, 38, 158-163.
- PARK, H.-D. & NOGUERA, D. R. 2004. Evaluating the effect of dissolved oxygen on ammonia-oxidizing bacterial communities in activated sludge. *Water Research*, 38, 3275-3286.
- PENG, L., DAI, H., WU, Y., PENG, Y. & LU, X. 2018. A Comprehensive Review of the Available Media and Approaches for Phosphorus Recovery from Wastewater. *Water, Air, & Soil Pollution*, 229, 115.
- PENG, Y. & ZHU, G. 2006. Biological nitrogen removal with nitrification and denitrification via nitrite pathway. *Applied Microbiology and Biotechnology*, 73, 15-26.
- PEYONG, Y. N., ZHOU, Y., ABDULLAH, A. Z. & VADIVELU, V. 2012. The effect of organic loading rates and nitrogenous compounds on the aerobic granules developed using low strength wastewater. *Biochemical Engineering Journal*, 67, 52-59.
- PICIOREANU, C., VAN LOOSDRECHT, M. C. & HEIJNEN, J. J. 1998. Mathematical modeling of biofilm structure with a hybrid differential-discrete cellular automaton approach. *Biotechnology and bioengineering*, 58, 101-116.
- PISHGAR, R., DOMINIC, J. A., SHENG, Z. AND TAY, J. H. 2019. Influence of operation mode and wastewater strength on aerobic granulation at pilot scale: Startup period, granular sludge characteristics and effluent quality. *Water Research*, 160, 81-96.
- PLANT, L. J. & HOUSE, W. A. 2002. Precipitation of calcite in the presence of inorganic phosphate. *Colloids and Surfaces A: Physicochemical and Engineering Aspects*, 203, 143-153.



- POOT, V., HOEKSTRA, M., GELEIJNSE, M. A., VAN LOOSDRECHT, M. C. & PÉREZ, J. 2016. Effects of the residual ammonium concentration on NOB repression during partial nitrification with granular sludge. *Water research*, 106, 518-530.
- PRESSLEY, T. A., BISHOP, D. F. & ROAN, S. G. 1972. Ammonia-Nitrogen Removal by Breakpoint Chlorination.
- PRONK, M., DE KREUK, M. K., DE BRUIN, B., KAMMINGA, P., KLEEREBEZEM, R., VAN LOOSDRECHT, M. C. M. 2015. Full scale performance of the aerobic granular sludge process for sewage treatment. *Water Research*, 84, 207-2017.
- QIAN, G., HU, X., LI, L., YE, L. & LV, W. 2017. Effect of iron ions and electric field on nitrification process in the periodic reversal bio-electrocoagulation system. *Bioresource technology*, 244, 382-390.
- QIAO, S., YAMAMOTO, T., MISAKA, M., ISAKA, K., SUMINO, T., BHATTI, Z. & FURUKAWA, K. 2010. High-rate nitrogen removal from livestock manure digester liquor by combined partial nitrification–anammox process. *Biodegradation*, 21, 11–20.
- QIAO, S., YIN, X., ZHOU, J. & FURUKAWA, K. 2013. Inhibition and recovery of continuous electric field application on the activity of anammox biomass. *Biodegradation*, 1-9.
- QIAO, S., YIN, X., ZHOU, J. & FURUKAWA, K. 2014. Inhibition and recovery of continuous electric field application on the activity of anammox biomass. *Biodegradation*, 25, 505-513.
- QIN, L. & LIU, Y. 2006. Aerobic granulation for organic carbon and nitrogen removal in alternating aerobic–anaerobic sequencing batch reactor. *Chemosphere*, 63, 926-933.
- QIN, L., LIU, Y. & TAY, J. H. 2004a. Effect of settling time on aerobic granulation in sequencing batch reactor. *Biochemical Engineering Journal*, 21, 47-52.
- QIN, L., TAY, J. H. & LIU, Y. 2004b. Selection pressure is a driving force of aerobic granulation in sequencing batch reactors. *Process Biochemistry*, 39, 579-584.
- QIN, L., TAY, J. H., YANG, S. F. & LIU, Y. Aerobic granulation under alternating aerobic and anaerobic conditions in sequencing batch reactors. 2nd Young Researchers Conference, University of Wageningen, Netherlands, 23-24 April 2004., 2004c. IWA Publishing, 3-10.
- QIU, G., MING LAW, Y., DAS, S. & TING, Y.-P. 2015. *Direct and Complete Phosphorus Recovery from Municipal Wastewater Using a Hybrid Microfiltration-Forward Osmosis Membrane Bioreactor Process with Seawater Brine as Draw Solution*.
- RAMESH, A., LEE, D.-J. & HONG, S. G. 2006. Soluble microbial products (SMP) and soluble extracellular polymeric substances (EPS) from wastewater sludge. *Applied Microbiology and Biotechnology*, 73, 219-225.
- RATHINAM, K., OREN, Y., PETRY, W., SCHWAHN, D. & KASHER, R. 2018. Calcium phosphate scaling during wastewater desalination on oligoamide surfaces mimicking reverse osmosis and nanofiltration membranes. *Water research*, 128, 217-225.
- REGMI, P., MILLER, M. W., HOLGATE, B., BUNCE, R., PARK, H., CHANDRAN, K., WETT, B., MURTHY, S. & BOTT, C. B. 2014. Control of aeration, aerobic SRT and COD input for mainstream nitrification/denitrification. *Water Research*, 57, 162-171.
- REN, T.-T., LIU, L., SHENG, G.-P., LIU, X.-W., YU, H.-Q., ZHANG, M.-C. & ZHU, J.-R. 2008. Calcium spatial distribution in aerobic granules and its effects on granule structure, strength and bioactivity. *Water research*, 42, 3343-3352.
- RITTMANN, B. E. & MCCARTY, P. L. 2001. *Environmental biotechnology: principles and applications*, 10020, New York, NY, McGraw-Hill.
- RUSCALLEDA, M., LÓPEZ, H., GANIGUÉ, R., PUIG, S., BALAGUER, M. D. & COLPRIM, J. 2008. Heterotrophic denitrification on granular anammox SBR treating urban landfill leachate. *Water Science & Technology*, 1749-1755.
- SADRIMOGHADDAM, S. & ALAVIMOGHADDAM, M. R. 2015. Cultivation of aerobic granules under different pre-anaerobic reaction times in sequencing batch reactors. *Separation and Purification Technology*, 142, 149-154.
- SALEM, S., MOUSSA, M. S. & VAN LOOSDRECHT, M. C. M. 2006. Determination of the decay rate of nitrifying bacteria. *Biotechnology and Bioengineering*, 94, 252-262.
- SARMA, S. & TAY, J. 2018a. Aerobic granulation for future wastewater treatment technology: challenges ahead. *Environmental Science: Water Research & Technology*, 4, 9-15.
- SARMA, S. J. & TAY, J.-H. 2018b. Carbon, nitrogen and phosphorus removal mechanisms of aerobic granules. *Critical Reviews in Biotechnology*, 1-12.

- SARMA, S. J., TAY, J. H. & CHU, A. 2017. Finding Knowledge Gaps in Aerobic Granulation Technology. *Trends in Biotechnology*, 35, 66-78.
- SCHAUBROECK, T., DE CLIPPELEIR, H., WEISSENBACHER, N., DEWULF, J., BOECKX, P., VLAEMINCK, S. E. & WETT, B. 2015. Environmental sustainability of an energy self-sufficient sewage treatment plant: Improvements through DEMON and co-digestion. *Water Research*, 74, 166-179.
- SEPÚLVEDA-MARDONES, M., CAMPOS, J. L., MAGRI, A. & VIDAL, G. 2019. Moving forward in the use of aerobic granular sludge for municipal wastewater treatment: an overview. *Reviews in Environmental Science and Bio/Technology*, 1-29.
- SHE, P., SONG, B., XING, X.-H., VAN LOOSDRECHT, M. & LIU, Z. 2006. Electrolytic stimulation of bacteria *Enterobacter dissolvens* by a direct current. *Biochemical Engineering Journal*, 28, 23-29.
- SHEN, Y.-X., XIAO, K., LIANG, P., MA, Y.-W. & HUANG, X. 2013. Improvement on the modified Lowry method against interference of divalent cations in soluble protein measurement. *Applied Microbiology and Biotechnology*, 97, 4167-4178.
- SHENG, G.-P., YU, H.-Q. & LI, X.-Y. 2010. Extracellular polymeric substances (EPS) of microbial aggregates in biological wastewater treatment systems: A review. *Biotechnology Advances*, 28, 882-894.
- SHI, X.-Y., YU, H.-Q., SUN, Y.-J. & HUANG, X. 2009. Characteristics of aerobic granules rich in autotrophic ammonium-oxidizing bacteria in a sequencing batch reactor. *Chemical Engineering Journal*, 147, 102-109.
- SHI, X. Y., SHENG, G. P., LI, X. Y. & YU, H. Q. 2010. Operation of a sequencing batch reactor for cultivating autotrophic nitrifying granules. *Bioresource Technology*.
- SHI, Y.-J., WANG, X.-H., YU, H.-B., XIE, H.-J., TENG, S.-X., SUN, X.-F., TIAN, B.-H. & WANG, S.-G. 2011. Aerobic granulation for nitrogen removal via nitrite in a sequencing batch reactor and the emission of nitrous oxide. *Bioresource technology*, 102, 2536-2541.
- SHIN, H. S. & LEE, S. M. 1998. Removal of nutrients in wastewater by using magnesium salts. *Environmental Technology*, 19, 283-290.
- SIMKISS, K. 1964. Variations in the crystalline form of calcium carbonate precipitated from artificial sea water. *Nature*, 201, 492.
- SINGH, R. P. & AGRAWAL, M. 2008. Potential benefits and risks of land application of sewage sludge. *Waste Management*, 28, 347-358.
- SINHA, B. & ANNACHATRE, A. P. 2007. Partial nitrification—operational parameters and microorganisms involved. *Reviews in Environmental Science and Bio/Technology*, 6, 285-313.
- SKERMAN, V. B. D. & MAC RAE, I. C. 1957. The influence of oxygen availability on the degree of nitrate reduction by *Pseudomonas denitrificans*. *J. Microbiol*, 3, 505-530.
- SMITH, P., KROHN, R., HERMANSON, G., MALLIA, A., GARTNER, F. & PROVENZANO, M. 1985. Measurement of protein using bicinchoninic acid *Anal Biochem* 150: 76–85. *Find this article online*.
- SOLIMAN, M. & ELDYASTI, A. 2018. Ammonia-Oxidizing Bacteria (AOB): opportunities and applications—a review. *Reviews in Environmental Science and Bio/Technology*, 1-37.
- SONG, Y., HAHN, H. H. & HOFFMANN, E. 2002. The Effect of Carbonate on the Precipitation of Calcium Phosphate. *Environmental Technology*, 23, 207-215.
- SONG, Y., ISHII, S., RATHNAYAK, L., ITO, T., SATOH, H. & OKABE, S. 2013. Development and characterization of the partial nitrification aerobic granules in a sequencing batch airlift reactor. *Bioresource Technology*.
- STROUS, M., HEIJNEN, J. J., KUENEN, J. G. & JETTEN, M. S. M. 1998. The sequencing batch reactor as a powerful tool for the study of slowly growing anaerobic ammonium oxidizing microorganisms. *Applied Microbiology & Biotechnology*, 50, 589–596.
- STROUS, M., KUENEN, J. G. & JETTEN, M. S. 1999. Key physiology of anaerobic ammonium oxidation. *Applied and Environmental Microbiology*, 65, 3248-50.
- SYUTSUBO, K., HARADA, H., OHASHI, A. & SUZUKI, H. 1997. An effective start-up of thermophilic UASB reactor by seeding mesophilically-grown granular sludge. *Water Science and Technology*, 36, 391-398.
- TANG, C. J., ZHENG, P., HU, B. L., CHEN, J. W. & WANG, C. H. 2010. Influence of substrates on nitrogen removal performance and microbiology of anaerobic ammonium oxidation by operating two UASB reactors fed with different substrate levels. *J Hazard Mater*, 181, 19–26.

- TAY, J., LIU, Q. & LIU, Y. 2004. The effect of upflow air velocity on the structure of aerobic granules cultivated in a sequencing batch reactor. *Water Science & Technology*, 49, 35-40.
- TAY, J. H., LIU, Q. S. & LIU, Y. 2001a. The effects of shear force on the formation, structure and metabolism of aerobic granules. *Applied Microbiology and Biotechnology*, 57, 227-233.
- TAY, J. H., LIU, Q. S. & LIU, Y. 2001b. Microscopic observation of aerobic granulation in sequential aerobic sludge blanket reactor. *Journal of Applied Microbiology*, 91, 168-175.
- TAY, J. H., LIU, Q. S. & LIU, Y. 2001c. The role of cellular polysaccharides in the formation and stability of aerobic granules. *Letters in Applied Microbiology*, 33, 222-226.
- TAY, J. H., YANG, S. F. & LIU, Y. 2002. Hydraulic selection pressure-induced nitrifying granulation in sequencing batch reactors. *Applied microbiology and biotechnology*, 59, 332-337.
- TAY, S. T.-L., MOY, B. Y.-P., MASZENAN, A. M. & TAY, J.-H. 2005. Comparing activated sludge and aerobic granules as microbial inocula for phenol biodegradation. *Applied Microbiology and Biotechnology*, 67, 708-713.
- TERVAHAUTA, T., VAN DER WEIJDEN, R. D., FLEMMING, R. L., HERNÁNDEZ LEAL, L., ZEEMAN, G. & BUISMAN, C. J. N. 2014. Calcium phosphate granulation in anaerobic treatment of black water: A new approach to phosphorus recovery. *Water Research*, 48, 632-642.
- TESKE, A., ALM, E., REGAN, J., TOZE, S., RITTMANN, B. & STAHL, D. 1994. Evolutionary relationships among ammonia- and nitrite-oxidizing bacteria. *Journal of bacteriology*, 176, 6623-6630.
- THRIVIKRAMAN, G., BODA, S. K. & BASU, B. 2018. Unraveling the mechanistic effects of electric field stimulation towards directing stem cell fate and function: A tissue engineering perspective. *Biomaterials*, 150, 60-86.
- TOH, S., TAY, J., MOY, B., IVANOV, V. & TAY, S. 2003. Size-effect on the physical characteristics of the aerobic granule in a SBR. *Applied Microbiology and Biotechnology*, 60, 687-695.
- TOKUTOMI, T. 2004. Operation of a nitrite-type airlift reactor at low DO concentration. *Water Science and Technology*, 49, 81-88.
- TSUNEDA, S., EJIRI, Y., NAGANO, T. & HIRATA, A. 2004. *Formation mechanism of nitrifying granules observed in an aerobic upflow fluidized bed (AUFB) reactor.*
- TSUNEDA, S., NAGANO, T., HOSHINO, T., EJIRI, Y., NODA, N. & HIRATA, A. 2003. Characterization of nitrifying granules produced in an aerobic upflow fluidized bed reactor. *Water Research*, 37, 4965-4973.
- TSUSHIMA, I., OGASAWARA, Y., SHIMOKAWA, M., KINDAICHI, T. & OKABE, S. 2007. Development of a super high-rate Anammox reactor and in situ analysis of biofilm structure and function. *Water Science & Technology*, 55, 9-17.
- TURK, O. & MAVINIC, D. S. 1989. MAINTAINING NITRITE BUILDUP IN A SYSTEM ACCLIMATED TO FREE AMMONIA. *Water Research*, 23, 1383-1388.
- VACCARI, D. A. & STRIGUL, N. 2011. Extrapolating phosphorus production to estimate resource reserves. *Chemosphere*, 84, 792-797.
- VAN DE GRAAF, A. A., DE BRUIJN, P., ROBERTSON, L. A., JETTEN, M. S. M. & KUENEN, J. G. 1996. Autotrophic growth of anaerobic ammonium-oxidizing micro-organisms in a fluidized bed reactor. *Microbiology*, 142, 2187-2196.
- VAN DER STAR, W. R. L., VAN DE GRAAF, M. J., KARTAL, B., PICIOREANU, C., JETTEN, M. S. M. & VAN LOOSDRECHT, M. C. M. 2008. Response of anaerobic ammonium-oxidizing bacteria to hydroxylamine. *Applied and Environmental Microbiology*, 74, 4417-4426.
- VAN DONGEN, U., JETTEN, M. S. M. & VAN LOOSDRECHT, M. C. M. 2001. The SHARON-ANAMMOX process for treatment of ammonium rich wastewater. *Water Science & Technology*, 44, 153-60.
- VAN HULLE, S. W. H., VANDEWEYER, H. J. P., MEESCHAERT, B. D., VANROLLEGHEM, P. A., DEJANS, P. & DUMOULIN, A. 2010. Engineering aspects and practical application of autotrophic nitrogen removal from nitrogen rich streams. *Chemical Engineering Journal*, 162, 1-20.
- VAN LANGERAK, E., GONZALEZ-GIL, G., VAN AELST, A., VAN LIER, J., HAMELERS, H. & LETTINGA, G. 1998. Effects of high calcium concentrations on the development of methanogenic sludge in upflow anaerobic sludge bed (UASB) reactors. *Water Research*, 32, 1255-1263.
- VAN LANGERAK, E., HAMELERS, H. & LETTINGA, G. 1997. Influent calcium removal by crystallization reusing anaerobic effluent alkalinity. *Water Science and Technology*, 36, 341-348.

- VAN LOOSDRECHT, M. C. M., EIKELBOOM, D., GJALTEMA, A., MULDER, A., TIJHUIS, L. & HEIJNEN, J. J. 1995. Biofilm structures. *Water Science and Technology*, 32, 35-43.
- VÁZQUEZ-PADÍN, J., FERNÁNDEZ, I., FIGUEROA, M., MOSQUERA-CORRAL, A., CAMPOS, J. AND MÉNDEZ, R. 2009. Applications of Anammox based processes to treat anaerobic digester supernatant at room temperature. *Bioresource Technology*, 100, 2988-2994.
- VÁZQUEZ-PADÍN, J. R., FIGUEROA, M., CAMPOS, J. L., MOSQUERA-CORRAL, A. & MÉNDEZ, R. 2010. Nitrifying granular systems: A suitable technology to obtain stable partial nitrification at room temperature. *Separation and Purification Technology*.
- VEYS, P., VANDEWEYER, H., AUDENAERT, W., MONBALLIU, A., DEJANS, P., JOOKEN, E., DUMOULIN, A., MEESSCHAERT, B. D. & VAN HULLE, S. W. H. 2010. Performance analysis and optimization of autotrophic nitrogen removal in different reactor configurations: a modelling study. *Environmental Technology*, 31, 1311-1324.
- VILLAIN, M., SIMON, S., BOURVEN, I. & GUIBAUD, G. 2010. The use of a new mobile phase, with no multivalent cation binding properties, to differentiate extracellular polymeric substances (EPS), by size exclusion chromatography (SEC), from biomass used for wastewater treatment. *Process Biochemistry*, 45, 1415-1421.
- VLAEMINCK, S. E. 2009. *Biofilm and granule applications for one-stage autotrophic nitrogen removal*. Phd, Ghent University.
- VLAEMINCK, S. E., CLOETENS, L. F.F., CARBALLA, M., BOON, N. & VERSTRAETE, W. 2008. Granular biomass capable of partial nitrification and anammox. *Water Science & Technology*, 58, 1113-1120.
- VLAEMINCK, S. E., TERADA, A., SMETS, B. F., DE CLIPPELEIR, H., SCHAUBROECK, T., BOLCA, S., DEMEESTERE, L., MAST, J., BOON, N. & CARBALLA, M. 2010. Aggregate size and architecture determine microbial activity balance for one-stage partial nitrification and anammox. *Applied and Environmental Microbiology*, 76, 900-909.
- VOLCKE, E. I., PICIOREANU, C., DE BAETS, B. & VAN LOOSDRECHT, M. C. M. 2010. Effect of granule size on autotrophic nitrogen removal in a granular sludge reactor. *Environmental Technology*, 31, 1271-80.
- WAN, C., SUN, S., LEE, D.-J., LIU, X., WANG, L., YANG, X. & PAN, X. 2013. Partial nitrification using aerobic granules in continuous-flow reactor: Rapid startup. *Bioresource Technology*, 142, 517-522.
- WAN, C., YANG, X., LEE, D.-J., SUN, S., LIU, X. & ZHANG, P. 2014. Influence of hydraulic retention time on partial nitrification of continuous-flow aerobic granular-sludge reactor. *Environmental Technology*, 35, 1760-1765.
- WAN, J., MOZO, I., FILALI, A., LINÉ, A., BESSIÈRE, Y. & SPÉRANDIO, M. 2011. Evolution of bioaggregate strength during aerobic granular sludge formation. *Biochemical engineering journal*, 58, 69-78.
- WANG, B.-B., CHANG, Q., PENG, D.-C., HOU, Y.-P., LI, H.-J. & PEI, L.-Y. 2014a. A new classification paradigm of extracellular polymeric substances (EPS) in activated sludge: Separation and characterization of exopolymers between floc level and microcolony level. *Water Research*, 64, 53-60.
- WANG, F., YANG, F.L., ZHANG, X.W., LIU, Y.H., ZHANG, H.M. AND ZHOU, J. 2005. Effects of cycle time on properties of aerobic granules in sequencing batch airlift reactors. *World Journal of Microbiology and Biotechnology*, 21, 1379-1384.
- WANG, J., QIAN, F., LIU, X., LIU, W., WANG, S. & SHEN, Y. 2016. Cultivation and characteristics of partial nitrification granular sludge in a sequencing batch reactor inoculated with heterotrophic granules. *Applied Microbiology and Biotechnology*, 100, 9381-9391.
- WANG, L. K. & IVANOV, V. 2010. *Environmental biotechnology*, Springer.
- WANG, M.-S., WANG, L.-H., BEKHIT, A. E.-D. A., YANG, J., HOU, Z.-P., WANG, Y.-Z., DAI, Q.-Z. & ZENG, X.-A. 2018. A review of sublethal effects of pulsed electric field on cells in food processing. *Journal of Food Engineering*, 223, 32-41.
- WANG, R., PENG, Y., CHENG, Z. & REN, N. 2014b. Understanding the role of extracellular polymeric substances in an enhanced biological phosphorus removal granular sludge system. *Bioresource technology*, 169, 307-312.
- WANG, X.-H., DIAO, M.-H., YANG, Y., SHI, Y.-J., GAO, M.-M. & WANG, S.-G. 2012. Enhanced aerobic nitrifying granulation by static magnetic field. *Bioresource technology*, 110, 105-110.
- WANG, X., ZHANG, B., SHEN, Z., QIU, Z., CHEN, Z., JIN, M., LI, J. & WANG, J. 2010. The EPS characteristics of sludge in an aerobic granule membrane bioreactor. *Bioresource technology*, 101, 8046-8050.

- WANG, X. H., ZHANG, H. M., YANG, F. L., XIA, L. P. & GAO, M. M. 2007a. Improved stability and performance of aerobic granules under stepwise increased selection pressure. *Enzyme and Microbial Technology*, 41, 205-211.
- WANG, Z.-P. & ZHANG, T. 2010. Characterization of soluble microbial products (SMP) under stressful conditions. *Water Research*, 44, 5499-5509.
- WANG, Z.-W., LI, Y. & LIU, Y. 2007b. Mechanism of calcium accumulation in acetate-fed aerobic granule. *Applied Microbiology and Biotechnology*, 74, 467-473.
- WANG, Z.-W., LI, Y., ZHOU, J.-Q. & LIU, Y. 2006. The influence of short-term starvation on aerobic granules. *Process Biochemistry*, 41, 2373-2378.
- WEI, D., XUE, X., YAN, L., SUN, M., ZHANG, G., SHI, L. & DU, B. 2014. Effect of influent ammonium concentration on the shift of full nitrification to partial nitrification in a sequencing batch reactor at ambient temperature. *Chemical Engineering Journal*, 235, 19-26.
- WEISS, C., TORRES-CANCEL, K., MOSER, R., ALLISON, P., GORE, E., CHANDLER, M. & MALONE, P. 2014. Influence of temperature on calcium carbonate polymorph formed from ammonium carbonate and calcium acetate. *J Nanotech Smart Mater*, 1, 1-6.
- WESTGATE, P. J. & PARK, C. 2010. Evaluation of proteins and organic nitrogen in wastewater treatment effluents. *Environmental science & technology*, 44, 5352-5357.
- WETT, B., OMARI, A., PODMIRSEG, S. M., HAN, M., AKINTAYO, O., BRANDON, M. G., MURTHY, S., BOTT, C., HELL, M., TAKACS, I., NYHUIS, G. & O'SHAUGHNESSY, M. 2013. Going for mainstream deammonification from bench to full scale for maximized resource efficiency. *Water Science and Technology*, 68, 283-289.
- WETT, B., PODMIRSEG, S., GÓMEZ - BRANDÓN, M., HELL, M., NYHUIS, G., BOTT, C. & MURTHY, S. 2015. Expanding DEMON sidestream deammonification technology towards mainstream application. *Water Environment Research*, 87, 2084-2089.
- WIESMANN, U. 1994. Biological nitrogen removal from wastewater. *Advances in biochemical engineering/biotechnology*, 51, 113-54.
- WINGENDER, J., NEU, T. R. & FLEMMING, H.-C. 1999. What are bacterial extracellular polymeric substances? *Microbial extracellular polymeric substances*. Springer.
- WINKLER, K. H., MARI AND STRAKA, LEVI 2019. New directions in biological nitrogen removal and. *Current Opinion in Biotechnology*, 57, 50-55.
- WINKLER, M.-K. H., KLEEREBEZEM, R., STROUS, M., CHANDRAN, K. & VAN LOOSDRECHT, M. C. M. 2013a. Factors influencing the density of aerobic granular sludge. *Applied Microbiology and Biotechnology*, 97, 7459-7468.
- WINKLER, M. H., KLEEREBEZEM, R., DE BRUIN, L., VERHEIJEN, P., ABBAS, B., HABERMACHER, J. & VAN LOOSDRECHT, M. 2013b. Microbial diversity differences within aerobic granular sludge and activated sludge flocs. *Applied microbiology and biotechnology*, 97, 7447-7458.
- WINKLER, M. K. & STRAKA, L. 2019. New directions in biological nitrogen removal and recovery from wastewater. *Current opinion in biotechnology*, 57, 50-55.
- WINKLER, M. K. H., KLEEREBEZEM, R., KHUNJAR, W. O., DE BRUIN, B. & VAN LOOSDRECHT, M. C. M. 2012a. Evaluating the solid retention time of bacteria in flocculent and granular sludge. *Water Research*, 46, 4973-4980.
- WINKLER, M. K. H., KLEEREBEZEM, R. & VAN LOOSDRECHT, M. C. M. 2012b. Integration of anammox into the aerobic granular sludge process for main stream wastewater treatment at ambient temperatures. *Water Research*, 46, 136-144.
- WU, J., BI, L., ZHANG, J. B., PONCIN, S., CAO, Z. P. & LI, H. Z. 2012. Effects of increase modes of shear force on granule disruption in upflow anaerobic reactors. *Water research*, 46, 3189-3196.
- WYFFELS, S., BOECKX, P., PYNAERT, K., ZHANG, D., VAN CLEEMPUT, O., CHEN, G. & VERSTRAETE, W. 2004. Nitrogen removal from sludge reject water by a two-stage oxygenlimited autotrophic nitrification denitrification process. *Water Science & Technology*, 49, 57-64.
- XIAO, F., YANG, S. F. & LI, X. Y. 2008. Physical and hydrodynamic properties of aerobic granules produced in sequencing batch reactors. *Separation and Purification Technology*, 63, 634-641.
- XIE, Q. & BURNELL, G. M. 1994. Interference of Mg<sup>2+</sup> and Ca<sup>2+</sup> on protein determination with Lowry's method. *Comparative Biochemistry and Physiology Part B: Comparative Biochemistry*, 107, 605-608.

- XIE, W.-M., NI, B.-J., SEVIOUR, T., SHENG, G.-P. & YU, H.-Q. 2012. Characterization of autotrophic and heterotrophic soluble microbial product (SMP) fractions from activated sludge. *Water Research*, 46, 6210-6217.
- XING, B.-S., JI, Y.-X., YANG, G.-F., CHEN, H., NI, W.-M. & JIN, R.-C. 2013. Start-up and stable operation of partial nitrification prior to ANAMMOX in an internal-loop airlift reactor. *Separation and Purification Technology*, 120, 458-466.
- XU, G., XU, X., YANG, F. & LIU, S. 2011. Selective inhibition of nitrite oxidation by chlorate dosing in aerobic granules. *J Hazard Mater*, 185, 249-54.
- XU, G., XU, X., YANG, F., LIU, S. & GAO, Y. 2012. Partial nitrification adjusted by hydroxylamine in aerobic granules under high DO and ambient temperature and subsequent Anammox for low C/N wastewater treatment. *Chemical Engineering Journal*, 213, 338-345.
- XU, Y., ZHOU, S. & LI, H. 2020. Landfill Leachate Treatment Using a Combination of Heterotrophic Denitrification and Partial Nitrification in a Single Sequencing Batch Reactor. *Polish Journal of Environmental Studies*, 29.
- YAMAMOTO, T., TAKAKI, K., KOYAMA, T. & FURUKAWA, K. 2008. Long-term stability of partial nitrification of swine wastewater digester liquor and its subsequent treatment by Anammox. *Bioresource Technology*, 99, 6419-6425.
- YAMASHITA, Y. & TANOUE, E. 2003. Chemical characterization of protein-like fluorophores in DOM in relation to aromatic amino acids. *Marine Chemistry*, 82, 255-271.
- YANG, J., TRELA, J., ZUBROWSKA-SUDOL, M. & PLAZA, E. 2015. Intermittent aeration in one-stage partial nitrification/anammox process. *Ecological Engineering*, 75, 413-420.
- YANG, J. C., ZHANG, L., DAISUKE, H., TAKAHIRO, S., MA, Y. G., LI, Z. G. & FURUKAWA, K. 2010. High rate partial nitrification treatment of reject wastewater. *Journal of Bioscience and Bioengineering*, 110, 436-440.
- YANG, L. & ALLEMAN, J. E. 1992. Investigation of batchwise nitrite build-up by an enriched nitrification culture. *Water Science & Technology*, 26, 997-1005.
- YANG, S. F., LIU, Q. S., TAY, J. H. & LIU, Y. 2004a. Growth kinetics of aerobic granules developed in sequencing batch reactors. *Letters in applied microbiology*, 38, 106-112.
- YANG, S. F., TAY, J. H. & LIU, Y. 2004b. Inhibition of free ammonia to the formation of aerobic granules. *Biochemical Engineering Journal*, 17, 41-48.
- YILMAZ, G., LEMAIRE, R., KELLER, J. & YUAN, Z. 2008. Simultaneous nitrification, denitrification, and phosphorus removal from nutrient-rich industrial wastewater using granular sludge. *Biotechnol Bioeng*, 100, 529-41.
- YIN, X., QIAO, S. & ZHOU, J. 2016. Effects of cycle duration of an external electrostatic field on anammox biomass activity. *Scientific reports*, 6, 19568.
- YU, H. Q., TAY, J. H. & FANG, H. H. P. 2001. The roles of calcium in sludge granulation during UASB reactor start-up. *Water Research*, 35, 1052-1060.
- YUAN, S., GAO, M., ZHU, F., AFZAL, M. Z., WANG, Y.-K., XU, H., WANG, M., WANG, S.-G. & WANG, X.-H. 2017. Disintegration of aerobic granules during prolonged operation. *Environmental Science: Water Research & Technology*, 3, 757-766.
- ZENG, X.-L., LONG, T., DING, W., XU, L. & ZOU, L. 2006. Improvement of biological activity of aerobic sludge by low energy ultrasonic irradiation. *China Water & Wastewater*, 22, 88-91.
- ZHANG, L., FENG, X., ZHU, N. & CHEN, J. 2007. Role of extracellular protein in the formation and stability of aerobic granules. *Enzyme and Microbial Technology*, 41, 551-557.
- ZHANG, L., REN, H. & DING, L. 2012. Comparison of extracellular polymeric substances (EPS) extraction from two different activated sludges. *Water Science and Technology*, 66, 1558-1564.
- ZHANG, L., YANG, J., HIRA, D., FUJII, T. & FURUKAWA, K. 2011. High-rate partial nitrification treatment of reject water as a pretreatment for anaerobic ammonium oxidation (anammox). *Bioresource Technology* 102, 3761-3767.
- ZHANG, Q.-Q. & JIN, R.-C. 2015. The Application of Low-Intensity Ultrasound Irradiation in Biological Wastewater Treatment: A Review. *Critical Reviews in Environmental Science and Technology*, 45, 2728-2761.
- ZHANG, X. & BISHOP, P. L. 2003. Biodegradability of biofilm extracellular polymeric substances. *Chemosphere*, 50, 63-69.

- ZHANG, Z.-Z., CHENG, Y.-F., ZHOU, Y.-H., BUAYI, X. & JIN, R.-C. 2015. A novel strategy for accelerating the recovery of an anammox reactor inhibited by copper (II): EDTA washing combined with biostimulation via low-intensity ultrasound. *Chemical Engineering Journal*, 279, 912-920.
- ZHENG, M., LIU, Y.-C., XIN, J., ZUO, H., WANG, C.-W. & WU, W.-M. 2015. Ultrasonic treatment enhanced ammonia-oxidizing bacterial (AOB) activity for nitrification process. *Environmental science & technology*, 50, 864-871.
- ZHOU, J.-H., ZHAO, H., HU, M., YU, H.-T., XU, X.-Y., VIDONISH, J., ALVAREZ, P. J. & ZHU, L. 2015. Granular activated carbon as nucleating agent for aerobic sludge granulation: effect of GAC size on velocity field differences (GAC versus flocs) and aggregation behavior. *Bioresource technology*, 198, 358-363.
- ZHOU, J. H., ZHOU, Y. C., YU, H. C., ZHAO, Y. Q., YE, K. Q., FANG, J. Y. & WANG, H. Y. 2019. Determining the effects of aeration intensity and reactor height to diameter (H/D) ratio on granule stability based on bubble behavior analysis. *Environmental Science and Pollution Research*, 26, 784-796.
- ZHU, L., LV, M.-L., DAI, X., ZHOU, J.-H. & XU, X.-Y. 2013. The stability of aerobic granular sludge under 4-chloroaniline shock in a sequential air-lift bioreactor (SABR). *Bioresource Technology*, 140, 126-130.